

# Carbon Dioxide Capture by Chemical Absorption: A Solvent Comparison Study

by

Anusha Kothandaraman

B. Chem. Eng.

Institute of Chemical Technology, University of Mumbai, 2005

M.S. Chemical Engineering Practice

Massachusetts Institute of Technology, 2006

SUBMITTED TO THE DEPARTMENT OF CHEMICAL ENGINEERING  
IN PARTIAL FULFILLMENT OF THE REQUIREMENTS FOR THE DEGREE OF

DOCTOR OF PHILOSOPHY IN CHEMICAL ENGINEERING PRACTICE  
AT THE  
MASSACHUSETTS INSTITUTE OF TECHNOLOGY

JUNE 2010

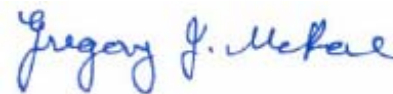
© 2010 Massachusetts Institute of Technology  
All rights reserved.

Signature of

Author.....

Department of Chemical Engineering

May 20, 2010



Certified

by.....

Gregory J. McRae

Hoyt C. Hottel Professor of Chemical Engineering

Thesis Supervisor

Accepted

by.....

William M. Deen

Carbon P. Dubbs Professor of Chemical Engineering

Chairman, Committee for Graduate Students



# **Carbon Dioxide Capture by Chemical Absorption: A Solvent Comparison Study**

by

Anusha Kothandaraman

Submitted to the Department of Chemical Engineering on May 20, 2010 in partial fulfillment of the requirements of the Degree of Doctor of Philosophy in Chemical Engineering Practice

## **Abstract**

In the light of increasing fears about climate change, greenhouse gas mitigation technologies have assumed growing importance. In the United States, energy related CO<sub>2</sub> emissions accounted for 98% of the total emissions in 2007 with electricity generation accounting for 40% of the total<sup>1</sup>. Carbon capture and sequestration (CCS) is one of the options that can enable the utilization of fossil fuels with lower CO<sub>2</sub> emissions. Of the different technologies for CO<sub>2</sub> capture, capture of CO<sub>2</sub> by chemical absorption is the technology that is closest to commercialization. While a number of different solvents for use in chemical absorption of CO<sub>2</sub> have been proposed, a systematic comparison of performance of different solvents has not been performed and claims on the performance of different solvents vary widely. This thesis focuses on developing a consistent framework for an objective comparison of the performance of different solvents. This framework has been applied to evaluate the performance of three different solvents – monoethanolamine, potassium carbonate and chilled ammonia.

In this thesis, comprehensive flowsheet models have been built for each of the solvent systems, using ASPEN Plus as the modeling tool. In order to ensure an objective and consistent comparison of the performance of different solvent systems, the representation of physical properties, thermodynamics and kinetics had to be verified and corrected as required in ASPEN Plus. The ASPEN RateSep module was used to facilitate the computation of mass transfer characteristics of the system for sizing calculations. For each solvent system, many parametric simulations were performed to identify the effect on energy consumption in the system. The overall energy consumption in the CO<sub>2</sub> capture and compression system was calculated and an evaluation of the required equipment size for critical equipment in the system was performed. The degradation characteristics and environmental impact of the solvents were also investigated. In addition, different flowsheet configurations were explored to optimize the energy recuperation for each system.

Monoethanolamine (MEA) was evaluated as the base case system in this thesis. Simulations showed the energy penalty for CO<sub>2</sub> capture from flue gas from coal-fired power plants to be 0.01572 kWh/gmol CO<sub>2</sub>. The energy penalty from CO<sub>2</sub> regeneration accounted for 60% of the energy penalty while the compression work accounted for 30%. The process flexibility in the MEA system was limited by degradation reactions. It was found that different flowsheet configurations for energy recuperation in the MEA system did not improve energy efficiency significantly.

Chilled ammonia was explored as an alternative to MEA for use in new coal-fired power plants as well as for retrofitting existing power plants. The overall energy penalty for CO<sub>2</sub> capture in chilled ammonia was found to be higher than in the MEA system, though energy requirements for CO<sub>2</sub> regeneration were found to be lower. The energy penalty for 85% capture of CO<sub>2</sub> in the chilled ammonia system was estimated to be 0.021 kWh/gmol CO<sub>2</sub>. As compared to the MEA system, the breakdown of the energy requirements was different with refrigeration in the absorber accounting for 44% of the energy penalty. This illustrates the need to perform a systemwide comparison of different solvents in order to evaluate the performance of various solvent systems.

The use of potassium carbonate as a solvent for CO<sub>2</sub> capture was evaluated for use in Integrated Reforming Combined Cycle (IRCC) system. With potassium carbonate, a high partial pressure of CO<sub>2</sub> in the flue gas is required. Different schemes for energy recuperation in the system were investigated and the energy consumption was reduced by 22% over the base case. An optimized version of the potassium carbonate flowsheet was developed for an IRCC application with a reboiler duty of 1980 kJ/kg.

In conclusion, a framework for the comparison of the performance of different solvents for CO<sub>2</sub> capture has been developed and the performance of monoethanolamine, chilled ammonia and potassium carbonate has been compared. From the standpoint of energy consumption, for existing power plants the use of MEA is found to be the best choice while for future design of power plants, potassium carbonate appears to be an attractive alternative. An economic analysis based on the technical findings in this thesis will help in identifying the optimal choices for various large, stationary sources of CO<sub>2</sub>.

Thesis Supervisor: Gregory J. McRae

Title: Hoyt C. Hottel Professor of Chemical Engineering

1: Energy Information Administration, Electric Power Annual 2007: A Summary. 2009: Washington D.C.

## Acknowledgements

I would like to begin by sincerely thanking my advisor, Prof. Greg McRae for his constant support, guidance and mentorship over the course of this thesis. He gave me the freedom to define my thesis statement and always acted as a very helpful sounding board for my ideas. Whenever I was bereft of ideas, my discussions with him and his insights always helped me get back on the right track. He has always encouraged me to explore a wide variety of opportunities. I have truly learnt a lot from him over the past 5 years and for this, I am very grateful.

I would also like to thank my thesis committee members – Howard Herzog, Prof. William Green and Prof. Ahmed Ghoniem for their valuable suggestions and advice. My collaborators at NTNU – Prof. Olav Bolland and Lars Nord were always ready to help me in understanding the power cycles and power plant modeling and I thank them for their time and helpful discussions. I am also very thankful to Randy Field for all his help with the ASPEN modeling in this work.

I am very grateful to the Norwegian Research Council, StatoilHydro, the Henry Bromfield Rogers Fellowship at MIT and the BPCL scholarship for the funding they have provided that has aided me greatly in the completion of this work.

Past and present members of the McRae group have been great sources of cheer and comfort during the past 5 years and I am grateful to them for their support. I would like to thank Ingrid Berkelmans, Bo Gong, Alex Lewis, Mihai Anton, Ken Hu, Carolyn Seto, Adekunle Adeyemo, Arman Haidari, Chuang-Chung Lee, Sara Passone, Jeremy Johnson and Patrick deMan for their friendship over the years. I would also like to thank Joan Chisholm, Liz Webb and Mary Gallagher for their support over the years and for making my life at MIT so much easier.

On a personal note, I know that this work could not have been completed without the tremendous support of my friends and family. I would like to thank my friends at MIT for all the good memories they have provided over the past few years. Ravi has been a great source of strength and support for me through each step of the journey and I thank him for his constant encouragement, optimism and belief in me. Finally, my gratitude to my parents is beyond measure – all through my life, they have always sacrificed to ensure that I had the best opportunities possible and they have constantly believed in me and encouraged me to dream big and to pursue those dreams. I cannot put into words what their support has meant to me over the years and I dedicate this thesis to them.

# Table of contents

<b>CHAPTER 1: INTRODUCTION.....</b>	<b>24</b>
<b>1.1 Motivation for carbon capture and sequestration .....</b>	<b>24</b>
<b>1.2 Brief overview of CO<sub>2</sub> capture systems.....</b>	<b>26</b>
1.2.1 Post-combustion capture.....	27
1.2.2 Oxyfuel combustion.....	29
1.2.3 Chemical looping combustion .....	32
1.2.4 Precombustion capture.....	34
<b>1.3 Current status of CO<sub>2</sub> capture technology .....</b>	<b>40</b>
<b>1.4 Solvent systems for chemical absorption .....</b>	<b>43</b>
<b>1.5 Thesis objectives.....</b>	<b>44</b>
<b>1.6 Thesis Overview .....</b>	<b>46</b>
<b>1.7 References.....</b>	<b>47</b>
<b>CHAPTER 2: ASPEN THERMODYNAMIC AND RATE MODELS .....</b>	<b>52</b>
<b>2.1 Electrolyte NRTL model .....</b>	<b>52</b>
2.1.1 Long range contribution.....	53
2.1.2 Born expression .....	55
2.1.3 Local contribution.....	55
<b>2.2 Soave-Reidlich-Kwong equation of state .....</b>	<b>57</b>
<b>2.3 Reidlich-Kwong-Soave-Boston-Mathias equation of state.....</b>	<b>59</b>
<b>2.4 Rate-based modeling with ASPEN RateSep.....</b>	<b>59</b>

2.4.1	Flow models.....	61
2.4.2	Film reactions.....	63
2.4.3	Column hydrodynamics.....	65
<b>2.5</b>	<b>Aspen Simulation Workbook.....</b>	<b>65</b>
<b>2.6</b>	<b>References.....</b>	<b>66</b>
<b>CHAPTER 3: MONOETHANOLAMINE SYSTEM.....</b>		<b>68</b>
<b>3.1</b>	<b>Process description.....</b>	<b>68</b>
<b>3.2</b>	<b>Chemistry of the MEA system.....</b>	<b>73</b>
3.2.1	Carbamate formation in the MEA system.....	74
<b>3.3</b>	<b>Thermochemistry in the MEA system.....</b>	<b>77</b>
<b>3.4</b>	<b>VLE in the MEA-CO<sub>2</sub>-H<sub>2</sub>O system.....</b>	<b>77</b>
<b>3.5</b>	<b>Degradation of MEA solvent.....</b>	<b>80</b>
3.5.1	Carbamate polymerization.....	80
3.5.2	Oxidative degradation.....	81
<b>3.6</b>	<b>MEA flowsheet development.....</b>	<b>82</b>
<b>3.7</b>	<b>MEA system equilibrium simulation results.....</b>	<b>84</b>
<b>3.8</b>	<b>Rate-based modeling of the MEA system.....</b>	<b>89</b>
3.8.1	Film discretization.....	89
3.8.2	Sizing of equipment.....	91
<b>3.9</b>	<b>Results from rate-based simulations for the MEA system.....</b>	<b>93</b>
3.9.1	Effect of capture percentage.....	97
3.9.2	Effect of packing.....	98

3.9.3	Effect of absorber height.....	100
3.9.4	Effect of solvent temperature.....	101
3.9.5	Effect of desorber height.....	102
3.9.6	Effect of desorber pressure .....	103
3.9.7	Breakdown of energy requirement in the reboiler .....	105
3.9.8	Effect of cross-heat exchanger.....	106
3.9.9	Other methods of energy recuperation.....	107
<b>3.10</b>	<b>Calculation of work for the MEA system .....</b>	<b>108</b>
<b>3.11</b>	<b>Total work for CO<sub>2</sub> capture and compression for NGCC plants.....</b>	<b>109</b>
<b>3.12</b>	<b>Total work for CO<sub>2</sub> capture and compression in coal-fired power plants ..</b>	<b>110</b>
<b>3.13</b>	<b>MEA conclusion .....</b>	<b>113</b>
<b>3.14</b>	<b>References.....</b>	<b>115</b>
<b>CHAPTER 4: POTASSIUM CARBONATE SYSTEM.....</b>		<b>119</b>
<b>4.1</b>	<b>Process description.....</b>	<b>119</b>
<b>4.2</b>	<b>Chemistry of the potassium carbonate system.....</b>	<b>121</b>
<b>4.3</b>	<b>Vapor-liquid equilibrium in K<sub>2</sub>CO<sub>3</sub>-H<sub>2</sub>O-CO<sub>2</sub> system.....</b>	<b>122</b>
<b>4.4</b>	<b>Difference in mode of operation between MEA and K<sub>2</sub>CO<sub>3</sub> systems.....</b>	<b>125</b>
<b>4.5</b>	<b>Flowsheet development for potassium carbonate system.....</b>	<b>127</b>
4.5.1	Effect of absorber pressure .....	128
<b>4.6</b>	<b>Equilibrium results with 40 wt. % eq.K<sub>2</sub>CO<sub>3</sub>.....</b>	<b>129</b>
<b>4.7</b>	<b>Rate-based modeling of the potassium carbonate system.....</b>	<b>130</b>
4.7.1	Film discretization .....	130

4.7.2	Definition of parameters used in the rate-based simulation.....	131
<b>4.8</b>	<b>Results from rate-based simulation of the potassium carbonate system.....</b>	<b>132</b>
4.8.1	Effect of packing.....	133
4.8.2	Effect of desorber height.....	134
4.8.3	Effect of desorber pressure .....	135
<b>4.9</b>	<b>Energy recuperation in the K<sub>2</sub>CO<sub>3</sub> system.....</b>	<b>136</b>
4.9.1	Flashing of rich solution and heat exchange with lean solution .....	136
4.9.2	Use of split-flow absorber.....	137
<b>4.10</b>	<b>Development of potassium carbonate model for Integrated Reforming Combined Cycle Plant.....</b>	<b>138</b>
<b>4.11</b>	<b>Use of potassium carbonate solvent with additives.....</b>	<b>140</b>
<b>4.12</b>	<b>Potassium carbonate system conclusion .....</b>	<b>141</b>
<b>4.13</b>	<b>References.....</b>	<b>142</b>
<b>CHAPTER 5: CHILLED AMMONIA SYSTEM .....</b>		<b>144</b>
<b>5.1</b>	<b>Chemistry of the chilled ammonia system.....</b>	<b>144</b>
<b>5.2</b>	<b>Thermodynamics of the chilled ammonia system .....</b>	<b>145</b>
<b>5.3</b>	<b>Process description.....</b>	<b>149</b>
<b>5.4</b>	<b>Thermochemistry in the chilled ammonia system .....</b>	<b>154</b>
5.4.1	Thermochemistry from Clausius-Clapeyron equation.....	154
5.4.2	Thermochemistry in ASPEN .....	156
<b>5.5</b>	<b>Analysis of the absorber .....</b>	<b>157</b>
5.5.1	Effect of absorber temperature.....	159

5.5.2	Effect of lean loading.....	161
5.5.3	Effect of molality of solution.....	163
<b>5.6</b>	<b>Analysis of the desorber .....</b>	<b>165</b>
<b>5.7</b>	<b>Discussion of mass transfer considerations .....</b>	<b>173</b>
5.7.1	Intrinsic mass transfer coefficient.....	173
5.7.2	Inhibition of mass transfer by precipitation .....	177
<b>5.8</b>	<b>Total energy utilization in the chilled ammonia system .....</b>	<b>178</b>
5.8.1	Coefficient of performance for refrigeration .....	179
5.8.2	Compression work .....	179
5.8.3	Flue gas chiller work.....	180
5.8.4	Steam extraction from power plant.....	180
<b>5.9</b>	<b>Conclusion for chilled ammonia system .....</b>	<b>184</b>
<b>5.10</b>	<b>References.....</b>	<b>185</b>
<b>CHAPTER 6: SUMMARY, CONCLUSIONS AND FUTURE WORK.....</b>		<b>187</b>
<b>6.1</b>	<b>Summary of research and thesis contributions.....</b>	<b>187</b>
<b>6.2</b>	<b>Future work.....</b>	<b>190</b>
<b>CHAPTER 7: PHD CEP CAPSTONE: CASE STUDY OF DIFFERENT ENVIRONMENTAL REGULATIONS IN THE US .....</b>		<b>192</b>
<b>7.1</b>	<b>Comparison of command-and-control environmental policies and market-based environmental policies .....</b>	<b>192</b>
<b>7.2</b>	<b>Phasedown of lead in gasoline in the United States .....</b>	<b>194</b>
7.2.1	History of lead as a fuel additive and regulations on leaded gasoline .....	194
7.2.2	Mechanics of the lead trading program in the US .....	196

7.2.3	How did refineries adopt to changing lead regulations?.....	200
7.2.4	Conclusion on phasedown of lead usage in gasoline.....	202
<b>7.3</b>	<b>Chlorofluorocarbon (CFC) reduction in the US.....</b>	<b>203</b>
7.3.1	What are CFCs and why are they harmful? .....	203
7.3.2	Regulation of CFC use.....	203
7.3.3	Effectiveness of the regulatory system in decreasing CFC production .....	209
7.3.4	Development of new technology and products.....	211
<b>7.4</b>	<b>Regulation of SO<sub>2</sub> emissions from power plants in the US .....</b>	<b>212</b>
7.4.1	Regulation of SO <sub>2</sub> in the 1970s.....	212
7.4.2	Regulation of SO <sub>2</sub> emissions from 1990.....	216
7.4.3	Compliance strategies of utilities.....	218
7.4.4	Effects of Clean Air Act on SO <sub>2</sub> emissions .....	219
7.4.5	Technology innovation and diffusion under the Clean Air Act.....	230
<b>7.5</b>	<b>Conclusion .....</b>	<b>238</b>
<b>7.6</b>	<b>References.....</b>	<b>241</b>
<b>APPENDIX A: OTHER POST-COMBUSTION CAPTURE TECHNOLOGIES</b>		<b>244</b>
<b>A.1</b>	<b>Physical absorption.....</b>	<b>244</b>
<b>A.2</b>	<b>Membrane separation.....</b>	<b>244</b>
<b>A.3</b>	<b>Adsorption .....</b>	<b>245</b>
<b>A.4</b>	<b>References.....</b>	<b>247</b>
<b>APPENDIX B: OXYFUEL CYCLES .....</b>		<b>248</b>
<b>B.1</b>	<b>Oxyfuel power boiler with steam cycle .....</b>	<b>248</b>

<b>B.2</b>	<b>Oxyfuel fired gas turbine.....</b>	<b>249</b>
<b>B.3</b>	<b>References.....</b>	<b>251</b>
<b>APPENDIX C: CHEMICAL LOOPING COMBUSTION AND REFORMING ..</b>		<b>252</b>
<b>C.1</b>	<b>Chemical looping steam reforming .....</b>	<b>254</b>
<b>C.2</b>	<b>Chemical looping autothermal reforming .....</b>	<b>255</b>
<b>C.3</b>	<b>References.....</b>	<b>258</b>
<b>APPENDIX D: CALCULATION OF MINIMUM WORK OF SEPARATION AND COMPRESSION.....</b>		<b>259</b>
<b>D.1</b>	<b>Minimum work of separation .....</b>	<b>259</b>
<b>D.2</b>	<b>Minimum work of compression.....</b>	<b>261</b>
<b>D.3</b>	<b>References.....</b>	<b>262</b>
<b>APPENDIX E: DEFINITION OF TERMS.....</b>		<b>263</b>

## List of figures

Figure 1-1: Plot of global instrumental temperature anomaly vs. time (temperature average from 1961-1990). Data for the figure from [1].....	24
Figure 1-2: Plot of atmospheric CO <sub>2</sub> concentration (ppmv) vs. time as measured at Mauna Loa, Hawaii. Data from [3].....	25
Figure 1-3: World Electricity Generation by Fuel, 2006-2030. Data from [5].....	26
Figure 1-4: Classification of CO <sub>2</sub> capture systems.....	27
Figure 1-5: Schematic of post-combustion capture ( Adapted from [2]).....	27
Figure 1-6: Schematic of oxyfuel combustion. Adapted from [2].....	30
Figure 1-7: Schematic of chemical looping combustion. Adapted from [11] .....	33
Figure 1-8: Schematic of chemical looping combustion system integrated with a power cycle. Adapted from [13]......	34
Figure 1-9: Schematic of precombustion decarbonization. Adapted from [2] .....	35
Figure 1-10: Flowsheet of autothermal reforming process. Adapted from [13].....	37
Figure 1-11: Block diagram of IGCC power plant. Adapted from [15].....	38
Figure 2-1: ASPEN representation of a stage (Adapted from [16]) .....	61
Figure 2-2: Mixed flow model in ASPEN RateSep (Adapted from [16]) .....	62
Figure 2-3: Concurrent flow model in ASPEN Plus (Adapted from [16]).....	62
Figure 2-4: VPlug flow model in ASPEN Plus (Adapted from [16]).....	63

Figure 2-5: VPlugP flow model in ASPEN Plus .....	63
Figure 3-1: Schematic of CO <sub>2</sub> capture by use of MEA solvent (Adapted from [7]) .....	69
Figure 3-2: Zwitterion mechanism for carbamate formation.....	74
Figure 3-3: Termolecular mechanism for carbamate formation.....	76
Figure 3-4: Comparison of ASPEN default VLE with experimental VLE at 60°C and 120°C. Experimental data from [17].....	78
Figure 3-5: Comparison of modified ASPEN VLE with experimental VLE at 60°C and 120°C. Modified interaction parameters from [18] and experimental data from [17].....	79
Figure 3-6: Process flow diagram of MEA system as developed in ASPEN Plus .....	82
Figure 3-7: Variation of L/G with lean loading for 85% CO <sub>2</sub> capture from NGCC flue gas; equilibrium simulation.....	85
Figure 3-8: Variation of reboiler duty and rich loading with L/G for 85% CO <sub>2</sub> capture from NGCC flue gas; equilibrium simulation .....	86
Figure 3-9: Variation of L/G with lean loading for 85% CO <sub>2</sub> capture from coal flue gas; equilibrium simulation.....	87
Figure 3-10: Variation of reboiler duty and rich loading with L/G for 85% CO <sub>2</sub> capture from coal flue gas; equilibrium simulation.....	88
Figure 3-11: Variation in ASPEN prediction of vented CO <sub>2</sub> with number of film segments.....	90
Figure 3-12: Variation of reboiler duty and rich loading with L/G for 85% CO <sub>2</sub> capture from NGCC flue gas: rate simulation .....	93

Figure 3-13: Variation of reboiler duty and rich loading with L/G for 85% CO <sub>2</sub> capture from coal flue gas: rate simulation.....	94
Figure 3-14: Variation of reboiler duty with rich loading for 85% CO <sub>2</sub> capture from coal flue gas and NGCC flue gas; rate simulation.....	95
Figure 3-15: Comparison of results from equilibrium and rate simulations for 85% CO <sub>2</sub> capture from NGCC flue gas .....	96
Figure 3-16: Variation of reboiler duty with lean loading for different capture percentages of CO <sub>2</sub> for NGCC flue gas.....	97
Figure 3-17: Variation in reboiler duty and rich loading with lean loading for different packing types .....	99
Figure 3-18: Variation in reboiler duty with absorber height for 85% CO <sub>2</sub> capture from NGCC flue gas.....	100
Figure 3-19: Absorber temperature profiles for 85% CO <sub>2</sub> capture from coal flue gas...	102
Figure 3-20: Variation in reboiler duty and temperature with reboiler pressure for 85% CO <sub>2</sub> capture from NGCC flue gas .....	103
Figure 3-21: Variation in electric work with reboiler pressure for 85% CO <sub>2</sub> capture from NGCC flue gas.....	105
Figure 3-22: Breakdown of energy requirements in reboiler.....	106
Figure 3-23: Variation in reboiler duty with lean loading for approach temperatures of 5 and 10°C for NGCC flue gas .....	107
Figure 3-24: Breakdown of energy consumption in CO <sub>2</sub> capture system of NGCC plant .....	110
Figure 3-25: Breakdown of total energy requirement for coal-fired power plants.....	111

Figure 3-26: Energy requirement for CO <sub>2</sub> capture in a NGCC plant .....	112
Figure 3-27: Energy requirement for CO <sub>2</sub> capture in a coal-fired power plant .....	113
Figure 4-1: Process flowsheet for a typical potassium carbonate process.....	120
Figure 4-2: Comparison of ASPEN default & experimental VLE for the K <sub>2</sub> CO <sub>3</sub> -CO <sub>2</sub> -H <sub>2</sub> O system (40 wt.% eq.K <sub>2</sub> CO <sub>3</sub> ) at 70, 90, 110 and 130 °C. Experimental data from [4] via [5].....	123
Figure 4-3: Comparison of ASPEN modified & experimental VLE for the K <sub>2</sub> CO <sub>3</sub> -CO <sub>2</sub> -H <sub>2</sub> O system (40 wt.% eq.K <sub>2</sub> CO <sub>3</sub> ) at 70, 90, 110 and 130 °C. Experimental data from [4] via [5]. Modified interaction parameters in ASPEN from [5] .....	124
Figure 4-4: Comparison of VLE of MEA-CO <sub>2</sub> -H <sub>2</sub> O system and K <sub>2</sub> CO <sub>3</sub> -CO <sub>2</sub> -H <sub>2</sub> O system .....	126
Figure 4-5: Flowsheet as developed in ASPEN Plus for the potassium carbonate system .....	127
Figure 4-6: Variation of rich loading and L/G with absorber pressure at a constant lean loading of 0.5 for the potassium carbonate system; equilibrium simulation .....	128
Figure 4-7: Variation of reboiler duty and L/G with lean loading for 85% capture of CO <sub>2</sub> ; equilibrium simulation .....	129
Figure 4-8: Variation of reboiler duty and rich loading with L/G for 85% CO <sub>2</sub> capture; rate-based simulation .....	132
Figure 4-9: Variation of reboiler duty with desorber height for 85% capture of CO <sub>2</sub> ; rate-based simulation.....	135
Figure 4-10: Flowsheet for energy recuperation by flashing of rich solution and heat exchange with lean solution.....	136

Figure 4-11: Energy recuperation by use of a split-flow absorber .....	138
Figure 4-12: Schematic of IRCC plant with CO <sub>2</sub> capture. Adapted from [11].....	139
Figure 4-13: Flowsheet of potassium carbonate system developed for application in IRCC plant.....	140
Figure 5-1: Comparison of ASPEN default VLE and experimental VLE for the NH <sub>3</sub> -CO <sub>2</sub> -H <sub>2</sub> O system for a 6.3M NH <sub>3</sub> solution at 40°C. Experimental data from [8] .....	146
Figure 5-2: Comparison of ASPEN default VLE and experimental VLE for the NH <sub>3</sub> -CO <sub>2</sub> -H <sub>2</sub> O system for a 11.9m NH <sub>3</sub> solution at 60°C. Experimental data from [8].....	147
Figure 5-3: Comparison of VLE of NH <sub>3</sub> -CO <sub>2</sub> -H <sub>2</sub> O system for 6.3M and 11.9M NH <sub>3</sub> solution at 313K. Data from [8].....	148
Figure 5-4: Comparison of VLE for NH <sub>3</sub> -CO <sub>2</sub> -H <sub>2</sub> O solution at 313K and 333K for 11.9m NH <sub>3</sub> solution. Data from [8].....	149
Figure 5-5: Flowsheet for chilled ammonia process.....	150
Figure 5-6: Variation in concentration of NH <sub>3</sub> in vent gas with temperature for a 20.9Mm NH <sub>3</sub> solution, with a lean loading of 0.4.....	158
Figure 5-7: Flowsheet as developed in ASPEN for the absorber section of the chilled ammonia process.....	159
Figure 5-8: Variation of rich loading and L/G in absorber with temperature for a 20.9m NH <sub>3</sub> solution at a lean loading of 0.42 for 85% CO <sub>2</sub> capture from coal flue gas .....	160
Figure 5-9: Variation in refrigerator load and water wash desorber duty with temperature for a 20.9m NH <sub>3</sub> solution, lean loading of 0.42, 85% CO <sub>2</sub> capture from coal flue gas ..	161
Figure 5-10: Variation of L/G and wt.% of solids in rich solution with lean loading for a 10.1m NH <sub>3</sub> solution at 5°C for 85% capture of CO <sub>2</sub> from coal flue gas .....	162

Figure 5-11: Variation of refrigeration, water wash desorber and total duty with lean loading for a 10.1m NH <sub>3</sub> solution at 5°C for 85% capture of CO <sub>2</sub> from coal flue gas...	163
Figure 5-12: Variation of L/G with molality of NH <sub>3</sub> for a lean loading of 0.4 and temperature of 5°C for 85% capture of CO <sub>2</sub> from coal flue gas.....	164
Figure 5-13: Variation of refrigeration duty and rich solids wt.% with molality of NH <sub>3</sub> for a lean loading of 0.4 and temperature of 5°C for 85% capture of CO <sub>2</sub> from coal flue gas .....	165
Figure 5-14: Desorber section of the flowsheet as developed in ASPEN Plus .....	167
Figure 5-15: Variation of L/G and solid% in rich stream vs. molality of NH <sub>3</sub> solution at lean loading of 0.4 and temperature of 5°C for 85% capture of CO <sub>2</sub> from coal flue gas. ....	168
Figure 5-16: Variation of refrigeration duty in absorber with molality of NH <sub>3</sub> solution for a lean loading of 0.4 and temperature of 5°C and 85% capture of CO <sub>2</sub> from coal flue gas. ....	169
Figure 5-17: Variation of wt.% of solids leaving heat exchanger and additional heat exchanger duty with molality of NH <sub>3</sub> at a lean loading of 0.4 and temperature of 5°C for 85% capture of CO <sub>2</sub> from coal flue gas .....	171
Figure 5-18: Variation of desorber and heat exchanger duties with molality of NH <sub>3</sub> solution at a lean loading of 0.4 and temperature of 5°C for 85% capture of CO <sub>2</sub> from coal flue gas .....	172
Figure 5-19: Distribution of energy requirements in chilled ammonia system for 85% capture of CO <sub>2</sub> from flue gas from coal-fired power plants .....	182
Figure 5-20: Energy requirement for 85% capture of CO <sub>2</sub> from flue gas from a coal-fired power plant using chilled ammonia solvent system .....	183

Figure 7-1: Effect of lead allowances trading on compliance with regulations. Figure adapted from [7].....	198
Figure 7-2: Effect of lead allowances banking on compliance with regulations. Figure adapted from [7].....	199
Figure 7-3: Trend of cumulative number of isomerization adoptions over time. Figure adapted from [5].....	201
Figure 7-4: Production of CFCs in the US from 1972 to 1988. Data from [11].....	204
Figure 7-5: Production of Annex I chemicals in the US after 1990. Figure adapted from [12].....	210
Figure 7-6: Worldwide production of Annex I chemicals after 1990. Figure adapted from [12].....	211
Figure 7-7: Comparison of actual SO <sub>2</sub> emissions in the US after enactment of Clean Air Act Amendment of 1990 with predicted SO <sub>2</sub> emissions. Figure adapted from [20] .....	220
Figure 7-8: Emissions from phase I units compared to allowance caps from 1995 to 1999. Data from [21].....	221
Figure 7-9: Comparison of usage levels of different coal types in 1990 and 1995. Data from [22].....	222
Figure 7-10: Percentage of electricity generating units employing each compliance strategy in 1995. Data from [22].....	223
Figure 7-11: Percentage reduction in emissions from each compliance strategy. Data from [22].....	224
Figure 7-12: Comparison of total SO <sub>2</sub> emissions from phase I and phase II units with allowed emissions from 1995 to 2006. Data from [21] .....	225

Figure 7-13: Size of SO <sub>2</sub> emissions bank from 1995-2006. Data from [21] .....	226
Figure 7-14: Volume of trade in SO <sub>2</sub> allowances from 1994 to 2003. Data from [23] ..	228
Figure 7-15: Price history for SO <sub>2</sub> allowances from 1994 to 2010. Adapted from [24-25] .....	229
Figure 7-16: Trend in US patents relevant to SO <sub>2</sub> control technologies from 1974-1993. Adapted from [26].....	231
Figure 7-17: Trend in US patents relevant to precombustion SO <sub>2</sub> control technologies from 1974-1993. Adapted from [26] .....	232
Figure 7-18: Variation of capital costs of FGD with cumulative FGD capacity. Adapted from [26].....	233
Figure 7-19: Variation of scrubbing efficiency with cumulative installed FGD capacity in the US. Adapted from [26].....	234
Figure 7-20: Variation of scrubbing efficiency of FGD with year of installation. Adapted from [15].....	235
Figure 7-21: Percentage of scrubbers with different removal efficiencies by regulatory regime. Data from [15] .....	237
Figure B-1: Schematic of oxyfuel fired gas turbine cycle. Adapted from [5] .....	249
Figure C-1: Flowsheet of chemical looping steam reforming. Adapted from [8]. .....	254
Figure C-2: Schematic of chemical looping autothermal reforming. Adapted from [9]	256
Figure C-3: Flowsheet of chemical looping autothermal reforming. Adapted from [10] .....	257
Figure D-1: Schematic of separation system .....	259

## List of tables

Table 1-1: : CO <sub>2</sub> partial pressure in flue gases of different combustion systems. (Data taken from [2]) .....	28
Table 1-2: Energy requirement to produce O <sub>2</sub> for combustion of different fuels. (Adapted from [10]).....	31
Table 1-3: Amine scrubbing technology. Data from [23-24] .....	42
Table 3-1: Values of temperature dependent parameters for equilibrium constant in MEA system .....	74
Table 3-2: Thermochemistry in the MEA system. Data from [16].....	77
Table 3-3: Specified discretization points in the liquid film.....	91
Table 3-4: Values of parameters used in the absorber for the MEA system .....	92
Table 3-5: Values of parameters used in the desorber of the MEA system.....	92
Table 3-6: Minimum reboiler duty obtained with different packings in the absorber.....	99
Table 3-7: Steam withdrawal conditions for coal and NGCC plants for use in reboiler of MEA system.....	109
Table 3-8: Total work in CO <sub>2</sub> capture system in NGCC plants.....	109
Table 3-9: Total work in CO <sub>2</sub> capture system in coal-fired power plants .....	111
Table 4-1: Values of parameters of equilibrium constants for the potassium carbonate system .....	122
Table 4-2: Location of discretization points in the liquid film .....	130

Table 4-3: Values of parameters used in the absorber of the potassium carbonate system .....	131
Table 4-4: Values of parameters used in the desorber of the potassium carbonate system .....	131
Table 4-5: Effect of packing type in the absorber.....	133
Table 4-6: Effect of packing type in the desorber.....	134
Table 5-1: Vapor pressure of CO <sub>2</sub> at different loadings and temperatures. Data from [10] .....	155
Table 5-2: Heat of reaction for different temperature ranges as calculated by the Clausius-Clapeyron equation .....	156
Table 5-3: Steam withdrawal condition for chilled ammonia system .....	181
Table 5-4: Work required in different components of the chilled ammonia system .....	182
Table 6-1: Summary of results from the three solvent systems.....	188
Table 7-1: Breakdown of banking of SO <sub>2</sub> allowances by compliance strategy. Data from [19].....	227
Table 7-2: Percentage of scrubbers with different removal efficiencies under each regulatory regime. Adapted from [15].....	236
Table D-1: Availability data for CO <sub>2</sub> at 1 bar and 110 bar. Data from [2].....	261
Table E-1: Definition of terms used in thesis .....	263

## List of symbols

$A_\phi$	:	Debye-Huckel parameter
$C_s$	:	Concentration of solvent
$d$	:	Solvent density
$D_{CO_2}$	:	Diffusivity of CO <sub>2</sub>
$D_s$	:	Dielectric constant of mixed solvent
$D_w$	:	Dielectric constant of water
$e$	:	Charge of an electron
$g^{ex*}$	:	Molar excess Gibbs free energy
$g^{ex*,local}$	:	Local interaction contribution to molar excess Gibbs free energy
$g^{ex*,LR}$	:	Long-range contribution to molar excess Gibbs free energy
$I_x$	:	Ionic strength on a mole fraction basis
$k_1$	:	First-order rate constant
$k_2$	:	Second-order rate constant
$k_B$	:	Boltzmann constant
$k_l$	:	Mass-transfer coefficient
$K_x$	:	Equilibrium constant (mole fraction based)
$M_s$	:	Molecular weight of solvent in kg/kmol
$N_{CO_2}$	:	Flux of CO <sub>2</sub>
$N_o$	:	Avogadro's number
$P$	:	Vapor pressure
$P_{ci}$	:	Critical pressure of species i
$Q_c$	:	Heat absorbed at lower temperature
$R$	:	Universal gas constant
$r_k$	:	Born radius of species k
$S$	:	Entropy
$T$	:	Temperature, in K
$T_{ci}$	:	Critical temperature of species i
$V_m$	:	Molar volume
$W$	:	Net work
$W_{min}$	:	Minimum thermodynamic work
$x_k$	:	Liquid-phase mole fraction of species k
$z_k$	:	Charge on species k
$\alpha$	:	Nonrandomness parameter
$\delta$	:	Film thickness
$\Delta H$	:	Heat of reaction (kcal/mol)
$\rho$	:	Closest approach parameter
$\tau$	:	Binary energy interaction parameter
$\omega$	:	Acentric factor

# Chapter 1

## Introduction

### 1.1 Motivation for carbon capture and sequestration

Greenhouse gas mitigation technology, particularly with respect to CO<sub>2</sub> is assuming increasing importance in the light of climate change fears. Over the past 30 years, there has been growing concern due to increasing global temperatures. Figure 1-1 shows the increase in the difference between the global mean surface temperature and the average temperature from 1961-1990 [1].

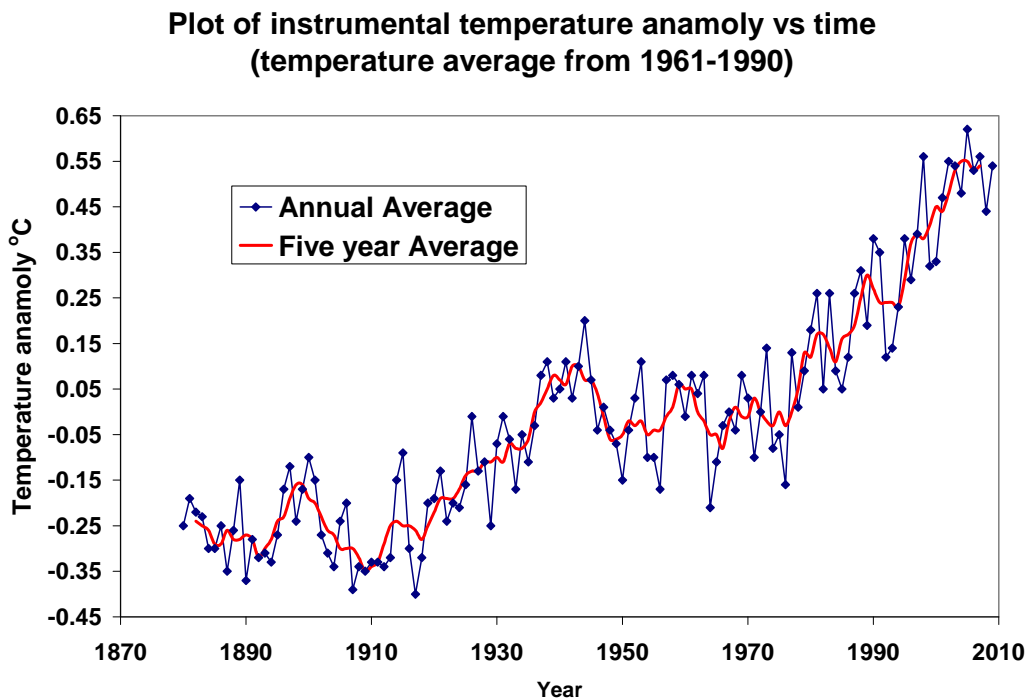


**Figure 1-1: Plot of global instrumental temperature anomaly vs. time (temperature average from 1961-1990). Data for the figure from [1]**

Much of the increase in global temperatures has been attributed to the increasing CO<sub>2</sub> concentration in the atmosphere due to human activity [2]. Figure 1-2 shows the trend in atmospheric CO<sub>2</sub> concentration as measured at Mauna Loa Observatory, Hawaii [3].

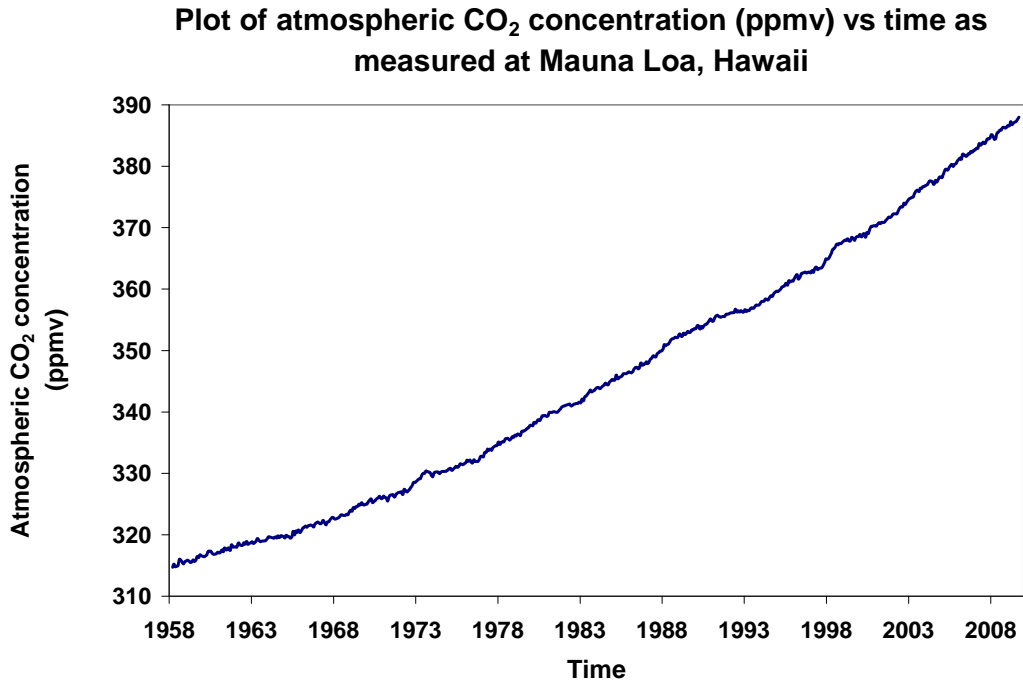


**Figure 1-2: Plot of atmospheric CO<sub>2</sub> concentration (ppmv) vs. time as measured at Mauna Loa, Hawaii. Data from [3].**

In the US, energy-related CO<sub>2</sub> emissions accounted for 98% of the total emissions in 2007, with electricity generation accounting for 40% of the total [4]. The electricity-generating sector – coal and natural gas fired power plants - creates concentrated and large sources of CO<sub>2</sub>, on which CO<sub>2</sub> mitigation technologies can be deployed first. The EIA predicts that in 2030, CO<sub>2</sub> emissions from electricity generation in the US will increase to 2700 million metric tons and account for 43% of the total US emissions [5]. This is because fossil fuels are expected to dominate the electricity generating mix for the next few decades. Figure 1-3 shows the expected utilization of different fuels for world electricity generation [5]. From Figure 1-3, it is apparent that coal will continue to be the

major fuel utilized for electricity generation in the near future. Hence, there is an urgent need to deploy technologies that will allow the utilization of fossil fuels in a cleaner way and provide a bridge to a more green economy in the future.

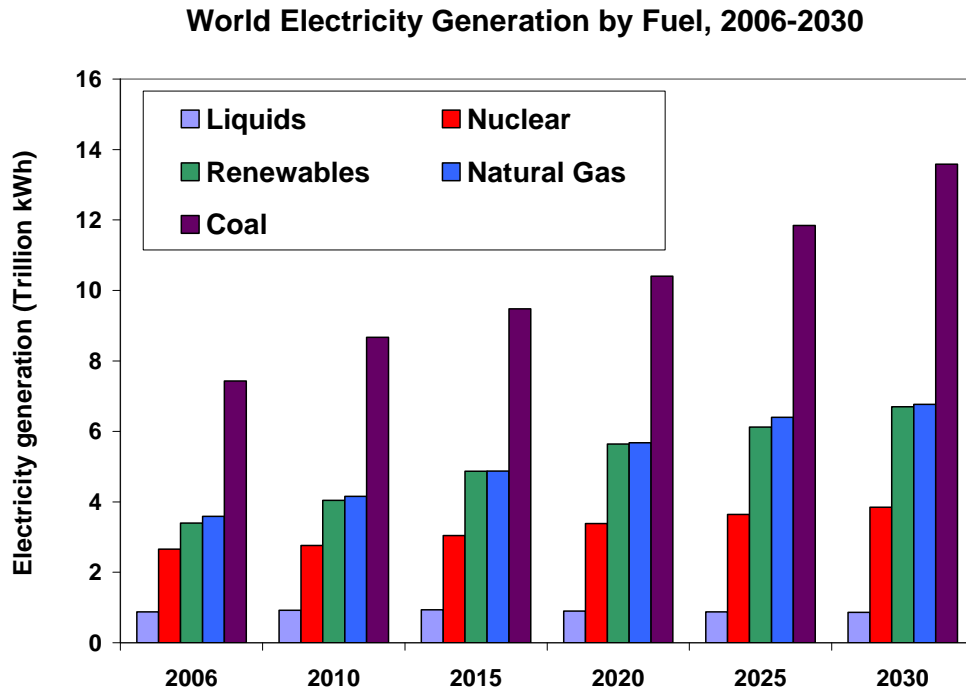
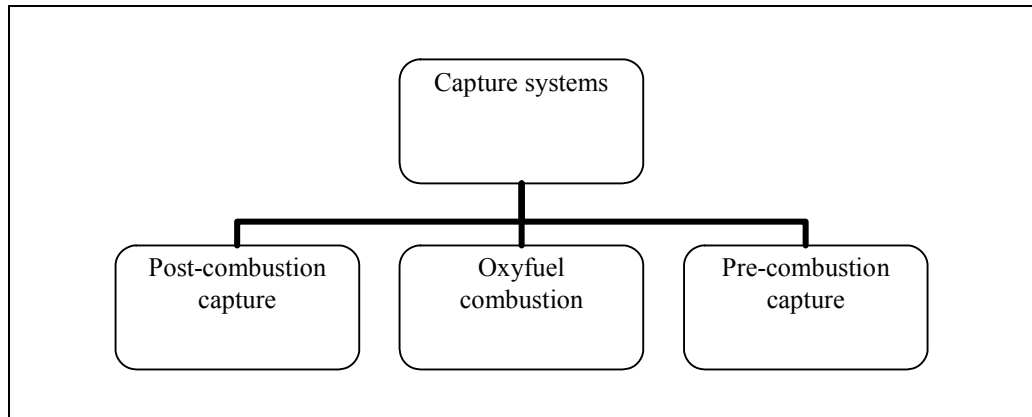


Figure 1-3: World Electricity Generation by Fuel, 2006-2030. Data from [5].

## 1.2 Brief overview of CO<sub>2</sub> capture systems

There are basically three systems for carbon dioxide capture and they are classified as shown in Figure 1-4.



**Figure 1-4: Classification of CO<sub>2</sub> capture systems**

### 1.2.1 Post-combustion capture

Post-combustion capture is a downstream process that is analogous to flue gas desulfurization. It involves the removal of CO<sub>2</sub> from the flue gas produced after the combustion of the fuel. A schematic of post-combustion capture is presented in Figure 1-5.

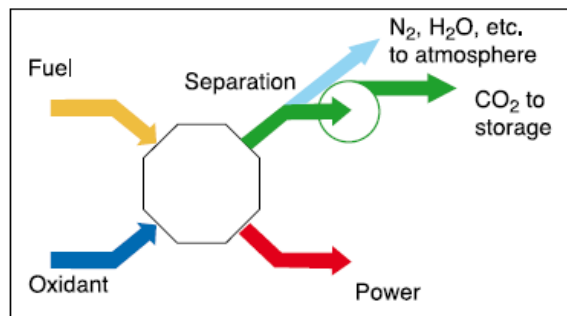


**Figure 1-5: Schematic of post-combustion capture ( Adapted from [2])**

The oxidant used for combustion is typically air and hence, the flue gases are diluted significantly with nitrogen. In addition, since the flue gases are at atmospheric pressure, a large volume of gas has to be treated. Table 1-1 presents the typical CO<sub>2</sub> percentage in the flue gases from different combustion systems.

**Table 1-1: CO<sub>2</sub> partial pressure in flue gases of different combustion systems. (Data taken from [2])**

<b>Flue gas source</b>	<b>CO<sub>2</sub> concentration, % vol (dry)</b>	<b>Pressure of gas stream, MPa</b>	<b>CO<sub>2</sub> partial pressure, MPa</b>
<b>Natural gas fired boilers</b>	7-10	0.1	0.007-0.01
<b>Gas turbines</b>	3-4	0.1	0.003-0.004
<b>Oil fired boilers</b>	11-13	0.1	0.011-0.013
<b>Coal fired boilers</b>	12-14	0.1	0.012-0.014
<b>IGCC after combustion</b>	12-14	0.1	0.012-0.014
<b>IGCC synthesis gas after gasification</b>	8-20	2-7	0.16-1.4 (before shift)

A number of methods exist for the post-combustion capture of CO<sub>2</sub> from flue gases. These include:

- Chemical absorption
- Physical absorptions
- Membrane separation
- Adsorption
- Cryogenic separation

### **1.2.1.1 Chemical absorption**

Chemical absorption systems at present are the preferred option for post-combustion capture of CO<sub>2</sub>. Chemical absorption systems have been in use since the 1930s for the

capture of CO<sub>2</sub> from ammonia plants for use in food applications and hence, are a commercially realized technology, though not at the scale required for power plants.

CO<sub>2</sub> is separated from the flue gas by passing the flue gas through a continuous scrubbing system. The system consists of an absorber and a desorber. Absorption processes utilize the reversible chemical reaction of CO<sub>2</sub> with an aqueous alkaline solvent, usually an amine. In the desorber, the absorbed CO<sub>2</sub> is stripped from the solution and a pure stream of CO<sub>2</sub> is sent for compression while the regenerated solvent is sent back to the absorber. The process of chemical absorption with different solvents is discussed in detail in the later chapters of this thesis. Heat is required in the reboiler to heat up the solvent to the required temperature; to provide the heat of desorption and to produce steam in order to establish the required driving force for CO<sub>2</sub> stripping from the solvent. This leads to the main energy penalty on the power plant. In addition, energy is required to compress the CO<sub>2</sub> to the conditions needed for storage and to operate the pumps and blowers in the process.

A discussion of physical absorption, membrane separation and adsorption is presented in Appendix A.

### **1.2.2 Oxyfuel combustion**

The main disadvantage of post-combustion capture systems is the dilution of the flue gases due to nitrogen. This problem can be mitigated if the combustion is carried out in the presence of oxygen instead of air. The burning of fossil fuel in an atmosphere of oxygen leads to excessively high temperatures – as high as 3500°C. The temperature is moderated to a level that the material of construction can withstand by recycling a fraction of the exhaust flue gases. Figure 1-6 depicts a schematic of oxyfuel combustion.

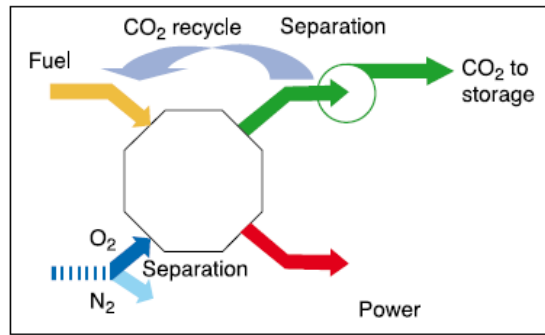


**Figure 1-6: Schematic of oxyfuel combustion. Adapted from [2]**

The flue gas contains mainly CO<sub>2</sub> and water. It may also contain other products of combustion, such as NO<sub>x</sub> and SO<sub>x</sub>, depending on the fuel employed. One of the advantages of oxyfuel combustion is that the formation of NO<sub>x</sub> is lowered since there is negligible amount of nitrogen in the oxidant. Any formation of NO<sub>x</sub> will only arise from the nitrogen in the fuel. However, if the amount of fuel-bound nitrogen is high, the concentration of NO<sub>x</sub> will be very high since it is not diluted by nitrogen. It is necessary that the NO<sub>x</sub> be removed prior to recycle of the flue gas [6]. After condensation of water, the flue gas contains 80-98% CO<sub>2</sub> depending on the type of the fuel used [2]. This is then compressed, dried and sent for storage. The CO<sub>2</sub> capture efficiency is very close to 100% in these systems. It may be necessary to remove acidic gases such as SO<sub>x</sub> and NO<sub>x</sub> if their levels are above those prescribed for CO<sub>2</sub> sequestration. Removal of noble gases such as argon may be necessary depending on the purity of O<sub>2</sub> employed for combustion. Since there is less NO<sub>x</sub>, the partial pressure of SO<sub>x</sub> and HCl are increased leading to an increase in the acid dew point. Hence, it may be necessary to employ dry recycle of CO<sub>2</sub> if the sulfur content of the fuel is high. Since the stream is pure in CO<sub>2</sub> and is directly sequestered, it may be possible to store the SO<sub>2</sub> along with the CO<sub>2</sub> and claim mixed credits for this. This will avoid the need for a flue gas desulfurization unit (FGD). Water however needs to be removed. Complete dehydration of the flue gas will reduce mass flow and prevent corrosion and hydrate precipitation [7].

The main energy penalty in oxyfuel combustion occurs due to the energy intensive separation of oxygen from air in the air separation unit (ASU). Cryogenic separation is employed to obtain an oxygen stream of 95% purity. At this level of purity, only separation of N<sub>2</sub> is needed and the energy requirement is typically around 0.2 kWh/kg O<sub>2</sub>, although some recent improvements may be able to reduce the energy requirement to 0.16 kWh/kg O<sub>2</sub> [8-9]. If the noble gases are removed in the ASU, then there will be less treatment of the flue gases required since the flue gas has to be stripped of the noble gases before storage. However, for energy efficiency of the plant, the production of 95% purity O<sub>2</sub> stream in the ASU has been found to be the optimum. The largest ASU in operation today produces around 5000 tonnes O<sub>2</sub> per day which is suitable for a 300 MWe coal fired boiler with flue gas recycle.

Table 1-2 presents the energy required to generate the amount of oxygen required for combustion of different fuels.

**Table 1-2: Energy requirement to produce O<sub>2</sub> for combustion of different fuels. (Adapted from [10])**

Fuel	Specific CO <sub>2</sub> emission		Oxygen required for combustion			Energy required to generate O <sub>2</sub> (at 0.20 kWh/kg O <sub>2</sub> )
	kg CO <sub>2</sub> /kg fuel	kg CO <sub>2</sub> /MJ fuel (LHV)	kg O <sub>2</sub> /kg CO <sub>2</sub>	kg O <sub>2</sub> /kg fuel	kg O <sub>2</sub> /MJ fuel	
<b>100%C</b>	3.7	0.108	0.726	2.67	0.79	0.145
<b>Hard coal</b>	2.9-3.4	0.09-0.1	0.75-0.92	2.4-3.0	0.076-0.11	0.15-0.184
<b>Lignite</b>	2.3-2.6	0.09-0.1	0.75-0.85	1.3-1.9	0.03-0.04	0.15-0.17
<b>Natural gas</b>	2.1-2.9	0.05-0.06	1.46-1.54	3.1-4.4	0.08-0.095	0.292-0.308

Appendix B presents a discussion of the cycles to integrate oxyfuel combustion with power production. One of the methods is through the use of a boiler and a steam cycle. To achieve this, boiler modifications are required with some redesign of the burner system. The air inleakage needs to be minimized and a recycle line needs to be provided for recycling flue gas to moderate the boiler temperature. In the case of natural gas, oxygen and natural gas can be sent to a gas turbine for combustion and power generation. However, for this to be implemented there needs to be commercialization of a gas turbine operating on CO<sub>2</sub> as the main working fluid.

A feature of oxyfuel combustion systems is that during start-up, air firing may be necessary so that sufficient recycle of the flue gas is established before oxygen firing is initiated. This necessitates the equipment for air firing and additional controls. The control of these systems is not yet well understood. In order, to evaluate the operability and reliability of these systems, large scale demonstration units need to be commissioned.

### **1.2.3 Chemical looping combustion**

Chemical looping combustion (CLC) is an indirect combustion system that avoids the direct contact of fuel with the oxidant. Oxygen is transferred to the fuel via a solid oxygen carrier. The combustion system is split into two reactors. In the reduction reactor (also called the fuel reactor), the fuel reduces the solid oxide material which is then transported to the oxidation reactor where the reduced metal oxide is oxidized with air. A schematic of a CLC system is shown in Figure 1-7.

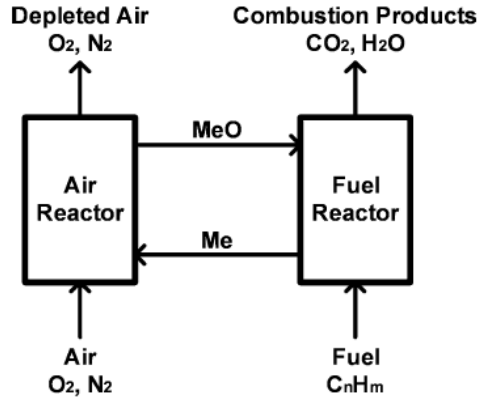
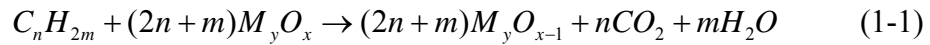


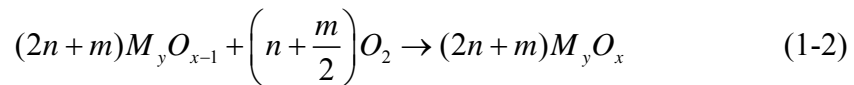
**Figure 1-7: Schematic of chemical looping combustion. Adapted from [11]**

The reaction scheme is shown below:

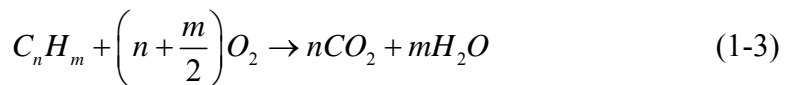
The reduction reaction in the fuel reactor is:



The oxidation reaction in the air reactor is:



The overall reaction is:



The overall reaction (1-3) is the equivalent of the combustion of the fuel. (1-1) is usually endothermic while (1-2) is exothermic. Hence, there needs to be transfer of heat from the oxidation reactor to the fuel reactor through the solid oxide particles. However, when CuO is used as the oxygen carrier, (1-1) is exothermic [12].

The flue gases from the reduction reactor consist mainly of CO<sub>2</sub> and H<sub>2</sub>O and a pure stream of CO<sub>2</sub> can be obtained by condensing the water. The flue gases can be integrated

into the power cycle either via a steam boiler or via a CO<sub>2</sub>/H<sub>2</sub>O turbine. Figure 1-8 shows a schematic of the integration of the CLC system with the power cycle.

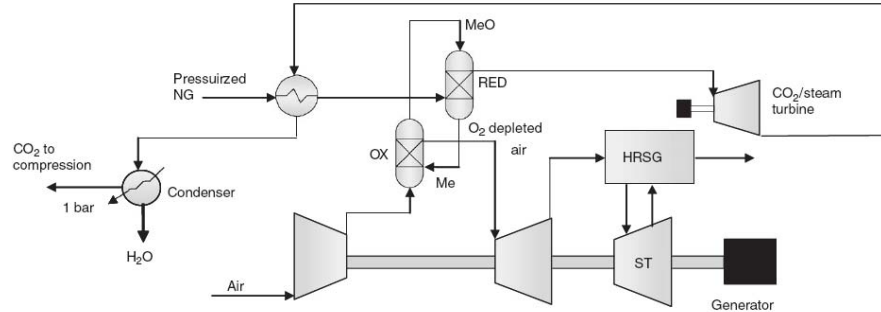


**Figure 1-8: Schematic of chemical looping combustion system integrated with a power cycle. Adapted from [13].**

The oxygen depleted air in the oxidation reactor contains sensible heat due to the exothermic oxidation reaction. This stream is also integrated into the power cycle.

Appendix C presents more details on chemical looping combustion and reforming.

## 1.2.4 Precombustion capture

In precombustion capture, the carbon content of the fuel is reduced prior to combustion, so that upon combustion, a stream of pure CO<sub>2</sub> is produced. Precombustion decarbonization can be used to produce hydrogen or generate electricity or both. Figure 1-9 presents a schematic of precombustion decarbonization [2].

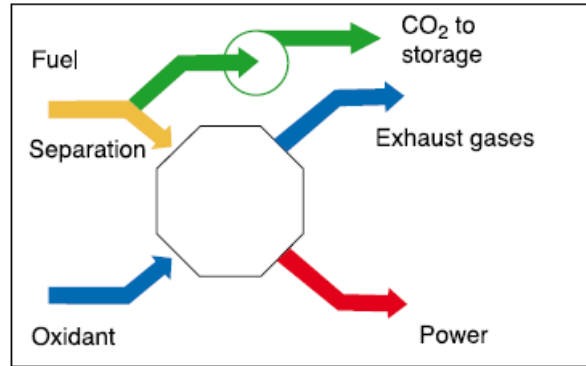
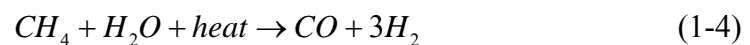


**Figure 1-9: Schematic of precombustion decarbonization. Adapted from [2]**

A synthesis gas is produced in the first step of precombustion decarbonization. If natural gas is used as a fuel, this is obtained by either steam reforming or autothermal reforming. If coal is used as the fuel, synthesis gas is obtained by gasification. In the next step, the synthesis gas is subjected to the water gas shift reaction to produce carbon dioxide and hydrogen. The hydrogen and carbon dioxide can be separated by pressure swing adsorption or physical absorption and the pure CO<sub>2</sub> stream is compressed and sent for storage. When pressure swing adsorption is used to produce a pure stream of CO<sub>2</sub> and another pure stream of H<sub>2</sub>, an additional step is needed for CO<sub>2</sub> purification before the H<sub>2</sub> purification. The hydrogen stream is either used as a feedstock for a chemical process or is burnt to produce electricity.

#### 1.2.4.1 Steam reforming

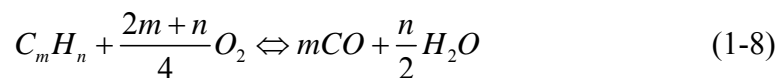
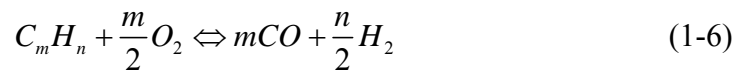
Natural gas can be steam reformed and then subjected to water gas shift reaction to produce a mixture consisting mainly of carbon dioxide and hydrogen. The reactions in steam reforming are outlined below:



Steam reforming is endothermic and hence, some of the natural gas has to be used for firing in the reformer furnace to provide the heat required for the reforming reaction. This can lead to significant exergy losses in the process. Since there is a more concentrated stream of CO<sub>2</sub> available, the energy penalty for absorption is not as high. The CO<sub>2</sub> can also be separated by pressure swing adsorption. However, the water gas shift reaction also requires steam to be withdrawn from the power cycle. Hence, this process is advantageous only if the energy savings made from capturing a purer stream of CO<sub>2</sub> are greater than the exergy losses due to loss of natural gas used for firing and loss of steam from the steam cycle for the shift reaction. If a CO<sub>2</sub> free process is desired, it is necessary to use the produced hydrogen for firing in the reformer, and this would lead to even higher exergy losses. The PSA offgas can be used for firing in the reformer with the natural gas or hydrogen.

#### 1.2.4.2 Autothermal reforming

Autothermal reforming is a combination of steam reforming and partial oxidation. Since the partial oxidation reaction is exothermic, it provides the energy required for the endothermic steam reforming and only minimal firing of additional natural gas as fuel is required. The reactions in autothermal reforming are given below. The autothermal reforming is the third reaction - (1-8)- and it is the sum of the first two reactions - (1-6) and(1-7).



A cycle integrating reforming with the power cycle is shown in Figure 1-10.

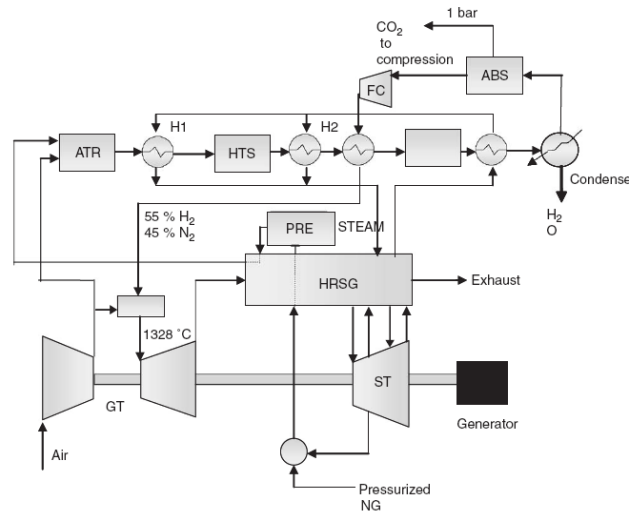


**Figure 1-10: Flowsheet of autothermal reforming process. Adapted from [13]**

After reforming and water gas shift reaction, the carbon dioxide is separated from the hydrogen and the nitrogen by absorption or by PSA. The hydrogen and nitrogen are then sent to a gas turbine for firing. Modern gas turbines with the low  $\text{NO}_x$  design cannot accommodate a fuel with hydrogen percentage much higher than 50%. Autothermal reforming rather than steam reforming provides a fuel which can meet this specification.

The main exergy loss in this scenario as compared to the conventional CC is due to the loss in the fuel heating value. It is expected that 20-25% of the energy of the fuel is dissipated irreversibly in the conversion of natural gas to hydrogen [14]. Methane is not completely reformed in the reformer. A typical conversion is 90% [8]. Some of the fuel has to be used for supplementary firing in the steam generator and some steam is also consumed in the water gas shift reaction. The gas from the reformer has to be compressed before it goes to the gas turbine and this leads to losses as well.

In this process, the capture of  $\text{CO}_2$  takes place at the same pressure as in the turbine. Hence, the stripping does not consume too much energy because of the pressure differential between the absorber and the stripper. When a lower pressure in the stripper is used, there is enough heat available from the cooling of the products from the water

gas shift reactor for the stripping process [8]. An optimization can be performed by not fully releasing the pressure in the stripper, thus saving on compression costs of CO<sub>2</sub> in the end.

A fuel containing more than 50% hydrogen may not be very well suited for a gas turbine with modern low NO<sub>x</sub> combustors. Hence, combustion issues need to be addressed. This is one of the major developmental issues before this technology can be demonstrated at a large scale.

### 1.2.4.3 Integrated Gasification Combined Cycle (IGCC)

If coal is to be integrated into a gas turbine cycle, it is necessary that it first be gasified to produce coal gas that can be combusted in a gas turbine. If CO<sub>2</sub> capture is desired, it is preferable to use O<sub>2</sub> blown systems at high pressures since this leads to higher CO<sub>2</sub> partial pressures. A flowsheet of an IGCC process with CO<sub>2</sub> capture is shown in Figure 1-11.

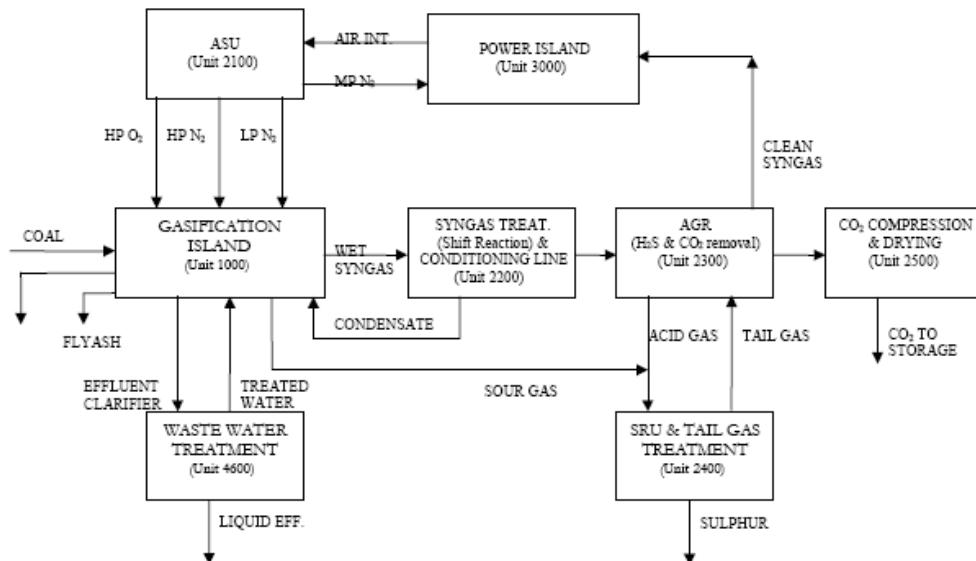


Figure 1-11: Block diagram of IGCC power plant. Adapted from [15]

The gasifier output contains syngas, CO<sub>2</sub> and impurities such as N<sub>2</sub>, H<sub>2</sub>S, COS, HCN, NH<sub>3</sub> and trace amounts of Hg which must be treated appropriately [2]. The syngas is

treated for removal of ash and particulates and then subjected to water gas shift to produce carbon dioxide and hydrogen. There will also be contamination due to H<sub>2</sub>S. This is treated and the gas is then sent for CO<sub>2</sub> capture. Since the CO<sub>2</sub> is at a relatively high pressure, it can be easily captured by a physical absorption process which is less energy intensive. Usually, H<sub>2</sub>S is removed in one physical absorption unit followed by recovery of CO<sub>2</sub> in the next one [16]. The recovered H<sub>2</sub>S is then sent to a Claus plant for reduction to elemental sulfur and tail gas clean-up. Recovered CO<sub>2</sub> is compressed and sent for storage. Hydrogen is then sent for combustion in the gas turbine and for power generation. In addition, power is generated from the steam cycle that utilizes the steam obtained from syngas cooling.

Sour gas shift is preferred to clean gas shift as far as exergy considerations are concerned due to the loss of steam in the gas cleanup process. This steam is utilized in the shift reaction. There can be some degree of integration between the ASU and the gas turbine with the ASU being fed by the exhaust from the gas turbine and the ASU supplying medium pressure N<sub>2</sub> to the gas turbine [15]. However, this may lead to problems in the startup of the plant. In addition, the gas turbine has to run only on hydrogen as the fuel. Such a gas turbine is not yet fully developed. GE supplies gas turbines where the maximum percentage of hydrogen should not exceed 65% [17]. This means that some amount of CO has to be left in the fuel entering the gas turbine limiting the maximum degree of capture to 85%. The hydrogen will be diluted with N<sub>2</sub> by-product from the ASU.

IGCC is a significantly more expensive technology than pulverized combustion for power generation because of all the capital costs involved. The performance however varies with the coal type. IGCC does not have the impetus for development due to the competition from efficient NGCC plants when the natural gas prices are stable. However, IGCC offers us a way to obtain electricity and syngas – an essential building block for the chemical industry – from coal. Due to the complexity of the system, IGCC plants are yet to demonstrate sufficient availability [6]. An IGCC plant incorporating CO<sub>2</sub> capture is yet to be demonstrated however [18].

### **1.3 Current status of CO<sub>2</sub> capture technology**

While there are a number of possible routes for carbon dioxide capture from power plants, a number of them are still in the developmental stage. All these technologies need to be evaluated when choosing the best one to incorporate in a power plant to be built in the future. However, the only immediately realizable capture technology for flue gases from power plants appears to be chemical absorption.

It is expected that in the near future, if oxyfuel combustion is employed, it will only be in a power boiler with an integrated steam cycle. A conceptual process flowsheet for a pulverized coal steam boiler operating on a supercritical steam cycle with CO<sub>2</sub> capture has been developed [19]. It has been found that the overall thermal efficiency on a LHV basis is reduced from 44.2% to 35.4%. For oxyfuel combustion to be incorporated, some modifications to the burner design are required. In addition, lines for recirculation of the CO<sub>2</sub> need to be provided. One of the other challenges is the lower purity of CO<sub>2</sub> produced in oxyfuel combustion. For the production of ultra-pure CO<sub>2</sub> (matching that produced in an amine absorption process), additional distillation steps would have to be added after the inert gas removal steps [20]. In order to understand the issues associated with the operability, startup and shutdown of these systems, demonstration plants employing oxyfuel combustion in boilers have to be commissioned. Recently, Vattenfall commissioned a 30MWth pilot plant facility for a detailed testing of the oxyfuel firing facility [21]. Design of new plants operating on a supercritical steam cycle can be considered since these plants inherently have a higher efficiency. For oxyfuel combustion to be incorporated in gas turbines, it is necessary that the technical and operational feasibility of turbines capable of operating on CO<sub>2</sub> as the main working fluid be demonstrated. A critical technology that needs to be improved for oxyfuel combustion to be more efficient is the air separation unit. Current cryogenic air separation plants are showing improvement in efficiency due to improved compressor efficiencies and larger scale plants [2]. It is necessary to optimize this further. Ion transport membranes which may offer more efficient separation of O<sub>2</sub> from air are presently under development [22].

Chemical looping combustion systems are a relatively new technology and are still in the development and pilot plant stage. In chemical looping systems, the research focus needs to be on developing better attrition resistant metal oxide carriers which have other desirable characteristics such as high rate of reaction. The thermal stability of these particles needs to be enhanced and their integrity in pressurized environments needs to be preserved if chemical looping systems are to be integrated efficiently with gas turbine power generation cycles. In addition, the compatibility of chemical looping systems with coal needs to be explored.

Gasification systems represent an attractive option since they allow us to obtain syngas and electricity from coal. However, the capital cost of the equipment is very high. The complexity of the system makes it difficult to operate and hence, the availability of these systems cannot be guaranteed. To date, there have been only a handful of demonstration power projects using IGCC. There is scope for more development work on gas turbines with low NO<sub>x</sub> combustors utilizing fuels containing more than 50% hydrogen. In addition, IGCC power plants with carbon capture are yet to be demonstrated. Producing hydrogen from natural gas for electricity production leads to a loss of around 20-25% of the fuel heating value. A point to be noted is that for coal to be integrated into a combined cycle, it is necessary to gasify it. However, this is not the case for gas. Hence, any technology employing gasification of natural gas for the purpose of carbon capture will appear to have an even more pronounced energy penalty. Hence, gasification of coal to produce electricity is the more feasible option. Full-scale implantation of coal gasification plants incorporating carbon dioxide capture is expected only in the medium to long time frame.

Chemical absorption systems seem to represent the best near-term option for CO<sub>2</sub> capture from power plants. There is commercial experience with operating these systems, albeit at a much smaller scale than required for power plants. A list of commercially available technologies for chemical absorption of CO<sub>2</sub> is presented in Table 1-3. In addition, HTC Purenergy and Aker Clean Carrbonin Norway have offered commercial packages with HTC Purenergy's process being based on mixed amines [23].

**Table 1-3: Amine scrubbing technology. Data from [23-24]**

<b>Process</b>	<b>Solvent</b>	<b>Source of CO<sub>2</sub></b>	<b>Commercial experience</b>
<b>Fluor (Econamine<sup>TM</sup> FG Plus)</b>	30 wt% aqueous MEA solution	Natural gas	Largest capacity of 330 tonnes/day CO <sub>2</sub> . Many plants operating worldwide for food applications
<b>KEPCO/MHI KS-1 process</b>	KS-1	Natural gas	Four commercial plants with four more under construction
<b>Cansolv process</b>	Tertiary amine with promoter	Coal and natural gas	One demonstration plant with coal and one with natural gas

During the oil price shock in the 1970s CO<sub>2</sub> capture was utilized in order to produce CO<sub>2</sub> for enhanced oil recovery applications. Once the oil prices stabilized, these capture plants were shut down. All the components of the system are well understood since acid gas scrubbing has been practiced in the industry for some time. There is no component of the system that is in the development stage. While new solvents are under investigation, existing solvents are already in use in commercial applications as can be seen from Table 1-3. The systems integration of the capture unit with the power plant needs to be studied in more detail. Chemical absorption is a downstream process and is very similar to flue gas desulfurization and other end of the pipeline solutions. A pilot plant has been set up as part of the CASTOR project at the Esbjerg Power Station operated by Esram in Denmark [25]. This unit is designed to capture 1 tonne CO<sub>2</sub> / hour. The hands on experience gained from this trial will help in gaining a better understanding of the technology. In addition, other demonstration projects such as the collaboration between Alstom and AEP in West Virginia are already underway [26]. The plant operates with the

chilled ammonia solvent and operation of the CO<sub>2</sub> capture system has commenced recently.

From a review of the literature on carbon dioxide technologies, it was concluded that scrubbing of CO<sub>2</sub> by chemical absorption represents the only immediately realizable option for CO<sub>2</sub> capture. The other systems are in the development stage and demonstration projects need to be commissioned before they can be implemented on a large scale. The technology for chemical absorption however is available and has been practiced in the industry. In order to employ it on the scale required for CO<sub>2</sub> capture, there needs to be development and identification of optimal solvents for absorption. To minimize the energy penalty of capture, the capture system needs to be well integrated with the power plant.

## **1.4 Solvent systems for chemical absorption**

An entropy of mixing approach was used to calculate the minimum work required for CO<sub>2</sub> capture. The minimum work for 90% CO<sub>2</sub> capture was calculated to be 0.001998 kWh/gmol CO<sub>2</sub>. The minimum work of compression for compressing the CO<sub>2</sub> to 110 bar is calculated to be 0.002677 kWh/gmol CO<sub>2</sub>. The calculation is shown in Appendix D. For a ultra supercritical coal-fired power plant, this represents a 8% decrease in efficiency of the power plant. Studies have shown that in actual applications, the efficiency loss from a power plant for CO<sub>2</sub> capture and compression to 150 bar, can range from 20 to 30% [27]. The reason for this difference between the actual energy loss and the ideal work loss is sought to be understood.

A number of solvent systems have been proposed and studied for CO<sub>2</sub> capture by chemical absorption. MEA has been the most widely studied system with a number of researchers developing flowsheet models to study its performance [28-31]. Other amines that have been studied include tertiary amines such as MDEA [32-35]. Sterically hindered amines such as AMP have also been investigated [36-41]. The performance of hindered amines was found to be better suited to absorption in higher CO<sub>2</sub> partial

pressure atmospheres ( 8-15% CO<sub>2</sub>) [38]. Mixed amine blends are designed to take advantage of the desirable properties in primary and tertiary amines. It is desired that these have the high capacity and low heat of absorption characteristic of tertiary amines and the fast rate of reaction characteristic of primary amines. This will lead to reduced circulation rates of the solvent and yield a lower heat duty in the stripper [34]. Particular interest has been focused on MEA/MDEA and MEA/AMP blends with pilot plant studies having been conducted [34, 42]. Investigation on DGA/MDEA blends has also been conducted [43]. Other systems that have been proposed include the potassium carbonate system [44-45] and using ammonia as a solvent for CO<sub>2</sub> capture [46-48].

While a number of different systems have been proposed and investigated, very few studies which compare the performance of different systems on a consistent basis have been performed. In addition, it was found that not many studies focused on incorporating the appropriate thermodynamic and rate models in the model development. Hence, it was decided to make these issues the focus of this thesis.

## 1.5 Thesis objectives

In this thesis, it was decided to investigate the MEA, potassium carbonate and chilled ammonia systems. The reasons for this choice are outlined below for each system:

- **Monoethanolamine (MEA):** MEA is the most widely-studied solvent for CO<sub>2</sub> capture and is the system for which abundant experimental data is available. It was hence decided to investigate MEA as the base system in this thesis and use it to validate the modeling methodologies. This would also facilitate a comparison of performance of different solvent systems.
- **Potassium carbonate:** Potassium carbonate was chosen as a system for utilization in high pressure CO<sub>2</sub> capture applications, particularly in Integrated Reforming Combined Cycle (IRCC). Potassium carbonate operates on a pressure swing absorption-desorption cycle as compared to MEA which operates on a temperature

swing absorption-desorption cycle. Hence, different modeling issues would have to be dealt with in this system.

- **Chilled ammonia:** The chilled ammonia system was evaluated since it has potential for direct application in post-combustion capture of CO<sub>2</sub> from power plants as well as in retrofitting of power plants and hence, would serve as a good comparison with the MEA system. In addition, since the chilled ammonia system has a desorber that operates at a high pressure, it allowed us to study the interplay between the energy required for regeneration of solvent and for CO<sub>2</sub> compression.

The main objectives of the thesis are as follows:

1. **Develop consistent flowsheet models in ASPEN Plus for each system:** The first objective of the thesis is to develop detailed flowsheet models in ASPEN Plus for each solvent system. It is necessary that each model have the accurate representation of physical properties, thermodynamics, thermochemistry and kinetics of the system. It is also necessary that the different flowsheet models be consistent with each other in terms of the input and outlet conditions utilized so that a consistent comparison of the performance of different solvent systems can be facilitated. The developed flowsheet models can then be utilized in future analysis for energy integration, costing, etc.
2. **Develop detailed rate-based models and understand the parameters that affect the performance of the system:** For each solvent system, it is desired to investigate and understand which parameters (e.g.: temperature, pressure, concentration, hydrodynamics) affect the performance of the system. Once this is done, the different parameters can be optimized in order to improve the overall performance of each solvent system. Another objective is to design rate-based simulations so that the effect of column hydrodynamics and the size of the equipment can be studied.

- 3. Identify possibilities for energy recuperation in the system:** In order to reduce the energy penalty of CO<sub>2</sub> capture, it is necessary to explore the potential for energy integration between the power plant and the capture system. The third objective of this thesis is to investigate different flowsheet configurations and modifications that will enable energy recuperation in the capture system.

## 1.6 Thesis Overview

Chapter 1 of this thesis introduces the concept of carbon capture and sequestration and motivates the need for a closer study of CO<sub>2</sub> capture by chemical absorption. In Chapter 2, a discussion of the thermodynamic and rate models utilized in this thesis is presented. The results from the three systems – MEA, potassium carbonate and chilled ammonia – are presented in Chapters 3, 4 and 5 respectively. Chapter 6 details the overall conclusions from the thesis and discusses further direction in which this study can be carried forth. Chapter 7 presents the capstone project where the effect of different types of environmental regulations on technology innovation, diffusion and adoption is discussed through case studies on the lead phasedown in gasoline, chlorofluorocarbons reduction in the US and the reduction in SO<sub>2</sub> emissions from power plants in the US. Appendix A describes post combustion capture systems besides chemical absorption; Appendix B discussed the oxyfuel integration cycles; Appendix C details chemical looping combustion and reforming and Appendix D presents the calculation of minimum work of separation and compression.

## 1.7 References

1. Goddard Institute of Space Studies NASA. 2009 [cited 2009 November 12]; Available from: <http://data.giss.nasa.gov/gistemp/graphs/Fig.A2.txt>.
2. IPCC, *IPCC Special Report on Carbon Dioxide Capture and Storage*, B. Metz, et al., Editors. 2005.
3. Earth System Research Laboratory Global Monitoring Division. 2009 [cited 2009 November 12]; Available from: [ftp://ftp.cmdl.noaa.gov/ccg/co2/trends/co2\\_mm\\_mlo.txt](ftp://ftp.cmdl.noaa.gov/ccg/co2/trends/co2_mm_mlo.txt).
4. Energy Information Administration, *Electric Power Annual 2007: A Summary*. 2009: Washington, D.C.
5. Energy Information Administration, *International Energy Outlook*. 2009: Washington, D.C.
6. Clarke, D.e.a., *CO<sub>2</sub> Capture and Storage - A VGB Report on the State of the Art*. 2004.
7. Andersson, K. and F. Johnsson, *Process evaluation of an 865 MWe lignite fired O<sub>2</sub>/CO<sub>2</sub> power plant*. *Energy Conversion and Management*, 2006. **47**(18-19): p. 3487-3498.
8. Bolland, O. and H. Undrum, *A novel methodology for comparing CO<sub>2</sub> capture options for natural gas-fired combined cycle plants*. *Advances in Environmental Research*, 2003. **7**(4): p. 901-911.
9. Darde, A., R. Prabhakar, J.-P. Tranier, and N. Perrin, *Air separation and flue gas compression and purification units for oxy-coal combustion systems*. *Energy Procedia*, 2009. **1**(1): p. 527-534.
10. Göttlicher, G., *The Energetics of Carbon Dioxide Capture in Power Plants*. 2004, NETL Report.
11. Ryden, M. and A. Lyngfelt, *Using steam reforming to produce hydrogen with carbon dioxide capture by chemical-looping combustion*. *International Journal of Hydrogen Energy*, 2006. **31**(10): p. 1271-1283.
12. Ryden, M., A. Lyngfelt, and T. Mattisson, *Synthesis gas generation by chemical-looping reforming in a continuously operating laboratory reactor*. *Fuel*, 2006. **85**(12-13): p. 1631-1641.

13. Kvamsdal, H.M., K. Jordal, and O. Bolland, *A quantitative comparison of gas turbine cycles with CO<sub>2</sub> capture*. Energy. **In Press, Corrected Proof**.
14. Corradetti, A. and U. Desideri, *Analysis of gas-steam combined cycles with natural gas reforming and CO<sub>2</sub> capture*. Journal of Engineering for Gas Turbines and Power-Transactions of the Asme, 2005. **127**(3): p. 545-552.
15. Davison, J., Bressan, L. and Domenichini, R. *CO<sub>2</sub> capture in coal-based IGCC power plants*. in *Seventh International Conference on Greenhouse Gas Control Technologies*. 2004. Vancouver, Canada.
16. Pruschek, R., G. Oeljeklaus, V. Brand, G. Haupt, G. Zimmermann, and J.S. Ribberink, *Combined-Cycle Power-Plant with Integrated Coal-Gasification, CO Shift and CO<sub>2</sub> Washing*. Energy Conversion and Management, 1995. **36**(6-9): p. 797-800.
17. Maurstad, O., *An overview of coal based Integrated Gasification Combined Cycle (IGCC) technology*. 2005, MIT LFEED: Cambridge, MA. p. 43.
18. Ordorica-Garcia, G., P. Douglas, E. Croiset, and L.G. Zheng, *Technoeconomic evaluation of IGCC power plants for CO<sub>2</sub> avoidance*. Energy Conversion and Management, 2006. **47**(15-16): p. 2250-2259.
19. Dillon, D.J., Panesar, R.S., Wall, R.A., Allam, R.J., White, V., Gibbons, J., and Haines, M.R., *Oxy-Combustion Processes for CO<sub>2</sub> Capture From Advanced Supercritical PF and NGCC Power Plant*, in *7th International Conference on Greenhouse Gas Control Technologies*. 2004: Vancouver, Canada.
20. Wilkinson, M.B., J.C. Boden, T. Gilmartin, C. Ward, D.A. Cross, R.J. Allam, and N.W. Ivens. *CO<sub>2</sub> capture from oil refinery process heaters through oxyfuel combustion*. in *Sixth International Conference on Greenhouse Gas Control Technologies*. 2002. Kyoto, Japan: Elsevier Science Ltd, Oxford UK.
21. Strömberg, L., G. Lindgren, J. Jacoby, R. Giering, M. Anheden, U. Burchhardt, H. Altmann, F. Kluger, and G.-N. Stamatelopoulos, *Update on Vattenfall's 30 MWth oxyfuel pilot plant in Schwarze Pumpe*. Energy Procedia, 2009. **1**(1): p. 581-589.
22. Dyer, P.N., R.E. Richards, S.L. Russek, and D.M. Taylor, *Ion transport membrane technology for oxygen separation and syngas production*. Solid State Ionics, 2000. **134**(1-2): p. 21-33.
23. Herzog, H., J. Meldon, and A. Hatton, *Advanced Post-Combustion CO<sub>2</sub> Capture*. 2009.

24. Steeneveldt, R., B. Berger, and T.A. Torp, *CO<sub>2</sub> capture and storage - Closing the knowing-doing gap*. Chemical Engineering Research & Design, 2006. **84**(A9): p. 739-763.
25. Le Thiez, P., G. Mosditchian, T. Torp, P. Feron, I. Ritesma, P. Zweigel, and E. Lindberg. *An innovative European integrated project: CASTOR - CO<sub>2</sub> from capture to storage*. in *Seventh International Conference on Greenhouse Gas Control Technologies*. 2004. Vancouver, Canada.
26. Wald, M., L., *Refitted to Bury Emissions, Plant Draws Attention in The New York Times*. 2009: New York.
27. Rochelle, G.T., *Amine Scrubbing for CO<sub>2</sub> Capture*. Science, 2009. **325**(5948): p. 1652-1654.
28. Singh, D., E. Croiset, P.L. Douglas, and M.A. Douglas, *Techno-economic study of CO<sub>2</sub> capture from an existing coal-fired power plant: MEA scrubbing vs. O<sub>2</sub>/CO<sub>2</sub> recycle combustion*. Energy Conversion and Management, 2003. **44**(19): p. 3073-3091.
29. Abu-Zahra, M.R.M., L.H.J. Schneiders, J.P.M. Niederer, P.H.M. Feron, and G.F. Versteeg, *CO<sub>2</sub> capture from power plants: Part I. A parametric study of the technical performance based on monoethanolamine*. International Journal of Greenhouse Gas Control, 2007. **1**(1): p. 37-46.
30. Freguia, S., *Modeling of CO<sub>2</sub> Removal from Flue Gases with Monoethanolamine*, in *Chemical Engineering*. 2002, University of Texas at Austin: Austin.
31. Alie, C., L. Backham, E. Croiset, and P.L. Douglas, *Simulation of CO<sub>2</sub> capture using MEA scrubbing: a flowsheet decomposition method*. Energy Conversion and Management, 2005. **46**(3): p. 475-487.
32. Lu, J.G., L.J. Wang, X.Y. Sun, J.S. Li, and X.D. Liu, *Absorption of CO<sub>2</sub> into aqueous solutions of methyldiethanolamine and activated methyldiethanolamine from a gas mixture in a hollow fiber contactor*. Industrial & Engineering Chemistry Research, 2005. **44**(24): p. 9230-9238.
33. McCann, N., M. Maeder, and M. Attalla, *Simulation of enthalpy and capacity of CO<sub>2</sub> absorption by aqueous amine systems*. Industrial & Engineering Chemistry Research, 2008. **47**(6): p. 2002-2009.
34. Idem, R., M. Wilson, P. Tontiwachwuthikul, A. Chakma, A. Veawab, A. Aroonwilas, and D. Gelowitz, *Pilot plant studies of the CO<sub>2</sub> capture performance of aqueous MEA and mixed MEA/MDEA solvents at the University of Regina CO<sub>2</sub> capture technology development plant and the Boundary Dam CO<sub>2</sub> capture*

- demonstration*. Industrial & Engineering Chemistry Research, 2006. **45**(8): p. 2414-2420.
35. Sakwattanapong, R., A. Aroonwilas, and A. Veawab, *Behavior of reboiler heat duty for CO<sub>2</sub> capture plants using regenerable single and blended alkanolamines*. Industrial & Engineering Chemistry Research, 2005. **44**(12): p. 4465-4473.
  36. Bosch, H., G.F. Versteeg, and W.P.M. Van Swaaij, *Kinetics of the reaction of CO<sub>2</sub> with the sterically hindered amine 2-Amino-2-methylpropanol at 298 K*. Chemical Engineering Science, 1990. **45**(5): p. 1167-1173.
  37. Sartori, G. and D.W. Savage, *Sterically hindered amines for carbon dioxide removal from gases*. Industrial & Engineering Chemistry Fundamentals, 2002. **22**(2): p. 239-249.
  38. Hook, R.J., *An Investigation of Some Sterically Hindered Amines as Potential Carbon Dioxide Scrubbing Compounds*. Industrial & Engineering Chemistry Research, 1997. **36**(5): p. 1779-1790.
  39. Alper, E., *Reaction mechanism and kinetics of aqueous solutions of 2-amino-2-methyl-1-propanol and carbon dioxide*. Industrial & Engineering Chemistry Research, 2002. **29**(8): p. 1725-1728.
  40. Yih, S.M. and K.P. Shen, *Kinetics of carbon dioxide reaction with sterically hindered 2-amino-2-methyl-1-propanol aqueous solutions*. Industrial & Engineering Chemistry Research, 2002. **27**(12): p. 2237-2241.
  41. Xu, S., Y.-W. Wang, F.D. Otto, and A.E. Mather, *Kinetics of the reaction of carbon dioxide with 2-amino-2-methyl-1-propanol solutions*. Chemical Engineering Science, 1996. **51**(6): p. 841-850.
  42. Aroonwilas, A. and A. Veawab, *Characterization and comparison of the CO<sub>2</sub> absorption performance into single and blended alkanolamines in a packed column*. Industrial & Engineering Chemistry Research, 2004. **43**(9): p. 2228-2237.
  43. Pacheco, M.A., *Mass transfer, kinetics and rate-based modelling of reactive absorption*, in *Chemical Engineering*. 1998, University of Texas, Austin: Austin.
  44. Benson, H.E., J.H. Field, and W.P. Haynes, *Improved process for CO<sub>2</sub> absorption used hot carbonate solutions*. Chemical Engineering Progress, 1956. **52**(10): p. 433-439.
  45. Tosh, J.S., J.H. Field, H.E. Benson, and W.P. Haynes, *Equilibrium Study of the System Potassium Carbonate, Potassium Bicarbonate, Carbon Dioxide, and Water*, U.S.B.o. Mines, Editor. 1959. p. 5484.

46. Bai, H.L. and A.C. Yeh, *Removal of CO<sub>2</sub> greenhouse gas by ammonia scrubbing*. Industrial & Engineering Chemistry Research, 1997. **36**(6): p. 2490-2493.
47. Yeh, A.C. and H.L. Bai, *Comparison of ammonia and monoethanolamine solvents to reduce CO<sub>2</sub> greenhouse gas emissions*. Science of the Total Environment, 1999. **228**(2-3): p. 121-133.
48. Yeh, J.T., K.P. Resnik, K. Rygle, and H.W. Pennline, *Semi-batch absorption and regeneration studies for CO<sub>2</sub> capture by aqueous ammonia*. Fuel Processing Technology, 2005. **86**(14-15): p. 1533-1546.

## Chapter 2

### ASPEN Thermodynamic and Rate Models

In this chapter, the thermodynamic and rate models that have been utilized in ASPEN Plus for modeling the systems are discussed.

#### 2.1 Electrolyte NRTL model

The Electrolyte NRTL model is the property model that is used to represent the CO<sub>2</sub> capture system in ASPEN. The ‘*ELECNRTL*’ model in ASPEN can handle a range of concentrations as well as aqueous and mixed solvents. In this section, the details of the Electrolyte NRTL model are elucidated.

The Electrolyte NRTL model was first proposed by Chen et al. [1-2] and then extended by Chen and Mock [3-4]. It is a model for the excess Gibbs free energy of an electrolytic solution. A summary of previous attempts to model the VLE of electrolyte systems is presented in Augsten et al. [5]. The Electrolyte NRTL model assumes that the excess Gibbs free energy in the electrolyte system is the sum of two contributions [2-3, 5]:

1. Short-range forces between all the species that includes the local ion-molecule, ion-ion, and molecule-molecule interactions.
2. Long-range electrostatic ion-ion interactions

The Electrolyte NRTL model is based on two fundamental assumptions [2]:

1. **Like-ion repulsion assumption:** Due to the large repulsive forces between ions of the same charge, it is assumed that the local composition of cations around cations and anions around anions is zero.
2. **Local electroneutrality assumption:** It is assumed that the distribution of cations and anions around a central solvent molecule is such that the net local ionic charge is zero.

Thus, the expression for the excess Gibbs free energy as calculated by the Electrolyte NRTL model can be expressed as:

$$g^{ex*} = g^{ex*,LR} + g^{ex*,local} \quad (2-1)$$

Where:

$g^{ex*}$  is the molar excess Gibbs free energy

$g^{ex*,LR}$  is the molar excess Gibbs free energy contribution from long range forces

$g^{ex*,local}$  is the molal excess Gibbs free energy contribution from local forces

The long range contributions are represented as a combination of the Pitzer-Debye-Hucel contribution [6] and the Born expression [7]. The local interaction contribution is derived as per the NRTL model.

### 2.1.1 Long range contribution

In the Electrolyte NRTL model, the Pitzer-Debye-Huckel formula [6] is used to model the contribution to molar excess Gibbs free energy from long-range interaction forces [5]. The long-range interaction contribution is given by (2-2).

$$g_{PDH}^{ex*} = -RT \left( \sum_k x_k \right) \left( \frac{1000}{M_s} \right)^{1/2} \left( \frac{4A_\phi I_x}{\rho} \right) \ln(1 + \rho I_x^{1/2}) \quad (2-2)$$

Where:

$x_k$  is the liquid-phase mole fraction

$M_s$  is the solvent molecular weight in kg/kmol

$A_\phi$  is the Debye-Huckel parameter

$I_x$  is the ionic strength on a mole fraction basis

$\rho$  is the closest approach parameter.

$$A_\phi = \frac{1}{3} \left( \frac{2\pi N_o d}{1000} \right)^{1/2} \left( \frac{e^2}{D_w k_B T} \right)^{1.5} \quad (2-3)$$

Where:

$N_o$  is the Avogadro's number

$d$  is the solvent density

$e$  is the charge of an electron

$D_w$  is the dielectric constant for water

$k_B$  is the Boltzmann constant

$T$  is temperature in K

$$I_x = 0.5 \sum_k x_k z_k^2 \quad (2-4)$$

Where:

$z_k$  is the charge on species  $k$

In this case, the reference state for ionic species is the ideal dilute state of electrolyte in the mixed solvent [5]. However, the Electrolyte NRTL model defines the reference state

for ionic species to be the ideal dilute state in water. Hence, the Born expression is used to correct for this [7]. The sum of the Pitzer-Debye-Huckel term and Born expression gives the excess Gibbs energy contribution from long-range interactions.

$$g^{ex*,LR} = g_{PDH}^{ex*} + g^{ex*,Born} \quad (2-5)$$

### 2.1.2 Born expression

The Born expression is given by (2-6) [7]:

$$g^{ex*,Born} = RT \left( \frac{e^2}{2k_B T} \right) \left( \frac{1}{D_s} - \frac{1}{D_w} \right) \left( \sum_k \frac{x_k z_k^2}{r_k} \right) 10^{-2} \quad (2-6)$$

Where:

$D_s$  is the dielectric constant of the mixed solvent

$r_k$  is the Born radius of species  $k$

### 2.1.3 Local contribution

The local contribution to the excess Gibbs free energy is modeled with the NRTL model [5, 8] and is given by (2-7) .

$$\begin{aligned}
g^{ex^*,local} = & \left( \sum_m X_m \frac{\sum_j X_j G_{jm} \tau_{jm}}{\sum_k X_k G_{km}} \right) \\
& + \sum_c X_c \sum_{a'} \frac{X_{a'} \sum_j G_{jc,a'} \tau_{jc,a'}}{\left( \sum_{a''} X_{a''} \right) \left( \sum_k X_k G_{kc,a'} \right)} + \dots \\
& + \dots + \sum_a X_a \sum_{c'} \frac{X_{c'} \sum_j G_{ja,c'} \tau_{ja,c'}}{\left( \sum_{c''} X_{c''} \right) \left( \sum_k X_k G_{ka,c'} \right)}
\end{aligned} \tag{2-7}$$

with

$$G_{cm} = \frac{\sum_a X_a G_{ca,m}}{\sum_{a'} X_{a'}} \tag{2-8}$$

$$G_{am} = \frac{\sum_c X_c G_{ca,m}}{\sum_{c'} X_{c'}} \tag{2-9}$$

$$\alpha_{cm} = \frac{\sum_a X_a \alpha_{ca,m}}{\sum_{a'} X_{a'}} \tag{2-10}$$

$$\alpha_{am} = \frac{\sum_c X_c \alpha_{ca,m}}{\sum_{c'} X_{c'}} \tag{2-11}$$

where the subscripts c, a and m refer to cations, anions and molecules respectively.

$$X_j = x_j C_j \quad (C_j = Z_j \text{ for ions; } C_j = 1 \text{ for molecules})$$

$$G_{jc,a'} = \exp(-\alpha_{jc,a'} \tau_{jc,a'}) \tag{2-12}$$

$$G_{ja,c'} = \exp(-\alpha_{ja,c'} \tau_{ja,c'}) \tag{2-13}$$

$$G_{ca,m} = \exp(-\alpha_{ca,m}\tau_{ca,m}) \quad (2-14)$$

$$G_{im} = \exp(-\alpha_{im}\tau_{im}) \quad (2-15)$$

$$\tau_{ma,ca} = \tau_{am} - \tau_{ca,m} + \tau_{m,ca} \quad (2-16)$$

$$\tau_{mc,ac} = \tau_{cm} - \tau_{ca,m} + \tau_{m,ca} \quad (2-17)$$

Where:

$\alpha$  is the nonrandomness parameter

$\tau$  is the binary energy interaction parameter

The only adjustable parameters in the Electrolyte NRTL model are the binary energy interaction parameters. These parameters are empirical and cannot be measured experimentally. They need to be regressed from available system data. In general, these interaction parameters have a temperature dependence of the form shown in (2-18) [5].

$$\tau = a + \frac{b}{T} \quad (2-18)$$

## 2.2 Soave-Reidlich-Kwong equation of state

The Soave-Reidlich-Kwong equation of state is used to model the vapor phase in the CO<sub>2</sub> capture system. The details of this equation of state are outlined below [9-11]:

$$P = \frac{RT}{V_m - b} - \frac{a}{V_m(V_m - b)} \quad (2-19)$$

Where:

$V_m$  is the molar volume

$$a = a_o + a_1 \quad (2-20)$$

$a_o$  is the standard quadratic mixing term:

$$a_o = \sum_{i=1}^n \sum_{j=1}^n x_i x_j (a_i a_j)^{1/2} (1 - k_{ij}) \quad (2-21)$$

$a_1$  is an additional, asymmetric term:

$$a_1 = \sum_{i=1}^n x_i \left( \sum_{i=1}^n x_i \left( (a_i a_j)^{1/2} l_{j,i} \right)^{1/3} \right)^3 \quad (2-22)$$

$$b = \sum_i x_i b_i \quad (2-23)$$

$$k_{ij} = k_{ji} \quad (2-24)$$

$$a_i = \alpha_i * 0.42747 \frac{R^2 T_{c_i}^2}{P_{c_i}} \quad (2-25)$$

$$b_i = 0.08664 \frac{RT_{c_i}}{P_{c_i}} \quad (2-26)$$

Where:

$T_{c_i}$  is the critical temperature of species i

$P_{c_i}$  is the critical pressure of species i

$\alpha_i$  is the temperature function added by Soave in order to improve the correlation of the pure component vapor pressure

$$\alpha_i(T) = \left( 1 + m_i (1 - T_{r,i})^{1/2} \right)^2 \quad (2-27)$$

$$m_i = 0.48508 + 1.55171 \omega_i - 0.15613 \omega_i^2 \quad (2-28)$$

Where:

$\omega$  is the acentric factor

$$k_{ij} = k_{ij}^{(1)} + k_{ij}^{(2)} T + \frac{k_{ij}^{(3)}}{T} \quad (2-29)$$

$$k_{ij} = k_{ji} \quad (2-30)$$

$$l_{ij} = l_{ij}^{(1)} + l_{ij}^{(2)}T + \frac{l_{ij}^{(3)}}{T} \quad (2-31)$$

The binary parameters  $k_{ij}$  are best determined from phase-equilibrium data regression.

### 2.3 Reidlich-Kwong-Soave-Boston-Mathias equation of state

The Reidlich-Kwong-Soave-Boston-Mathias equation of state is used in the ASPEN model to model the compression section of the flowsheet. This incorporates a modified alpha function for temperatures higher than the critical temperature [9-12].

$$\alpha_i(T) = \left( \exp\left( c_i \left( 1 - T_{r,i}^d \right) \right) \right)^2 \quad (2-32)$$

$$d_i = 1 + \frac{m_i}{2} \quad (2-33)$$

$$c_i = 1 - \frac{1}{d_i} \quad (2-34)$$

Where:

$m_i$  is calculated as above in (2-28)

With the Reidlich-Kwong-Soave-Boston-Mathias equation of state, (2-27) is used to calculate the alpha function at temperatures below critical and (2-32) is used to calculate the alpha function at temperatures above critical

### 2.4 Rate-based modeling with ASPEN RateSep

The traditional way of modeling absorption and desorption columns has been through the use of equilibrium models. In these models, the column is divided into a number of stages and the assumption is that the vapor and liquid phase leaving a stage in the column are at

equilibrium [13]. However, this is a very simplistic assumption and is not valid in actual cases. In order to correct for this, factors such as the height equivalent to a theoretical plate (HETP), stage and Murphee efficiencies are employed [14]. However, particularly for reactive separation processes, the use of efficiencies does not work well because the deviations from the equilibrium model are very large [15]. Hence, in these cases, it is necessary to model these systems with rate-based models.

ASPEN RateSep, the rate-based mode of RadFrac allows for the rate-based modeling of absorption and desorption columns [16]. It is a stage based model as shown in Figure 2-1 [16] and allows the modeling of mass and heat transfer phenomena as well as the kinetics of chemical reactions. The various equations that are solved in ASPEN RateSep include [16]:

- Mass and heat balances for the vapor and liquid phases
- Mass and heat transfer rate models to determine interphase transfer rates
- Vapor-liquid equilibrium equations for the interphase
- Estimation of mass and heat transfer coefficients and interfacial areas
- Enhancement of mass and heat transfer processes by chemical reactions

Aspen RateSep uses the solution proposed by Alopaeus [17] to solve the Maxwell-Stefan multicomponent mass transfer equation [18]. It uses the two-film theory and allows for film discretization which is useful to get an accurate concentration profile in the film for fast reactions. It also combines the film equations with separate balance equations for the liquid and vapor phase, diffusion and reaction kinetics, electrolyte solution chemistry and thermodynamics [18].

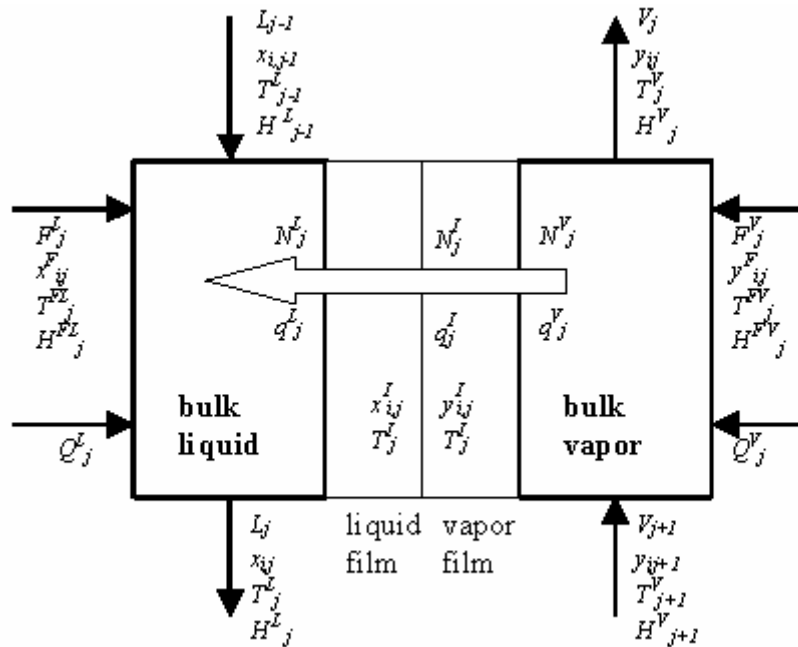


Figure 2-1: ASPEN representation of a stage (Adapted from [16])

## 2.4.1 Flow models

ASPEN RateSep provides a number of flow models that can be used in the rate modeling. These flow models are used to determine the bulk properties that are used in calculating the mass and heat fluxes and the reaction rates [16]. Different bulk properties are calculated for each of the stages shown in Figure 2-1.

### 2.4.1.1 Mixed flow model

The mixed flow model is shown in Figure 2-2. In this model, the bulk properties for each phase are taken to be the same as the outlet conditions for that phase when it leaves that stage. This is the default flow model in ASPEN RateSep and the model that is adopted in this work.

$x_{i,j}$ $T_j^L$ $P_j$ $L_j$	$x'_{i,j}$ $T_j$	$y'_{i,j}$ $T_j$	$y_{i,j}$ $T_j^V$ $P_j$ $V_j$
<b>bulk liquid</b>	liquid film	vapor film	<b>bulk vapor</b>

Figure 2-2: Mixed flow model in ASPEN RateSep (Adapted from [16])

### 2.4.1.2 Countercurrent flow model

In the countercurrent flow model shown in Figure 2-3, ASPEN calculates the bulk properties for each phase as an average of the inlet and outlet properties [16]. This method is computationally much more intensive and is recommended only when a very low outlet composition is specified.

$x_{i,avg}$ $T_{avg}^L$ $P_{avg}$ $L_{avg}$	$x'_{i,j}$ $T_j$	$y'_{i,j}$ $T_j$	$y_{i,avg}$ $T_{avg}^V$ $P_{avg}$ $V_{avg}$
<b>bulk liquid</b>	liquid film	vapor film	<b>bulk vapor</b>

Figure 2-3: Concurrent flow model in ASPEN Plus (Adapted from [16])

### 2.4.1.3 VPlug flow model

The VPlug flow model is shown in Figure 2-4 . In this model, the properties of the liquid are calculated to be the same as that of the outlet leaving the stage. For the vapor, average conditions are used as in the countercurrent flow model. The pressure is assumed to be the same as the outlet pressure.

$x_{i,j}$ $T_j^L$ $P_j$ $L_j$	$x'_{i,j}$ $T_j$	$y'_{i,j}$ $T_j$	$y_{i,j}^{avg}$ $T_j^{avg}$ $P_j$ $V_j^{avg}$
<b>bulk liquid</b>	liquid film	vapor film	<b>bulk vapor</b>

Figure 2-4: VPlug flow model in ASPEN Plus (Adapted from [16])

#### 2.4.1.4 VPlugP flow model

The VPlugP flow model is shown in Figure 2-5. This is identical to the VPlug model except that the average pressure is used instead of the outlet pressure.

$x_{i,j}$ $T_j^L$ $P^{avg}$ $L_j$	$x'_{i,j}$ $T_j$	$y'_{i,j}$ $T_j$	$y_{i,j}^{avg}$ $T_j^{avg}$ $P^{avg}$ $V_j^{avg}$
<b>bulk liquid</b>	liquid film	vapor film	<b>bulk vapor</b>

Figure 2-5: VPlugP flow model in ASPEN Plus

#### 2.4.2 Film reactions

RateSep uses a two-film model to perform mass and heat transfer models. It provides a number of options for film discretization [16]:

1. **Nofilm:** When this mode is specified for a phase, ASPEN assumes that there is no film resistance for this phase. Hence, it performs an equilibrium calculation in this phase.

2. **Film:** When this mode is specified for a phase, ASPEN performs diffusion resistance calculations but no reaction calculations for the film in this phase.
3. **Filmrxn:** This is one of the modes that can be specified for a phase in order to perform reaction calculations in this phase. In this case ASPEN uses the reaction condition factor to calculate the rate of reaction in the film. This is the weighting factor used for calculating compositions and temperature that are to be used in the evaluation of rate. The reaction condition factor varies between 0 and 1 with 0 being the interphase condition and 1 being the bulk condition. The reaction condition factor is an adjustable parameter that can be specified by the user.
4. **Discrxn:** This is the most robust of the methods that ASPEN offers to consider reactions in the film and is the most applicable one when there are fast reactions in the film. In this case, ASPEN allows the discretization of the film into distinct segments and calculates the concentrations of the species at each of these discrete points so that an accurate concentration profile in the film is obtained. It allows the user to set the number of discretization points as well as the discretization ratio. The discretization ratio is the ‘ratio of the thicknesses of adjacent discretization regions in the film’[16]. It also allows the specification of locations in the film where additional discretization points are desired. This is particularly useful in specifying points close to the interphase. The optimization of the discretization points is very important in CO<sub>2</sub> capture systems since there are fast reactions occurring in the system. Kucka at al. [19] and Aspiron [15] showed that for systems in which there is sour gas absorption by aqueous amines, the film segments need to be thinner at the boundaries of the film than at the middle of the film.

### **2.4.3 Column hydrodynamics**

ASPEN RateSep allows the consideration of column hydrodynamics through a number of models and correlations. For many different types of packing, ASPEN has built-in correlations for the mass transfer coefficient, heat transfer coefficient, interfacial area and the holdup. In addition, ASPEN provides a design mode in which the column can be sized by setting a base approach to a flooding on a chosen stage.

## **2.5 Aspen Simulation Workbook**

Aspen Simulation Workbook was used as a tool in this thesis to run parametric simulations with different solvent systems. It is a tool that allows ASPEN to link process models to an Excel workbook [20]. It allows the user to set up a number of different scenario runs for a simulation in Excel. The user can decide on a number of variables, whose values they want to vary and enter these in Excel. Excel feeds these values to ASPEN and runs the simulation for each of the scenarios. The user can define which output values they want ASPEN to feed to Excel. Thus, the simulation is run from Excel and Excel becomes the controlling program. This tool is very useful when parametric studies have to be performed and the output format allows for easy data analysis.

## 2.6 References

1. Chen, C.-C., H.I. Britt, J.F. Boston, and L.B. Evans, *Extension and application of the pitzer equation for vapor-liquid equilibrium of aqueous electrolyte systems with molecular solutes*. AIChE Journal, 1979. **25**(5): p. 820-831.
2. Chen, C.-C., H.I. Britt, J.F. Boston, and L.B. Evans, *Local composition model for excess Gibbs energy of electrolyte systems. Part I: Single solvent, single completely dissociated electrolyte systems*. AIChE Journal, 1982. **28**(4): p. 588-596.
3. Chen, C.-C. and L.B. Evans, *A local composition model for the excess Gibbs energy of aqueous electrolyte systems*. AIChE Journal, 1986. **32**(3): p. 444-454.
4. Mock, B., L.B. Evans, and C.-C. Chen, *Thermodynamic representation of phase equilibria of mixed-solvent electrolyte systems*. AIChE Journal, 1986. **32**(10): p. 1655-1664.
5. Augsten, D.M., *A model for vapor-liquid equilibria for acid gas-alkanolamine-H<sub>2</sub>O systems*, in *Chemical Engineering*. 1989, University of Texas at Austin: Austin.
6. Pitzer, K.S., *Electrolytes. From dilute solutions to fused salts*. Journal of the American Chemical Society, 2002. **102**(9): p. 2902-2906.
7. Robinson, R.A. and R.H. Stokes, eds. *Electrolyte Solutions*. 2nd ed. 1970: London.
8. Renon, H. and J.M. Prausnitz, *Local compositions in thermodynamic excess functions for liquid mixtures*. AIChE Journal, 1968. **14**(1): p. 135-144.
9. ASPEN, *Rate-based model of the CO<sub>2</sub> capture process by NH<sub>3</sub> using Aspen Plus*. 2008, Aspen Plus.
10. Soave, G., *Equilibrium Constants for a Modified Reidlich-Kwong Equation-of-State* Chemical Engineering Science, 1972. **27**: p. 1169-1203.
11. Redlich, O. and J.N.S. Kwong, *On the Thermodynamics of Solutions V. An Equation-of-State: Fugacities of Gaseous Solutions*. Chem. Rev., 1949. **44**: p. 223-244.
12. Boston, J.F. and P.M. Mathias. *Phase Equilibria in a Third-Generation Process Simulator*. in *2nd International Conference on Phase Equilibria and Fluid Properties in the Chemical Process Industries*. 1980. West Berlin.

13. Treybal, R.E., *Mass-Transfer Operations, 3rd edition*. 3rd edition ed. Chemical Engineering Series, ed. McGraw-Hill. 1981.
14. Taylor, R., R. Krishna, and H. Kooijman, *Real-World Modeling of Distillation*. Chemical Engineering Progress, 2003. **99**: p. 28-39.
15. Aspron, N., *Nonequilibrium Rate-Based Simulation of Reactive Systems: Simulation Model, Heat Transfer, and Influence of Film Discretization*. Industrial & Engineering Chemistry Research, 2006. **45**: p. 2054-2069.
16. ASPEN, *User Online Documentation*. 2008.
17. Alopaeus, V., J. Aittamaa, and H.V. Nordén, *Approximate high flux corrections for multicomponent mass transfer models and some explicit methods*. Chemical Engineering Science, 1999. **54**(19): p. 4267-4271.
18. Zhang, Y., H. Chen, C.-C. Chen, J.M. Plaza, R. Dugas, and G.T. Rochelle, *Rate-Based Process Modeling Study of CO<sub>2</sub> Capture with Aqueous Monoethanolamine Solution*. Industrial & Engineering Chemistry Research, 2009. **48**(20): p. 9233-9246.
19. Kucka, L., I. Müller, E.Y. Kenig, and A. Górak, *On the modelling and simulation of sour gas absorption by aqueous amine solutions*. Chemical Engineering Science, 2003. **58**(16): p. 3571-3578.
20. ASPEN, *Aspen Simulation Workbook User Guide*. 2006.

## Chapter 3

### Monoethanolamine system

The use of aqueous monoethanolamine (MEA) for the removal of CO<sub>2</sub> from flue gases is an available technology and has been described in detail in a number of sources [1-4]. MEA has been used as a solvent for non-selective removal of acidic gases for the past 60 years [4]. Presently, Fluor is actively trying to commercialize CO<sub>2</sub> capture technologies based on MEA as a solvent [5]. The Fluor process utilizes a 30 wt.% MEA solvent with inhibitors to prevent degradation and equipment corrosion. The Fluor process has until now mainly been used on natural gas derived flue gases. In general, amine concentrations of up to 32 wt.% may be used provided CO<sub>2</sub> is the only acidic gas being absorbed and that a corrosion inhibitor is added [6].

#### 3.1 Process description

The process for CO<sub>2</sub> capture using MEA can be broken into 3 different sections:

1. Flue gas cooling and compression
2. Absorption of CO<sub>2</sub> and regeneration of solvent
3. CO<sub>2</sub> compression

A schematic of the process is shown in Figure 3-1 [7]. Each of these steps is now discussed in detail below.

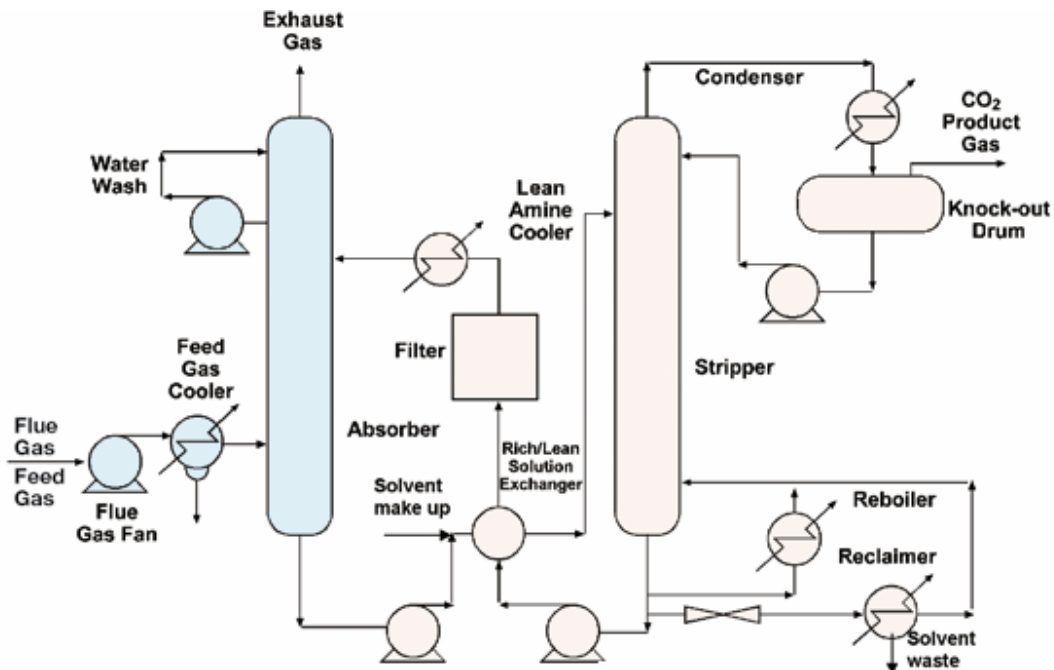


Figure 3-1: Schematic of CO<sub>2</sub> capture by use of MEA solvent (Adapted from [7])

### Flue gas cooling and compression:

The absorber in the MEA system operates at a temperature of approximately 40°C and hence, the inlet temperature of the gases to the absorber system needs to be around 40-50°C. In the case of natural gas combined cycle plants (NGCC), the temperature of the flue gas at the exhaust of the power plant is around 110-120°C and these gases need to be cooled before being fed to the absorption system. Cooling is required for flue gases derived from coal-fired power plants as well unless the flue gases have been through a wet flue gas desulfurization scrubber, in which case they may already have been cooled to the requisite temperature.

The flue gas is typically cooled by passing it through a direct contact cooling tower (DCC). The DCC is a packed tower in which there is counter-current flow of cooling water and the flue gases. The flue gases enter at the bottom of the tower with the cooling

water entering at the top. In the tower, the flue gas is cooled by evaporation of water and hence, the water content of the flue gas is reduced at the exit of the tower. The cooling water is collected at the bottom of the DCC and is sent to a cooling water in order to have its temperature reduced before being used in the DCC again.

The flue gas exits at the top of the DCC and is sent to a blower where it is slightly compressed. Since the flue gas stream has to flow upward through a packed absorber, it is necessary to increase the pressure of the flue gas before sending it to the absorber. This is also accompanied by attendant temperature increase.

It is necessary that prior to chemical absorption with MEA, the flue gas be scrubbed to remove  $\text{NO}_x$ ,  $\text{SO}_x$  and similar impurities. The presence of  $\text{NO}_x$  and  $\text{SO}_x$  in the flue gas is undesirable since they react irreversibly with the amine solvent to form heat stable salts that cannot be reclaimed. In  $\text{NO}_x$ , it is  $\text{NO}_2$  which is responsible for the irreversible reaction. A  $\text{NO}_2$  level of less than 20 ppmv is recommended [8]. Most modern plants produce a flue gas with a  $\text{NO}_2$  content lower than this and hence, this does not pose too much of a problem. For  $\text{SO}_x$ , there is a tradeoff between the cost of the flue gas desulfurization and the cost of the makeup solvent required to compensate the degradation of the solvent due to  $\text{SO}_x$ . For MEA, a  $\text{SO}_x$  level of less than 10 ppmv is desired for the Fluor Daniel Econamine<sup>TM</sup> process [8].  $\text{SO}_3$  can also form corrosive sulfuric acid aerosol in wet scrubbers. A special mist eliminator or a wet electrostatic precipitator needs to be employed in the flue gas desulfurization unit [8].

#### **Absorption of $\text{CO}_2$ and regeneration of solvent:**

The absorber utilized is typically a packed column, in which a packing that provides sufficient surface area for the absorption of  $\text{CO}_2$  is used. The flue gas enters at the bottom of the absorber with the lean amine solvent entering at the top of the absorber. The lean amine comes in at a loading of between 0.2- 0.3 and leaves at a loading close to 0.5. In a MEA system, the loading is defined on a mole basis as given by

$$\text{Loading} = \frac{\text{Moles of all CO}_2 \text{ carrying species}}{\text{Moles of all MEA carrying species}} \quad (3-1)$$

$$\text{Loading} = \frac{[\text{CO}_2] + [\text{HCO}_3^-] + [\text{CO}_3^{2-}] + [\text{MEACOO}^-]}{[\text{MEA}] + [\text{MEA}^+] + [\text{MEACOO}^-]} \quad (3-2)$$

In this case, lean amine refers to the amine stream that is stripped of CO<sub>2</sub> i.e. the amine stream that enters the top of the absorber. When the amine stream is loaded with CO<sub>2</sub>, as is the case with the stream that leaves the bottom of the absorber, it is referred to as a rich amine stream. The amine stream is usually introduced on the second stage from the top with make-up water entering at the first stage. This allows the first stage to function as a water wash to remove any entrained MEA that may be carried out along with the vent gas that is stripped of CO<sub>2</sub>. It also serves the function of cooling the vent gas before it is released to the atmosphere. In some cases, it may be necessary to have a separate water wash tower after the absorber.

The rich amine leaves from the bottom of the absorber from where it is sent to a pump before being sent to the cross-heat exchanger. In the cross heat-exchanger, the rich stream from the absorber exchanges heat with the lean stream from the desorber. This allows the rich stream to be heated and the lean stream to be cooled down. Before proceeding to the absorber, the lean stream is further cooled to bring its temperature down to 40°C or so.

The rich stream is taken from the cross-heat exchanger to the desorber. The desorber is a packed column that has a kettle reboiler. The desorber typically operates at slightly elevated pressures (~1.5-1.8 atm). The rich amine enters at the second stage of the desorber and flows down the column, counter to the direction of the vapors from the reboiler. The stream from the top of the column is taken to a condenser in order to condense the water and lower the temperature and then to a flash in order to separate the CO<sub>2</sub> and H<sub>2</sub>O. A part of the liquid reflux (pure water) is returned to the top of the desorber column while a purge stream is sent to storage. As in the absorber, the first stage in the desorber acts as a water wash stage to remove any entrained MEA in the vapor

leaving the top of the desorber. In the reboiler of the desorber, steam from the power plant is used to produce the heat duty. The heat duty in the reboiler arises from three different requirements:

1. Sensible heat to raise the temperature of the rich stream to that in the desorber
2. Heat of reaction to reverse the absorption reaction and release CO<sub>2</sub>
3. Heat to produce steam to maintain driving force for transfer of CO<sub>2</sub> from liquid phase to gas phase

### **Reclaiming of solvent:**

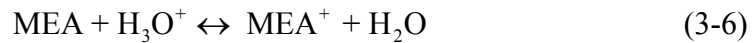
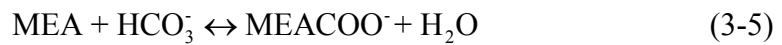
Particularly in the case of flue gas from coal fired power plants, it will be necessary to use a MEA reclaimer to treat some of the heat stable salts that form due to the NO<sub>x</sub> and SO<sub>x</sub>. The continued buildup of these salts in the amine stream is undesirable since it lowers the capacity of the solvent for CO<sub>2</sub> absorption. A purge stream of the solvent is removed and taken to a reclaimer where in the presence of a strong alkali like NaOH and with the application of heat, some of the heat stable salts can be dissociated, resulting in the recovery of some of the solvent. The sludge that is produced in the reclaimer is sent for disposal in a landfill.

### **CO<sub>2</sub> compression:**

The CO<sub>2</sub> gas that is released from the desorber needs to be dried and compressed before being sent for storage. Drying is an important step since the presence of moisture in the stream can cause corrosion in the pipelines used for CO<sub>2</sub> transport. Typically, a 4-stage reciprocating compressor is used with cooling between the stages. The compressor is used to compress the CO<sub>2</sub> to 90 atm, beyond which the supercritical liquid CO<sub>2</sub> can be pumped to the discharge pressure of 130 atm.

### 3.2 Chemistry of the MEA system

In the MEA system, CO<sub>2</sub> is solubilized in the liquid phase either in a carbamate, carbonate or bicarbonate form. The following reversible reactions occur in the MEA system:



The equilibrium constants for the reaction are temperature dependent and follow the dependence given in (3-8).

$$\ln K_x = A + \frac{B}{T} + C \ln T + DT \quad (3-8)$$

In this case, T is the temperature in °K. The constants A, B, C, D for the different reactions are presented in Table 3-1 and are referenced from Augsten's work [9].

**Table 3-1: Values of temperature dependent parameters for equilibrium constant in MEA system**

Reaction	A	B	C	D
(3-3)	132.89	-13445.9	-22.47	0
(3-4)	231.46	-12092.1	-36.78	0
(3-5) (reverse)	-0.52	-2545.53	0	0
(3-6)(reverse)	-3.038	-7008.3	0	-0.00313
(3-7)	216.05	-12431.7	-35.48	0

### 3.2.1 Carbamate formation in the MEA system

Carbamate formation is an important reaction in CO<sub>2</sub> absorption. There is much discussion in the literature on the mechanism of formation of the carbamate. Two mechanisms have been proposed for the formation of the carbamate – the zwitterion mechanism and the termolecular mechanism.

#### 3.2.1.1 Zwitterion mechanism

This mechanism was proposed by Caplow in 1968 [10] and is shown below in Figure 3-2

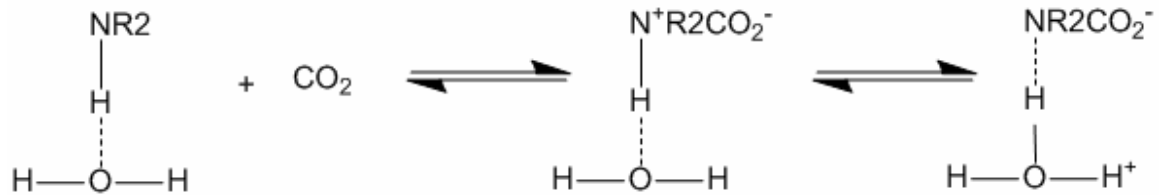


**Figure 3-2: Zwitterion mechanism for carbamate formation**

Caplow assumed that the amine molecule forms a hydrogen bond with the water molecule before reacting with CO<sub>2</sub>. The first step was the formation of an unstable intermediate by the bonding of the CO<sub>2</sub> molecule to the amine. In the second step, the

amine proton is transferred to a basic molecule to form the carbamate. The base can be a water molecule or an amine.

The kinetic expressions for this have been elucidated by Kumar *et al.* in 2003 [11].

QSSA on zwitterion gives:

$$r_{CO_2} = \frac{k_2[CO_2][Am]}{1 + \frac{k_{-1}}{\sum k_b[B]}} = \frac{[CO_2][Am]}{\frac{1}{k_2} + \frac{k_{-1}}{k_2} \frac{1}{\sum k_b[B]}} \quad (3-9)$$

The summation term is the contribution of all the bases present in the solution for the removal of protons. In lean aqueous solutions, the amine, water, OH<sup>-</sup> can act as bases causing the deprotonation of the zwitterion to form the carbamate species

1. For low amine concentrations,  $k_b \sim k_{H_2O}$

$$r_{CO_2} = k_2[CO_2][Am] \left( \frac{k_{H_2O}[H_2O]}{k_{-1}} \right) \quad (3-10)$$

2. At moderately high amine concentrations, the contribution of the amine and the water to the zwitterion's deprotonation are equally important and hence the contribution of all must be considered.
3. At very high amine concentrations, the contribution of water to the deprotonation is insignificant and also  $k_{-1}/(k_{Am}[am])$  is low. Hence,

$$r_{CO_2} = k_2[CO_2][Am] \quad (3-11)$$

### 3.2.1.2 Termolecular mechanism

A termolecular single-step mechanism for carbamate formation was proposed in 1989 [12] and is shown in Figure 3-3 .

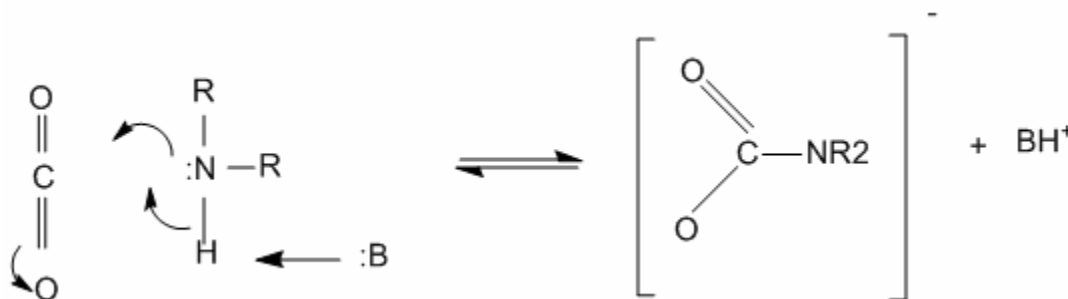


**Figure 3-3: Termolecular mechanism for carbamate formation**

In this mechanism, the bond formation with  $\text{CO}_2$  and the proton transfer take place simultaneously. This mechanism is not very different from that proposed by Caplow. However, the recent literature cites Caplow's mechanism as shown below [11, 13]. In this the formation of hydrogen bond with the base is ignored. If the lifetime of the zwitterion is very small, then Caplow's mechanism approaches the termolecular mechanism.



The experimental data can be represented by either mechanism [14]. However, ab initio computations show that the single step termolecular reaction is more likely. In addition, for some systems reported in literature, the zwitterion mechanism gives implausible values of parameters [15]. Other mechanisms have also been proposed to explain the carbamate formation and so as of yet, there is no consensus on which the correct mechanism is.

### 3.3 Thermochemistry in the MEA system

The thermochemistry of the MEA system has been elucidated by Rochelle et al. [16]. The values as presented in Rochelle et al. [16] are presented below:

**Table 3-2: Thermochemistry in the MEA system. Data from [16]**

Reaction	-ΔH (kcal/gmol)		
	25°C	80°C	120°C
$\text{CO}_2(\text{g}) \rightarrow \text{CO}_2(\text{aq.})$	4.9	2.9	1.3
$\text{CO}_2(\text{aq}) + \text{H}_2\text{O} \rightarrow \text{HCO}_3^- + \text{H}^+$	-2.2	1.7	4.7
$\text{MEA}(\text{aq}) + \text{H}^+ \rightarrow \text{MEA}^+$	12.0	12.2	12.1
$\text{MEA}(\text{aq}) + \text{HCO}_3^- \rightarrow \text{MEACOO}^- + \text{H}_2\text{O}$	4.3	5.1	5.4
<b>Overall reaction</b>	18.9	21.9	23.6

Hence, at 25°C, the heat of reaction of MEA with CO<sub>2</sub> is 18.9 kcal/gmol CO<sub>2</sub>.

### 3.4 VLE in the MEA-CO<sub>2</sub>-H<sub>2</sub>O system

The VLE in the MEA-CO<sub>2</sub>-H<sub>2</sub>O system is complex since the liquid phase is ionic. Hence, an electrolyte model is needed and the model that is utilized is the ENRTL model that was described earlier. In the ENRTL model, the NRTL component of the Gibbs free energy calculation has a number of temperature dependent interaction parameters, whose value cannot be measured independently, but rather needs to be regressed.

Using a flash calculation in ASPEN, it is possible to compute the VLE that ASPEN predicts will exist in the system for different conditions of temperature and liquid loading. Figure 3-4 shows a comparison between the VLE predicted by ASPEN and the experimental VLE obtained by Jou et al. [17].

### Comparison of ASPEN default VLE with experimental VLE at 60 °C and 120°C

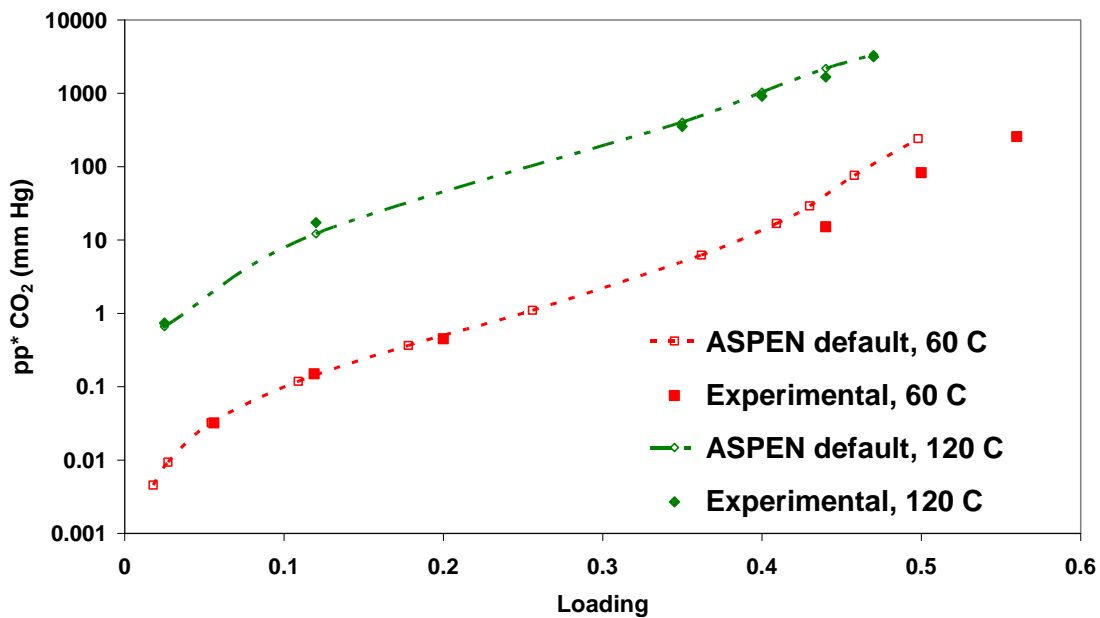
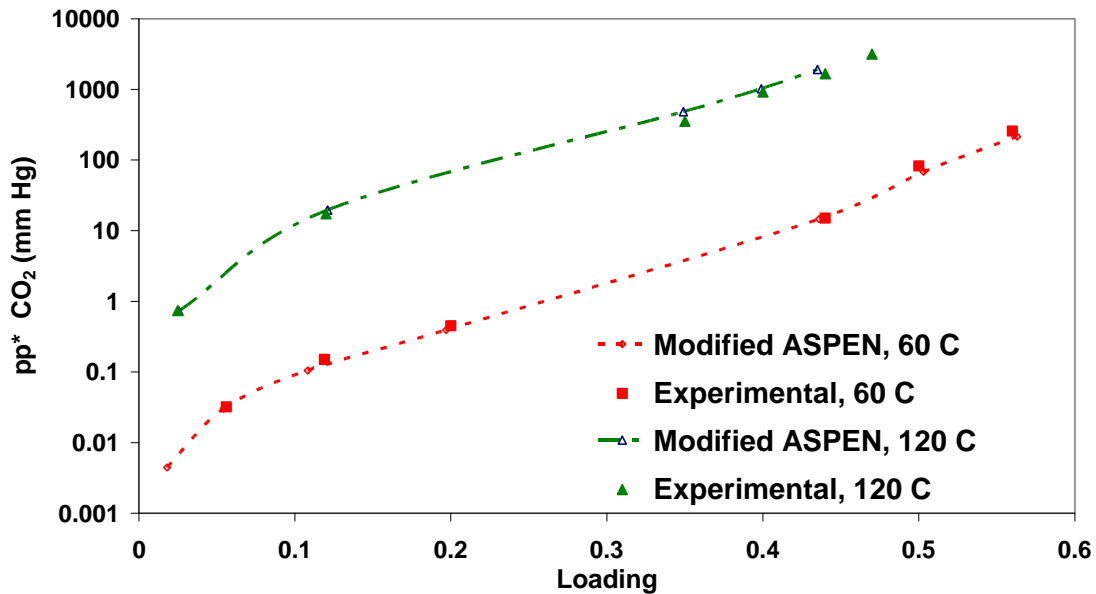


Figure 3-4: Comparison of ASPEN default VLE with experimental VLE at 60°C and 120°C. Experimental data from [17]

As can be seen from Figure 3-4, there is some discrepancy between the VLE predicted by ASPEN and that obtained by experiments, particularly at high loadings. In order to model the performance of the system adequately in ASPEN, it is necessary to have a good match of the ASPEN VLE with what is predicted by experiments. For this purpose, the temperature-dependent interaction parameters in the NRTL portion of the ENRTL model were modified as described by Ferguia [18]. He has described the regression of new values of the interaction parameters using the ASPEN Data Regression System by incorporating more accurate VLE data. When these values are incorporated in ASPEN, a much better agreement of the VLE with the experimental values is obtained. This is shown in Figure 3-5.

**Comparison of modified ASPEN VLE with  
experimental VLE at 60°C and 120°C**



**Figure 3-5: Comparison of modified ASPEN VLE with experimental VLE at 60°C and 120°C. Modified interaction parameters from [18] and experimental data from [17].**

These diagrams also serve to illustrate the mechanism of separation of CO<sub>2</sub> from the rest of the flue gas using a MEA solution by a temperature swing absorption-desorption cycle. At lower temperatures, the equilibrium partial pressure of CO<sub>2</sub> over the MEA solution is low and hence this creates the driving force for CO<sub>2</sub> transfer from the gas phase to the liquid phase. In the gas phase, the partial pressure of CO<sub>2</sub> is around 0.04 atm in the case of flue gas from natural gas-fired power plants and 0.13 atm in the case of flue gas from coal-fired power plants. This is much higher than the equilibrium partial pressure of CO<sub>2</sub> and hence, the CO<sub>2</sub> is forced into the liquid solution.

At higher temperatures, however, the equilibrium partial pressure of CO<sub>2</sub> over the MEA solution is much higher. Hence, once the reaction has been reversed in the liquid phase, there is driving force for transport of CO<sub>2</sub> from the liquid phase to the gas phase.

### **3.5 Degradation of MEA solvent**

One of the concerns with using MEA as a solvent is that it is prone to degradation at high temperatures by a number of mechanisms as outlined in this section.

#### **3.5.1 Carbamate polymerization**

Carbamate polymerization is the most common mechanism of amine degradation. It occurs in the presence of CO<sub>2</sub> and high temperature [19]. The rate of degradation is a strong function of CO<sub>2</sub> partial pressure and temperature [16]. Carbamate polymerization is initiated by the formation of an oxazolidone. This forms as a five-member ring by the internal reaction of an alcohol and a carbamate. The parent amine then reacts with the oxazolidone to produce a substituted ethylenediamine. The final step in the degradation is the condensation of the substituted ethylenediamine to a substituted piperazine. Sterically hindered amines and tertiary amines do not have a strong tendency to form carbamate and hence, are not subjected to this form of degradation.

Degradation by carbamate polymerization is insignificant at temperatures lower than 100°C and hence, will be important only around the stripper and the reboiler sump. Since,

the degradation reactions are favored at high CO<sub>2</sub> loading, the degradation is more probable at the rich end of the stripper. In addition, the rate of polymerization has a high dependence on amine concentration and hence, solvents that use a lower amine concentration will have a lower rate of degradation. Carbamate polymerization has been studied by a number of authors [20-21]. However, there is not much literature on the kinetics of the carbamate polymerization reaction.

### **3.5.2 Oxidative degradation**

Oxidative degradation occurs due to the presence of oxygen in the flue gas. Neither carbon dioxide nor high temperature is required for oxidative degradation to occur. The products of oxidative degradation include various aldehydes, organic acids such as acetate, formate, glycolate, acetate and oxalate amines, NH<sub>3</sub> and nitrosoamines [22-23]. These products can have significant environmental impacts if released into the environment. Nitrosoamines are known to be carcinogens. Oxidative degradation also results in the formation of heat stable salts and loss of the solvent. The degraded solvent has to be replaced with make-up and this can be a significant cost in the process. In addition, the degradation reactions can significantly enhance the corrosion of the column and its internals [24-25]. In industrial applications, Fe and Cu are likely to be catalysts that promote the degradation of the amine.

Oxidative degradation will most likely occur at short times and low temperature with contact in the absorber and at longer times and high temperature in the stripper [16]. A number of authors have studied the oxidative degradation of MEA [26-29]. A study at the University of Texas has identified that the oxidative degradation of MEA under industrial conditions is controlled by O<sub>2</sub> mass transfer and that the degradation rate is likely to be 0.29-0.73 kg MEA/m ton of CO<sub>2</sub> [30]. In general, inhibitors are added to the system to prevent the oxidative degradation of MEA.

### 3.6 MEA flowsheet development

As described before, the flowsheet for CO<sub>2</sub> capture with MEA consists of a three different sections. The RKS-BM model was used in the CO<sub>2</sub> compression section with the ENRTL model being used in the other sections. This is because the property model used in the CO<sub>2</sub> compression section had to be capable of handling supercritical CO<sub>2</sub>.

Since the intent of the study was to perform parametric studies on the system, it was decided to model the flowsheet as an open-loop simulation since this would allow easier convergence and facilitate performing multiple runs quickly. However, design specifications were put in place to ensure that the simulation would converge in the closed form as well. The developed flowsheet is shown in Figure 3-6.

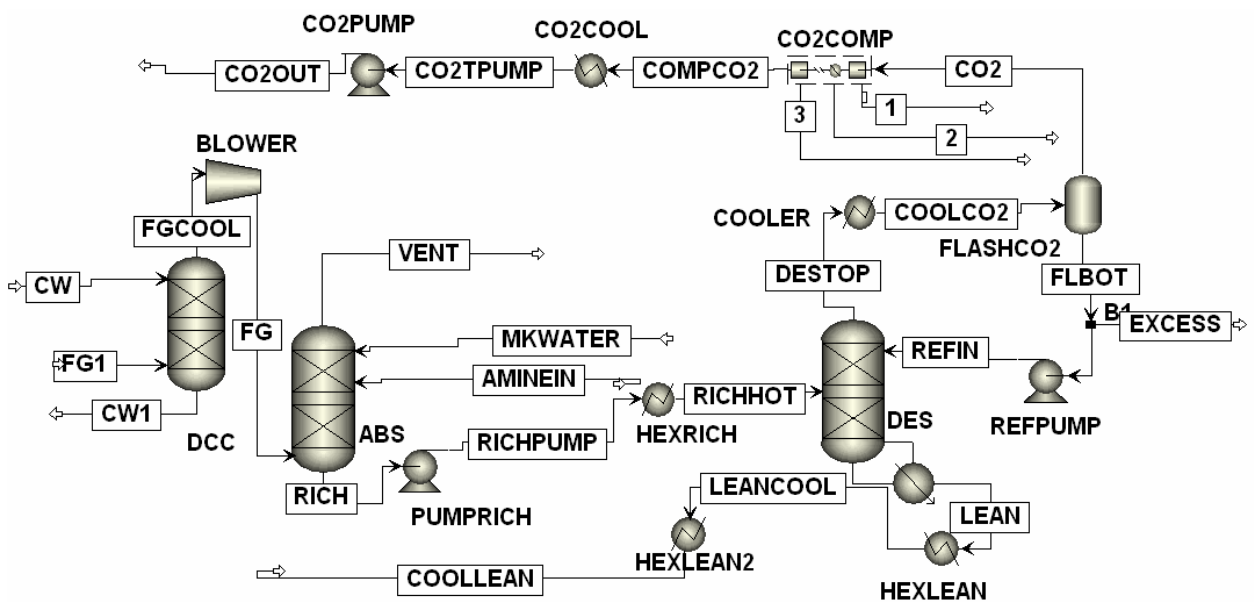


Figure 3-6: Process flow diagram of MEA system as developed in ASPEN Plus

The absorber, desorber and direct contact cooling tower (DCC) were modeled as RADFRAC columns. The desorber was modeled with a kettle reboiler. The compressor

was modeled as a four-stage reciprocating compressor with cooling in between the stages. The design specifications in the flowsheet are outlined below:

- 1. Vent CO<sub>2</sub>:** The absorber has a design specification which regulates the amount of CO<sub>2</sub> that is vented from the top of the absorber. The desired extent of capture is achieved by varying the amount of amine flow into the absorber column. This design specification is specified in the *Flowsheeting Options* tab.
- 2. Reboiler Duty:** The reboiler duty is varied so that the composition of the stream COOLLEAN (output from second heat exchanger after desorber) is equivalent to that of the stream AMINEIN. This ensures that the simulation would converge in a closed loop manner as well. This is done by matching the loading of the two streams. In the *Prop Sets* tab, two property sets FAPPCO2 and FAPPMEA are defined. These calculate the apparent molar flows of CO<sub>2</sub> and MEA in the stream. The ratio of FAPPCO2 to FAPPMEA is the loading of the stream. This property is set to the desired value (the value in the AMINEIN stream) and the reboiler duty is varied till the desired value is reached.
- 3. Cross-exchanger duty:** In this flowsheet, the cross exchanger is simulated as two separate heat exchangers – HEXRICH and HEXLEAN. This is so that a closed loop will not be formed. However, it is necessary to match the heat duties of the two heat exchangers so that they effectively function as a cross-heat exchanger. This is achieved through this design specification in the *Flowsheeting Options* tab. The heat duty of the HEXLEAN heat exchanger is set equal to the negative of the heat duty of the HEXRICH heat exchanger.
- 4. Cross-exchanger approach temperature:** In addition to matching the heat duties of HEXLEAN and HEXRICH, it is necessary to set a design specification on the approach temperature to the cross-exchanger. For this purpose, the

temperature of the outlet stream of HEXLEAN is set to 10°C above the temperature of the inlet stream to HEXRICH.

- 5. Water balance:** It is necessary to maintain water balance in the plant in order to have closed loop convergence. For this purpose, the flowrate of the make up water stream is varied to achieve an overall water balance.

### **3.7 MEA system equilibrium simulation results**

In equilibrium simulations, the absorber and desorber column were modeled as a set of stages, with each stage in equilibrium. The reactions occurring in the column were also considered to be at equilibrium. Hence, these simulations present the most optimistic results attainable since in reality, the reactions will not be at equilibrium and mass transfer considerations in the column will invalidate the equilibrium simulation. The main purpose of these simulations is to obtain a lower bound on the heat duty and to provide good estimates for converging the system with the more complex rate-based method.

Figure 3-7 shows the variation in L/G in absorber with lean loading for flue gas from a natural gas fired power plant. L/G is the ratio of the total molar liquid flow to the total molar gas flow in the column. The absorber was simulated with 12 equilibrium stages and the desorber was simulated with 8 equilibrium stages.

**Variation of L/G in absorber with lean loading for for 85% CO<sub>2</sub> capture from NGCC flue gas; equilibrium simulation**

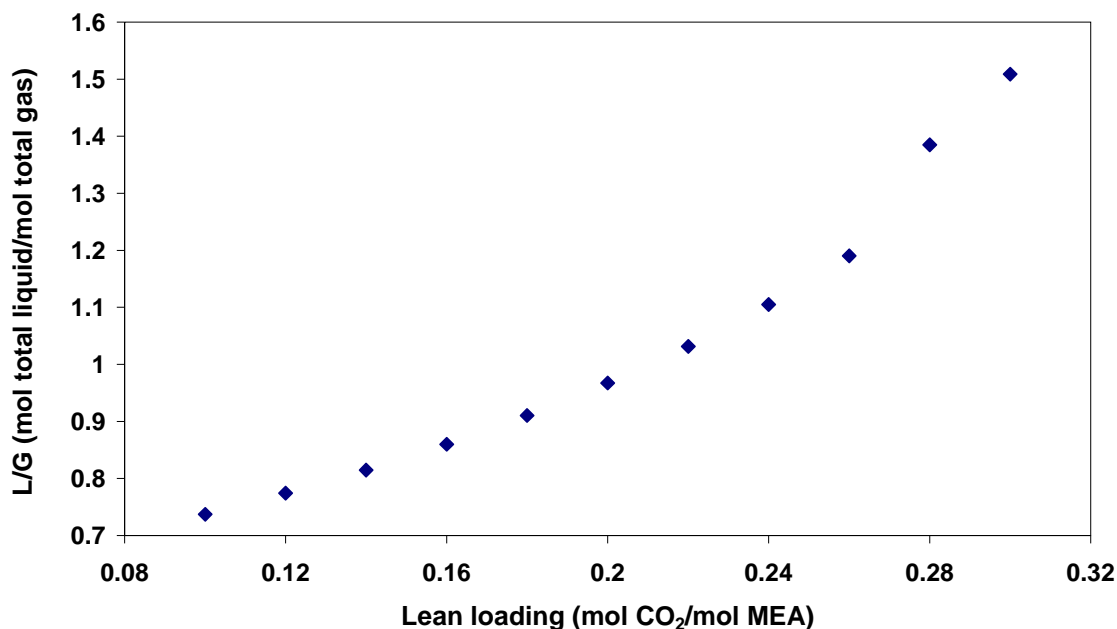


**Figure 3-7: Variation of L/G with lean loading for 85% CO<sub>2</sub> capture from NGCC flue gas; equilibrium simulation**

The required amine flowrate increases as the lean loading increases since with increasing lean loading, the capacity of the solvent for CO<sub>2</sub> absorption decreases. As can be seen from the figure, beyond a certain lean loading, there is a sharp increase in the liquid flowrate required to achieve the 85% capture..

An interesting trend is observed when we study the variation of reboiler duty with the lean loading (and hence L/G). This trend is shown in Figure 3-8 for flue gas from a NGCC plant.

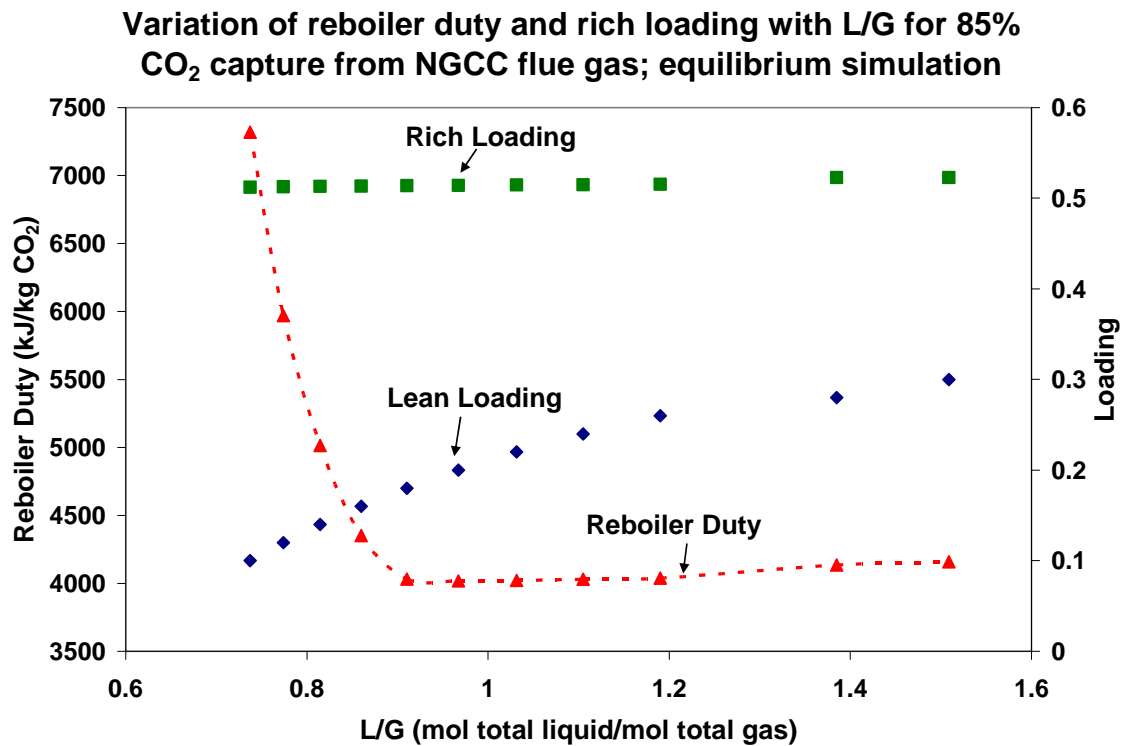


**Figure 3-8: Variation of reboiler duty and rich loading with L/G for 85% CO<sub>2</sub> capture from NGCC flue gas; equilibrium simulation**

The reboiler duty is very high at low lean loadings, since the partial pressure of CO<sub>2</sub> in equilibrium with the liquid phase is low at low loadings. Hence, to strip the solution to the required low lean loading, a substantial amount of steam has to be supplied. Hence, in this case, the amount of energy lost due to the vaporization and subsequent condensation of water is high. However, as the lean loading increases, the equilibrium partial pressure of CO<sub>2</sub> increases and the relative amount of steam that needs to be vaporized decreases. This causes the reboiler duty to fall. However beyond a certain lean loading, it is the sensible heat component that dominates because the liquid flowrate that is required to achieve the 85% capture has increased as shown above in Figure 3-8. Hence, there exists the potential for optimization of the loading range to operate in.

When similar simulations are performed for flue gas derived from a coal fired power plant that has higher CO<sub>2</sub> content, similar trends are observed though the numerical values are different. These trends are shown in Figure 3-9 and Figure 3-10 below.

**Variation of L/G in absorber with lean loading for for 85% CO<sub>2</sub> capture from coal flue gas; equilibrium simulation**

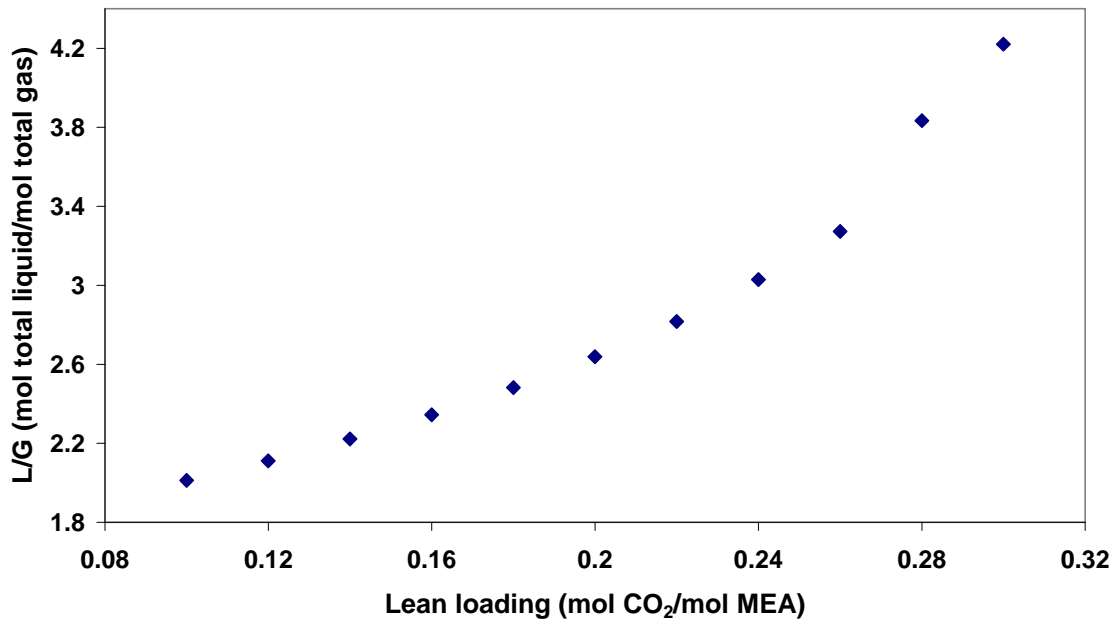


**Figure 3-9: Variation of L/G with lean loading for 85% CO<sub>2</sub> capture from coal flue gas; equilibrium simulation**

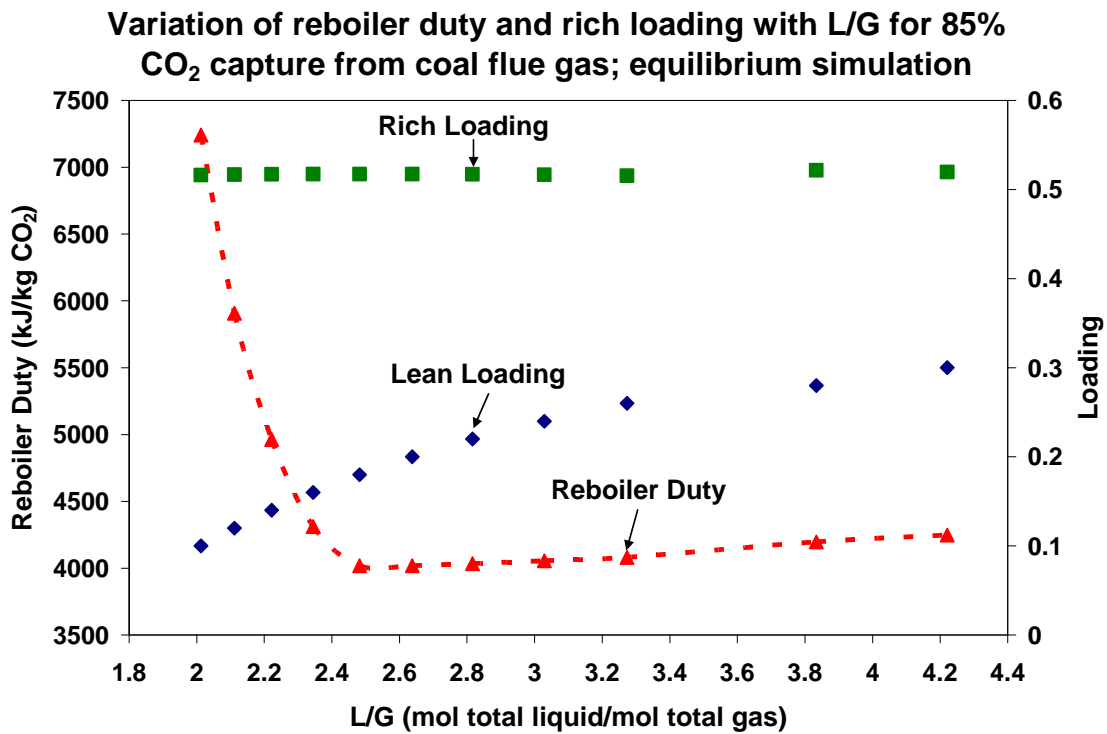


**Figure 3-10: Variation of reboiler duty and rich loading with L/G for 85% CO<sub>2</sub> capture from coal flue gas; equilibrium simulation**

In order to test the validity of the assumptions that reactions are at equilibrium in the absorber, simulations were performed including the kinetics of the reactions. In this case, the column was modeled as a series of equilibrium stages, but the kinetics of the reactions were incorporated. It was found that unrealistically large holdups needed to be specified in order to obtain results that approached the results from the equilibrium simulations. This clearly indicates that the chemical kinetics of the reactions are not fast enough to consider the reactions to be at equilibrium and that the kinetics need to be incorporated in the analysis.

In addition, it is not realistic to model the column as a set of equilibrium stages. It is necessary to take the mass transfer resistance and enhancement of mass transfer due to reaction into account and this is done by using the ASPEN RateSep module.

## 3.8 Rate-based modeling of the MEA system

ASPEN RateSep is a module within ASPEN Plus that allows the rate-based simulation of absorber and desorber columns. A detailed discussion of the models utilized in ASPEN RateSep has been provided in an earlier section. The modifications that were made for the MEA system are discussed in this section.

### 3.8.1 Film discretization

As detailed before, ASPEN RateSep allows a number of different ways of calculating the resistance in the vapor and liquid films. If the reaction is fast and the film is not discretized, RateSep will calculate the rate of reaction in the film based on the concentration at the interface. For the MEA system, since there are rapid reactions that occur in the liquid film, the *Discrxn* option was chosen for the liquid film. For the vapor film, the *Film* option was chosen, since there are no reactions, but the calculation of the mass transfer resistance was desired. In the MEA model, the film discretization is an important component in accurately modeling the performance of the system. Both the number of discretization points as well as the relative spacing of the points is important in order to calculate a representative rate of reaction within the film.

Since there is a rapid reaction in the film, it is necessary to have more discretization points at the boundary of the film than in the middle regions [31]. The number of discretization points needs to be optimized for solution stability and computational speed. Beyond a certain number of points, the solution does not change as the number of points is increased and this indicates that the calculated concentration profile in the film is constant. Hence, beyond this, by increasing the number of points, we would only be increasing the computational time without improving the accuracy of the solution. In order to determine the number of points required, a number of simulation runs were performed where all parameters in the system were kept constant except for the number of discretization points. The amount of CO<sub>2</sub> that was predicted to escape from the

absorber was noted and plotted against the number of discretization points. This graph is shown below in Figure 3-11.

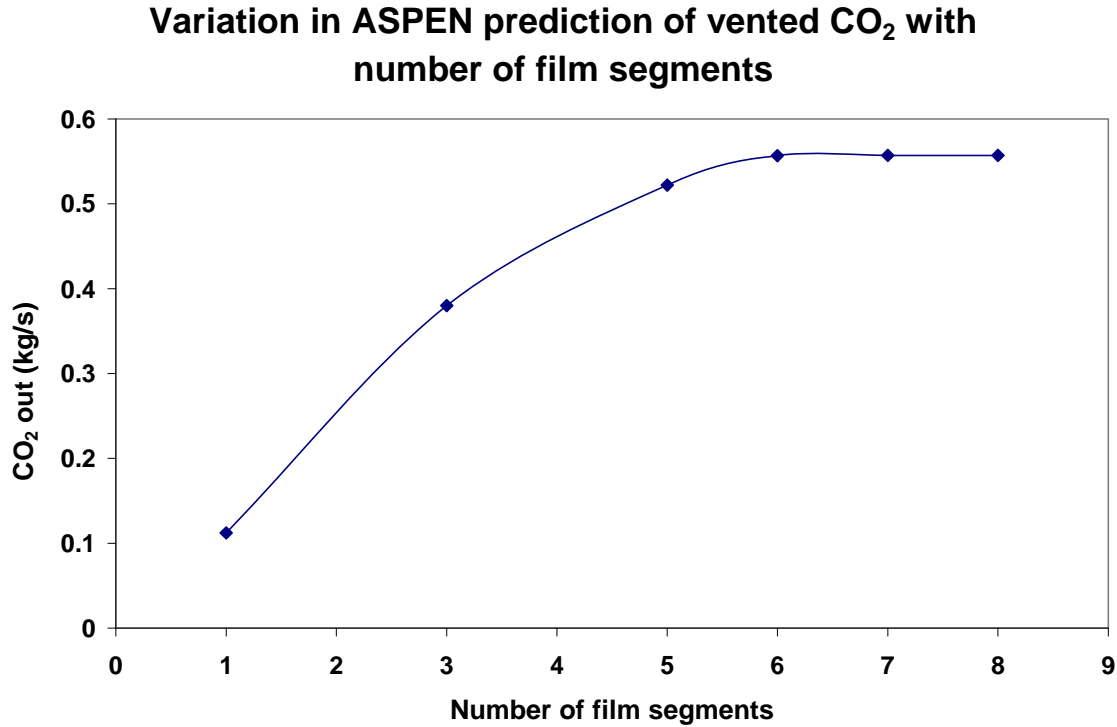


**Figure 3-11: Variation in ASPEN prediction of vented CO<sub>2</sub> with number of film segments**

As can be seen from Figure 3-11, upto 6 discretization points, the amount of CO<sub>2</sub> predicted to be vented increases as the discretization points increase. This is because when the number of points is lower, ASPEN calculates an artificially high rate of reaction in the film due to improper prediction of the concentration profile. Beyond 6 points, the solution is stable. Hence, at least 6 points are required in order to compute an accurate and stable solution. In our simulations, we decided to use 8 additional points for discretizing the film. The discretization points are given in Table 3-3.

**Table 3-3: Specified discretization points in the liquid film**

<b>Point</b>	<b>Non-dimensional distance from vapor side in the liquid film</b>
<b>1</b>	0.001
<b>2</b>	0.005
<b>3</b>	0.01
<b>4</b>	0.05
<b>5</b>	0.1
<b>6</b>	0.15
<b>7</b>	0.2
<b>8</b>	0.3

### **3.8.2 Sizing of equipment**

As part of the rate-based calculations in ASPEN RateSep, it is necessary to provide either the height of the column or the packed height per stage and the number of stages. The diameter of the column can either be provided or ASPEN can calculate it based on a fractional approach to maximum capacity. A design factor of 70% approach to flooding was chosen since this allows some safety factor in case operating conditions in the column change suddenly. Since the flowrate of flue gas from the power plant is very high, it was decided to divide the capture plant into 4 trains for the NGCC case and into 3 trains for the coal power plant case. This allowed the use of absorbers and strippers with diameters which are found in commercial units now. The range of diameters looked at was from 5-13m. The kinetics in the system were modeled as per the parameters set out by Kvamsdal et al [32-33].

### 3.8.2.1 Definition of parameters used in the simulation

The basic parameters used in the absorber and the desorber for the simulations are presented in Table 3-4 and Table 3-5 respectively. When parametric simulations were performed, these parameters were changed accordingly.

**Table 3-4: Values of parameters used in the absorber for the MEA system**

<b>Parameter</b>	<b>Value</b>
<b>Diameter</b>	12 m
<b>Height</b>	17 m
<b>Packing</b>	Norton IMTP Metal 1 in
<b>Lean solvent inlet temperature</b>	40°C
<b>Absorber pressure</b>	1 atm

**Table 3-5: Values of parameters used in the desorber of the MEA system**

<b>Parameter</b>	<b>Value</b>
<b>Diameter</b>	7 m
<b>Height</b>	15 m
<b>Packing</b>	Norton IMTP Metal 1 in
<b>Desorber pressure</b>	1.7 atm
<b>Solvent feed stage</b>	2 (above stage)
<b>Reflux feed stage</b>	1 (on stage)

### 3.9 Results from rate-based simulations for the MEA system

As with the equilibrium simulations, parametric simulations were run for flue gas from NGCC and coal-fired power plants. The first simulation was to investigate the effect of lean loading of the solvent on the reboiler duty. Figure 3-12 shows the results obtained for flue gas from NGCC and Figure 3-13 shows the results obtained for flue gas from coal-fired power plants.

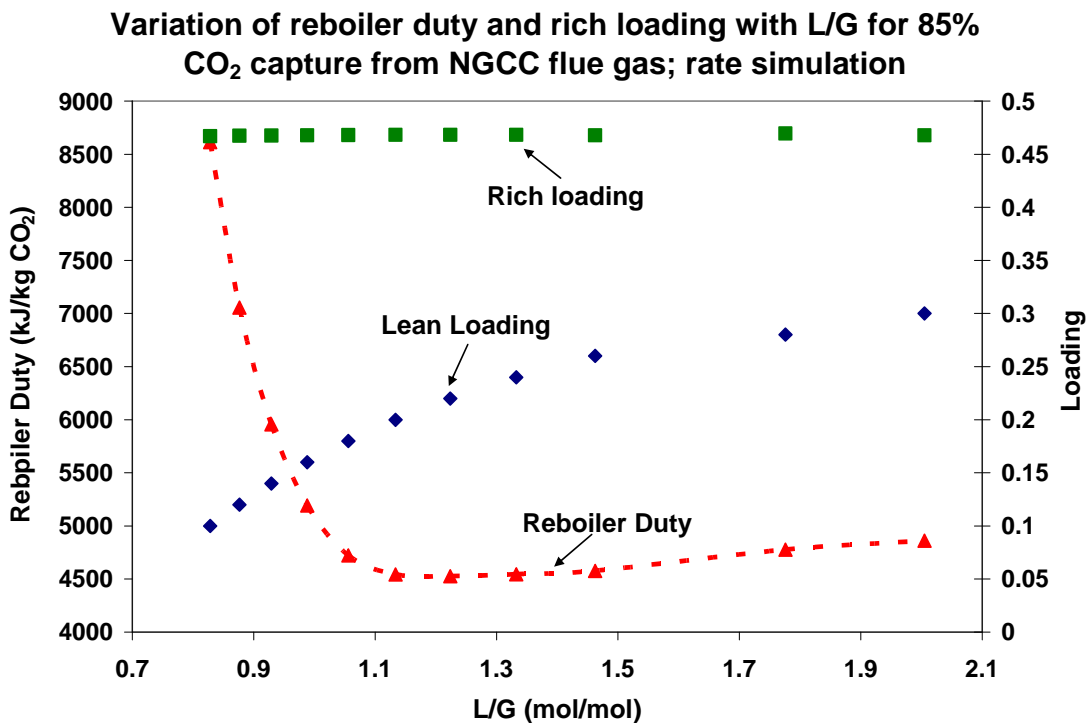


**Figure 3-12: Variation of reboiler duty and rich loading with L/G for 85% CO<sub>2</sub> capture from NGCC flue gas: rate simulation**

As can be seen from Figure 3-12, the same trend in reboiler duty with lean loading as observed in equilibrium simulations is observed with the rate based simulations as well. This is because of the trade-off between the sensible heat requirements and the heat

required to generate steam to maintain driving force for CO<sub>2</sub> transfer from liquid to the gas phase.

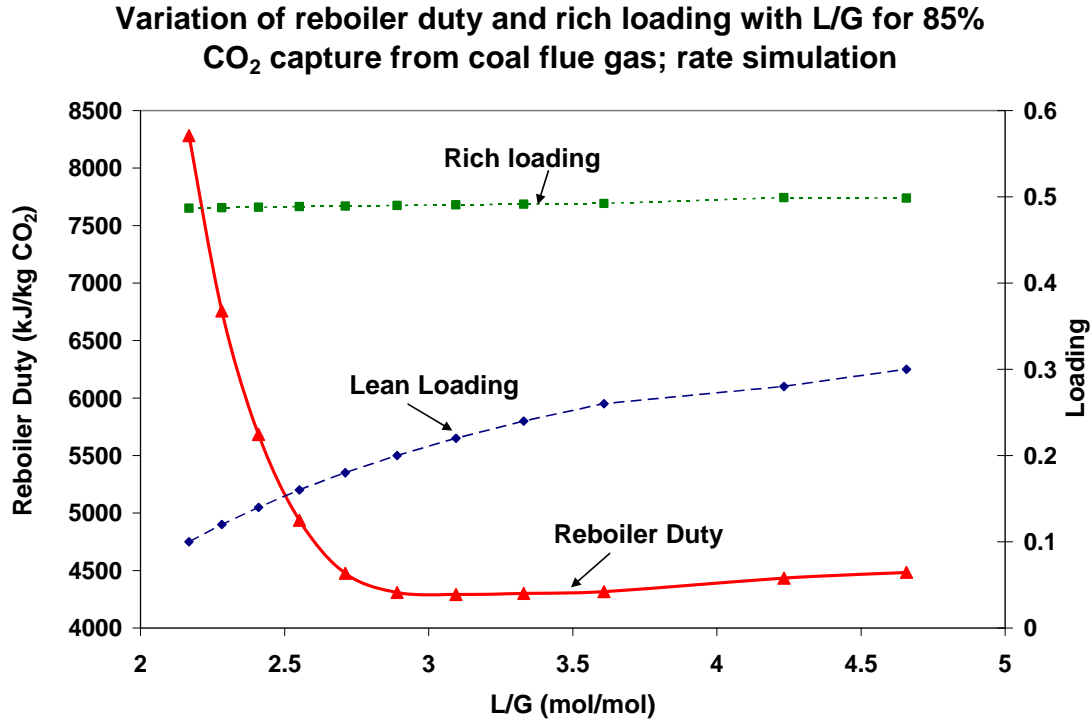


**Figure 3-13: Variation of reboiler duty and rich loading with L/G for 85% CO<sub>2</sub> capture from coal flue gas: rate simulation**

The predicted reboiler duties for the higher CO<sub>2</sub> content flue gas (coal-fired) are always higher than that predicted for flue gas from the NGCC plant. This is because the higher CO<sub>2</sub> content in the flue gas results in a higher driving force at the bottom of the absorber tower, where the amine solution is the most loaded and thus, the rich loading of the amine stream is higher in the case of the coal-fired power plant flue gas than it is in the NGCC flue gas. A higher rich loading leads to a lower steam requirement since the equilibrium partial pressure of CO<sub>2</sub> increases with loading and hence, there is less steam that leaves the desorber with the CO<sub>2</sub>. Figure 3-14 shows the predicted reboiler duties and rich loadings for coal-fired and NGCC flue gas.

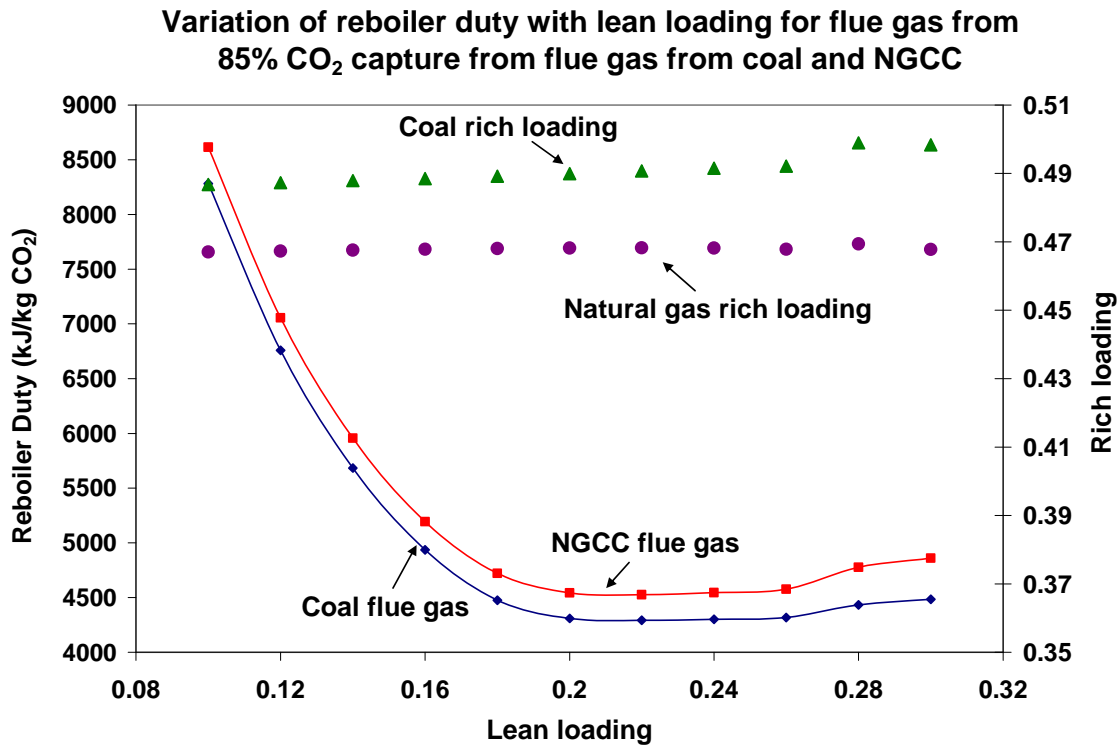


**Figure 3-14: Variation of reboiler duty with rich loading for 85% CO<sub>2</sub> capture from coal flue gas and NGCC flue gas; rate simulation**

In addition, we can compare the reboiler duties and rich loading obtained from the equilibrium and rate-based simulations. It is found that the reboiler duty predicted for the rate-based simulations is always higher than that predicted for the equilibrium simulations. This is to be expected since the equilibrium simulation predicts that the rich loading will always approach 0.5. However, the driving force that exists at the bottom of the column when the solution is highly loaded is small and hence, it is difficult to attain a rich loading of 0.5. Thus, the equilibrium simulation does not capture the driving force limitation that exists at the bottom of the column. Hence, rate-based simulations are required in order to model the system well and to accurately predict the energy consumption in the system. Figure 3-15 shows the comparison between reboiler duties

and rich loadings predicted by the equilibrium and rate-based simulations for flue gas from a NGCC plant.

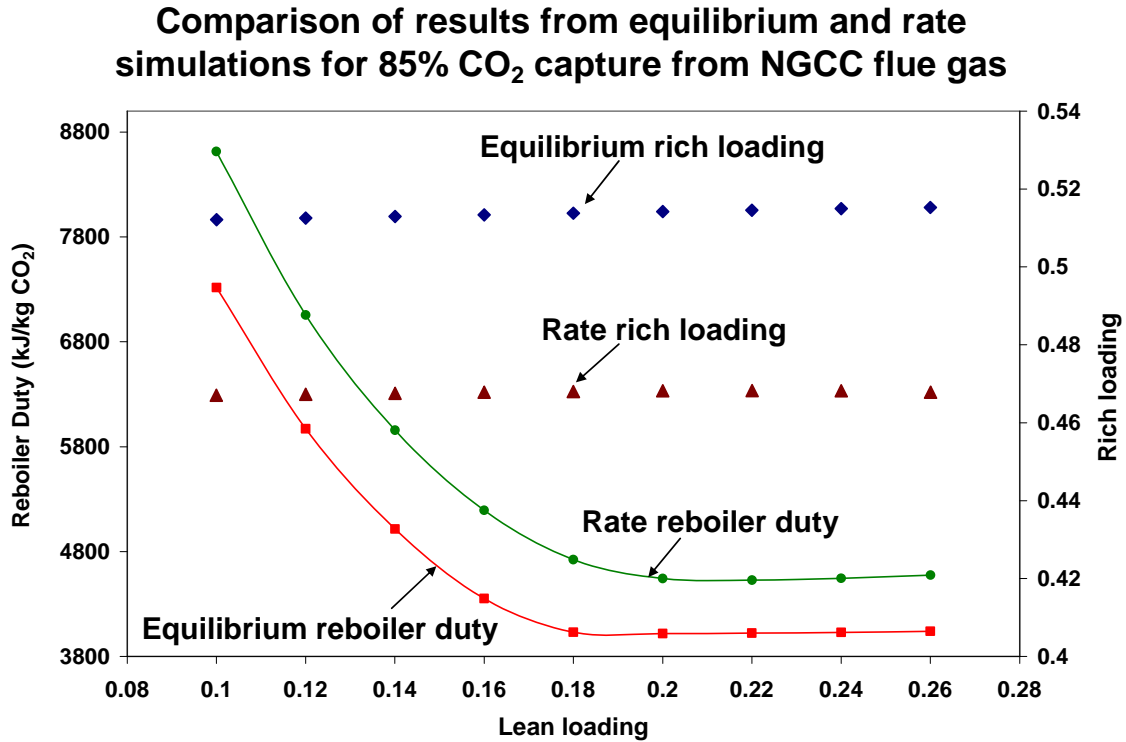


**Figure 3-15: Comparison of results from equilibrium and rate simulations for 85% CO<sub>2</sub> capture from NGCC flue gas**

Thus, the simulations predict a reboiler duty of 4500 kJ/kg CO<sub>2</sub> for natural gas and a duty of 4250 kJ/kg CO<sub>2</sub> for gas from a coal power plant. The difference between the two is due to the higher rich loading that can be obtained with the coal system. These results match very well with the reported results from the Fluor Econamine FG<sup>TM</sup> process which reports a value of 4200 kJ/kg CO<sub>2</sub> for flue gas from coal-fired power plants [1]. The PH4-33 report states a lower value but that is based on the Fluor Econamine FG Plus<sup>TM</sup> process which incorporates a better solvent formulation and significant heat integration [4].

### 3.9.1 Effect of capture percentage

The first set of parametric simulations was performed to investigate the effect of capture % on the reboiler duty. Capture extents of 65, 85 and 90% were investigated. The reboiler duty for different loadings was calculated for each of these capture extents. Figure 3-16 shows the variation in reboiler duty with lean loading for the different capture percentages for NGCC flue gas.

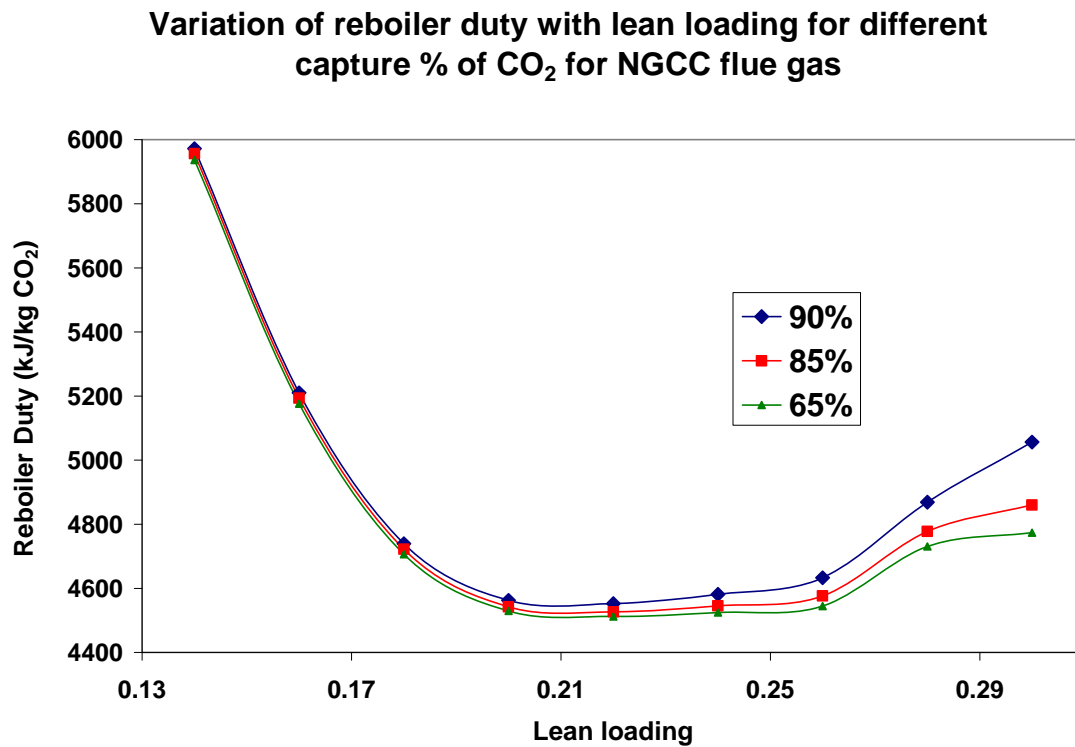


Figure 3-16: Variation of reboiler duty with lean loading for different capture percentages of CO<sub>2</sub> for NGCC flue gas

As can be seen from Figure 3-16, the reboiler duty per kg of CO<sub>2</sub> captured increases as the capture percentage increases. This is because, as the capture percentage increases, the solvent flowrate required increases and this increases the sensible heat requirements in the system. However, it should be noted that as the capture percentage decreases, the size

of the towers required will be lower due to the lower flowrates and hence, the overall cost will decrease.

### **3.9.2 Effect of packing**

ASPEN RateSep allows the use of different packings – both random and structured – in the column. The packing that is used, particularly in the absorber influences the reboiler duty, since the amount of surface area that is created is important in determining the final rich loading of the solvent. In this study, both random and structured packings were investigated. The random packing studied was the Norton IMTP Metal 25 mm packing. The structured packings investigated were the Sulzer MellaPak 752Y packing and the SuperPak Metal 300 packing. ASPEN uses different correlations to calculate the mass transfer coefficient and interfacial area depending on the packing employed. In our study, the Onda correlation [34] was employed for the Norton IMTP packing, the Bravo and Fair correlation (1985) [35] was utilized for the MellaPak packing and the Billet and Schultes correlation [36] was used for the SuperPak packing.

Each of the packings has a different specific surface area. As the surface area of the packings increase, the rich loading obtained increases and hence, the reboiler duty decreases. Figure 3-17 presents the variation of reboiler duty and rich loading with lean loading for each of the different packings for coal-fired power plant flue gas.

### Variation in reboiler duty and rich loading with lean loading for different packing types

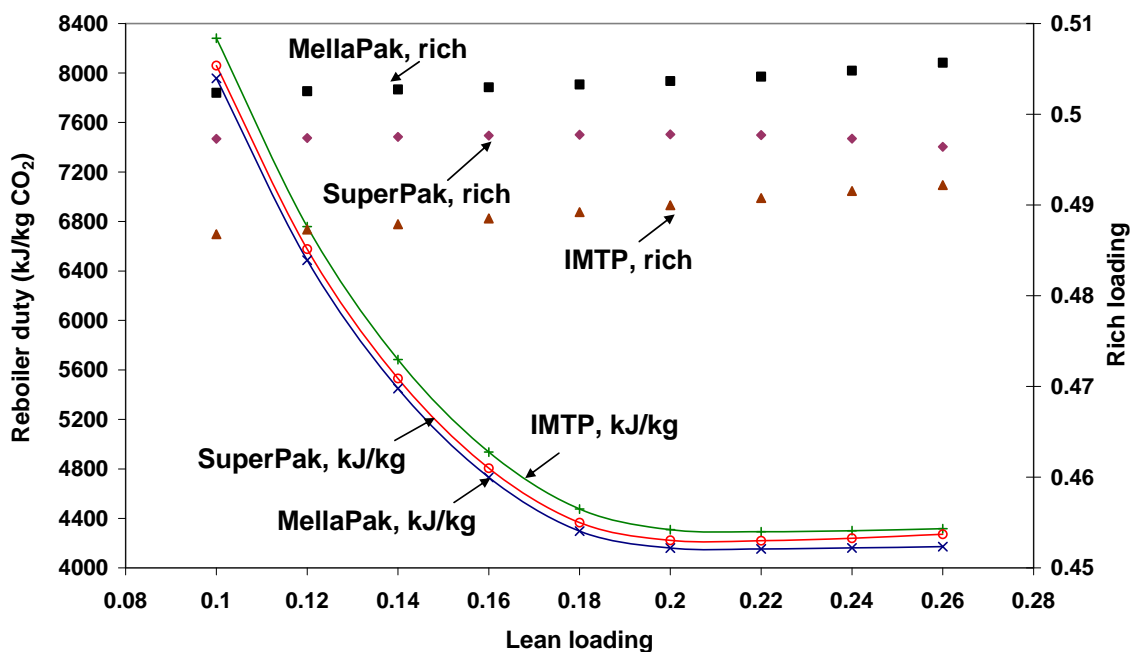


Figure 3-17: Variation in reboiler duty and rich loading with lean loading for different packing types

Table 3-6 presents the result that corresponds to the minimum reboiler duty for each of the packings as well as the specific surface area of each packing.

Table 3-6: Minimum reboiler duty obtained with different packings in the absorber

Packing	SA (sqm/cum)	Rich Load	Reboiler Duty (kJ/kg CO <sub>2</sub> )
IMTP Norton 25 mm	226	0.491	4292
SuperPak Metal 300	300	0.498	4219
MellaPak Sulzer 752Y	495	0.504	4152

It should be noted that as the packing specific surface area increases, the pressure drop in the column increases and the fractional approach to maximum capacity increases. Hence, the diameter of the column needs to be adjusted so that the column can operate in a loading zone. Thus, an economic optimization has to be performed between the cost of the packing and the attendant increase in size and pressure drop with the decrease in the reboiler duty to determine which packing should be used in the column.

### 3.9.3 Effect of absorber height

In order to study the effect of the absorber height on the energy consumption in the reboiler, the diameter of the column was kept constant and the absorber height was varied. As was expected, with increase in the absorber height, the attained rich loading increased and hence, the reboiler duty decreased. Figure 3-18 shows the variation of minimum reboiler duty with height of the absorber for NGCC flue gas.

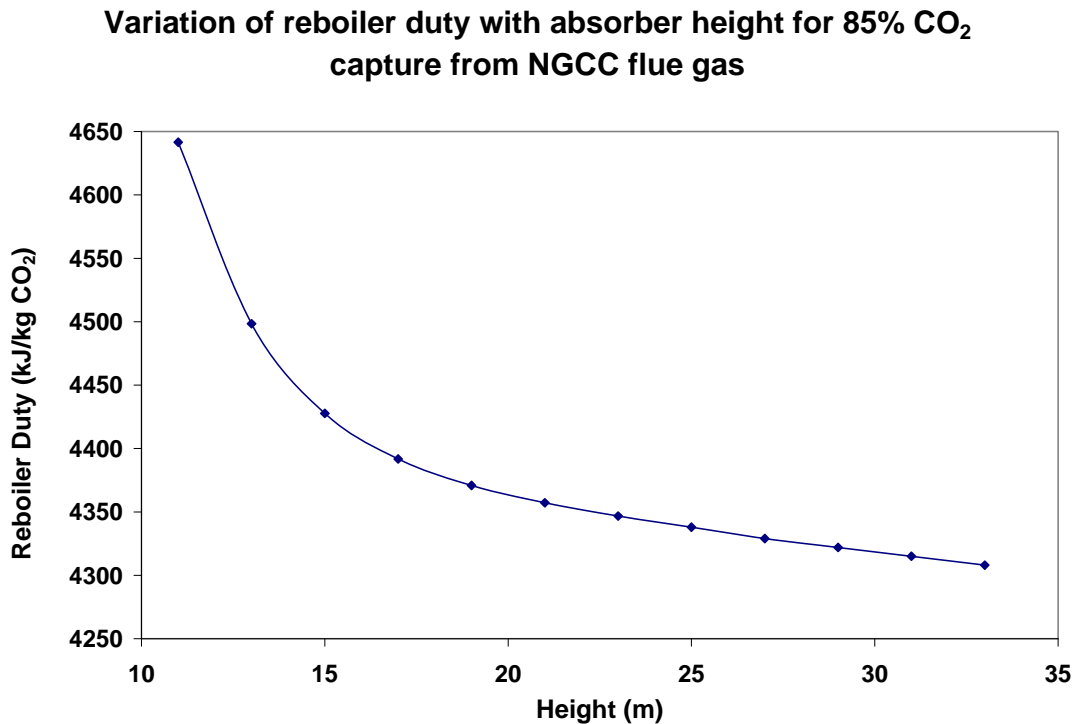


Figure 3-18: Variation in reboiler duty with absorber height for 85% CO<sub>2</sub> capture from NGCC flue gas

At each height, the simulation was performed for different lean loadings and the minimum reboiler duty attained for each height is shown in Figure 3-18. The minimum reboiler duty decreases with increase in height upto a certain height, beyond which there is not much effect of height on the reboiler duty. This is because, the rich loading does not increase significantly and hence the reboiler duty does not decrease. The increase in height of the absorber entails two additional costs:

1. Capital cost: As the height of the absorber increases, the capital cost of the equipment increases.
2. Power required in blower: The pressure drop in the absorber increases as the height of the absorber increases and hence, the power required in the blower will increase.

An optimization between these costs and the savings in the reboiler duty needs to be performed in order to arrive at the optimum height.

### **3.9.4 Effect of solvent temperature**

As the temperature of absorption decreases, the driving force for absorption increases. However, the rate of the reaction and diffusivity decrease as temperature is decreased. An analysis was performed to see the effect of temperature on the performance of the system. Simulations were run at solvent temperatures of 20, 30 and 40°C. The reboiler duty for these runs did not differ significantly. Hence, the temperature of the solvent does not have a significant effect on the performance of the system. This is mainly because the solvent has a low specific heat and it takes up the heat of absorption quickly. This causes the temperature of the solvent to rise upon reaction with CO<sub>2</sub> and negates the effect of having lower solvent temperature.

The absorber tends to exhibit a temperature bulge at the top of the column. There is a significant amount of reaction at the top of the column when the lean liquid enters. Due to the highly exothermic nature of the reaction, a lot of heat is released. The liquid takes

up this heat and since the liquid has low specific heat, its temperature rises. This causes the bulge at the top of the column. As the liquid proceeds down the column, it exchanges heat with the gas and hence gets cooled. Figure 3-19 shows the temperature profiles in the absorber for the liquid for coal fired flue gas.

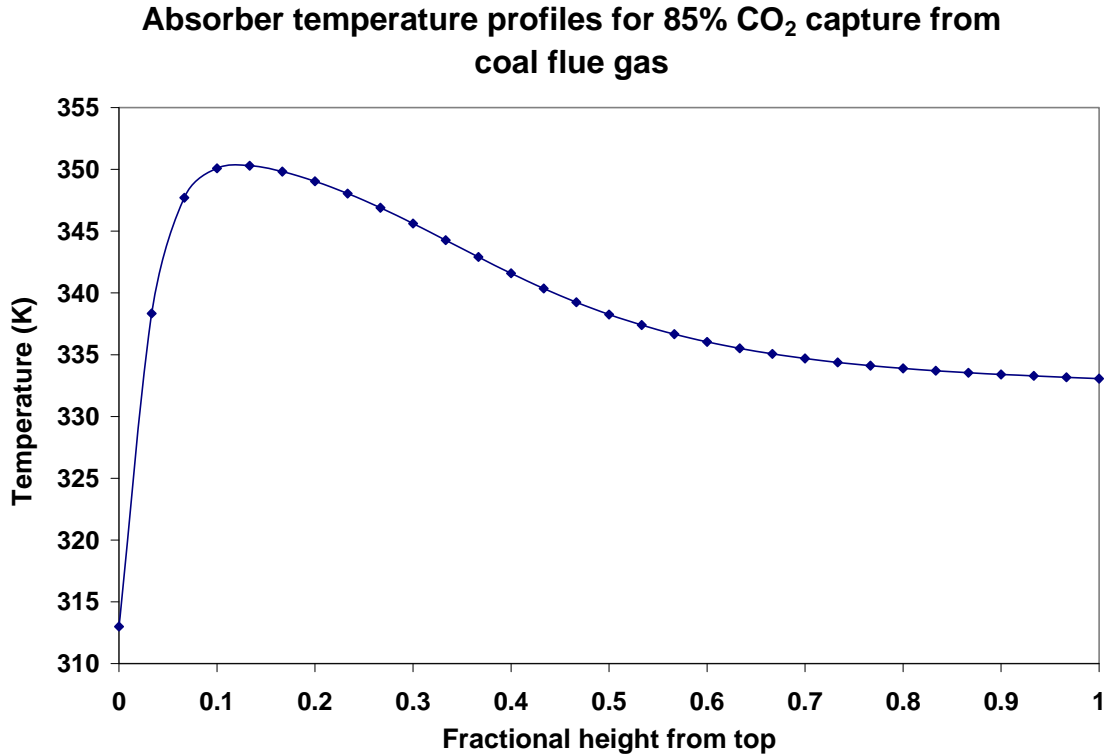


Figure 3-19: Absorber temperature profiles for 85% CO<sub>2</sub> capture from coal flue gas

### 3.9.5 Effect of desorber height

The absorber height and diameter and the desorber diameter were kept constant and the effect of desorber height on the reboiler duty was studied. It was found that the effect of the desorber height on the reboiler height was not very significant except at very low heights at which the desorber heat duty was very high.

### 3.9.6 Effect of desorber pressure

The pressure in the reboiler has a significant effect on the performance of the process. The pressure increase in the reboiler is accompanied by an attendant increase in the temperature. As the temperature increases, the conditions become favorable for transfer of CO<sub>2</sub> to the gas phase and hence, less steam is required to maintain the driving force for CO<sub>2</sub> transfer for every mole of CO<sub>2</sub>. Thus, it is favorable to operate the desorber at as high pressures and hence temperatures as possible. However, the operating conditions in the desorber are limited by the fact that the degradation of MEA is accelerated with increasing temperatures. A temperature of greater than 125°C in the reboiler is not recommended. The desorber needs to be operated at a pressure that corresponds to a temperature of 125°C or less in the reboiler. Figure 3-20 shows how the reboiler duty and temperature vary with pressure in the reboiler for NGCC flue gas.

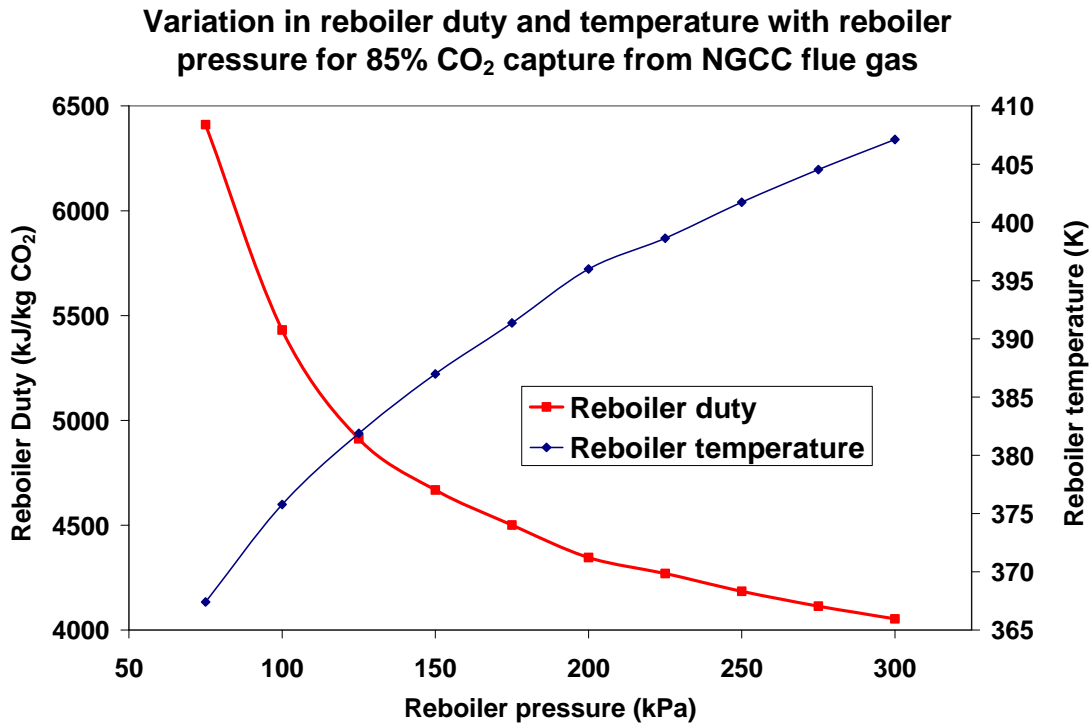


Figure 3-20: Variation in reboiler duty and temperature with reboiler pressure for 85% CO<sub>2</sub> capture from NGCC flue gas

The reboiler pressure that corresponds to a temperature of 125°C is around 170 kPa and this is the pressure that is used in the reboiler. As the reboiler pressure increases, it affects the total electric power consumption in two ways:

- 1. Power lost due to steam consumption in reboiler:** As the reboiler pressure and temperature increase, the temperature of steam used in the reboiler will also have to increase. Typically, steam that condenses at a temperature that is 10°C greater than the temperature in the reboiler is used so that the heat transfer area required is not too large. Thus, this means that as the reboiler pressure increases, the work lost due to steam extraction will increase due to the extraction of higher quality steam.
- 2. Compression power:** As the reboiler pressure increases, the power required for compressing the CO<sub>2</sub> to the discharge conditions decreases.

An analysis was performed to quantify the effect of these two factors at different pressures. The work lost due to steam extraction and the compression power were calculated for each reboiler pressure and added to give the total electric work required. Figure 3-21 shows how the total electric power consumption required varies as a function of the reboiler pressure for NGCC flue gas. As can be seen from Figure 3-21, the total electric power consumption decreases as the reboiler pressure increases. The decrease is steep until a pressure of approximately 1.25 atm. In the MEA system, a pressure of 1.7 atm was maintained in the reboiler. It should also be noted that at higher pressures, the material of construction used in the stripper may have to change to accommodate corrosion problems.

**Variation in electric work with reboiler pressure for 85% CO<sub>2</sub> capture from NGCC flue gas**

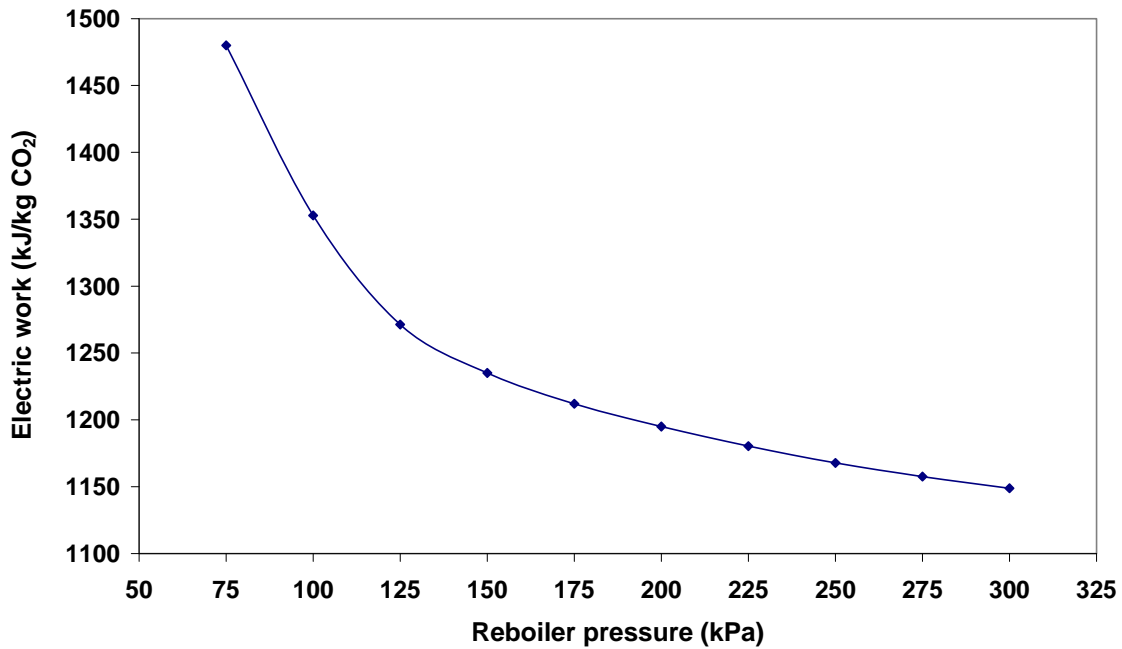


**Figure 3-21: Variation in electric work with reboiler pressure for 85% CO<sub>2</sub> capture from NGCC flue gas**

### **3.9.7 Breakdown of energy requirement in the reboiler**

Using ASPEN, it is possible to break down the energy requirement in the reboiler into the three components of heat of reaction, sensible heat and heat for steam production. The breakdown is shown in Figure 3-22.

The heat of desorption accounts for the biggest fraction of the energy requirements in the reboiler with the stripping steam and sensible heat requirement accounting almost evenly for the rest. A method to reduce the sensible heat requirement in the reboiler is to have a lower approach temperature in the cross-heat exchanger.

### Breakdown of energy requirements in reboiler

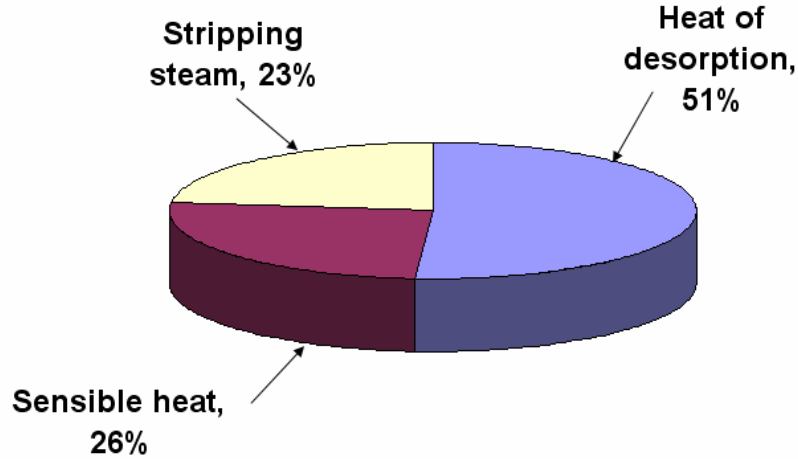
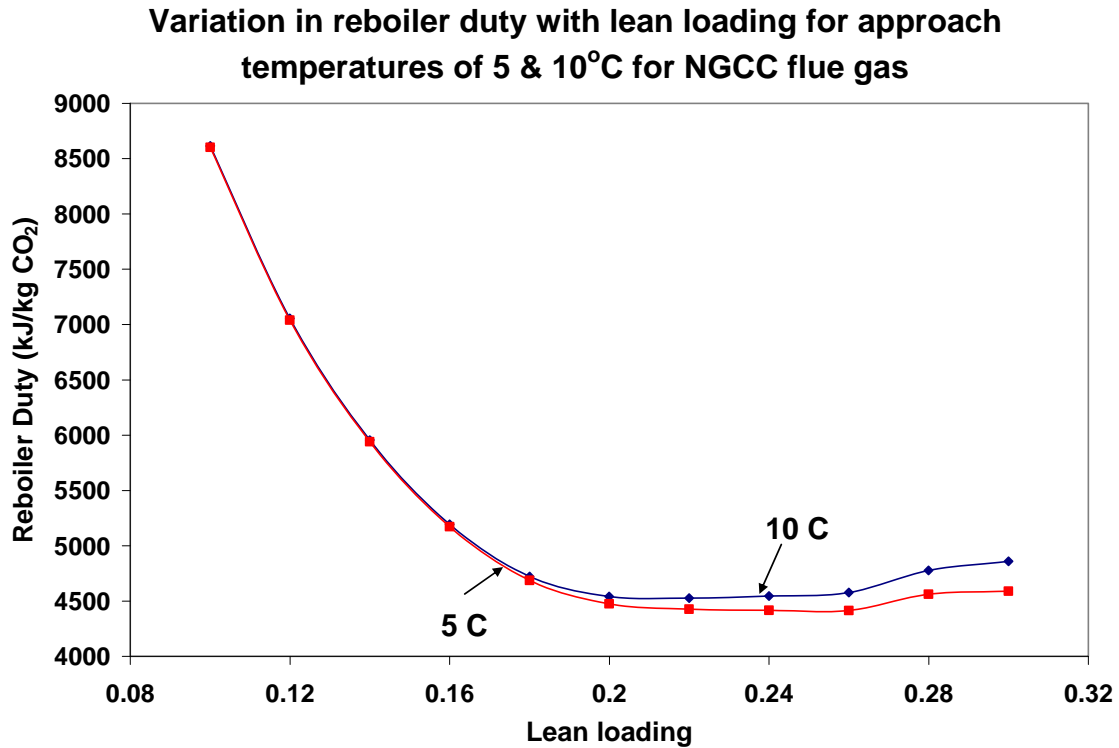


Figure 3-22: Breakdown of energy requirements in reboiler

### 3.9.8 Effect of cross-heat exchanger

The performance of the cross-heat exchanger is determined by the approach temperature on the cold side [37]. In the cross-heat exchanger, the pinch is more likely to occur on the cold side than on the hot side. This is because the flowrate of the lean stream is lower as is its sensible heat capacity.

In the base-case scenario, the cross-heat exchanger was modeled with an approach temperature of 10°C. If this approach temperature can be reduced, it will lead to lowering of the sensible heat requirements in the process. The heat exchanger is one of the main sources of A study was performed to vary the approach temperature and analyze the effect on the reboiler duty. Figure 3-23 presents the variation of reboiler duty with the approach temperature on the cold side for NGCC flue gas.



**Figure 3-23: Variation in reboiler duty with lean loading for approach temperatures of 5 and 10°C for NGCC flue gas**

Thus, the reboiler duty decreases by approximately 3% as the approach temperature decreases from 10°C to 5°C. However, this comes at the expense of greater surface area in the heat exchanger and hence, a cost optimization has to be performed to determine the feasibility of lowering the approach temperature.

### **3.9.9 Other methods of energy recuperation**

A number of different configurations have been explored for the energy recuperation in the MEA system. A succinct summary has been presented by Rochelle [38], in which the concepts of vapor recompression and multi-pressure stripper have been discussed. Vapor recompression aims to take advantage of the heat content of the water leaving the top of the desorber along with the CO<sub>2</sub>. The entire stream is compressed and for intercooling,

the reboiler bottoms is used. Thus, the amount of steam required in the reboiler is lower, but the compression duty will be higher. However, as shown by Jassim and Rochelle [39], there was no significant reduction in the total work in the system. They showed that the net effect of these configurations is to shift the energy use from heat to work.

### **3.10 Calculation of work for the MEA system**

In this section, the process of calculating the total work in the system is detailed. In the MEA process, the main components of energy consumption are:

1. Desorber steam requirement
2. CO<sub>2</sub> compressor
3. Blower
4. Auxiliaries

The steam that is used to provide heat in the reboiler of the desorber is extracted from the steam turbine in the power plant. The work that is lost by not having this steam pass through the turbines needs to be calculated. For this purpose, a turbine model is set up in ASPEN Plus to calculate the discharge conditions of the steam from the turbine [40]. In the reboiler, we need steam that condenses at approximately 135°C in order to provide a 10°C temperature difference across the reboiler tube. Using this saturation pressure, the discharge conditions for steam for a USC coal fired power plant and a NGCC plant can be calculated. The discharge conditions as calculated for our configurations are detailed in Table 3-7. Using these values, the work that is lost because of reboiler energy requirements can be calculated. In Table 3-7, the % power lost refers to the percentage of electric power that is lost from the plant due to the extraction of steam with the base case plant being an ultra supercritical plant for the coal-fired power plant case. When steam is extracted for use in the reboiler, the power plant output lost is less than the heat content of the steam because not all of the heat content of the steam would have been converted to power. [41]. The percentage of power lost from the power plant is calculated as per the

guidelines set out by Bolland and Undrum [41]. The compression work in the system is calculated in ASPEN Plus, by first compressing the CO<sub>2</sub> stream to 90 atm and then pumping the stream to the discharge conditions.

**Table 3-7: Steam withdrawal conditions for coal and NGCC plants for use in reboiler of MEA system**

Steam conditions	Coal	Natural gas
Saturation pressure (bar)	3.5	3.5
Saturation temperature (°C)	138.87	138.87
Withdrawal temperature (°C)	241	292
% power lost from power plant due to steam extraction	18.24%	22.96%

### 3.11 Total work for CO<sub>2</sub> capture and compression for NGCC plants

The work required for the different power sinks in CO<sub>2</sub> capture from NGCC plants is shown in Table 3-8.

**Table 3-8: Total work in CO<sub>2</sub> capture system in NGCC plants**

Power sink	Work (kWh/gmol CO <sub>2</sub> )
Reboiler steam	0.0126
CO <sub>2</sub> compressor	0.0043
Blower and auxiliaries	0.0070
Total	0.0239

Thus, the total work required for CO<sub>2</sub> capture and compression in a NGCC plant with MEA is 0.0239 kWh/gmol CO<sub>2</sub>. The energy requirements in the reboiler are the major component, though the energy consumption in the blower and auxiliaries is also significant. The breakdown of the total work into the work required in the desorber, in compression as well as in blower and auxiliary requirements is shown in Figure 3-24.

### Breakdown of energy consumption in NGCC plant

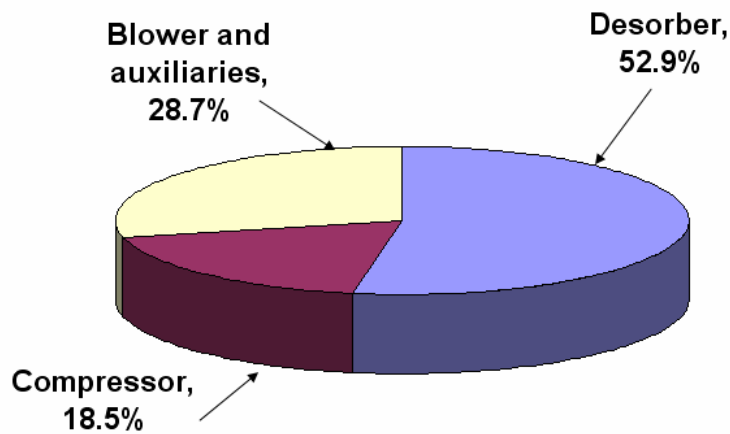


Figure 3-24: Breakdown of energy consumption in CO<sub>2</sub> capture system of NGCC plant

### 3.12 Total work for CO<sub>2</sub> capture and compression in coal-fired power plants

The work required for the different power sinks in CO<sub>2</sub> capture from a coal-fired power plant is shown in Table 3-9. The breakdown of the total work into the work required in the desorber, in compression as well as in blower and auxiliary requirements is shown in Figure 3-25.

**Table 3-9: Total work in CO<sub>2</sub> capture system in coal-fired power plants**

Power sink	Work (kWh/gmol CO <sub>2</sub> )
Reboiler steam	0.00936
CO <sub>2</sub> compressor	0.0044
Blower and auxiliaries	0.00196
<b>Total</b>	<b>0.01572</b>

**Breakdown of energy requirement for coal-fired power plants**

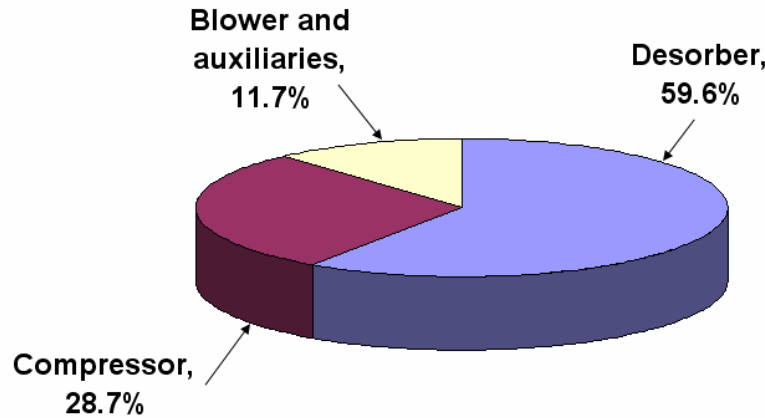


**Figure 3-25: Breakdown of total energy requirement for coal-fired power plants**

Thus, the total work required for CO<sub>2</sub> capture and compression in a coal-fired power plant with MEA is 0.0157 kWh/gmol CO<sub>2</sub>. The energy requirements in the reboiler are the major component. As compared to the NGCC plant with capture, the energy requirements in the compressor are much higher. The work per gmol CO<sub>2</sub> is lower in the coal-fired power plant because the higher CO<sub>2</sub> content in the flue gas leads to a lower energy requirement in the reboiler. The overall derating of the power plant is higher for the coal-fired power plant than for the NGCC case. Figure 3-26 and Figure 3-27 compare

the energy requirement for CO<sub>2</sub> capture in a NGCC and coal-fired power plant respectively. Thus, the derating for the natural gas fired power plant with MEA is 17% while the derating of the coal-fired power plant is 23%.

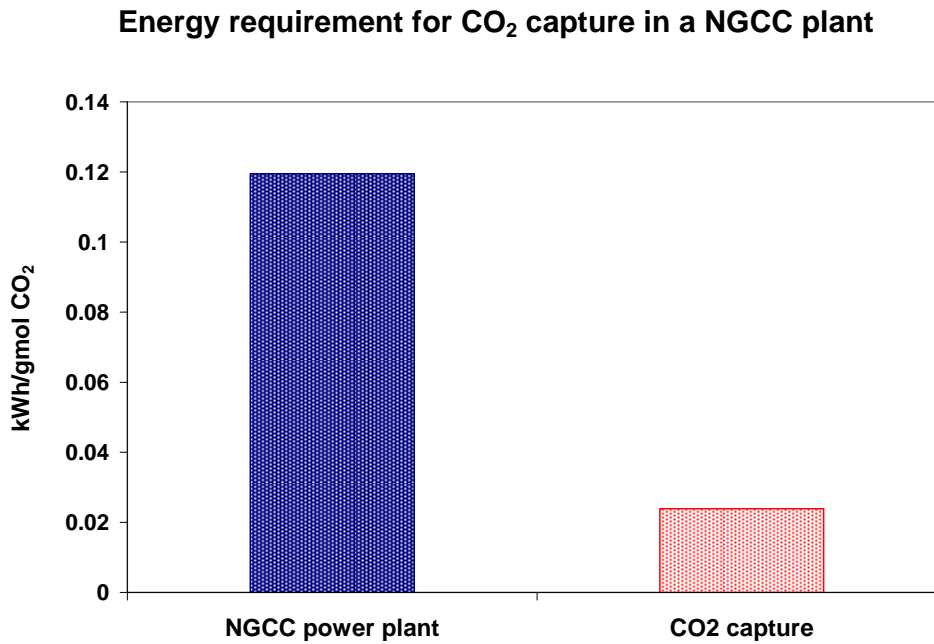


**Figure 3-26: Energy requirement for CO<sub>2</sub> capture in a NGCC plant**

The energy requirements for CO<sub>2</sub> capture in a NGCC plant compare well with values reported in literature for similar plants [1, 4, 18]. The derating of the NGCC plant is in the range of 16-19% and that for the coal-fired power plant is in the range of 22-28%.

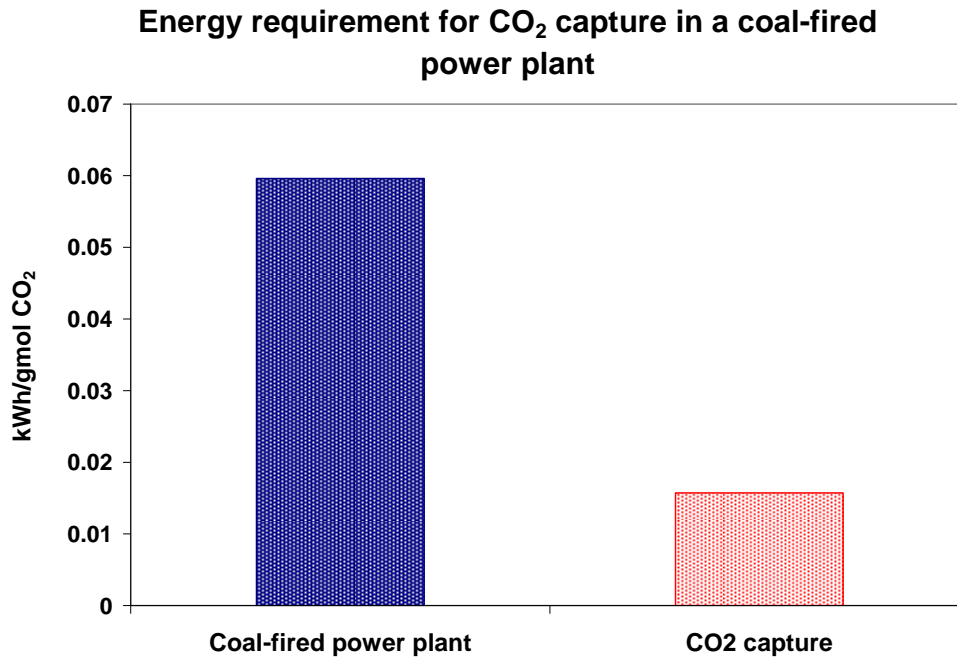


**Figure 3-27: Energy requirement for CO<sub>2</sub> capture in a coal-fired power plant**

### **3.13 MEA conclusion**

In this chapter, the details of the MEA system have been presented. Rate-based simulations for the absorption of CO<sub>2</sub> from NGCC and coal-fired power plants into MEA have been developed in ASPEN. The simulations show that the energy penalty for CO<sub>2</sub> capture from flue gas from coal-fired power plants is 0.01572 kWh/gmol CO<sub>2</sub> and from NGCC plants is 0.02388 kWh/gmol CO<sub>2</sub>. This leads to a derating of 17% for the NGCC plant and 24% for the coal-fired power plant. The importance of using rate-based simulations was demonstrated. The simulations were rigorous and were developed with the RateSep module in ASPEN and incorporated film discretization. Different factors that influence the performance of the system such as the lean loading, packing and height of the absorber and desorber, temperature in the absorber, pressure in the desorber and capture percentage were investigated. The possibility of energy recuperation in the MEA

system was also looked at. These simulations represent one of the few attempts to model the rate behavior of the system with the correct thermodynamic representation in ASPEN.

With the MEA system, the main factors that limit a significant reduction in energy consumption are the kinetics and the lack of process flexibility in the reboiler due to degradation considerations. If the kinetics are enhanced, it would be possible to increase the rich loading and hence, decrease the reboiler duty. Hence, an activated MEA system could be considered in order to improve the performance of the system.

### 3.14 References

1. Chapel, D. and Ernst J., *Recovery of CO<sub>2</sub> from Flue Gases: Commercial Trends*, in *Canadian Society of Chemical Engineers Annual Meeting*. 1999: Saskatchewan, Canada.
2. Reddy, S., D. Johnson, and J. Gilmartin, *Fluor's Econamine FG Plus<sup>SM</sup> Technology for CO<sub>2</sub> Capture at Coal-fired Power Plants*, in *Power Plant Air Pollutant Control "Mega" Symposium*. 2008: Baltimore, MD.
3. Reddy, S., J. Scherffius, S. Freguia, and R. C., *Fluor's Econamine FG Plus<sup>SM</sup> Technology: An Enhanced Amine-Based CO<sub>2</sub> Capture Process*, in *Second National Conference on Carbon Sequestration*. 2003: Alexandria, VA.
4. IEA Greenhouse Gas R&D Programme, *Improvement in power generation with post-combustion capture of CO<sub>2</sub>*. 2004.
5. Rao, A., E. Rubin, and M. Berkenpas, *An Integrated Modeling Framework for Carbon Management Technologies - Volume 1 - Technical Documentation: Amine Based CO<sub>2</sub> Capture and Storage Systems for Fossil Fuel Power Plant*, C.M.U. Department of Engineering and Public Policy, Editor. 2004.
6. Kohl, A.L. and F.C. Riesenfeld, *Gas Purification*. 5th edition ed, ed. A.L. Kohl and F.C. Riesenfeld. 1997, New York: Elsevier. 1439.
7. IPCC, *IPCC Special Report on Carbon Dioxide Capture and Storage*, B. Metz, et al., Editors. 2005.
8. VGB PowerTech, *CO<sub>2</sub> Capture and Storage: VGB Report on the State of the Art*. 2004.
9. Augsten, D.M., *A model for vapor-liquid equilibria for acid gas-alkanolamine-H<sub>2</sub>O systems*, in *Chemical Engineering*. 1989, University of Texas at Austin: Austin.
10. Caplow, M., *Kinetics of carbamate formation and breakdown*. *Journal of the American Chemical Society*, 1969. **90**(24): p. 6795-6803.
11. Kumar, P.S., J.A. Hogendoorn, G.F. Versteeg, and P.H.M. Feron, *Kinetics of the reaction of CO<sub>2</sub> with aqueous potassium salt of taurine and glycine*. *Aiche Journal*, 2003. **49**(1): p. 203-213.

12. Crooks, J.E. and J.P. Donnellan, *Kinetics and Mechanism of the Reaction between Carbon-Dioxide and Amines in Aqueous-Solution*. Journal of the Chemical Society-Perkin Transactions 2, 1989(4): p. 331-333.
13. Versteeg, G.F., L.A.J. Van Dijck, and W.P.M. Van Swaaij, *On the kinetics between CO<sub>2</sub> and alkanolamines both in aqueous and non-aqueous solutions. An overview*. Chemical Engineering Communications, 1996. **144**: p. 113-158.
14. Da Silva, E.F. and H.F. Svendsen, *Ab initio study of the reaction of carbamate formation from CO<sub>2</sub> and alkanolamines*. Industrial and Engineering Chemistry Research, 2004. **43**(13): p. 3413-3418.
15. Aboudheir, A., P. Tontiwachwuthikul, A. Chakma, and R. Idem, *Kinetics of the reactive absorption of carbon dioxide in high CO<sub>2</sub>-loaded, concentrated aqueous monoethanolamine solutions*. Chemical Engineering Science, 2003. **58**(23-24): p. 5195-5210.
16. Rochelle, G., S. Bishnoi, S. Chi, H. Dang, and J. Santos, *Research Needs for CO<sub>2</sub> Capture from Flue Gas by Aqueous Absorption/Stripping*. 2001, University of Texas at Austin: Austin.
17. Jou, F.Y., A.E. Mather, and F.D. Otto, *The solubility of CO<sub>2</sub> in a 30 mass percent monoethanolamine solution*. Can. J. Chem. Eng., 1995. **73**.
18. Freguia, S., *Modeling of CO<sub>2</sub> Removal from Flue Gases with Monoethanolamine*, in *Chemical Engineering*. 2002, University of Texas at Austin: Austin.
19. Goff, G.S. and G.T. Rochelle, *Oxidation inhibitors for copper and iron catalyzed degradation of monoethanolamine in CO<sub>2</sub> capture processes*. Industrial & Engineering Chemistry Research, 2006. **45**(8): p. 2513-2521.
20. Chakma, A. and A. Meisen, *Degradation of Aqueous DEA Solutions in a Heat-Transfer Tube*. Canadian Journal of Chemical Engineering, 1987. **65**(2): p. 264-273.
21. Dawodu, O.F. and A. Meisen, *Degradation of alkanolamine blends by carbon dioxide*. Canadian Journal of Chemical Engineering, 1996. **74**(6): p. 960-966.
22. Goff, G.S., *Oxidative degradation of aqueous monoethanolamine in CO<sub>2</sub> capture processes: iron and copper catalysis, inhibition and O<sub>2</sub> mass transfer*, in *Chemical Engineering*. 2005, University of Texas: Austin.
23. Sexton, A. and G.T. Rochelle, *Oxidation products of amines in CO<sub>2</sub> capture*, in *Eighth International Conference on Greenhouse Gas Control Technologies*. 2006: Trondheim, Norway.

24. Veawab, A. and A. Aroonwilas, *Identification of oxidizing agents in aqueous amine-CO<sub>2</sub> systems using a mechanistic corrosion model*. Corrosion Science, 2002. **44**(5): p. 967-987.
25. Veawab, A., P. Tontiwachwuthikul, and A. Chakma, *Corrosion behavior of carbon steel in the CO<sub>2</sub> absorption process using aqueous amine solutions*. Industrial & Engineering Chemistry Research, 1999. **38**(10): p. 3917-3924.
26. Supap, T., R. Idem, A. Veawab, A. Aroonwilas, P. Tontiwachwuthikul, A. Chakma, and B.D. Kybett, *Kinetics of the oxidative degradation of aqueous monoethanolamine in a flue gas treating unit*. Industrial and Engineering Chemistry Research, 2001. **40**(16): p. 3445-3450.
27. Chi, S. and G.T. Rochelle, *Oxidative degradation of monoethanolamine*. Industrial & Engineering Chemistry Research, 2002. **41**(17): p. 4178-4186.
28. Bello, A. and R.O. Idem, *Comprehensive study of the kinetics of the oxidative degradation of CO<sub>2</sub> loaded and concentrated aqueous monoethanolamine (MEA) with and without sodium metavanadate during CO<sub>2</sub> absorption from flue gases*. Industrial & Engineering Chemistry Research, 2006. **45**(8): p. 2569-2579.
29. Bello, A. and R.O. Idem, *Pathways for the formation of products of the oxidative degradation of CO<sub>2</sub>-loaded concentrated aqueous monoethanolamine solutions during CO<sub>2</sub> absorption from flue gases*. Industrial & Engineering Chemistry Research, 2005. **44**(4): p. 945-969.
30. Goff, G.S. and G.T. Rochelle, *Monoethanolamine degradation: O<sub>2</sub> mass transfer effects under CO<sub>2</sub> capture conditions*. Industrial & Engineering Chemistry Research, 2004. **43**(20): p. 6400-6408.
31. Kucka, L., I. Müller, E.Y. Kenig, and A. Górak, *On the modelling and simulation of sour gas absorption by aqueous amine solutions*. Chemical Engineering Science, 2003. **58**(16): p. 3571-3578.
32. Kvamsdal, H.M. and G.T. Rochelle, *Effects of the temperature bulge in CO<sub>2</sub> absorption from flue gas by aqueous monoethanolamine*. Industrial & Engineering Chemistry Research, 2008. **47**(3): p. 867-875.
33. Kvamsdal, H.M., *Personal Communication*. 2007.
34. Onda, K., H. Takuechi, and Y. Okumoto, *Mass transfer coefficients between gas and liquid phases in packed column*. J. Chem. Eng. Jap., 1968. **1**.
35. Bravo, J.L., J.A. Rocha, and J.R. Fair, *Mass transfer in gauze packings*. Hydrocarbon Processing, 1985(January).

36. Billet, R. and M. Schultes, *Predicting Mass Transfer in Packed Columns*. Chem. Eng. Technol., 1993. **16**: p. 1.
37. Tobiesen, F.A., H.F. Svendsen, and K.A. Hoff, *Desorber Energy Consumption Amine Based Absorption Plants*. International Journal of Green Energy, 2005(2).
38. Rochelle, G., *Innovative Stripper Configurations to Reduce the Energy Cost of CO<sub>2</sub> Capture*, in *Second Annual Carbon Sequestration Conference*. 2003: Alexandria, VA.
39. Jassim, M.S. and G.T. Rochelle, *Innovative Absorber/Stripper Configurations for CO<sub>2</sub> Capture by Aqueous Monoethanolamine*. Industrial & Engineering Chemistry Research, 2005. **45**(8): p. 2465-2472.
40. Nord, L.O., *Personal Communication*. 2009.
41. Bolland, O. and H. Undrum, *A novel methodology for comparing CO<sub>2</sub> capture options for natural gas-fired combined cycle plants*. Advances in Environmental Research, 2003. **7**: p. 901-911.

## Chapter 4

### Potassium Carbonate System

The absorption of carbon dioxide by ‘hot’ potassium carbonate was first demonstrated by Benson in 1954 [1]. This process was proposed in order to remove CO<sub>2</sub> from synthesis gas manufactured for Fischer-Tropsch synthesis. Since the synthesis gas was available at higher pressures, it was beneficial to employ a CO<sub>2</sub> absorption process that operated at higher pressures as well. Hence, it was proposed to use hot, concentrated alkaline solutions of potassium carbonate under pressure. It was decided to investigate this process as part of this thesis since it could potentially have very useful applications in pressurized combustion and reforming processes such as IRCC.

#### 4.1 Process description

Benson [1] performed solubility studies on the K<sub>2</sub>CO<sub>3</sub>-KHCO<sub>3</sub>-CO<sub>2</sub> system and found that the use of a 60% solution was prohibitive near 120°C (boiling point) because precipitation occurred at a bicarbonate conversion of only 35%. The 50% solution was also not useful, because near the boiling point of 113 C, precipitation takes place when the conversion to bicarbonate exceeded 48%. However, with a 40% solution, precipitation did not take place at 107 C (boiling point) until a bicarbonate conversion of 90%. Hence, it is feasible to employ a 40 or 45% K<sub>2</sub>CO<sub>3</sub> solution if the conversion to bicarbonate does not exceed 90 or 80% respectively.

A flow diagram for a typical hot potassium carbonate process is shown in Figure 4-1. In the potassium carbonate process, the absorber typically operates at high pressures (> 10 atm). At these high pressures, there is sufficient driving force in the absorber for transfer of CO<sub>2</sub> from the gas phase to the liquid phase. The process operates at a high temperature (> 100 °C) and CO<sub>2</sub> is absorbed at nearly the same temperature as it is desorbed. Thus, the need for cooling the flue gas before entry into the absorber is eliminated as is the need

for cross-heat exchanger between the absorber and desorber. Upon introduction into the desorber, the solution flashes, releasing dissolved  $\text{CO}_2$  and some steam. This results in some cooling of the solution. Hence, some steam needs to be supplied in the desorber for providing sensible heat to the solution. This sensible heat requirement however is much lower than that in the amine process. In addition, since the heat of reaction of  $\text{CO}_2$  with  $\text{K}_2\text{CO}_3$  is much lower than with MEA, the overall heat duty is lower in the process.

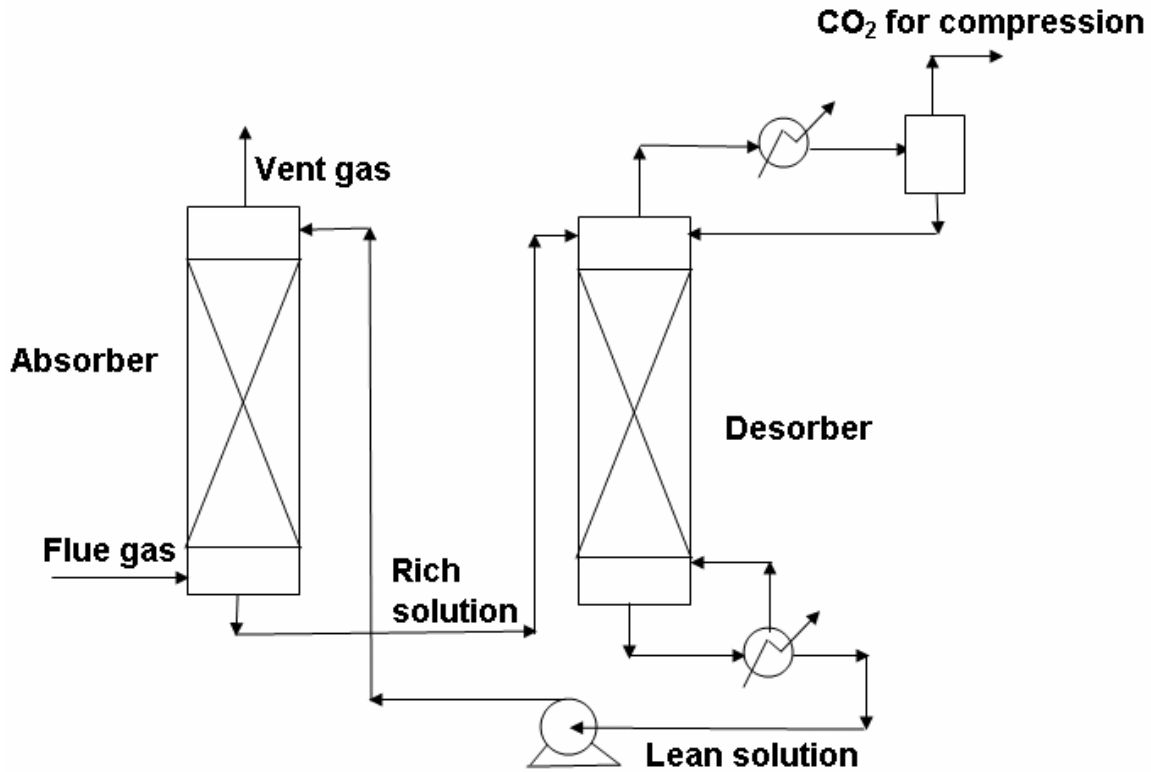


**Figure 4-1: Process flowsheet for a typical potassium carbonate process**

Since potassium carbonate is not volatile, there are minimal losses of the solvent with the exit gas. In addition, since potassium carbonate is not prone to the degradation reactions associated with MEA, there is no loss of solvent associated with degradation.

## 4.2 Chemistry of the potassium carbonate system

The overall reaction when carbon dioxide is absorbed in a solution of potassium carbonate and potassium bicarbonate is given by (4-1) [2].



Potassium carbonate and potassium bicarbonate are both strong electrolytes and hence, the metal will be present only in the ionic form. Thus (4-1) can be represented as (4-2).



Reaction (4-2) is trimolecular and is made up of a number of elementary steps. Carbon dioxide can undergo two direct reactions in an alkaline solution [3].



Both of these reactions are accompanied with the instantaneous dissociation of water.



The prevailing chemical reactions are hence (4-3), (4-4) and (4-5). Reactions (4-4) and (4-5) are instantaneous reactions and hence it is reaction (4-3) that is the rate controlling step for absorption of  $\text{CO}_2$  [3].

In ASPEN, the equilibrium constants of the reactions are calculated with a temperature dependence as:

$$\ln K_x = A + \frac{B}{T} + C \cdot \ln T + D \cdot T \quad (4-6)$$

The values of the parameters A, B, C and D for the reactions are built into ASPEN and are shown in Table 4-1.

**Table 4-1: Values of parameters of equilibrium constants for the potassium carbonate system**

Reaction	A	B	C	D
$CO_2 + 2H_2O \leftrightarrow H_3O^+ + HCO_3^-$	231.465437	-12092.1	-36.7816	0
$HCO_3^- + H_2O \leftrightarrow CO_3^{2-} + H_3O^+$	216.050437	-12431.7	-35.4819	0

### 4.3 Vapor-liquid equilibrium in $K_2CO_3$ - $H_2O$ - $CO_2$ system

Tosh et al. [4] performed studies to determine the equilibrium behavior of the  $K_2CO_3$ - $KHCO_3$ - $CO_2$ - $H_2O$  system at various temperatures (343 to 413 K) and concentrations (20, 30 and 40 wt.%) of  $K_2CO_3$ . Flash calculations were performed in ASPEN to obtain the VLE results embedded in ASPEN. Calculations were performed for 40 wt.%  $K_2CO_3$  at temperatures of 70, 90, 110 and 130°C. Figure 4-2 shows a comparison of the results from ASPEN with those obtained experimentally by Tosh [4-5].

As can be seen from Figure 4-2, there is significant deviation in the ASPEN values from those obtained experimentally. The deviation is particularly significant at higher temperatures and loadings. The higher temperature condition is important since the solution will remain at a temperature close to 110°C (boiling point of 40 wt.% solution)

**Experimental and ASPEN default VLE for  $K_2CO_3$ - $CO_2$ - $H_2O$  system (40 wt%  $K_2CO_3$ )**

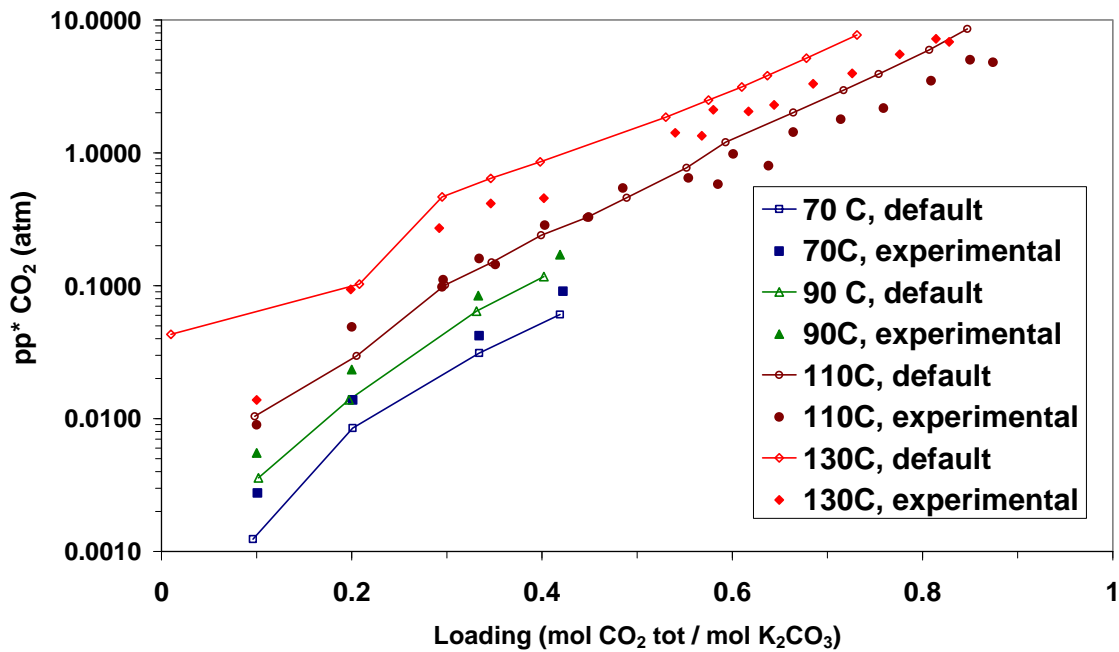


**Figure 4-2: Comparison of ASPEN default & experimental VLE for the  $K_2CO_3$ - $CO_2$ - $H_2O$  system (40 wt.% eq. $K_2CO_3$ ) at 70, 90, 110 and 130 °C. Experimental data from [4] via [5]**

Cullinane [2] and Hilliard [5] have investigated the representation of VLE behavior of this system in ASPEN using the ENRTL model and regressed values for the temperature-dependent interaction parameters. In his analysis, Cullinane [2] only used the VLE data of Tosh et al. [4] to regress the parameters. This may not provide an accurate representation of all the interactions in the systems especially since there can be significant experimental errors in the VLE measurements. Hilliard [5] in his analysis uses data from a number of sources to regress the values of the interaction parameters. In particular, Hilliard used the following sources of data:

- For the  $H_2O - K_2CO_3$  system, the mean ionic activity coefficient data of Aseyev and Zaystev [6], the water vapor pressure depression data of Aseyev [7] and Puchkov and Kurochkina [8] and calorimetry data of Aseyev and Zaystev [6]

were regressed. The data provided a range of temperatures from 298 to 403 K and 0.014 to 50 wt.%  $K_2CO_3$  solutions.

- For the  $H_2O-KHCO_3$  system, the vapor pressure depression data of Aseyev [7] and calorimetry data of Aseyev and Zaystev [6] was regressed. The data provided a range of temperature from 278 to 403 K.
- For the  $K_2CO_3-H_2O-CO_2$  system, the VLE data of Tosh et al. [4] was regressed.

Utilizing the regressed values from Hilliard [5], the modified VLE for the system was calculated in ASPEN Plus and is shown in Figure 4-3.

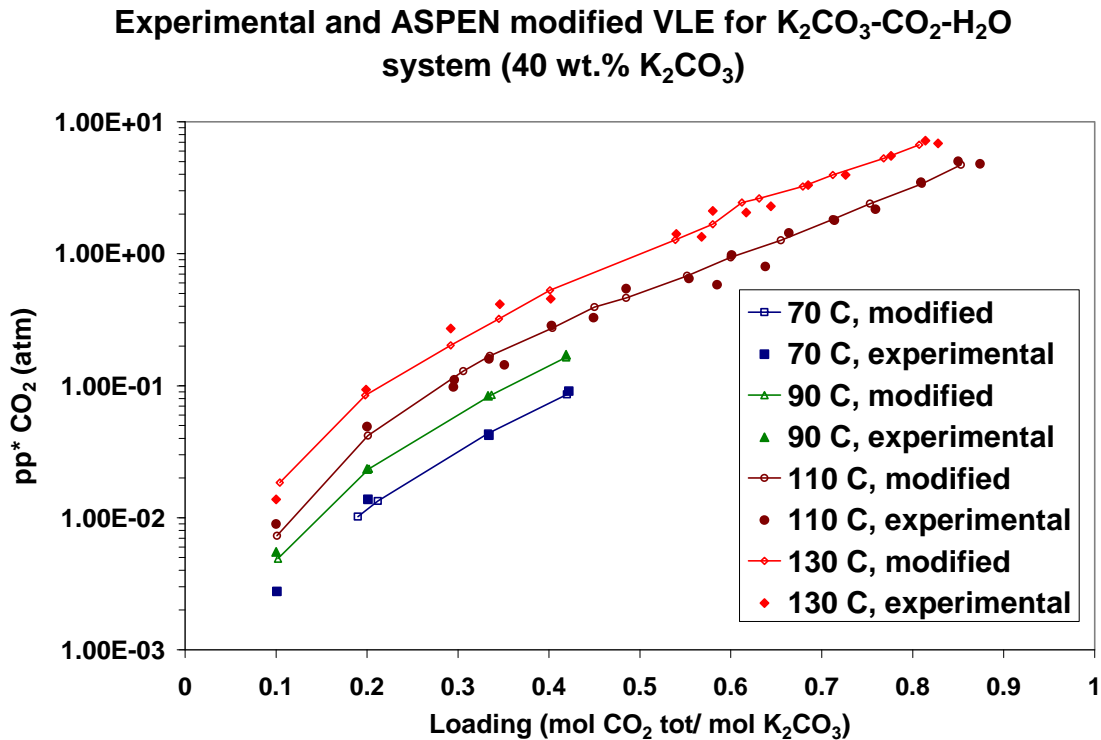


**Figure 4-3: Comparison of ASPEN modified & experimental VLE for the  $K_2CO_3-CO_2-H_2O$  system (40 wt.% eq. $K_2CO_3$ ) at 70, 90, 110 and 130 °C. Experimental data from [4] via [5]. Modified interaction parameters in ASPEN from [5]**

Thus, utilizing the modified parameters gives a much better representation of the VLE of the system and these parameters were used in the rest of the analyses.

For the definition of loading as referred to in the VLE diagrams, the following formula is used:

$$Loading = \frac{[\text{Moles of HCO}_3^-] - ([\text{Initial moles of CO}_3^{2-}] - [\text{Final moles of CO}_3^{2-}])}{([\text{Moles of K}^+]/2)} \quad (4-7)$$

In this definition, the numerator is the total number of moles of CO<sub>2</sub> absorbed by the solution. HCO<sub>3</sub><sup>-</sup> is formed by the absorption of CO<sub>2</sub> and the dissociation of CO<sub>3</sub><sup>2-</sup>. The difference gives the moles of CO<sub>2</sub> absorbed. The denominator represents the moles of K<sub>2</sub>CO<sub>3</sub> if all of the potassium existed as K<sub>2</sub>CO<sub>3</sub>. Hence, this definition can also be represented as:

$$Loading = \frac{[\text{Total moles of CO}_2 \text{ absorbed}]}{[\text{Moles of K}_2\text{CO}_3]} \quad (4-8)$$

This was the chosen form for the VLE diagrams since the data of Tosh [4] was available in this format. However, in the rest of this document, the following definition of loading is used since it facilitates and easy comparison with MEA.

$$Loading = \frac{[\text{Moles of CO}_3^{2-}] + [\text{Moles of HCO}_3^-] + [\text{Moles of CO}_2]}{[\text{Moles of K}^+]} \quad (4-9)$$

#### **4.4 Difference in mode of operation between MEA and K<sub>2</sub>CO<sub>3</sub> systems**

In MEA, the absorption-desorption was essentially driven by the temperature swing between the absorber and the desorber due to the high heat of absorption of CO<sub>2</sub> with MEA. The equilibrium partial pressure of CO<sub>2</sub> over a loaded solution of MEA is very different between 60°C and 120°C as shown in Figure 3-5 and it is this difference that is

exploited for the separation of CO<sub>2</sub> from the loaded solution. In the case of K<sub>2</sub>CO<sub>3</sub>, the effect of temperature on the partial pressure is not as pronounced as shown in Figure 4-3. This is because of the low heat of absorption of CO<sub>2</sub> in K<sub>2</sub>CO<sub>3</sub>. Since temperature swing absorption-desorption would not work effectively in the potassium carbonate system, the mode of operation is by pressure swing. Figure 4-4 shows the equilibrium partial pressure of CO<sub>2</sub> over loaded MEA and K<sub>2</sub>CO<sub>3</sub> solutions at different pressures.

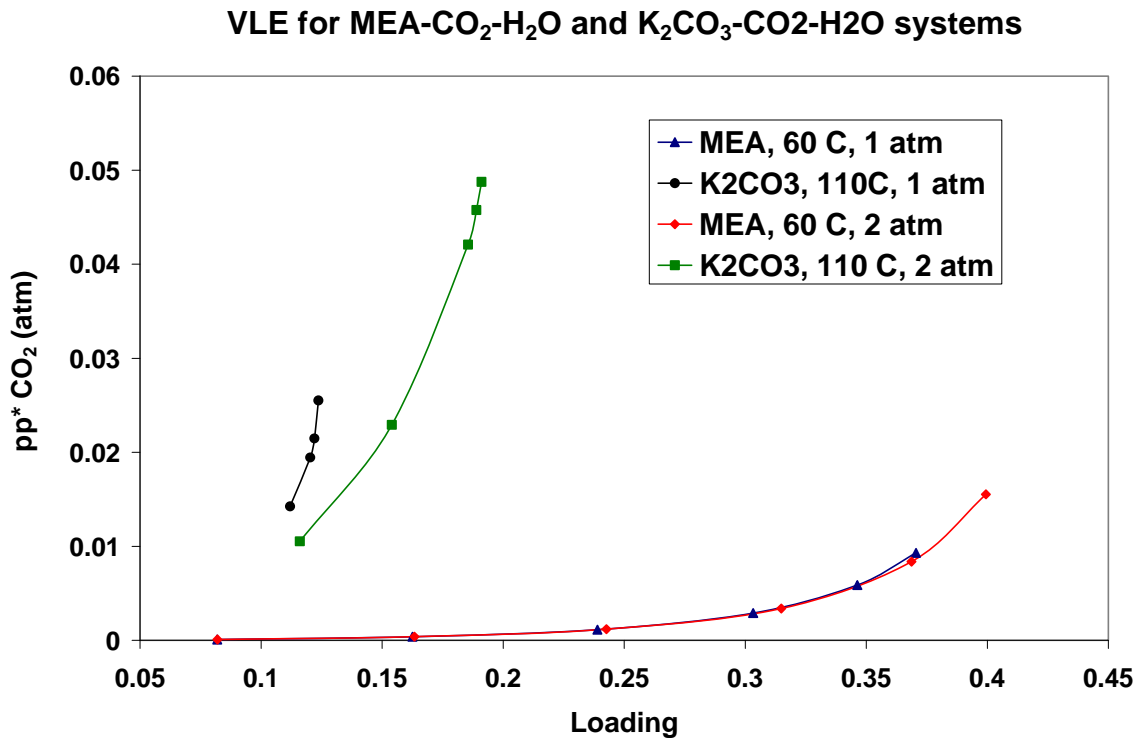


**Figure 4-4: Comparison of VLE of MEA-CO<sub>2</sub>-H<sub>2</sub>O system and K<sub>2</sub>CO<sub>3</sub>-CO<sub>2</sub>-H<sub>2</sub>O system**

While the effect of system pressure on the equilibrium pressure of CO<sub>2</sub> over the K<sub>2</sub>CO<sub>3</sub> system is significant, it is negligible in the case of the MEA system. As the pressure increases, the equilibrium partial pressure of CO<sub>2</sub> over the K<sub>2</sub>CO<sub>3</sub> system decreases. This difference is used to perform the absorption-desorption cycle in the K<sub>2</sub>CO<sub>3</sub> system. In order to provide a sufficient driving force for absorption, the absorber needs to be

operated at a high pressure. From the figure it can be seen that the equilibrium partial pressure of CO<sub>2</sub> over K<sub>2</sub>CO<sub>3</sub> is much higher than that over MEA at 1 atm. This necessitates a higher pressure in the absorber. The higher pressure provides sufficient driving force to push the reaction forward in the absorber and attain higher loadings which are essential to maintaining the capacity of the solution.

## 4.5 Flowsheet development for potassium carbonate system

For the purpose of parametric simulations, the simulation was developed as an open-loop flowsheet in ASPEN. The basic version of the flowsheet used is shown in Figure 4-5.

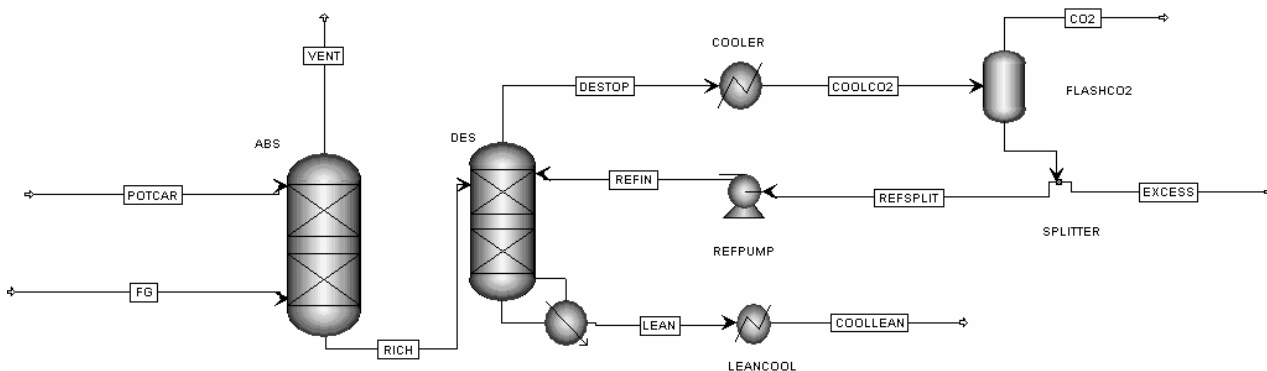


**Figure 4-5: Flowsheet as developed in ASPEN Plus for the potassium carbonate system**

As with the MEA system, there were design specifications on the inlet flowrate of the solvent to the absorber to ensure the required amount of capture and on the reboiler duty such that the composition of the regenerated solvent matches that of the input to the absorber. The absorber and desorber were modeled as packed towers. In all the simulations, a 40 wt. % eq. K<sub>2</sub>CO<sub>3</sub> solution was used.

### 4.5.1 Effect of absorber pressure

In order to determine a suitable absorber pressure to be used in the simulations, it was decided to run the absorber at different pressures to see the effect on the liquid solvent flowrate required to achieve 85% capture and the rich solvent loading that could be attained. Figure 4-6 shows how these quantities change with the absorber pressure.

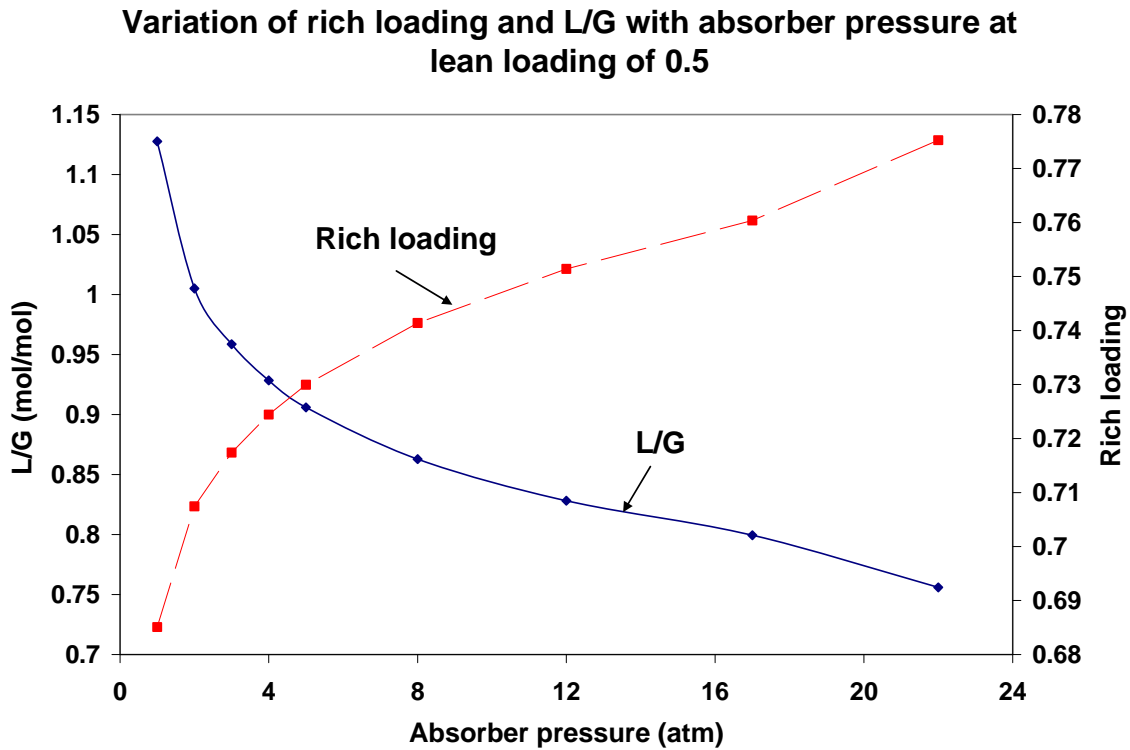


**Figure 4-6: Variation of rich loading and L/G with absorber pressure at a constant lean loading of 0.5 for the potassium carbonate system; equilibrium simulation**

As the absorber pressure increases, the driving force for absorption increases and hence the rich loading of the solution increases. This causes the required solvent flowrate to decrease. Based on this, it was decided to use a pressure of 15 atm for the analysis.

## 4.6 Equilibrium results with 40 wt. % eq.K<sub>2</sub>CO<sub>3</sub>

Equilibrium simulations were performed in ASPEN Plus for the absorption of CO<sub>2</sub> in aqueous K<sub>2</sub>CO<sub>3</sub>. These simulations were performed only for coal-fired power plant flue gas since it was found that the low CO<sub>2</sub> content of natural gas-fired power plant flue gas would make it unsuitable for operation with the K<sub>2</sub>CO<sub>3</sub> system. The absorber and desorber were modeled as RADFRAC columns with a number of equilibrium stages with all the reactions assumed to be at equilibrium. Figure 4-7 shows the variation in reboiler duty and L/G with lean loading for 85% capture and an absorber pressure of 15 atm.

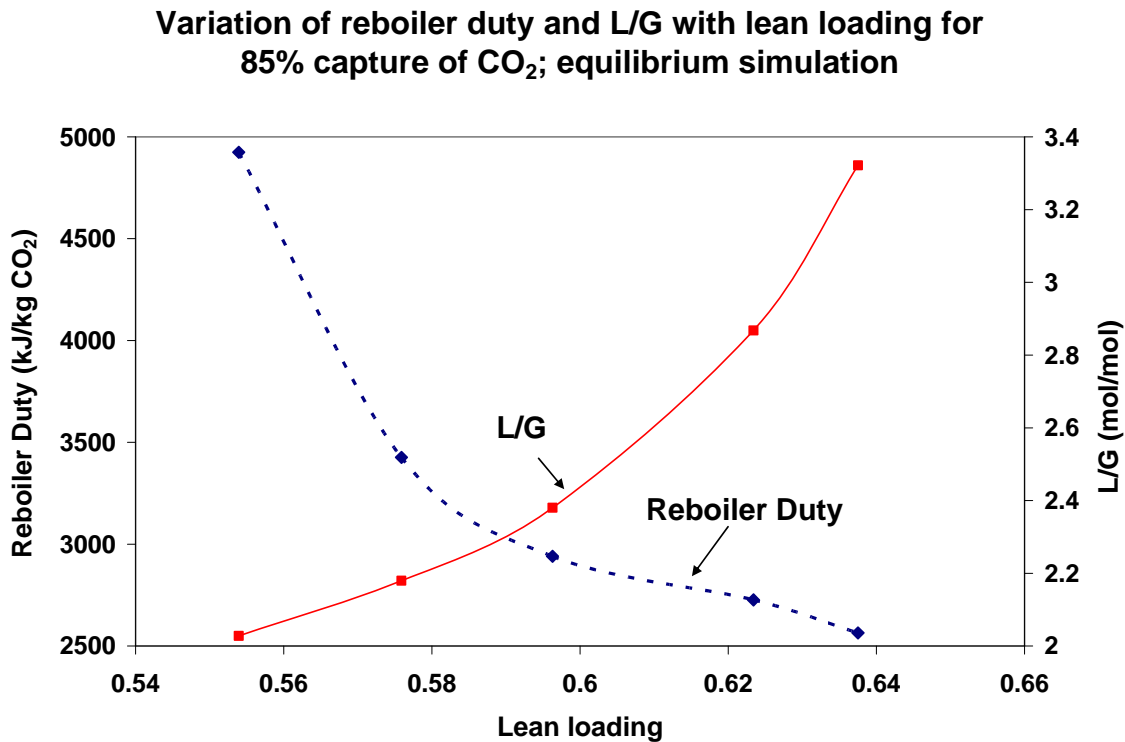


**Figure 4-7: Variation of reboiler duty and L/G with lean loading for 85% capture of CO<sub>2</sub>; equilibrium simulation**

The reactions of CO<sub>2</sub> with K<sub>2</sub>CO<sub>3</sub> have intrinsically fast kinetics. However, because the concentration of the reactive species is low, the rate of reaction is low and assuming that

the reactions proceed to equilibrium is not realistic. It is necessary to perform rate based modeling in order to obtain an accurate representation of the system.

## 4.7 Rate-based modeling of the potassium carbonate system

This section describes the various settings and values of hydrodynamic parameters that were employed in the rate-based modeling of the potassium carbonate system.

### 4.7.1 Film discretization

For the rate-based modeling of the  $K_2CO_3$  system ASPEN RateSep was used with the same film discretization and sizing considerations as in the MEA system. It was found that the use of 10 additional points was necessary in the film discretization in order to obtain a good representation of the reaction in the film. The position of these points is given in Table 4-2.

**Table 4-2: Location of discretization points in the liquid film**

<b>Point</b>	<b>Non-dimensional distance from vapor side in the liquid film</b>
1	0.0001
2	0.0003
3	0.0005
4	0.001
5	0.007
6	0.009
7	0.01
8	0.03
9	0.05
10	0.07

#### 4.7.2 Definition of parameters used in the rate-based simulation

The basic parameters used in the absorber and the desorber for the simulations are presented in Table 4-3 and Table 4-4 respectively. When parametric simulations were performed, these parameters were changed accordingly.

**Table 4-3: Values of parameters used in the absorber of the potassium carbonate system**

<b>Parameter</b>	<b>Value</b>
<b>Diameter</b>	12 m
<b>Height</b>	20 m
<b>Packing</b>	Norton Raschig Metal 10 mm
<b>Lean solvent inlet temperature</b>	80°C
<b>Absorber pressure</b>	15 atm

**Table 4-4: Values of parameters used in the desorber of the potassium carbonate system**

<b>Parameter</b>	<b>Value</b>
<b>Diameter</b>	13 m
<b>Height</b>	18 m
<b>Packing</b>	Norton Raschig Metal 6 mm
<b>Desorber pressure</b>	1 atm
<b>Solvent feed stage</b>	2 (above stage)
<b>Reflux feed stage</b>	1 (on stage)

## 4.8 Results from rate-based simulation of the potassium carbonate system

Rate-based simulations were performed in ASPEN Plus using the parameters detailed above. All the simulations were performed with 40 wt.% eq.  $K_2CO_3$  solution. Figure 4-8 shows the variation of reboiler duty and rich loading as the lean loading is changed.

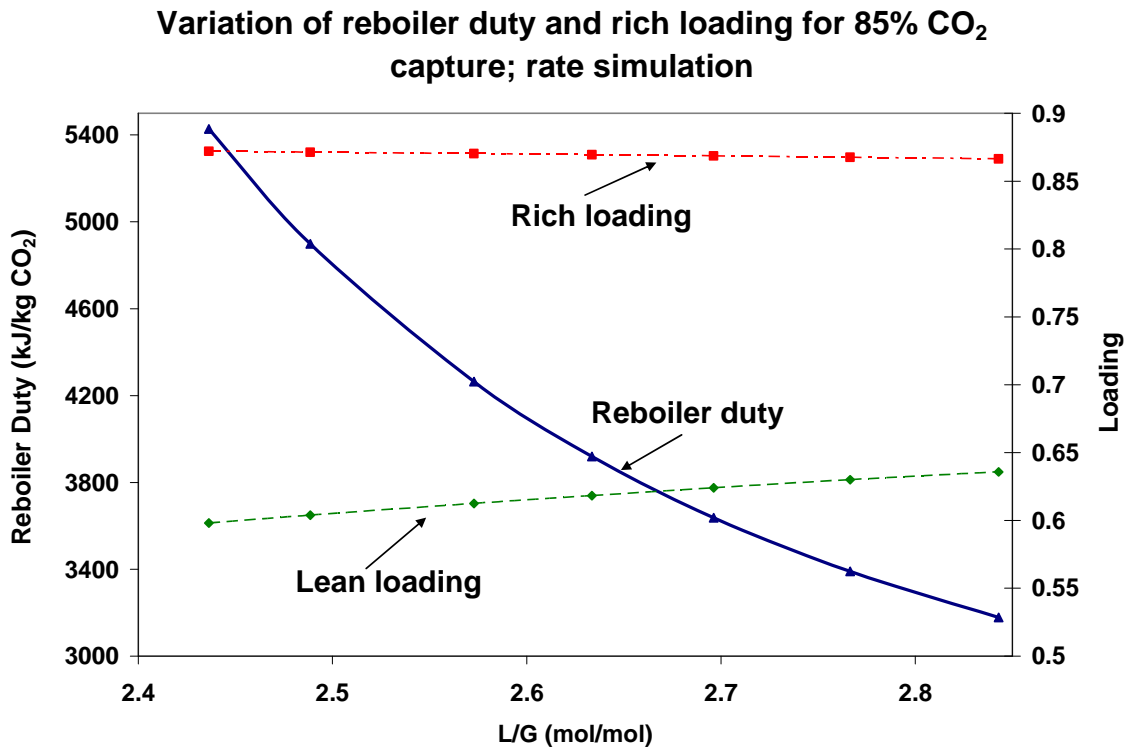


**Figure 4-8: Variation of reboiler duty and rich loading with L/G for 85%  $CO_2$  capture; rate-based simulation**

The minimum reboiler duty obtained is approximately 3200 kJ/kg. This is without any heat integration in the system. As can be seen, in this system, it is not the balance between sensible heat and heat for steam stripping that is important. The sensible heat is a much smaller component than in MEA and the heat of providing steam for stripping is much more important. This is why as the lean loading increases, the reboiler duty

decreases. Further decrease in the lean loading is not advisable since it may lead to precipitation of bicarbonate in the system, especially in the cooled streams and this is not desirable.

A point of difference between the two systems was found to be in the design of the desorber. In the MEA system, the reactions in the desorber are very fast due to the high temperature in the desorber and it was the absorber which was the critical piece of equipment. However, in the case of  $K_2CO_3$ , the reactions are not faster in the desorber since both the absorber and desorber operate at nearly the same temperatures. In addition, the pressure is lower in the desorber. As compared to the MEA system, the equilibrium pressure of  $CO_2$  over the  $K_2CO_3$  system in the desorber is much lower. Hence, the kinetics of the stripping reaction and the mass transfer of  $CO_2$  to the vapor phase in the desorber are very important and the desorber becomes the critical piece of equipment.

A number of parametric simulations were performed with the  $K_2CO_3$  system, particularly to investigate the effect of different hydraulic parameters on the performance of the system.

#### 4.8.1 Effect of packing

The effect of packing on the performance of the system is quite pronounced in the case of  $K_2CO_3$ . The rich loading obtained in the absorber is influenced significantly by the packing employed. The rich loading attained subsequently affects the reboiler duty in the desorber. Table 4-5 presents the results with different packings.

**Table 4-5: Effect of packing type in the absorber**

Packing type	Size	Surface area (sqm/cum)	Lean loading	Rich loading
IMTP Metal	1 inch	185	0.517	0.7
Raschig Metal	16 mm	325.5	0.517	0.718
Raschig 10mm	10 mm	543	0.517	0.758

Hence, it is necessary to use a high mass transfer packing that provides sufficient area for the transfer of CO<sub>2</sub> from vapor to liquid phase in the absorber.

The effect of packing in the desorber is even more pronounced. This is because the equilibrium partial pressure of CO<sub>2</sub> over the solution is low in the desorber and hence, a high mass transfer packing is essential in the desorber to transfer the CO<sub>2</sub> into the vapor phase. Table 4-6 presents the reboiler duties obtained with different packings. The rich loading of the solution was 0.866 and the lean loading was 0.636 and the height of the desorber was 18 m for all these cases.

**Table 4-6: Effect of packing type in the desorber**

<b>Packing</b>	<b>Size (mm)</b>	<b>Surface area (sqm/cum)</b>	<b>Reboiler Duty (kJ/kg CO<sub>2</sub>)</b>
<b>Raschig</b>	6	814.5	3180.33
<b>Raschig</b>	10	543	3422.3
<b>Raschig</b>	16	325.5	3796.72
<b>Raschig</b>	25	185	4215.41
<b>IMTP</b>	50	102	4557.38

#### **4.8.2 Effect of desorber height**

Parametric simulations were carried out to investigate the effect of desorber height on the reboiler duty. It was found that as the desorber height increased, the reboiler duty decreased. Figure 4-9 shows the variation of reboiler duty with the desorber height. As can be seen from Figure 4-9, the reboiler duty first decreases steeply with height and beyond, a certain height, it starts to flatten out. Hence, an optimization can be performed on the desorber height which takes into consideration the lowering in reboiler duty but increase in capital cost with increasing height.

**Variation of reboiler duty with desorber height for 85% capture of CO<sub>2</sub>; rate simulation**

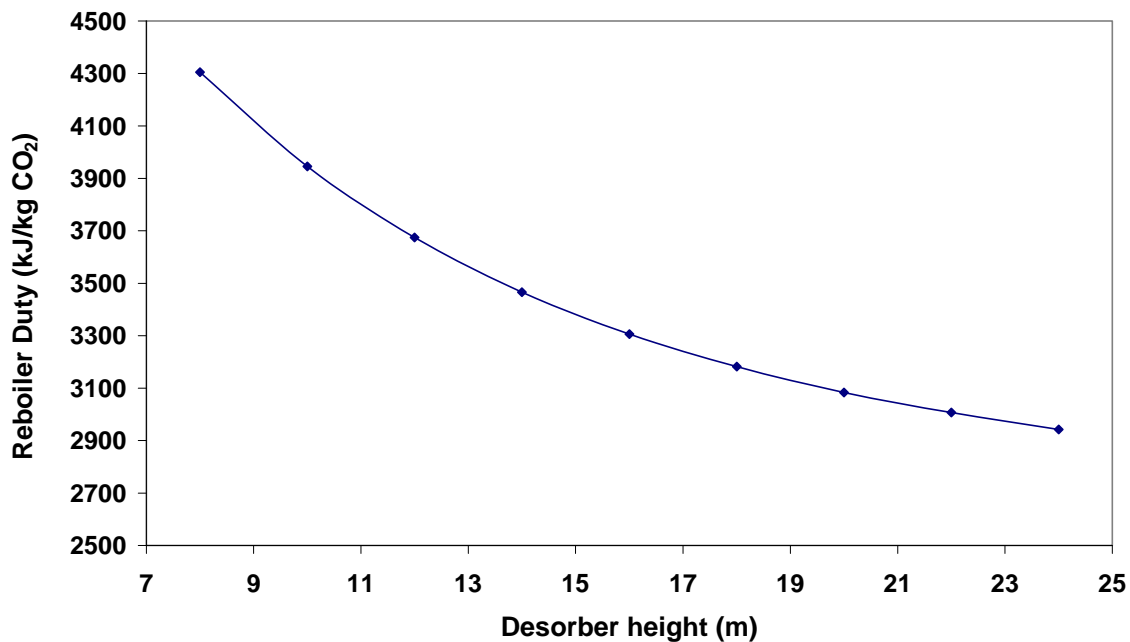


**Figure 4-9: Variation of reboiler duty with desorber height for 85% capture of CO<sub>2</sub>; rate-based simulation**

### **4.8.3 Effect of desorber pressure**

For K<sub>2</sub>CO<sub>3</sub>, the ratio of the heat of absorption to the heat of vaporization of water is less than 1. Hence, as the pressure increases, the amount of water vapor that leaves along with the CO<sub>2</sub> at the top of the column increases significantly. Energy has to be supplied in the reboiler to produce this steam and this represents a major portion of the energy consumption in this system. Hence, for the potassium carbonate system, it is particularly beneficial to operate the desorber at low pressures. By operating under a slight vacuum, it is possible to reduce the energy consumption by 100 kJ/kg. However, when operating under vacuum, it will be necessary to have larger diameter columns due to the higher vapor flows. In addition, the power required to compress the CO<sub>2</sub> to discharge conditions will increase.

## 4.9 Energy recuperation in the $K_2CO_3$ system

A number of schemes were investigated to perform energy recuperation in system:

- Flashing of rich solution and heat exchange with the lean stream from the desorber
- Using a split-flow absorber with semi-regeneration of the rich stream

These schemes are discussed in detail in the following section.

### 4.9.1 Flashing of rich solution and heat exchange with lean solution

When the rich solution is introduced in the desorber, it flashes due to the lower pressure in the desorber. However, at the same time cooling occurs and hence, some sensible heat has to be supplied to bring the liquid back up to the temperature in the desorber. This can be avoided by having a separate flash tank before the desorber and performing heat exchange of the flashed liquid with the lean stream from the desorber. In this case, some dissolved  $CO_2$  would be flashed and the partially regenerated rich stream will have its temperature raised before it is introduced into the desorber. A flowsheet for this configuration is shown in Figure 4-10.

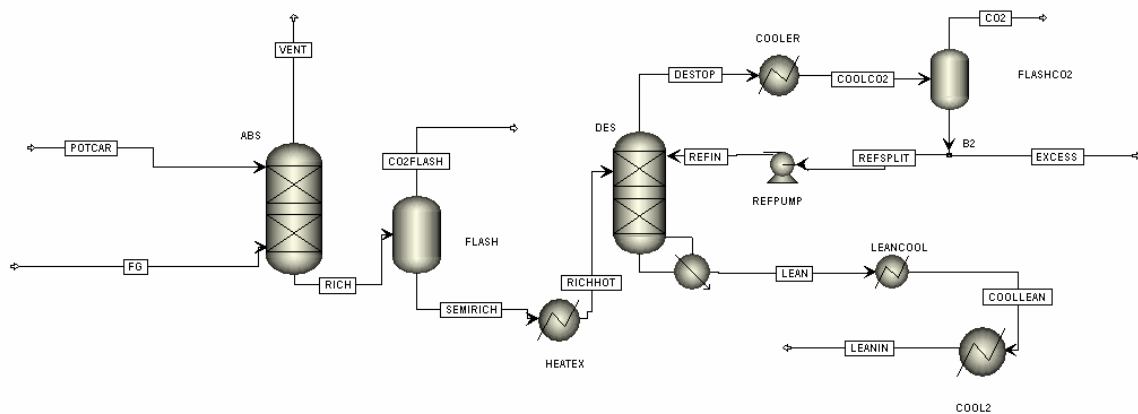


Figure 4-10: Flowsheet for energy recuperation by flashing of rich solution and heat exchange with lean solution

In this configuration, the stream 'SEMIRICH' would undergo heat exchange with the stream 'LEAN' in a cross heat exchanger before passing onto the desorber. The lean stream from this heat exchanger would be further cooled before entering the absorber.

Using this approach, the energy consumption can be reduced to 2850 kJ/kg. This represents a reduction of around 10% in the reboiler duty from the base case and hence offers significant savings.

#### **4.9.2 Use of split-flow absorber**

With the use of a split flow absorber, the following two properties can be taken advantage of in order to reduce the energy consumption in the desorber [9]:

- Heat of desorption decreases as the loading increases
- Steam required for stripping decreases as the loading increases

In absorption systems, the driving force is improved when the temperature is lower. Hence, having a lower solvent inlet temperature into the absorber will help increase the driving force at the top of the absorber where the gas is the leanest. In the split flow absorber system, only a part of the solution is thoroughly stripped to low lean loadings. This solution is then cooled and sent to the top of the absorber where there are the lowest driving forces. The rest of the rich solution is stripped less thoroughly and is introduced into the absorber at an intermediate point [9-10]. The flowsheet setup of the system is shown in Figure 4-11.

Around 25% of the total rich stream is stripped completely and cooled to 60 C and fed to the top of the absorber. The rest of the rich stream is removed from an intermediate point in the desorber (stage 11) and fed to stage 5 of the absorber. The lean loading of the intermediate steam is 0.74. The lean loading of the completely regenerated stream is 0.61.

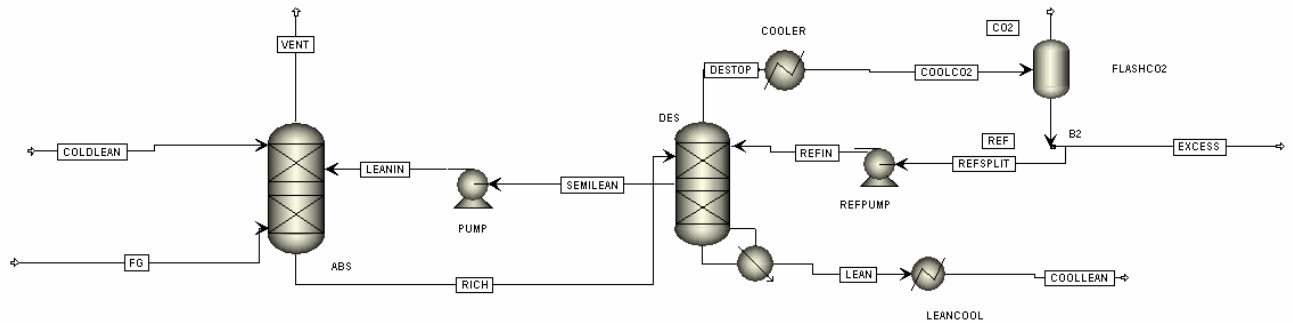


**Figure 4-11: Energy recuperation by use of a split-flow absorber**

The reboiler duty for such a setup is around 2650 kJ/kg. This represents a 22% savings over the base case scenario. The size of the absorber will however be greater in this setup because more liquid flow will be required in the column due to the partial regeneration of the rich solution. The fraction of the split stream as well as the point of entry into the absorber can be optimized for.

## **4.10 Development of potassium carbonate model for Integrated Reforming Combined Cycle Plant**

One of the applications of the hot potassium carbonate process is in CO<sub>2</sub> capture in an Integrated Reforming Combined Cycle plant (IRCC) as described by Nord et al [11]. An optimized potassium carbonate process was developed for the IRCC configuration described by Nord [11-12] and is described in this section.

An IRCC plant uses natural gas as the fuel and reforms the natural gas to syngas. This is followed by a water gas shift reaction to shift carbon monoxide to carbon dioxide and hydrogen. After the water gas shift reaction, CO<sub>2</sub> is captured and the hydrogen-rich gas is combusted in a gas turbine. A schematic of this process as developed by Nord [11] is shown in Figure 4-12.



the desorber where CO<sub>2</sub> stripping occurs. By optimizing various parameters in the model, the reboiler duty was reduced to 1980 kJ/kg CO<sub>2</sub>. The steam required for the reboiler is extracted from the steam turbine [11].

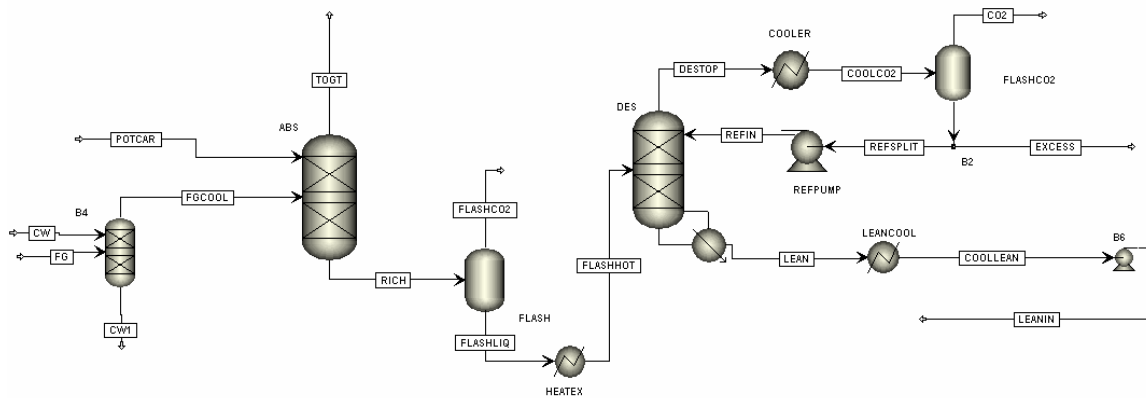


**Figure 4-13: Flowsheet of potassium carbonate system developed for application in IRCC plant**

## 4.11 Use of potassium carbonate solvent with additives

The use of an additive that reacts quickly with CO<sub>2</sub> will significantly increase the rate of reaction in a K<sub>2</sub>CO<sub>3</sub> system and enable operation of the process at pressures close to 1 atm. A number of such additives have been proposed in literature. The use of DEA [13] as an additive increases the mass transfer rate by a factor of 3 while the use of a hindered amine increases it by a factor of 2 [9]. The use of 3% boric acid as an activator has also been investigated [14-15]. This was found to increase the rate of CO<sub>2</sub> transfer by a factor of 2, though this is still slower than in MEA [14]. A number of investigations into the use of piperazine as an activator for the potassium carbonate process have also been carried out [5, 16]. It was found that the addition of 0.6m piperazine to potassium carbonate caused the rate of absorption to compare favorably with that in 5 M MEA [16]. However, whenever an additive such as an amine is added to the solution, the heat of reaction in the system increases due to the formation of the amine carbamate species. Hence, the

addition of an activator will increase the rate of mass transfer but also increase the heat of reaction in the system.

#### **4.12 Potassium carbonate system conclusion**

A rate-based model was developed in ASPEN to analyze the performance of the potassium carbonate system. Potassium carbonate has some properties that make its utilization as a solvent for CO<sub>2</sub> capture attractive – namely, low heat of reaction, low volatility and not prone to degradation. It was found that a high pressure (15 atm) was required in the absorber in order to make the operation feasible. Thus, potassium carbonate can be of particular use in pressurized combustion systems as well as in systems with reforming of fuel such as IRCC.

The effect of lean loading, absorber and desorber height, absorber and desorber packing, pressure and temperature on the heat requirements in the system was studied. The reboiler duty in the desorber was found to be 3200 kJ/kg for the standard configuration. Different schemes for energy recuperation in the system were investigated and it was found that the use of a split flow absorber could reduce the heat duty by 22%. An optimized version of the potassium carbonate flowsheet was developed for an IRCC application and the reboiler duty for this case was 1980 kJ/kg.

## 4.13 References

1. Benson, H.E., Field, J.H. and Jameson, R.M., *CO<sub>2</sub> absorption employing hot potassium carbonate solutions*. Chemical Engineering Progress, 1954. **50**: p. 356-364.
2. Cullinane, J.T., *Thermodynamics and kinetics of aqueous piperazine with potassium carbonate for carbon dioxide absorption*, in *Chemical Engineering*. 2005, University of Texas: Austin.
3. Sanyal, D., N. Vasishtha, and D. Saraf, N., *Modeling of Carbon Dioxide Absorber Using Hot Carbonate Process*. Industrial & Engineering Chemistry Research, 1988. **27**: p. 2149-2156.
4. Tosh, J.S., J.H. Field, H.E. Benson, and W.P. Haynes, *Equilibrium Study of the System Potassium Carbonate, Potassium Bicarbonate, Carbon Dioxide, and Water*, U.S.B.o. Mines, Editor. 1959. p. 5484.
5. Hilliard, M., *Thermodynamics of aqueous piperazine/potassium carbonate/carbon dioxide characterized by the Electrolyte NRTL model within ASPEN Plus 2004*. 2004.
6. Aseyev, G.G. and I.D. Zaytsev, *Volumetric Properties of Electrolyte Solutions: Estimation Methods and Experimental Data*. 1996, New York: Begell House.
7. Aseyev, G.G., *Electrolytes: Equilibria in Solutions and Phase Equilibria. Calculation of Multicomponent Systems and Experimental Data on the Activities of Water, Vapor Pressures, and Osmotic Coefficients*. 1999, New York: Begell House.
8. Puchkov, L.V. and V.V. Kurochkina, *Saturated Vapor Pressure over Aqueous Solutions of Potassium Carbonate*. Zhur. Priklad. Khim, 1970. **43**(1): p. 181-183.
9. Kohl, A.L. and F.C. Riesenfeld, *Gas Purification*. 5th edition ed, ed. A.L. Kohl and F.C. Riesenfeld. 1997, New York: Elsevier. 1439.
10. Bartoo, R.K., *Removing Acid Gas by the Benfield Process*. Chemical Engineering Progress, 1984.
11. Nord, L.O., A. Kothandaraman, H. Herzog, G. McRae, and O. Bolland, *A modeling software linking approach for the analysis of an integrated reforming combined cycle with hot potassium carbonate CO<sub>2</sub> capture*. Energy Procedia, 2009. **1**(1): p. 741-748.
12. Nord, L.O., *Personal Communication*. 2008.

13. Rahimpour, M.R. and A.Z. Kashkooli, *Enhanced carbon dioxide removal by promoted hot potassium carbonate in a split-flow absorber*. Chemical Engineering and Processing, 2004. **43**(7): p. 857-865.
14. Ghosh, U.K., S.E. Kentish, and G.W. Stevens, *Absorption of carbon dioxide into aqueous potassium carbonate promoted by boric acid*. Energy Procedia, 2009. **1**(1): p. 1075-1081.
15. Smith, K., U. Ghosh, A. Khan, M. Simioni, K. Endo, X. Zhao, S. Kentish, A. Qader, B. Hooper, and G. Stevens, *Recent developments in solvent absorption technologies at the CO2CRC in Australia*. Energy Procedia, 2009. **1**(1): p. 1549-1555.
16. Cullinane, J.T. and G.T. Rochelle, *Carbon dioxide absorption with aqueous potassium carbonate promoted by piperazine*. Chemical Engineering Science, 2004. **59**(17): p. 3619-3630.

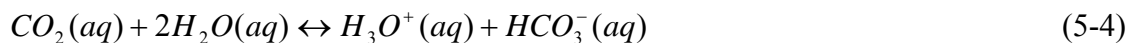
## Chapter 5

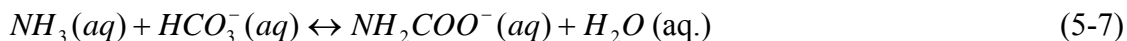
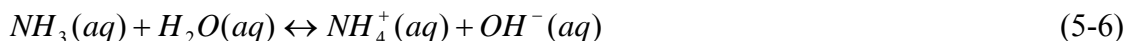
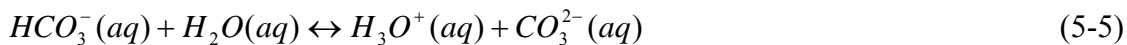
### Chilled ammonia system

The use of ammonia as a solvent for absorption of CO<sub>2</sub> has seen increasing interest over the past few years. Two variations of this process have been discussed in this literature. The first is the Aqua Ammonia process in which an aqueous ammonia solution is used to capture CO<sub>2</sub> with the absorption occurring at room temperature [1-2]. The Powerspan ECO<sub>2</sub> process is based on an adaptation of the aqueous ammonia process[3]. The second variation is the chilled ammonia process that was patented by Gal in 2006 [4]. In this process, the absorption of CO<sub>2</sub> in the ammonia solution is carried out under refrigerated conditions in the temperature range of 0 to 10 °C. The process engineering for the chilled ammonia process has been carried out by Alstom Power [5]. The focus of this chapter is on an analysis of the energy consumption in the chilled ammonia process.

#### 5.1 Chemistry of the chilled ammonia system

The chemistry of the system is based on the reaction of CO<sub>2</sub> with an ammonium carbonate solution. The chilled ammonia process also involves the precipitation of ammonium bicarbonate due to the low temperature in the absorber. The reactions involved are detailed under:





CO<sub>2</sub> is solubilized in the solution in the carbonate, bicarbonate and carbamate forms. It is important to consider the carbamate formation since this is a significant reaction. Many studies of the ammonia system ignore the formation of the carbamate species and this results in a much lower estimated heat of reaction. The detailed thermochemistry will be discussed in the later sections of this chapter.

## 5.2 Thermodynamics of the chilled ammonia system

The thermodynamics of the NH<sub>3</sub> – CO<sub>2</sub> – H<sub>2</sub>O system are complex since it is a vapor-liquid-solid system with ions present in the liquid state. The ERNTL model that was described earlier is used to model this system. In the case of this system, in addition to representing adequately the vapor pressures of NH<sub>3</sub>, CO<sub>2</sub> and H<sub>2</sub>O at different temperatures, it is necessary that the model also predict the precipitation of solids in the appropriate temperature and concentration ranges.

The in-built ASPEN values for the NRTL parameters provide an adequate representation of the VLE of the NH<sub>3</sub>-CO<sub>2</sub>-H<sub>2</sub>O system. The NRTL pairs in the ASPEN database have been regressed against VLE data from Goppert [6-7]. All the other property models have been updated as per the guidelines laid out in the ASPEN Plus report on the system [7].

Figure 5-1 shows the VLE behavior of the NH<sub>3</sub>-CO<sub>2</sub>-H<sub>2</sub>O system for a 6.3 M NH<sub>3</sub> solution at 313 K and Figure 5-2 shows the VLE behavior of the NH<sub>3</sub>-CO<sub>2</sub>-H<sub>2</sub>O system for a 11.9M NH<sub>3</sub> solution at 333K .

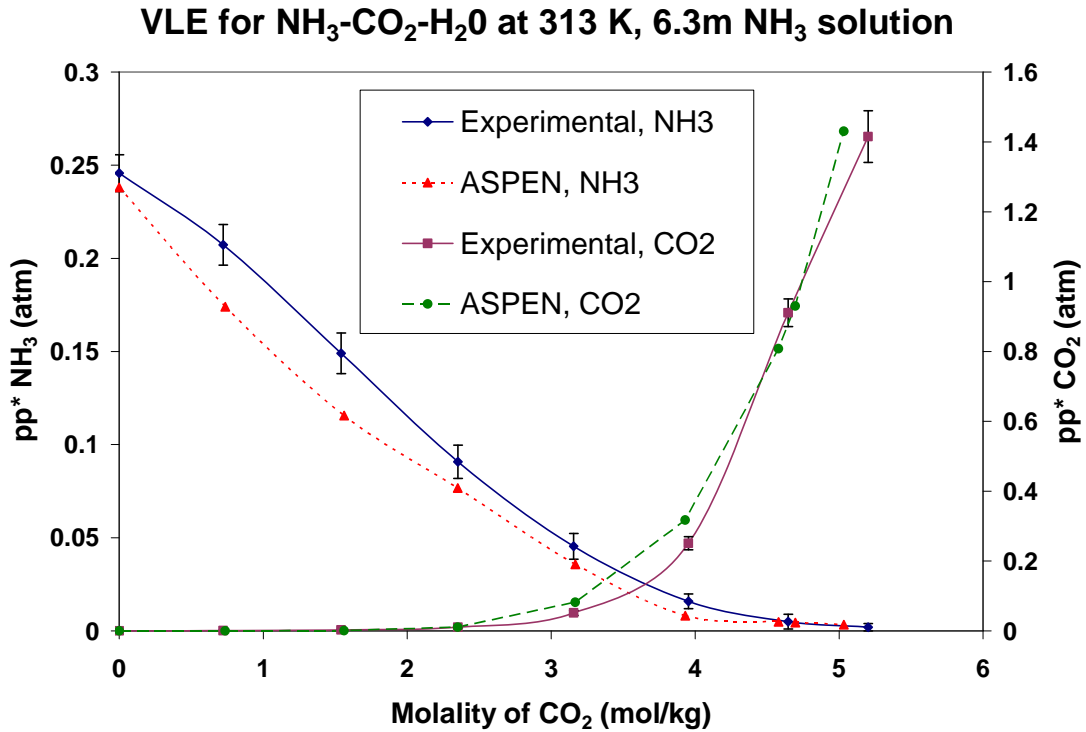


Figure 5-1: Comparison of ASPEN default VLE and experimental VLE for the NH<sub>3</sub>-CO<sub>2</sub>-H<sub>2</sub>O system for a 6.3M NH<sub>3</sub> solution at 40°C. Experimental data from [8]

### VLE for NH<sub>3</sub>-CO<sub>2</sub>-H<sub>2</sub>O at 333K, 11.9 m NH<sub>3</sub> solution

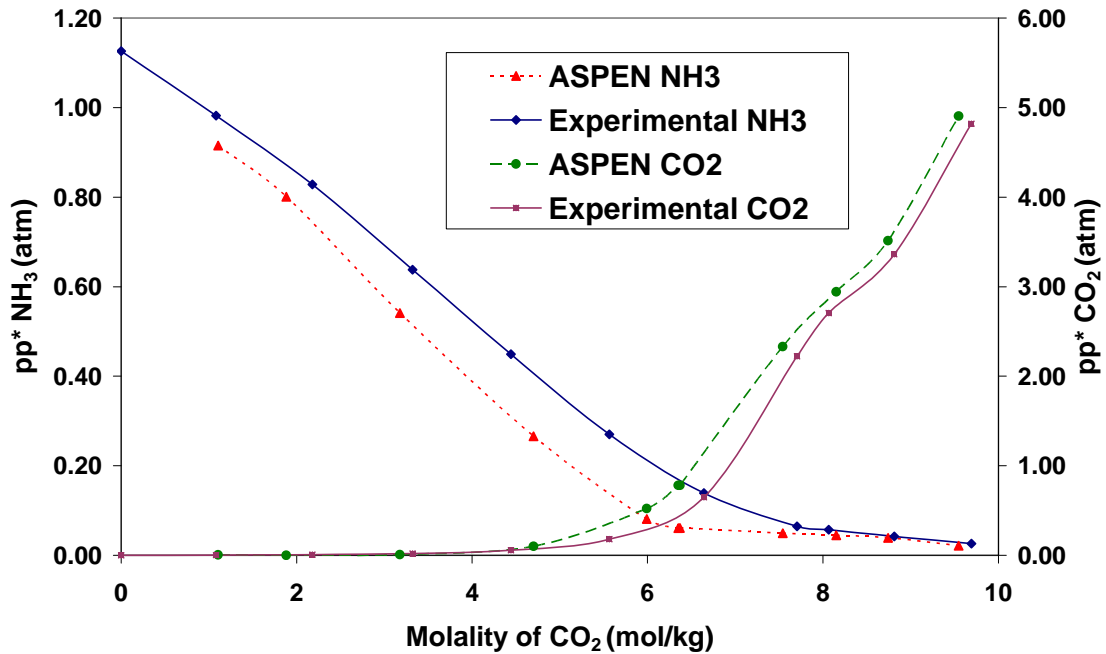
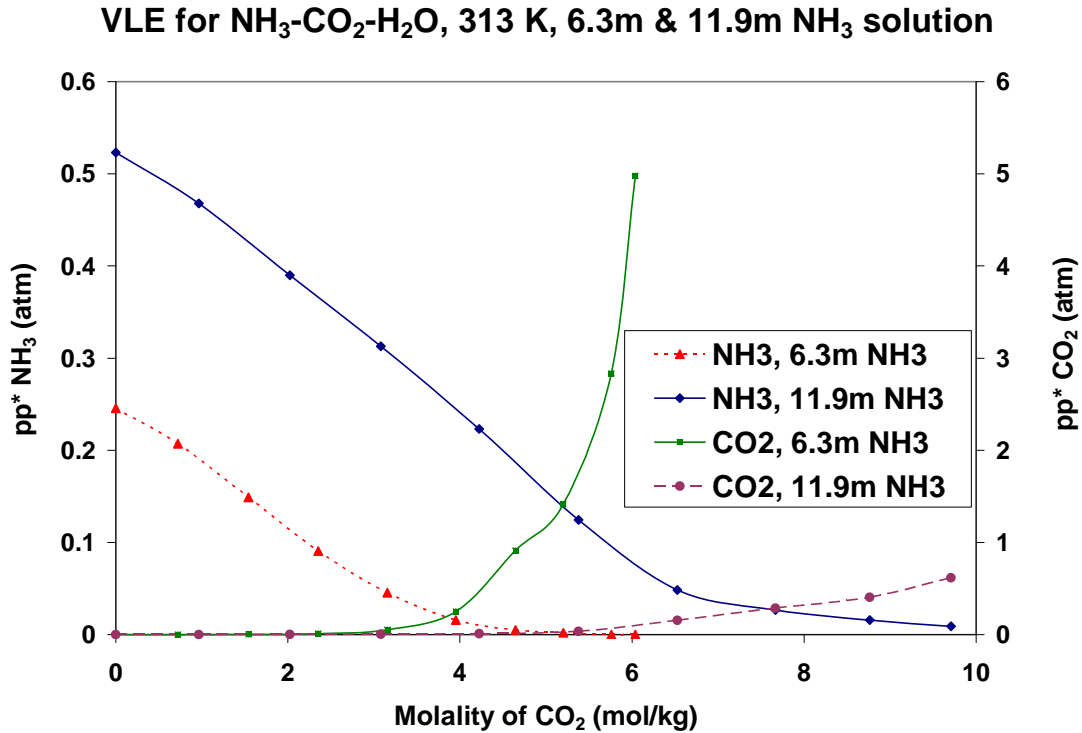


Figure 5-2: Comparison of ASPEN default VLE and experimental VLE for the NH<sub>3</sub>-CO<sub>2</sub>-H<sub>2</sub>O system for a 11.9m NH<sub>3</sub> solution at 60°C. Experimental data from [8]

Upon inspection, it was found that ASEPN accurately predicts the formation of bicarbonate when it occurs. As can be seen from the above graphs, when the molality of CO<sub>2</sub> in the solution is low, the equilibrium partial pressure of NH<sub>3</sub> is high since much of the NH<sub>3</sub> is in an unbound state. As the CO<sub>2</sub> content of the solution increases however, there is a steep decrease in the equilibrium partial pressure of NH<sub>3</sub> since the ammonia in the solution becomes bound in the form of ammonium carbonate and ammonium bicarbonate. This has important implications in the amount of regeneration to be performed on the lean solution. Regenerating the lean solution below a certain CO<sub>2</sub> content can cause excessive NH<sub>3</sub> in the vent gas from the absorber, thus necessitating large energy requirements in the stripping of NH<sub>3</sub> for the vent gas before release. The equilibrium partial pressure of NH<sub>3</sub> depends both on the temperature and the

concentration of the  $\text{NH}_3$  solution. Figure 5-3 presents the variation in  $\text{NH}_3$  partial pressure with  $\text{NH}_3$  concentration. As can be seen from the figure, at higher  $\text{NH}_3$  concentrations, the degree of slip increases dramatically especially at low lean loadings. This can be potentially problematic depending on the extent of regeneration of the rich solution in the stripper.



**Figure 5-3: Comparison of VLE of  $\text{NH}_3\text{-CO}_2\text{-H}_2\text{O}$  system for 6.3M and 11.9M  $\text{NH}_3$  solution at 313K. Data from [8]**

Figure 5-4 presents the variation of the equilibrium partial pressures of  $\text{CO}_2$  and  $\text{NH}_3$  at different temperatures for the same concentration of  $\text{NH}_3$  and  $\text{CO}_2$  in the solution. The equilibrium partial pressure of  $\text{NH}_3$  is lower for the same  $\text{NH}_3$  and  $\text{CO}_2$  concentrations at a lower temperature. This is the main reason for operating the absorber at a low temperature.

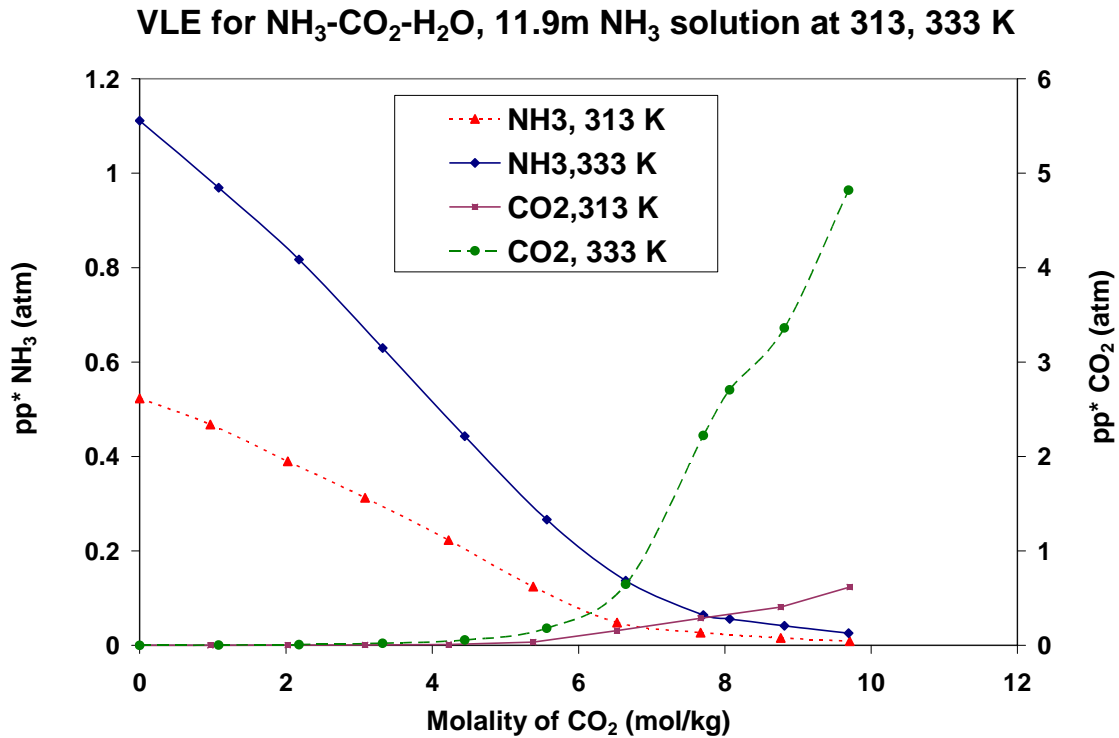


Figure 5-4: Comparison of VLE for NH<sub>3</sub>-CO<sub>2</sub>-H<sub>2</sub>O solution at 313K and 333K for 11.9m NH<sub>3</sub> solution. Data from [8]

### 5.3 Process description

The process for CO<sub>2</sub> capture using chilled ammonia can be divided into 5 sections:

1. Flue gas cooling
2. Absorption of CO<sub>2</sub> into solution
3. Stripping of NH<sub>3</sub> from the vent gas
4. Desorption of CO<sub>2</sub> from the solution
5. Compression of CO<sub>2</sub>

The overall flowsheet for CO<sub>2</sub> capture is presented in Figure 5-5. Each of the sections is described in detail below.

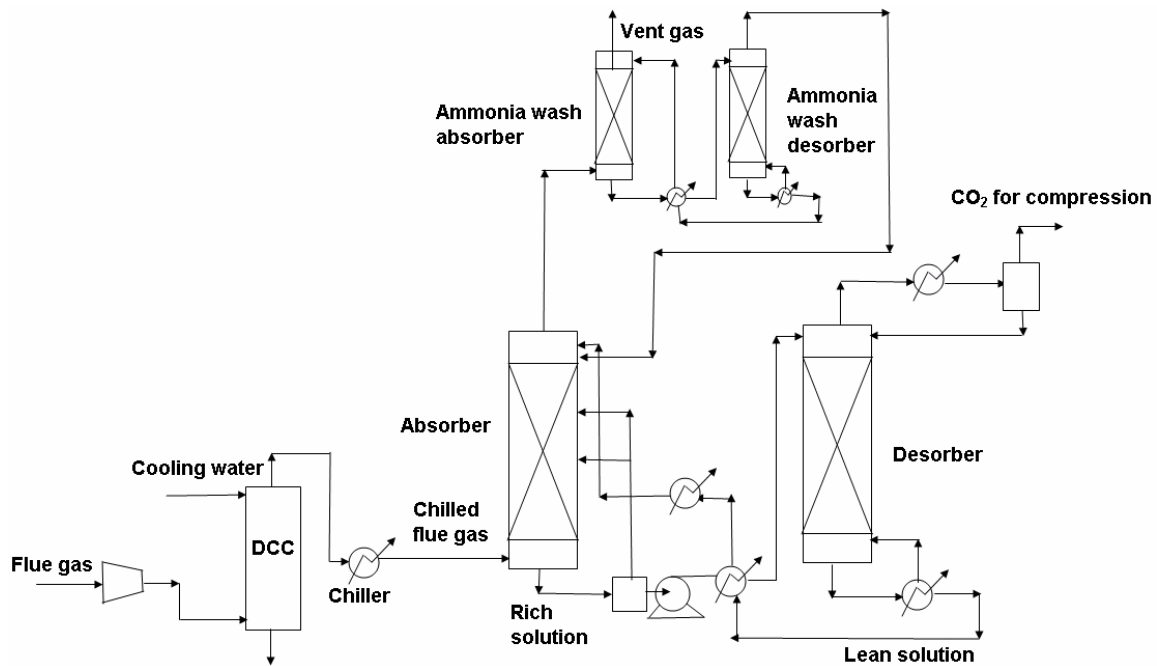


**Figure 5-5: Flowsheet for chilled ammonia process**

**Flue gas cooling:** The temperature in the absorber in the chilled ammonia process is to be maintained between 1- 10 °C for optimal operation [4]. Due to this, it is necessary to cool the flue gas from the outlet of the power plant to this temperature. The flue gas from the power plant, after desulfurization, is passed through a Direct Contact Cooler (DCC) where it is cooled to around 25°C. The DCC is a packed column in which there is counter-current flow of flue gas and water. Cold water is sprayed from the top of the tower with the flue gas entering at the bottom. As the flue gas contacts the cold water, there is cooling of the flue gas and condensation of most of the water in the flue gas stream. The water is collected at the bottom of the DCC and is recycled to the top after cooling. A small purge stream is removed from the water and fresh water is added to the DCC to make up for this purge stream. The flue gas exits the top of the DCC and is then passed through chillers in order to reduce its temperature to around 7°C before entering the absorber.

**Absorption of CO<sub>2</sub> into the ammonia solution:** The absorption of CO<sub>2</sub> into the ammonia solution occurs mainly through the precipitation of ammonium bicarbonate. The cooled flue gas enters at the bottom of the absorber while the chilled lean ammonium carbonate solution enters at the top of the absorber. According to Gal's patent [4], the CO<sub>2</sub> loading of the lean solvent should be between 0.25 and 0.67 and for optimal performance, should be between 0.33 and 0.67. There are two competing forces that dictate what the loading of the lean stream should be. Lower the loading, the higher the absorption capacity of the solvent. However, as the CO<sub>2</sub> loading of the solvent decreases, the equilibrium partial pressure of NH<sub>3</sub> in the system increases, thus increasing the NH<sub>3</sub> slip from the absorber.

In the absorber, there is recirculation of chilled ammonium bicarbonate at different stages. Of critical importance, is that the absorber be refrigerated through the use of chillers and that the temperature in the absorber not exceed 10°C. The chilling load in the absorber comes from two sources:

1. The reaction of CO<sub>2</sub> with NH<sub>3</sub> is exothermic and hence, the heat of reaction needs to be removed in order to maintain low temperatures in the absorber.
2. The precipitation of ammonium bicarbonate is an exothermic reaction and the heat of precipitation needs to be removed as well.

After the desired degree of CO<sub>2</sub> absorption, the rich solvent leaves from the bottom of the absorber, while the CO<sub>2</sub> stripped gas leaves from the top of the absorber and passes to the ammonia recovery system for stripping of the ammonia vapors in the gas. The rich stream is pumped to a pressure of 30 atm before passing on to the cross heat exchanger.

**Stripping of NH<sub>3</sub> from the vent gas:** The vent gas that exits the top of the absorber has an ammonia content ranging from 500-3000 ppmv. This level of ammonia is unacceptable for gases vented to the atmosphere. In addition, this lost ammonia has to be made up by the addition of fresh solvent and this makes it economically more costly.

Hence, an ammonia recovery system is needed after the absorber. As described in Kohl and Riesenfeld [9], this is an elaborate system with an absorber with a major two-section water wash and a desorber to strip the ammonia from the water. The quantity of water required to strip the ammonia from the gas stream in the absorber is large. This aqueous ammonia stream is too dilute to be recycled directly to the CO<sub>2</sub> absorber for it will affect the water balance of the plant. Hence, it is necessary to strip ammonia from the aqueous solution and recycle the water to the ammonia wash absorber.

The vent gas from the absorber enters the bottom of the wash absorber and cold water flows from the top. Ammonia is absorbed into the aqueous solution and vent gas containing less than 10 ppmv ammonia is released from the top of the wash absorber. This vent gas needs to be heated to around 45°C before it can be released to the atmosphere in order to satisfy flume conditions. The aqueous solution containing ammonia exits the bottom of the absorber and flows to the wash desorber. There is a heat exchanger between the water wash absorber and desorber, in which the minimum approach temperature is set to 10 °C. In the desorber, ammonia is stripped from the aqueous solution and is released from the top while the water stream removed from the bottom of the desorber is sent back to the absorber for a fresh batch of absorption.

**Desorption of CO<sub>2</sub> from the solution:** The CO<sub>2</sub> laden rich stream that leaves the bottom of the CO<sub>2</sub> absorber is taken to the desorber after being pumped to 30 atm and passing through the cross heat exchanger. In the cross heat exchanger, the cold rich stream from the absorber bottom exchanges heat with the hot lean stream from the desorber. The minimum approach temperature in the cross heat exchanger is set to 10 °C. In the heat exchanger, there are two components of heat required:

1. **Sensible heat requirement:** Heat is required to raise the temperature of the rich stream
2. **Heat of solution:** Heat is required to dissolve the ammonium bicarbonate solids which are in the rich solution

In some cases, not all the ammonium bicarbonate solid is dissolved in the cross heat-exchanger. In these instances, the rich stream has to be sent to another heat exchanger. In this study, it has been assumed that the desorber design will not accommodate solids and hence, it is necessary to have all the solids dissolved before the stream enters the desorber.

The CO<sub>2</sub> stream enters at the top of the desorber and as it flows down the tower, it contacts with the vapors generated in the reboiler. The prevailing VLE causes the transfer of the CO<sub>2</sub> from the liquid to gas phase. The desorber is operated at a pressure of 30 atm and the temperature in the reboiler can range from 120 – 145°C. At this temperature, the equilibrium partial pressure of ammonia is low and hence, there is low vaporization of ammonia from the solution. The high pressure in the desorber serves to reduce the heat consumption in two ways:

- 1. Lowers the compression energy:** Since the gas leaving the desorber is at 30 atm, lesser amount of compression work is needed in order to compress CO<sub>2</sub> to the required 110 atm.
- 2. Lessens the steam required to maintain driving force for transfer:** At these high pressures, the VLE in the system is favorable to the desorption of CO<sub>2</sub>. This means that less steam is needed to maintain the driving force for transfer of CO<sub>2</sub> from the liquid to gas phase.

The CO<sub>2</sub> lean solution that leaves from the bottom of the absorber is passed back to the cross heat exchanger where it is cooled. It is then further cooled in chillers to a temperature of 10 ° C or less, before being returned to the absorber. The CO<sub>2</sub> rich gas that leaves at the top of the desorber is cooled and sent to a receiver to condense the ammonia and water present in the solution. The gas is then sent for CO<sub>2</sub> compression and handling. Prior to this step, it may be necessary to have a water wash to remove the residual ammonia present in the stream.

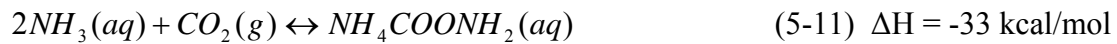
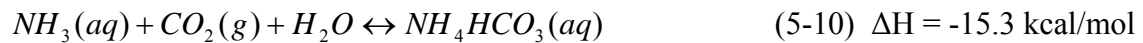
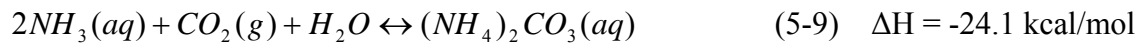
**Compression of CO<sub>2</sub>:** The gas that is received from the desorber is at 30 atm. This is then passed to a two or three stage compressor with intercoolers in order to produce supercritical CO<sub>2</sub> of the required specification.

## 5.4 Thermochemistry in the chilled ammonia system

In this section, the calculation of the thermochemistry of the chilled ammonia system from the Clausius-Clapeyron equation as well as in ASPEN is detailed.

### 5.4.1 Thermochemistry from Clausius-Clapeyron equation

With the ammonia system, one of the important issues is the thermochemistry. It is claimed that the chilled ammonia process has a heat of reaction that is 3 times lower than MEA. This is based on the claim that the only reaction that occurs for the absorption of CO<sub>2</sub> is the conversion of ammonium carbonate to ammonium bicarbonate. However, this is not the case. CO<sub>2</sub> is solubilized by a number of reactions as outline below:



Hence, the heat of reaction is much higher than what it would be if the reaction was only the cycling between ammonium carbonate and ammonium bicarbonate. The actual heat of reaction can be calculated from the Clausius-Clapeyron equation as given below:

$$\ln\left(\frac{P_2}{P_1}\right) = \frac{-\Delta H * \left(\frac{1}{T_2} - \frac{1}{T_1}\right)}{R} \quad (5-13)$$

where  $P_2$  refers to the vapor pressure at temperature  $T_2$  and  $P_1$  refers to the vapor pressure at temperature  $T_1$  and  $R$  is the universal gas constant. Using the data of van Krevelen [10-11], we can calculate the heat of reaction from the Clausius-Clapeyron equation [11]. In the chilled ammonia process, the typical lean loading is 0.4 and the typical rich loading is 0.8. Table 5-1 presents the vapor pressure of  $\text{CO}_2$  at different temperatures at these mole ratios for a 2N  $\text{NH}_3$  solution.

**Table 5-1: Vapor pressure of  $\text{CO}_2$  at different loadings and temperatures. Data from [10]**

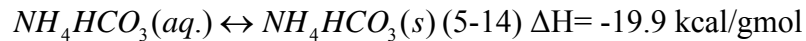
<b>Temperature, in °C</b>	<b>Vapor pressure of <math>\text{CO}_2</math> for loading of 0.4</b>	<b>Vapor pressure of <math>\text{CO}_2</math> for loading of 0.8</b>
<b>20</b>	2.8	95
<b>40</b>	9.5	430
<b>60</b>	50	1600
<b>80</b>	190	5000
<b>90</b>	310	8000

Now, using the Clausius-Clapeyron equation, we can calculate the heat of reaction for different ranges. Table 5-2 presents these calculations.

**Table 5-2: Heat of reaction for different temperature ranges as calculated by the Clausius-Clapeyron equation**

Temperature range	Heat of reaction, kcal/mol	
	Loading = 0.4	Loading = 0.8
20-40 °C	11.13	13.76
40-60°C	17.20	13.61
60-80 °C	15.59	13.31
80-90 °C	12.47	11.97

The average heat of reaction for in the 20-40°C range is 12.445 kcal/mol and in the 80-90°C, it is 12.2 kcal/mol. This is approximately twice the heat of reaction for the conversion of ammonium carbonate to ammonium bicarbonate. This suggests that the actual reactions occurring in the system is a combination of (5-9) - (5-12) and also indicates the presence of free ammonia in the system. In addition, it needs to be noted, that the heat of reaction in the absorber will be higher than this due to the precipitation of ammonium bicarbonate crystals. The reaction through which this occurs is:



Before taking the lean stream to the desorber, this heat of solution has to be provided in order to avoid fouling problems due to solids in the stripper.

#### **5.4.2 Thermochemistry in ASPEN**

An ASPEN simulation was setup in order to calculate the heat of reaction for the solubilization of CO<sub>2</sub> predicted by ASPEN. The simulation was set up a single stage flash calculation at 40 °C. The inlet lean stream had a loading of 0.4. The outlet stream had a CO<sub>2</sub> loading of 0.8. The heat of absorption was calculated to be 13.4 kcal/mol which lies within the values predicted by the Clausius-Clapeyron equation.

## 5.5 Analysis of the absorber

In the chilled ammonia process, the absorber is a critical piece of equipment that is of complex design. The temperature in the absorber needs to be maintained below 10 °C even with exothermic reactions occurring and hence, it is necessary to keep the absorber refrigerated. Since precipitation reactions occur in the absorber, the internal design is also important. A packed tower may not be appropriate to accommodate the required precipitation; however, a slurry tower will severely inhibit mass transfer from the gas phase to the liquid phase. In this study, the only equilibrium simulations were carried out and hence, the internal design of the column was not considered.

The absorber is modeled in ASPEN using the RADFRAC column. The lean stream containing mainly ammonium carbonate is introduced at the top of the absorber with the cooled flue gas stream entering the absorber at the bottom. The absorber is refrigerated using the *utility exchangers* option in the *heaters and coolers* setting. In the individual study of the absorber, the flowrate of the lean stream was varied in order to get 85% capture of the CO<sub>2</sub> in the flue gas stream. This meant that manual adjustment of the refrigeration settings was required in order to maintain the required temperature profile in the absorber. As the absorber is cooled, there is more precipitation and hence, the absorption capacity of the solution for CO<sub>2</sub> increases. As the temperature in the absorber decreases, the NH<sub>3</sub> slip from the absorber decreases. However, this is also accompanied by an increase in the refrigeration load.

A number of parametric studies were carried out in the absorber in order to study the influence of these various parameters. In the first set of simulations, the solution was maintained at 20.9 M NH<sub>3</sub> with a lean CO<sub>2</sub> to NH<sub>3</sub> ratio of 0.42. The temperature in the absorber was varied from 1°C to 10°C to study the effect on the NH<sub>3</sub> slip from the absorber. The CO<sub>2</sub> capture percentage was kept constant at 85%. Figure 5-6 shows the partial pressure of NH<sub>3</sub> in the vent gas at different temperatures. As can be seen from Figure 5-6, the concentration of NH<sub>3</sub> in the vent gas even when the temperature in the

absorber is 1°C is as high as 600 ppmv. An acceptable concentration for emitting into the atmosphere is 10 ppmv NH<sub>3</sub>. Hence, a water wash absorber and desorber for scrubbing NH<sub>3</sub> in the vent gas is necessary after the main absorber. The flowsheet of the absorber section incorporating this is shown in Figure 5-7.

**Concentration of NH<sub>3</sub> in vent gas vs. temperature,  
20.9m NH<sub>3</sub> solution, lean CO<sub>2</sub> to NH<sub>3</sub> ratio of 0.4**

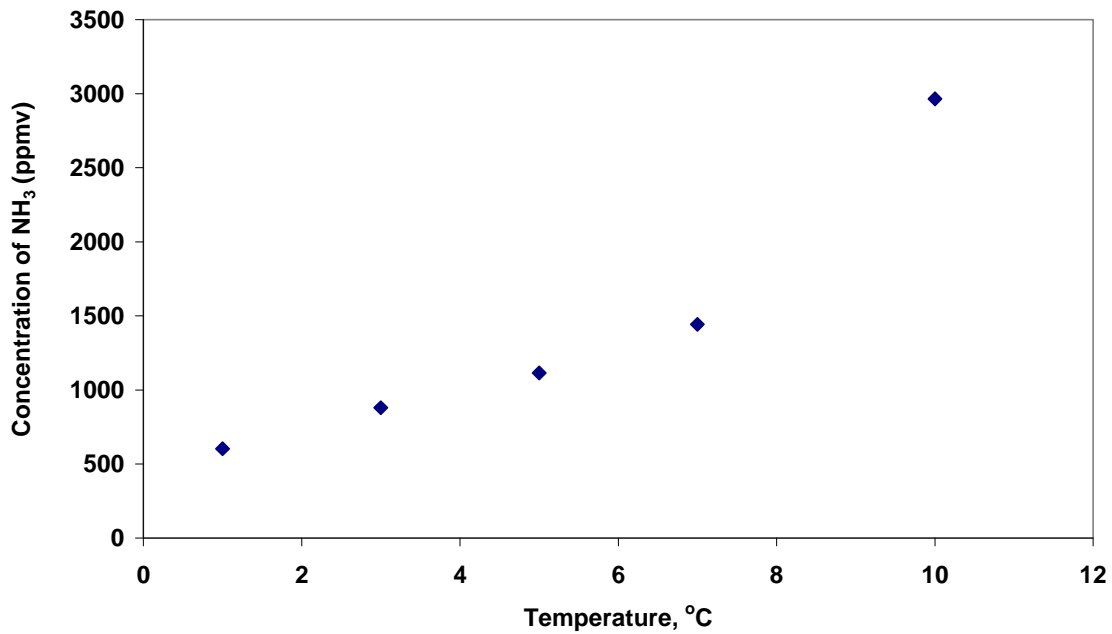


**Figure 5-6: Variation in concentration of NH<sub>3</sub> in vent gas with temperature for a 20.9Mm NH<sub>3</sub> solution, with a lean loading of 0.4**

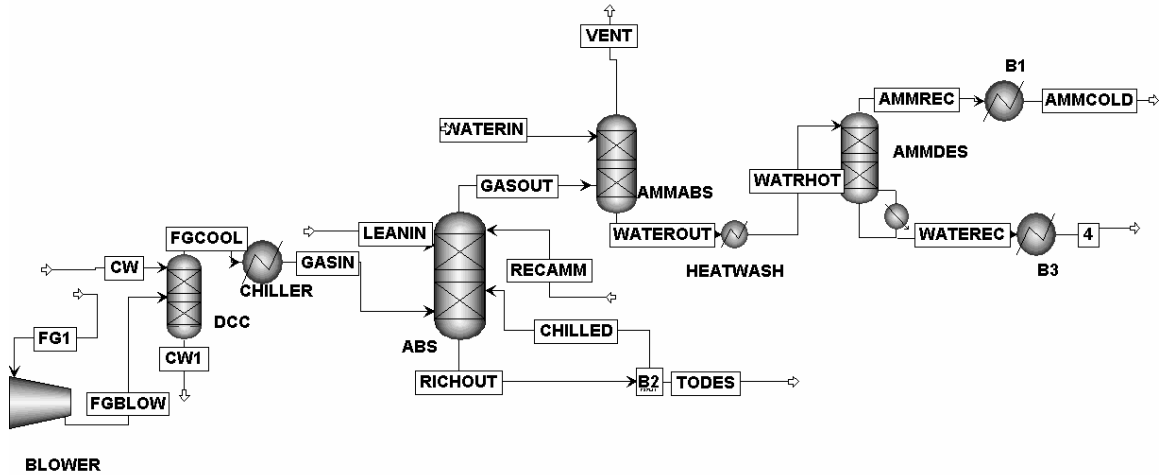
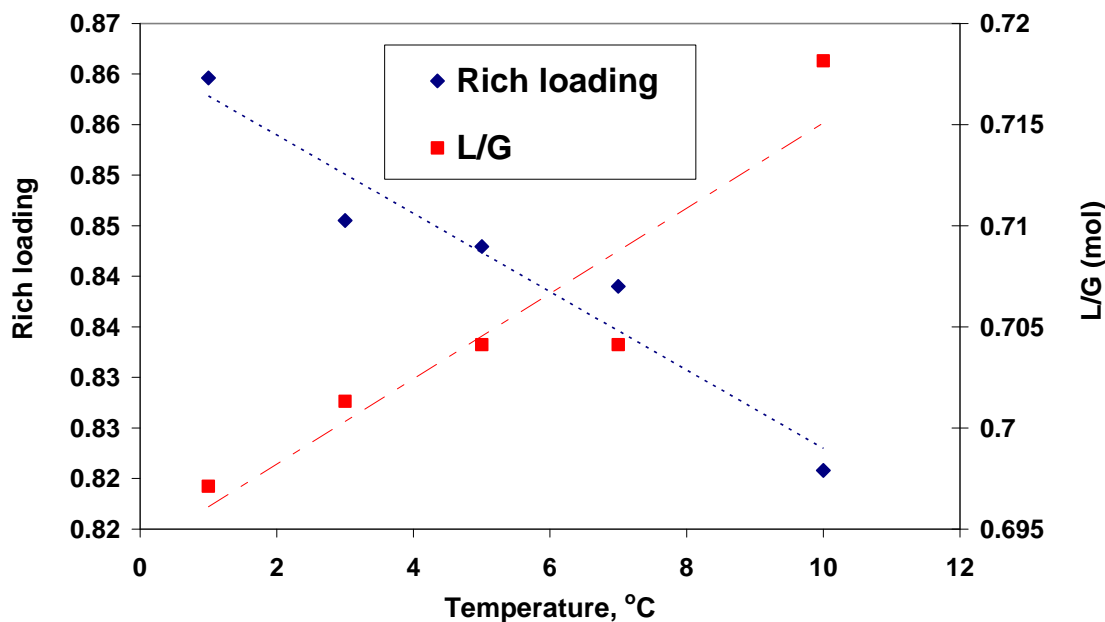


Figure 5-7: Flowsheet as developed in ASPEN for the absorber section of the chilled ammonia process

### 5.5.1 Effect of absorber temperature

Figure 5-8 shows the variation of the rich loading and L/G with temperature. As the temperature increases, the attained rich loading decreases. Consequently, there is an increase required in the amount of solvent that needs to be circulated to achieve 85% capture. This is because as the temperature increases, precipitation of ammonium bicarbonate is hindered and this reduces the capacity of the solvent for CO<sub>2</sub> absorption.

**Rich loading and L/G variation with temperature in absorber, 20.9m NH<sub>3</sub> solution, lean loading of 0.42**



**Figure 5-8: Variation of rich loading and L/G in absorber with temperature for a 20.9m NH<sub>3</sub> solution at a lean loading of 0.42 for 85% CO<sub>2</sub> capture from coal flue gas**

Figure 5-9 shows the refrigeration load requirement as well as the water wash desorber heat duty requirement for different temperatures for a 20.9 M NH<sub>3</sub> solution with a lean loading of 0.42. As the temperature decreases, the refrigeration load increases; however, the water wash desorber heat duty decreases since the concentration of NH<sub>3</sub> in the vent gas is lower and less water is needed to scrub the solution from the wash absorber. Hence, there is an optimization to be performed on the temperature in the absorber based on the different heat duties that are needed to be satisfied. In addition, another factor that influences this will be the kinetics of the reaction. This is not reflected in these simulations since the system has been modeled as an equilibrium system. However, as the temperature decreases, the kinetics of the system will become slower and hence, this will have an effect on the size of the absorber tower.

### Refrigeration load and water wash desorber duty vs. temperature for 20.9 M NH<sub>3</sub> solution, lean loading

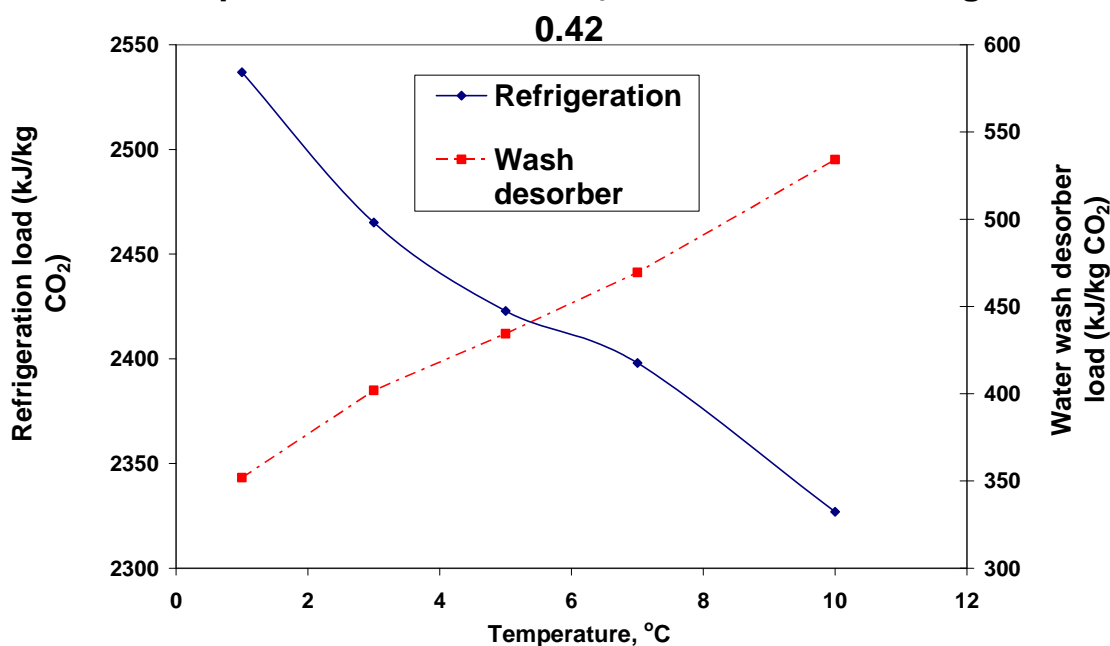
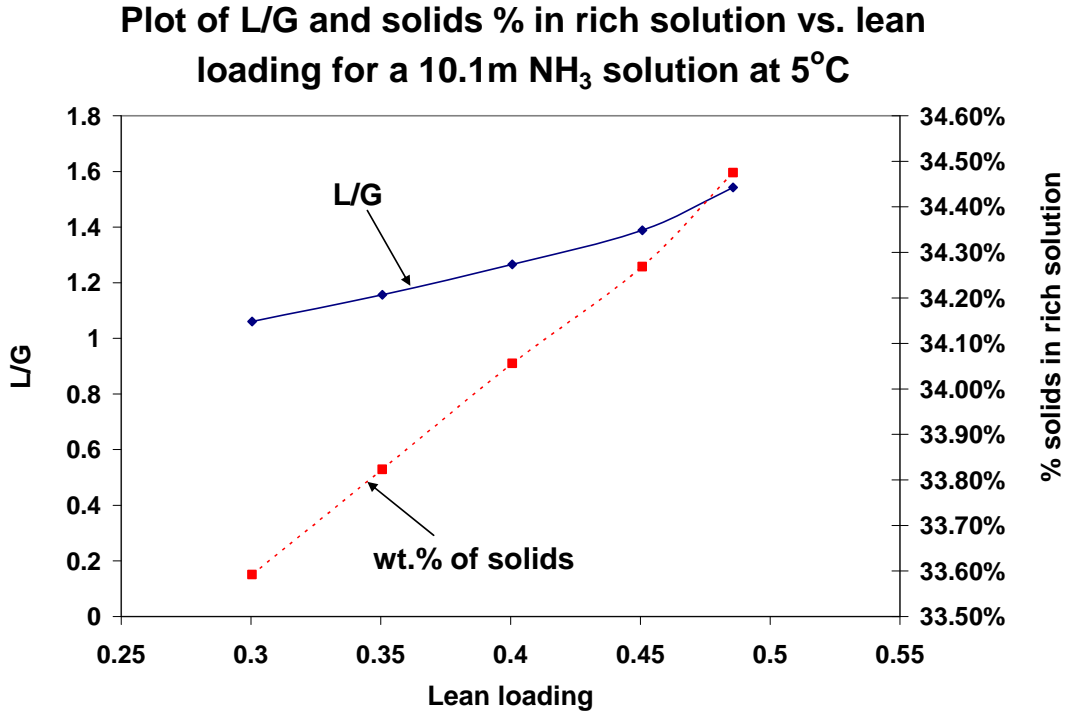


Figure 5-9: Variation in refrigerator load and water wash desorber duty with temperature for a 20.9m NH<sub>3</sub> solution, lean loading of 0.42, 85% CO<sub>2</sub> capture from coal flue gas

### 5.5.2 Effect of lean loading

In the next set of simulations, it was decided to investigate the effect of the lean loading (lean CO<sub>2</sub> to NH<sub>3</sub> ratio) on different parameters. A 10.1 M NH<sub>3</sub> solution was used and the temperature in the absorber was kept at 5°C. As the lean loading decreases, there is more free NH<sub>3</sub> in the solution and hence, the absorption capacity is greater. We would expect that as the lean loading increases, the flowrate of liquid required to achieve 85% would increase. Figure 5-10 shows that this is the trend that is predicted by ASPEN. In addition, as the lean loading increases, we would expect that the % of solids in the rich solution would increase. As can be seen in Figure 5-10, this can be confirmed from the ASPEN simulation. Beyond a lean loading of 0.45, for a 10.1 M NH<sub>3</sub> solution at 5 °C, there is some ammonium bicarbonate solid present in the lean solution and this is responsible for

the kink in the graphs in Figure 5-10. Since this solid has no absorption capacity, the actual flowrate of the liquid stream through the column will be greater.



**Figure 5-10: Variation of L/G and wt.% of solids in rich solution with lean loading for a 10.1m NH<sub>3</sub> solution at 5°C for 85% capture of CO<sub>2</sub> from coal flue gas**

An interesting trend is also observed in the interaction between the wash desorber reboiler duty and the absorber refrigeration duty. As the lean loading increases, there is increased precipitation and hence, the refrigeration duty in the absorber is higher because of the exothermic nature of the precipitation reaction. However, at low lean loadings, there is free NH<sub>3</sub> in the solution. This leads to increased slip from the absorber at the same temperature. The water flow and hence, the desorber reboiler duty required to scrub this stream increases. Hence, as the lean loading increases, the water wash reboiler duty decreases, but the refrigeration duty in the absorber increases. The trend of the refrigeration duty and water wash desorber duty is shown in Figure 5-11.

**Plot of heat duty vs. lean loading for a 10.1m NH<sub>3</sub> solution at 5°C**

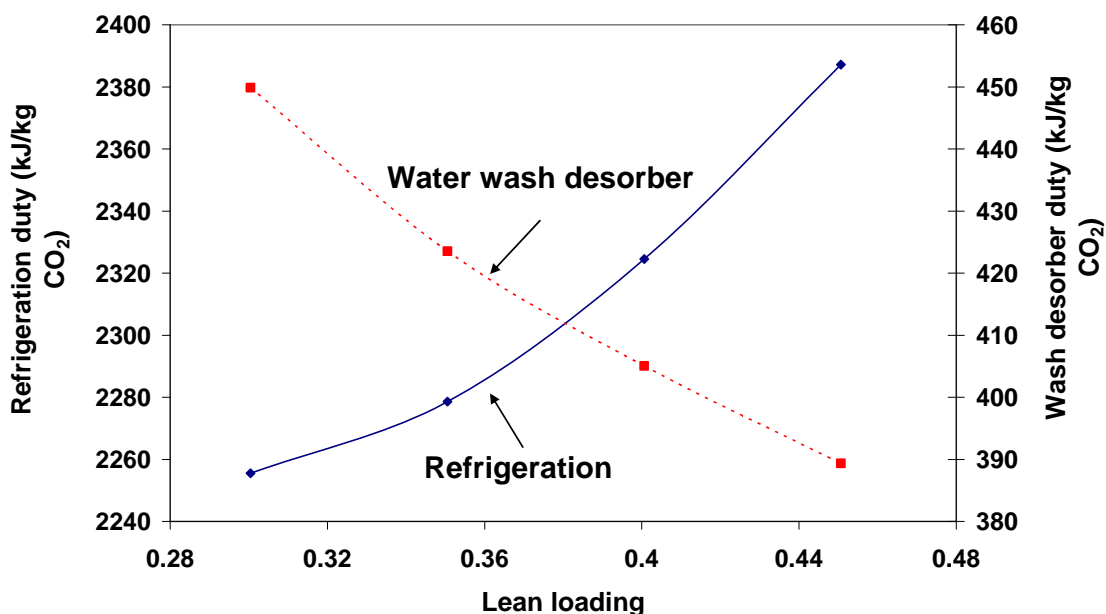


**Figure 5-11: Variation of refrigeration, water wash desorber and total duty with lean loading for a 10.1m NH<sub>3</sub> solution at 5°C for 85% capture of CO<sub>2</sub> from coal flue gas**

This suggests that there is some scope for optimization in terms of the lean loading to be used. Further implications of the lean loading on the heat duties in the desorber will be discussed in subsequent sections.

### 5.5.3 Effect of molality of solution

In the next set of parametric studies, it was decided to investigate the effect of changing the NH<sub>3</sub> molality in the solution while keeping the lean loading of the solution constant at 0.4 with the temperature at 5°C. The performance of the system at a variety of molalities from 10m to 30m NH<sub>3</sub> was studied. In particular, we were interested in how the liquid flow required to achieve 85% capture would vary with increasing molality. As the molality of the solution increases, it was observed that the liquid flow required decreased

since there is more available ammonia for binding the carbon dioxide, as shown in Figure 5-12.

**L/G vs. molality of NH<sub>3</sub> for a lean loading of 0.4 and temperature of 5°C**

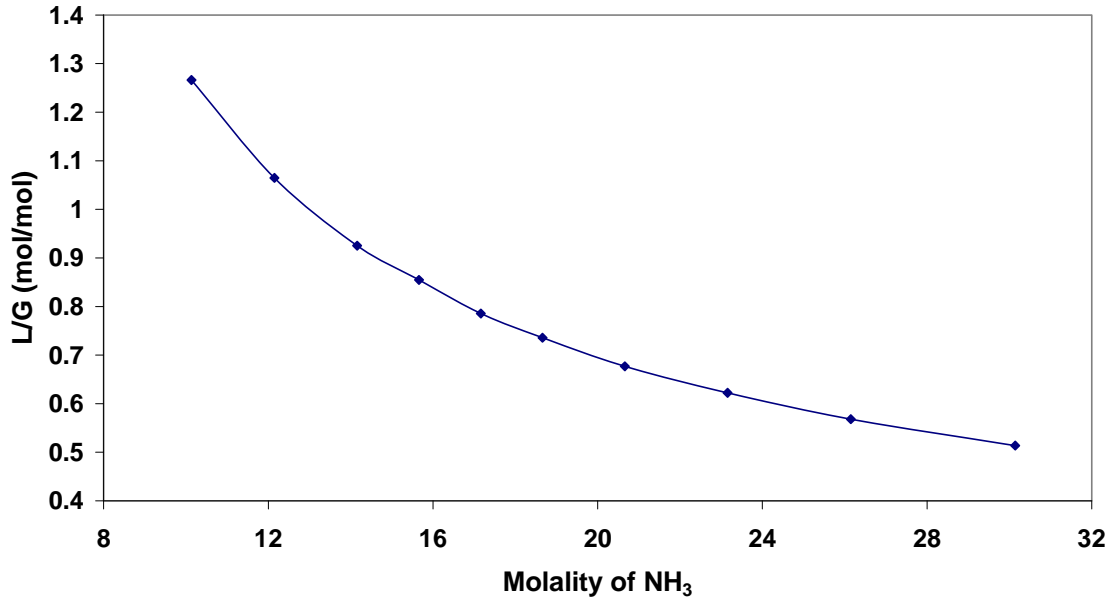


**Figure 5-12: Variation of L/G with molality of NH<sub>3</sub> for a lean loading of 0.4 and temperature of 5°C for 85% capture of CO<sub>2</sub> from coal flue gas**

As the molality continues to increase, a flattening of the L/G curve is observed. In addition, as the molality of the solution increases, the wt. % of solids in the resulting rich solution also increases. This, in turn, increases the refrigeration duty in the absorber. Figure 5-13 shows the variation in wt.% of rich solids and refrigeration load with molality. This increase in the amount of solids in the rich solution also has implications on the heat duty in the heat exchanger prior to the desorber. It is necessary that all solids go into solution before the rich stream proceeds to the desorber in order to avoid fouling. As the wt. % of the solids increases, a greater amount of solids will remain undissolved

after the cross heat exchanger and a higher heat duty will be required in the subsequent heat exchanger.

### Refrigeration duty and rich solids wt.% vs molality of NH<sub>3</sub> for a lean loading of 0.40 and temperature of 5°C

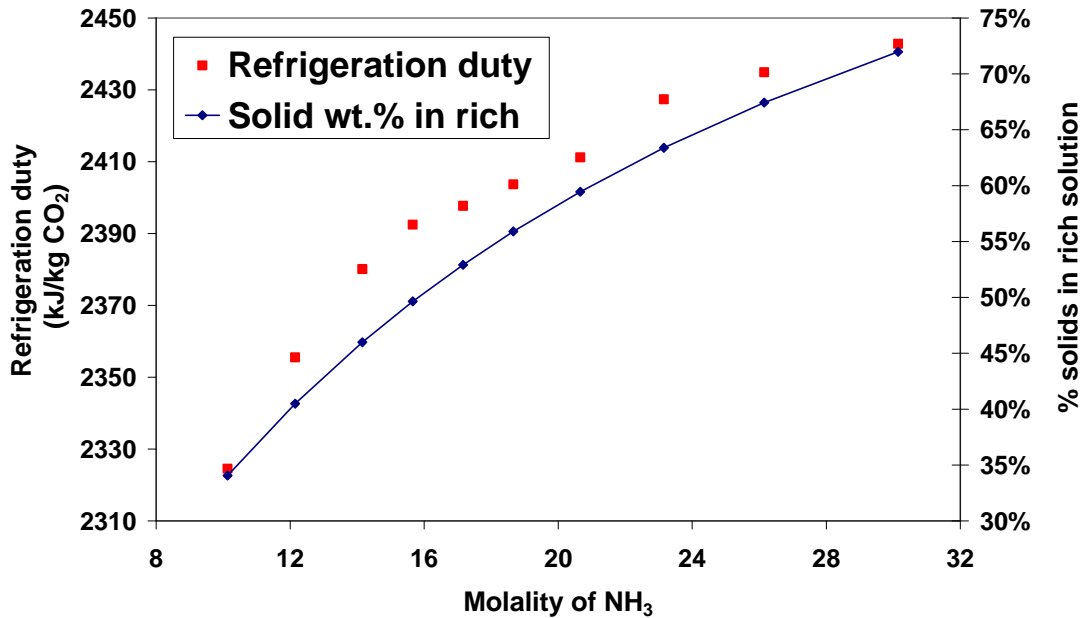


Figure 5-13: Variation of refrigeration duty and rich solids wt.% with molality of NH<sub>3</sub> for a lean loading of 0.4 and temperature of 5°C for 85% capture of CO<sub>2</sub> from coal flue gas

## 5.6 Analysis of the desorber

The next set of parametric simulations focused on getting an understanding of the different factors that influence the performance of the desorber system. The rich stream, after leaving the absorber is pumped to 30 atm and is then taken to a cross heat exchanger, where it exchanges heat with the lean stream leaving the desorber. In some cases, it may be necessary that there is further heat treatment before the stream is taken to the desorber, so that solids are completely dissolved and there is no issue of fouling in the desorber. The flowsheet as set up in ASPEN for this section of the simulation is shown in

Figure 5-14. In this case, there are two heat exchangers. The first heat exchanger is the cross heat exchanger. In the second heat exchanger, heat is supplied in order to dissolve the solids before the stream goes to the desorber. The convergence process is a three-step procedure:

1. Initially, the temperature at the outlet of the second heat exchanger at which the solids will completely be in solution is determined. This is done by varying the outlet temperature till there are no solids remaining in the outlet stream.
2. The heat duty in the desorber is varied till the required regeneration of CO<sub>2</sub> is achieved. Once this is done, it fixes the temperature in the reboiler and hence, the temperature of the lean stream that exits the desorber.
3. Once the temperature of the lean stream that exits the desorber is fixed, the heat duty in the lean heat exchanger can be determined since the outlet temperature from this heat exchanger is fixed at the inlet temperature of the stream to the absorber. This is the heat duty that needs to be matched with the first rich heat exchanger and this is done by varying the outlet temperature of the rich heat exchanger.

The desorber is modeled as a packed column in ASPEN Plus using the Radfrac module. The pressure in the condenser stage of the desorber is set at 30 atm. In some cases, it may also be necessary to have a water wash column after the desorber so that any traces of NH<sub>3</sub> that are present in the CO<sub>2</sub> outlet stream can be combined. Given the high pressure and temperature in the desorber, this is not likely; however, if such a wash is needed, the outlet from the wash can be sent to the wash desorber that handles the stream from the absorber section.

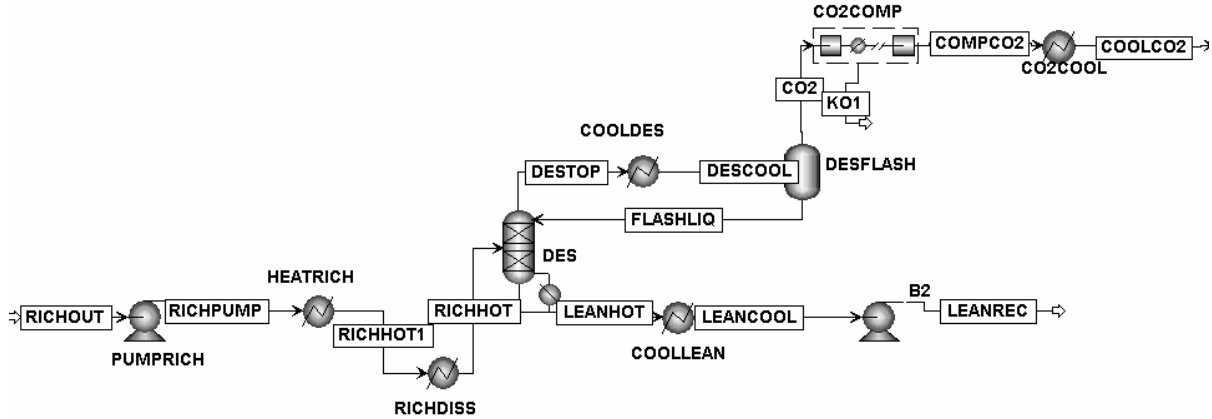


**Figure 5-14: Desorber section of the flowsheet as developed in ASPEN Plus**

The parametric simulations on the desorber were carried out for cases where the absorber inlet temperature was 5°C and the lean loading (CO<sub>2</sub> to NH<sub>3</sub> mole ratio in the lean solution) was 0.4. The simulations were performed at different molalities in order to investigate the effect of concentration of solution on the performance of the system.

Since this was a combined study of the absorber and desorber, the first analysis was to look at how the flowrate and composition of the stream from the absorber varied as the concentration of NH<sub>3</sub> in the solution increased. As the molality of NH<sub>3</sub> increases, at a constant inlet lean loading, we would expect that the precipitation of ammonium bicarbonate would be increased. This increase in precipitation should result in the system needing a lower flowrate of the lean solution in order to achieve 85% capture. This is what was observed from the simulations as shown in Figure 5-15.

It is notable that as the molality increases from 12M NH<sub>3</sub> to 28M NH<sub>3</sub>, the required liquid flowrate in the column almost halves. This is significant because the sensible heat swing required in the desorber is quite large.

**Plot of L/G and solid % in rich stream vs molality of NH<sub>3</sub> solution, lean loading of 0.4, temperature of 5°C**

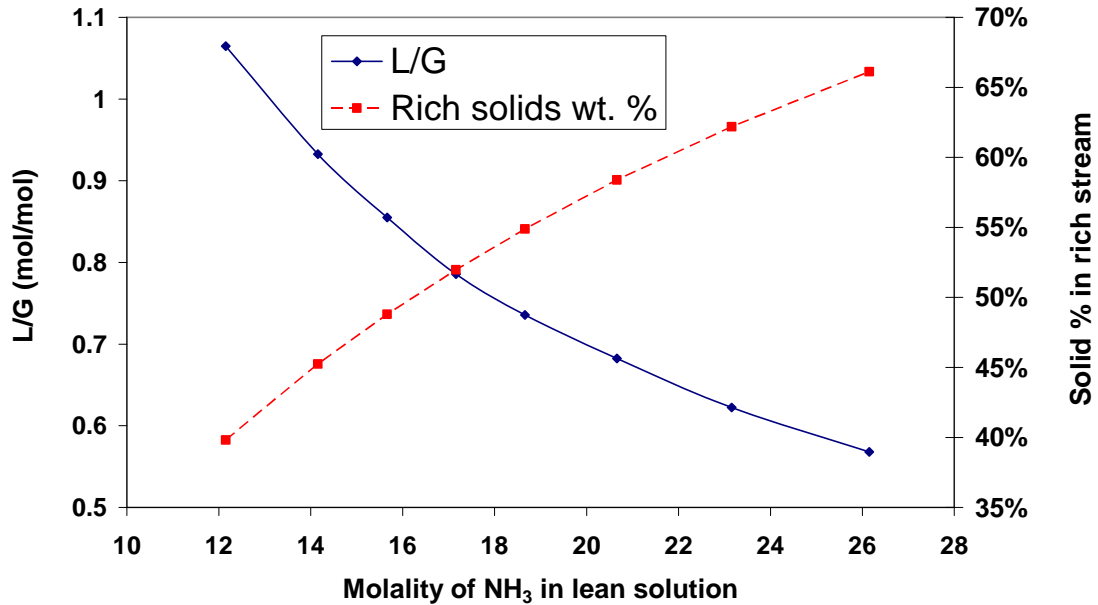


**Figure 5-15: Variation of L/G and solid% in rich stream vs. molality of NH<sub>3</sub> solution at lean loading of 0.4 and temperature of 5°C for 85% capture of CO<sub>2</sub> from coal flue gas.**

However, as the molality of the solution increases, the precipitation of ammonium bicarbonate and hence, the refrigeration duty required to maintain a temperature of 5°C in the absorber increases due to the exothermic nature of the precipitation reaction. Figure 5-16 shows the change in refrigeration duty (kJ/kg CO<sub>2</sub>) with molality of NH<sub>3</sub>.

### Plot of refrigeration duty vs. molality of NH<sub>3</sub> in solution

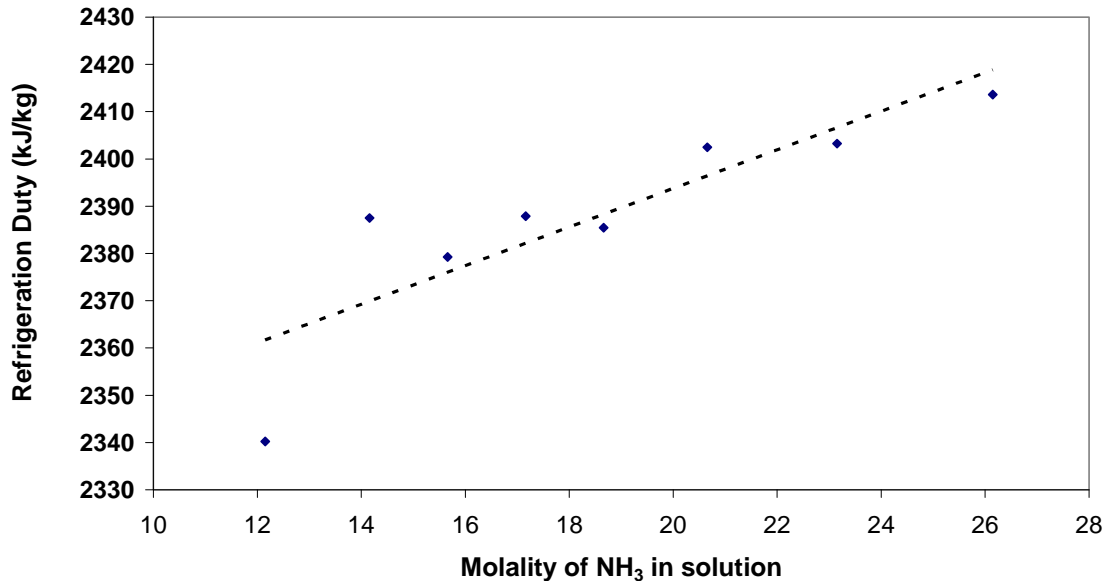


**Figure 5-16: Variation of refrigeration duty in absorber with molality of NH<sub>3</sub> solution for a lean loading of 0.4 and temperature of 5°C and 85% capture of CO<sub>2</sub> from coal flue gas.**

The heat duty in the desorber and heat exchangers arise from 4 different sources:

- 1. Sensible heat requirement:** The temperature in the reboiler of the desorber ranges between 140 – 150 °C, thus necessitating a temperature swing of 135-145°C between the absorber and the desorber. This means that there is a large sensible heat requirement in the system. Though some of this is mitigated by the cross-heat exchanger, it does not provide the entire sensible heat required by the rich stream.
- 2. Heat of dissolution of ammonium bicarbonate:** The reaction that causes the ammonium bicarbonate solid to go into solution is endothermic and has a heat of

reaction of 19.9 kcal/mol. Thus, heat has to be supplied in the heat exchanger for this reaction.

- 3. Heat of reaction to regenerate solvent:** The regeneration of the lean ammonium carbonate solution is a series of endothermic reactions for which heat needs to be supplied.
- 4. Steam for stripping:** In order to maintain the driving force for transfer of CO<sub>2</sub> from liquid phase to gas phase in the desorber, steam is required in order due to dilute the gas phase. This adds an additional heat requirement in the desorber.

Depending on the molality, the heat duty in the cross heat exchanger is either sufficient or insufficient to dissolve all the solids present in the rich stream. When the heat duty is not sufficient, further heating is required in a second heat exchanger before the desorber. As the molality increases, it is found that the wt.% of solids leaving the heat exchanger increases, thus necessitating higher heat duties in the second heat exchanger. This is shown in Figure 5-17. Thus, upto 17m NH<sub>3</sub> in solution, there is no solid left in the stream leaving the cross heat exchanger and a second heat exchanger does not need to be utilized. Beyond 17m NH<sub>3</sub> solution, when the lean loading is 0.4, a second heat exchanger is required before the rich stream is sent to the desorber. This will be an additional capital cost consideration. Both heat exchangers operate at 30 atm. However, the temperature of the solution in these heat exchangers is lower than that in the desorber and hence a lower quality heat source can be utilized in these exchangers. This is an area where there is potential for heat integration of the capture system with the power plant.

**Plot of wt.% of solids leaving heat exchanger and addnl. heat exchanger duty vs. molality of NH<sub>3</sub> in solution, lean loading of 0.4 and temperature of 5°C**

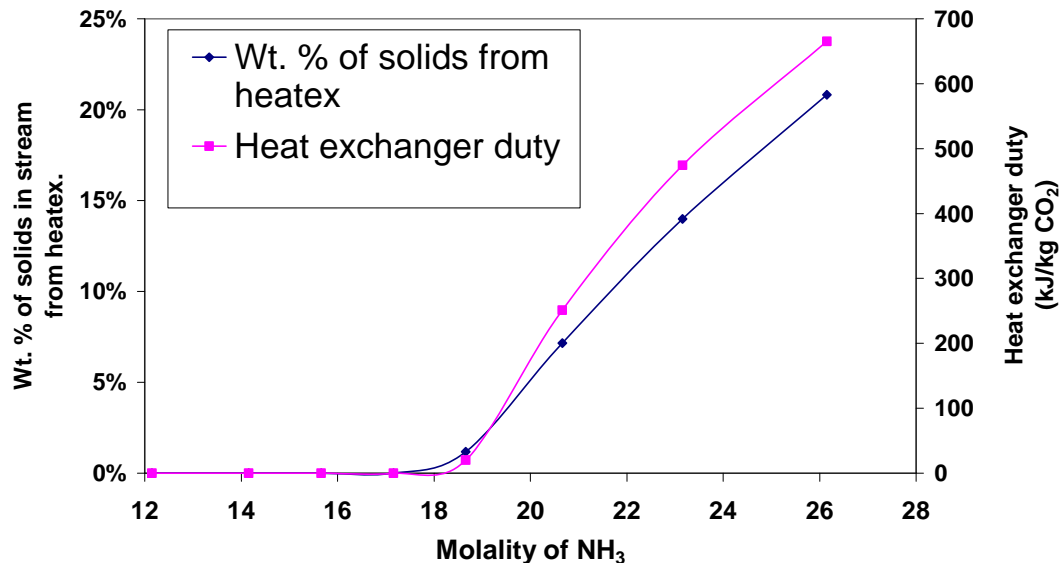


**Figure 5-17: Variation of wt.% of solids leaving heat exchanger and additional heat exchanger duty with molality of NH<sub>3</sub> at a lean loading of 0.4 and temperature of 5°C for 85% capture of CO<sub>2</sub> from coal flue gas**

The rich stream is taken to the desorber, where the desorber duty is varied till all the CO<sub>2</sub> that was absorbed into the solution in the absorber is removed. As the molality of the solution and hence, the amount of heat supplied in the second heat exchanger increases, the amount of heat that needs to be supplied in the desorber decreases. This is because, in the second heat exchanger, in addition to the heat being used to dissolve the solids, heat is also used to carry out the reaction for the removal of CO<sub>2</sub> and to increase the temperature of the solution. Hence, in these cases, less heat is required in the desorber. Figure 5-18 shows how the duty in the heat exchanger and desorber vary with the molality of NH<sub>3</sub> in the solution at a constant lean loading of 0.4 and temperature of 5°C.

**Plot of desorber and heat exchanger duties vs. molality of NH<sub>3</sub> solution at lean loading of 0.4 and temperature of 5°C**

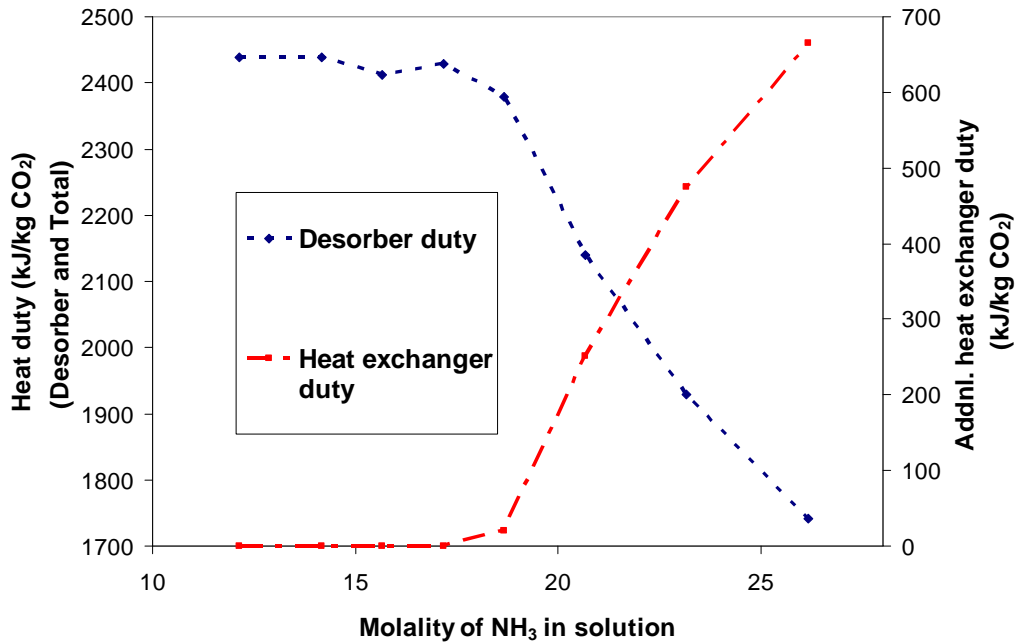


**Figure 5-18: Variation of desorber and heat exchanger duties with molality of NH<sub>3</sub> solution at a lean loading of 0.4 and temperature of 5°C for 85% capture of CO<sub>2</sub> from coal flue gas**

The average total heat duty is in the range of 2400 kJ/kg CO<sub>2</sub> while the distribution between the heat exchanger and the desorber varies. Since the heat in the heat exchanger is of lower quality it is beneficial to shift as much of the heat duty to the heat exchanger as possible by heat integration with the power plant. While the overall heat duty is significantly lower than the heat duty in a typical MEA stripper (4000 kJ/kg CO<sub>2</sub>), it should be noted that most of this heat needs to be supplied by steam that condenses at 160°C while the MEA process needs steam that condenses at 135°C and thus the effective work does not decrease in the same ratio. In addition, the ammonia process has significant work requirements in the refrigeration of the absorber as well as in the water wash desorber. These simulations were also performed using the equilibrium method and when the rate method is employed, the heat requirements will only increase.

## 5.7 Discussion of mass transfer considerations

In the modeling of the chilled ammonia system, the absorber was modeled as made up of a number of equilibrium stages – both from the kinetics viewpoint as well as the mass transfer view. However, it is important to consider the mass transfer implications in the chilled ammonia system, particularly given the precipitation that occurs in the system. In this section, a preliminary discussion on the comparison of the mass transfer coefficient in the chilled ammonia system with the MEA system is presented.

### 5.7.1 Intrinsic mass transfer coefficient

If we assume the reaction of CO<sub>2</sub> with the solvent to be a pseudo-first order reaction as an approximation, we have:

$$r_{CO_2} = k_1[CO_2] \quad (5-15)$$

with

$$k_1 = k_2[C_s] \quad (5-16)$$

Where:

$k_1$  is the pseudo-first order rate constant

$k_2$  is the second order rate constant

$C_s$  is the concentration of the solvent

The differential equation representing the steady state transfer is then given by:

$$D_{CO_2} \frac{\partial^2 [CO_2]}{\partial x^2} - k_1 [CO_2] = 0 \quad (5-17)$$

Where:

$D_{CO_2}$  is the diffusivity of CO<sub>2</sub>

The boundary conditions are:

$$[CO_2] = [CO_2]_i \quad @ \quad x = 0 \quad (5-18)$$

$$[CO_2] = 0 \quad @ \quad x = \delta \quad (5-19)$$

Where

$x = 0$  and  $x = \delta$  are the boundaries of the liquid film

The general solution of this equation as given by Danckwerts [12] is:

$$[CO_2] = \frac{1}{\sinh \sqrt{M}} \left[ [CO_2]_b \sinh \left( x \sqrt{\frac{k_1}{D_{CO_2}}} \right) + [CO_2]_i \sinh \left( \frac{D_{CO_2}}{k_1} - x \right) \sqrt{\frac{k_1}{D_{CO_2}}} \right] \quad (5-20)$$

Where:

$$M = \frac{D_{CO_2} k_1}{k_l^2} \quad (5-21)$$

Where:

$M = (\text{Hatta number})^2$

$k_l$  is the mass transfer coefficient in m/s

Now applying Fick's law at the gas-liquid interface, we have

$$N_{CO_2} = - \frac{d[CO_2]}{dx} \Big|_{x=0} \quad (5-22)$$

Where:

$N_{CO_2}$  is the flux of  $CO_2$

This gives us an expression for  $CO_2$  flux under first and pseudo first-order conditions [12]:

$$N_{CO_2} = k_i \left( [CO_2]_i - \frac{[CO_2]_b}{\cosh \sqrt{M}} \right) \frac{\sqrt{M}}{\tanh \sqrt{M}} \quad (5-23)$$

As the rate of the reaction increases, the Hatta number increases and the reaction becomes completed in the film and  $[CO_2]_b \rightarrow 0$  and the tanh contribution tends to 1. Hence we obtain,

$$N_{CO_2} = k_i \sqrt{M} [CO_2]_i \quad (5-24)$$

$$N_{CO_2} = \sqrt{k_1 D_{CO_2}} [CO_2]_i \quad (5-25)$$

Equation (5-25) and equation (5-16) can be combined to give equation (5-26)

$$N_{CO_2} = \sqrt{k_2 C_s D_{CO_2}} [CO_2]_i \quad (5-26)$$

The equation for the  $CO_2$  flux can also be given as in (5-27)

$$N_{CO_2} = k_L (CO_{2i} - CO_{2b}) \quad (5-27)$$

Since  $CO_{2b} \rightarrow 0$ , we have

$$N_{CO_2} = k_L [CO_2]_i \quad (5-28)$$

Comparing (5-26) and (5-28), we have

$$k_L = \sqrt{k_2 [C_s] D_{CO_2}} \quad (5-29)$$

Thus, using the above equation it is possible to compare the mass transfer coefficients that are obtainable in different solutions. In particular, we can compare the mass transfer coefficients that will exist in the absorption of CO<sub>2</sub> in the MEA process as well as in the chilled ammonia process.

#### 5.7.1.1 Kinetic constant for MEA system

A number of researchers have investigated the kinetic of CO<sub>2</sub> absorption in MEA [13-17]. Bishnoi [18] provides a compilation of the various results and suggests that the rate expression provided by Hikita [16] fits the data the best. The rate expression is:

$$\log_{10}k_2 = 10.99 - \frac{2152}{T} \quad (5-30)$$

This was measured in the range of temperature of 278 – 315 K. However, none of the researchers have performed measurements at concentrations of 5M which is what is prevalent in industrial applications or in partially loaded MEA solutions. For the purpose of this discussion, we will utilize the above expression to calculate the rate.

Using the above expression, at 313 K, which is the normal temperature in a MEA absorber, we obtain a value of k<sub>2</sub> of 13.02 m<sup>3</sup>/mol-s. In our calculations, we will also use a MEA concentration of 5M in the absorber which is the concentration corresponding to a 30 wt.% MEA solution.

#### 5.7.1.2 Kinetic constant for ammonia system

For the rate constant for the reaction of CO<sub>2</sub> with NH<sub>3</sub>, the expression of Pinsent [19] was utilized. The reaction constant is given by:

$$\log_{10} k_2 = 11.13 - \frac{2530}{T} \quad (5-31)$$

The measurements were conducted at temperatures between 0 – 40°C and at low molalities of NH<sub>3</sub>. Using the above expression, at 5°C, we get a rate constant for the reaction as 0.107 m<sup>3</sup>/mol-s. In our calculations, we will use a 16 M NH<sub>3</sub> solution. We can assume that the diffusivity of CO<sub>2</sub> in both MEA and NH<sub>3</sub> is the same as in water.

### 5.7.1.3 Comparison of mass transfer coefficient in MEA system with chilled ammonia system

Using (5-29), we have

$$\frac{k_{L,MEA}}{k_{L,NH_3}} = \sqrt{\frac{k_{2,MEA} C_{MEA}}{k_{2,NH_3} C_{NH_3}}}$$

$$\frac{k_{L,MEA}}{k_{L,NH_3}} = \sqrt{\frac{13.02 * 5 * 1000}{0.107 * 16 * 1000}}$$

Hence, we have

$$\frac{k_{L,MEA}}{k_{L,NH_3}} = 6.17$$

Thus, the mass transfer coefficient in the chilled ammonia process is 6 times lower than that in the MEA process. This means that the absorbers utilized in the chilled ammonia process will have to be much bigger than those in the MEA process. This adds additional capital cost to the plant.

## 5.7.2 Inhibition of mass transfer by precipitation

The second issue with the ammonia absorbers is that of precipitation. Since there is significant solid precipitation, it may not be appropriate to use a packed tower to avoid problems with the clogging of packing. A design such as a spray tower may have to be employed. However, the mass transfer obtained in spray towers is inherently poorer than in packed columns. Given the lower intrinsic mass transfer coefficient in the ammonia

process as compared to the MEA process, this will pose a significant problem. Alternative absorber designs that will allow sufficient mass transfer without being inhibited by solid precipitation will need to be investigated.

## **5.8 Total energy utilization in the chilled ammonia system**

In order to compare the performance of the chilled ammonia system to the MEA system, it is necessary to quantify the total energy use in the system. In the chilled ammonia system, energy requirements in the form of power and heat occur in different sections of the system. These are outlined below:

### **Heat requirements:**

1. Main CO<sub>2</sub> desorber
2. Heat exchanger following the cross heat exchanger
3. Water wash desorber

### **Electric work requirements:**

1. Blower for flue gas
2. Refrigeration for absorber
3. Flue gas chiller
4. Various pumps
5. CO<sub>2</sub> compressor
6. Flue gas blower

In this section, the calculation procedure for some of these quantities has been detailed and the overall expected energy consumption is presented.

### 5.8.1 Coefficient of performance for refrigeration

As discussed in previous sections, the absorber in the chilled ammonia process needs to be refrigerated. ASPEN provides the thermal refrigeration duty that is required to maintain a certain temperature profile in the absorber. In order to calculate the effect on the electrical efficiency of the power plant, we need to convert the thermal refrigeration duty to electric work. This is done through the utilization of the coefficient of performance COP [20].

$$COP = \frac{Q_c}{W} \quad (5-32)$$

Where:

$Q_c$  is the heat absorbed at the lower temperature

$W$  is the net work

In an optimistic case, we can assume that the coefficient of performance (COP) for the refrigeration is 4. In this scenario, when the refrigeration duty is 2500 kJ/kg, we obtain a net work (refrigeration compressor load) of 625 kJ/kg of CO<sub>2</sub>.

### 5.8.2 Compression work

The amount of compression work required in the chilled ammonia system will be lower than in the MEA system due to the fact that the desorber in the chilled ammonia system operates at 30 atm. This means that the CO<sub>2</sub> product only has to be compressed from 30 atm to the discharge pressure rather than from 1.7 atm as is the case with the MEA system.

In the flowsheet, the CO<sub>2</sub> compression system was modeled with the MCOMPR model with a two stage reciprocating compressor with interstage cooling. The discharge pressure from the compressor unit was set at 90 MPa after which the stream was cooled

before sending it to a pump where the discharge pressure was 139 MPa. The thermodynamics of the compression section was modeled using the Reidlich Kwong Soave equation with the Boston-Mathias correction (RKS-BM). For this purpose, the compression section was specified as a new section in the ASPEN flowsheet.

### **5.8.3 Flue gas chiller work**

The flue gas from the power plant is passed through a blower to raise its pressure and then passed through a DCC. At the exit of the DCC, the temperature of the flue gas is 25°C. It is necessary to cool this flue gas further to 10°C before it can be introduced into the absorber. For this purpose, mechanical chillers are employed. Thus, this is another chilling load in the plant.

### **5.8.4 Steam extraction from power plant**

Steam needs to be extracted from the power plant to satisfy two requirements. In the water wash desorber, the reboiler temperature is at 100°C. Hence, the condensing temperature of the steam utilized in the desorber needs to be at least 10°C higher. For the purposes of the calculation, we choose to use steam which is at 1.5 bar and has a saturation temperature of 112°C.

In the main CO<sub>2</sub> desorber, the reboiler temperature is as high as 150°C. Hence, we need steam that has a condensing temperature of around 160°C. We choose to use steam at 6.25 bar that has a saturation temperature of 160°C.

In the heat exchanger prior to the desorber, the temperature that exists is around 75°C. Hence, to provide heat in this exchanger, we need steam at around 85°C. We choose to use steam at 0.75 bar that has a saturation temperature of 90°C.

Hence, steam needs to be extracted from the power plant at 3 different conditions. This may create complications in the design of the steam cycle. In addition, the extraction of steam at the high pressure that is required for use in the main desorber may prove to be difficult since these needs to be done from the IP casing. Typically, only small amounts

of steam are withdrawn from the IP casing and it may be difficult to withdraw the large flow that is required in the desorber. This is an area of design of the plant that needs to be investigated further. It may also be possible to use flue gas from the power plant to provide heat in the second heat exchanger before the desorber. If this is done, the third steam extraction can be avoided and the efficiency of the process would improve.

The different steam conditions required and the extraction conditions are summarized in Table 5-3.

**Table 5-3: Steam withdrawal condition for chilled ammonia system**

<b>Steam conditions</b>	<b>CO<sub>2</sub> desorber</b>	<b>Water wash desorber</b>	<b>Auxiliary heat exchanger</b>
<b>Saturation pressure (bar)</b>	6.25	1.5	0.75
<b>Saturation temperature (°C)</b>	160	111.37	91.79
<b>Withdrawal temperature (°C)</b>	300	167	107
<b>% power lost from power plant due to extraction of steam</b>	24.41%	10.92%	6.58%

Using these values, the work that is lost because of steam requirements in the ammonia system can be calculated.

The work that is required for different power sinks in CO<sub>2</sub> capture is shown in Table 5-4. The total work required in the chilled ammonia system is 0.020867 kWh/gmol CO<sub>2</sub> for 85% capture of CO<sub>2</sub> from flue gas from coal-fired power plants. The distribution of this work between the different components is shown in Figure 5-19.

**Table 5-4: Work required in different components of the chilled ammonia system**

Power sink	Work (kWh/gmol CO <sub>2</sub> )
Reboiler duty	0.006587
Water wash desorber duty	0.000697
Refrigeration	0.009285
CO <sub>2</sub> compression	0.001228
Blower and auxiliaries	0.00307
<b>Total</b>	<b>0.020867</b>

**Distribution of energy requirements in chilled ammonia system**

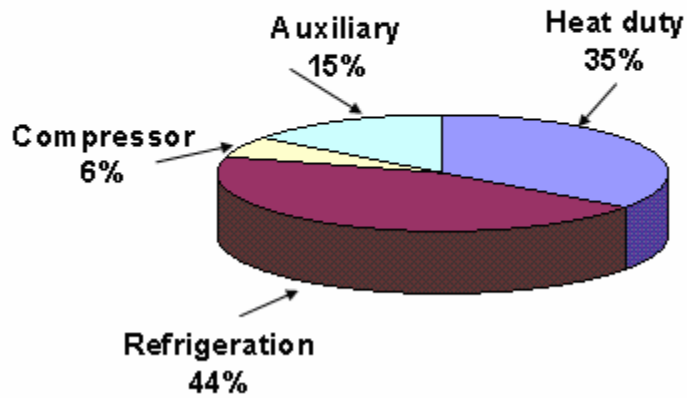


**Figure 5-19: Distribution of energy requirements in chilled ammonia system for 85% capture of CO<sub>2</sub> from flue gas from coal-fired power plants**

Figure 5-20 compares the power requirement for CO<sub>2</sub> capture to the total output of the power plant.

### Energy requirement for CO<sub>2</sub> capture in a coal-fired power plant using chilled ammonia

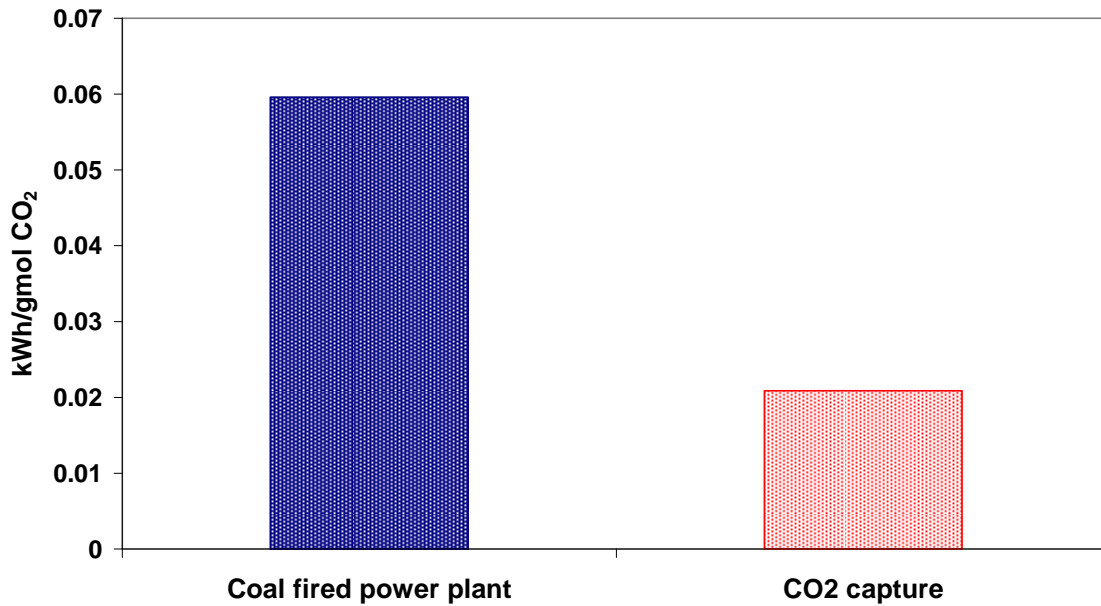


**Figure 5-20: Energy requirement for 85% capture of CO<sub>2</sub> from flue gas from a coal-fired power plant using chilled ammonia solvent system**

The derating of the coal-fired power plant for 85% capture of CO<sub>2</sub> is 29.5%. The derating when MEA was used as the solvent was 23%. Hence, chilled ammonia has a higher energy penalty than MEA. Refrigeration in the absorber and chilling of flue gas accounts for the largest fraction of the power requirements. The heat duty in the main desorber as well as the water wash desorber is the next biggest requirement. The compression work is much lower than with MEA. In order to improve the efficiency of the process, heat integration options for the absorber refrigeration and flue gas chilling need to be investigated.

## 5.9 Conclusion for chilled ammonia system

A complete flowsheet model has been developed for CO<sub>2</sub> capture using chilled ammonia solvent. The SVLE and thermochemistry of the system were investigated and it was found that the formation of ammonium carbamate occurred in the system, thus increasing the heat of reaction. It was found that in order to control the amount of ammonia that is released to the atmosphere, a water wash absorber and desorber are needed after the main CO<sub>2</sub> absorber. The effect of absorber temperature on the slip was found to be substantial.

In order to have a high percentage of capture of CO<sub>2</sub>, a concentrated solution of ammonium carbonate was needed and this led to precipitation in the absorber. The occurrence of exothermic reactions in the absorber along with the exothermic precipitation reaction and the necessity of maintaining the absorber at a low temperature led to significant refrigeration needs in the absorber. The work load for flue gas chilling was high as well. The effect of lean loading and molality of the solution on the refrigeration requirements in the absorber and the water wash desorber duty was investigated and it was seen that a trade-off between the two was required. Since the desorber is operated at a high pressure (30 atm), the compression work is lower than with MEA. The total work for CO<sub>2</sub> capture from a coal fired power plant was estimated to be 0.021 kWh/gmol CO<sub>2</sub> with refrigeration accounting for 44% of the duty. This leads to a 29% derating in the power plant output. As shown before, the use of the MEA system leads to a 22% derating of the power plant output. The mass transfer rate in the chilled ammonia absorber is estimated to be much lower than in the case of MEA and hence, larger absorbers will be required.

## 5.10 References

1. Bai, H.L. and A.C. Yeh, *Removal of CO<sub>2</sub> greenhouse gas by ammonia scrubbing*. Industrial & Engineering Chemistry Research, 1997. **36**(6): p. 2490-2493.
2. Yeh, J.T., K.P. Resnik, K. Rygle, and H.W. Pennline, *Semi-batch absorption and regeneration studies for CO<sub>2</sub> capture by aqueous ammonia*. Fuel Processing Technology, 2005. **86**(14-15): p. 1533-1546.
3. McLarnon, C.R. and J.L. Duncan, *Testing of ammonia based CO<sub>2</sub> capture with multi-pollutant control technology*. Energy Procedia, 2008.
4. Gal, E., *Ultra cleaning combustion gas including the removal of CO<sub>2</sub>*, W.I. Property, Editor. 2006.
5. Kozak, F., A. Petig, E. Morris, R. Rhudy, and D. Thimsen, *Chilled ammonia process for CO<sub>2</sub> capture*. Energy Procedia, 2008.
6. Goppert, U. and G. Maurer, *Vapor Liquid Equilibria in Aqueous-Solutions of Ammonia and Carbon-Dioxide at Temperatures between 333-K and 393-K and Pressures up to 7 Mpa*. Fluid Phase Equilibria, 1988. **41**(1-2): p. 153-185.
7. ASPEN, *Rate-based model of the CO<sub>2</sub> capture process by NH<sub>3</sub> using Aspen Plus*. 2008, Aspen Plus.
8. Kurz, F., B. Rumpf, and G. Maurer, *Vapor-Liquid-Solid Equilibria in the System Nh<sub>3</sub>-Co<sub>2</sub>-H<sub>2</sub>o from around 310-K to 470-K - New Experimental-Data and Modeling*. Fluid Phase Equilibria, 1995. **104**: p. 261-275.
9. Kohl, A.L. and F.C. Riesenfeld, *Gas Purification*. 5th edition ed, ed. A.L. Kohl and F.C. Riesenfeld. 1997, New York: Elsevier. 1439.
10. Van Krevelen, D.W., P.J. Hoftijzer, and F.Y. Huntjens, *Composition and vapour pressures of aqueous solutions of ammonia, carbon dioxide and hydrogen sulphide*. Rec. Trav. Chim., 1949. **68**: p. 191-216.
11. Herzog, H., *Personal Communication*.
12. Danckwerts, P.V., *Gas Liquid Reactions*. 1970, New York: McGraw Hill.
13. Astarita, G., *Carbon dioxide absorption in aqueous monoethanolamine solutions*. Chem. Eng. Sci., 1961. **16**.
14. Danckwerts, P.V., *The reaction of CO<sub>2</sub> with ethanolamines*. Chem. Eng. Sci., 1979. **34**.

15. Jou, F.Y., A.E. Mather, and F.D. Otto, *The solubility of CO<sub>2</sub> in a 30 mass percent monoethanolamine solution*. Can. J. Chem. Eng., 1995. **73**.
16. Hikita, H., S. Asai, H. Ishikawa, and M. Honda, *The Kinetics of Reactions of Carbon Dioxide with Monoethanolamine, Diethanolamine and Triethanolamine by a Rapid Mixing Method*. Chem. Eng. J., 1977. **14**.
17. Hikita, H., S. Asai, Y. Katsu, and S. Ikuno, *Absorption of Carbon Dioxide into Aqueous Monoethanolamine*. AIChE Journal, 1979. **25**(5).
18. Bishnoi, S., *Carbon Dioxide Absorption and Solution Equilibrium in Piperazine Activated Methyldiethanolamine*, in *Chemical Engineering*. 2000, The University of Texas at Austin: Austin.
19. Pinsent, B.R.W., L. Pearson, and F.J.W. Roughton, *The Kinetics of Combination of Carbon Dioxide with Ammonia*. Trans. Faraday. Soc., 1956. **52**.
20. Smith, J.M., H.C. Van Ness, and M.M. Abbott, *Introduction to Chemical Engineering Thermodynamics*. 6 ed. 2001, New York: McGraw-Hill.

## Chapter 6

### Summary, Conclusions and Future Work

The need for CO<sub>2</sub> capture technologies is a pressing one and is assuming growing importance everyday. Post-combustion capture technologies represent one of the most promising methods of CO<sub>2</sub> capture and are the closest to commercialization. They also represent the class of technology that can most easily be retrofitted onto the existing fleet of power plants. The need of the hour is to identify and evaluate the performance of different solvents that can be used for post-combustion capture on a number of different dimensions – energy consumption, size of equipment, degradation and environmental impact. In this thesis, comprehensive process flowsheet simulations have been developed to obtain an objective and consistent comparison of the performance of MEA, potassium carbonate and chilled ammonia as solvents for capture of CO<sub>2</sub>.

#### 6.1 Summary of research and thesis contributions

ASPEN Plus was used as the tool in this thesis to develop detailed flowsheet models for the comparison of the performance of the different solvents systems. This allows an understanding of the process configuration required for each system. For each system, initially equilibrium-based simulations were performed in order to gain an understanding of the system. Following this, detailed rate-based models were developed for the MEA and potassium carbonate systems. The overall energy consumption in the CO<sub>2</sub> capture system, with proper definition of the system boundaries was calculated. In addition, an evaluation of the required equipment size for the critical equipment in the system was performed and the degradation characteristics and environmental impact of the solvent was investigated.

An important portion of this thesis was focused on developing a framework for building simulations that will allow an objective and consistent comparison of the performance of

different solvent systems. In order to carry this out, it was necessary to ensure that the physical properties, thermodynamics, thermochemistry and kinetics of the various systems were represented accurately in the simulation tool and that the mass transfer characteristics of the system were captured when sizing calculations were performed. Additionally, the boundaries of the CO<sub>2</sub> capture process have to be set appropriately so as to include all the attendant energy requirements in the system.

The thesis has also focused on performing parametric simulations to identify which variables have the most influence on the energy consumption in the system. This will be of help in guiding future investigations to identify optimal operating parameters for these solvent systems. The methodology developed in this thesis has been utilized in analyzing the performance of three solvent systems – MEA, potassium carbonate and chilled ammonia. A summary of the results from the three systems is presented below in Table 6-1.

**Table 6-1: Summary of results from the three solvent systems**

<b>Criteria</b>	<b>MEA</b>	<b>Chilled ammonia</b>	<b>K<sub>2</sub>CO<sub>3</sub></b>
<b>Work for 85% capture</b>	0.0157 kWh/gmol (24% derate)	0.0209 kWh/gmol (29% derate)	0.0095 kWh/gmol
<b>Operating pressure</b>	Abs: 1 atm Des: 1.7 atm	Abs: 1 atm Des: 30 atm	Abs: 15 atm Des: 1 atm
<b>Operating temperature</b>	Abs: 40-60 C Des: 115 C	Abs: 3-10 C Des: 130-150 C	Abs: 90-95 C Des: 105-110 C
<b>Size of equipment</b>	Absorber is bigger than desorber	Absorber will be bigger than MEA	Absorber same size as MEA; desorber bigger
<b>Degradation and volatility</b>	Degrades at high temp, volatile	Volatile, addnl. water wash required	Non volatile; no degradation

The base case system that was investigated in this thesis is the MEA system. Since, experimental data on the MEA system is available in literature, it served as a good system

to validate the modeling methodologies employed in this thesis. Rate-based simulations for the absorption of CO<sub>2</sub> from NGCC and coal-fired power plants into MEA were developed in ASPEN. The simulations showed that the energy penalty for 85% CO<sub>2</sub> capture from flue gas from coal-fired power plants is 0.01572 kWh/gmol CO<sub>2</sub> and from NGCC plants is 0.02388 kWh/gmol CO<sub>2</sub>. The reboiler duty in the case of CO<sub>2</sub> capture from coal-fired power plants was found to be 4200 kJ/kg. Different factors that influence the performance of the system such as the temperature in the absorber, pressure in the desorber and absorber packing and height were investigated. It was found that the energy penalty from CO<sub>2</sub> regeneration accounted for 60% of the energy penalty and that the compression work accounted for approximately 30% of the energy penalty. The process flexibility of the MEA system was limited by the MEA degradation reactions, the rate of which becomes unacceptably high beyond a temperature of 125°C. This restricted the maximum pressure that could be used in the desorber.

The second system investigated in this thesis was the potassium carbonate system. In comparison to MEA, it offers greater process flexibility due to lack of solvent degradation as well as the ability to operate the absorber and desorber at high temperatures. The heat of reaction for CO<sub>2</sub> with potassium carbonate is much lower than with MEA. A rate-based model was developed in ASPEN to analyze the performance of the potassium carbonate system. It was found that a high pressure (15 atm) was required in the absorber in order to make the operation feasible. Thus, potassium carbonate can be of particular use in pressurized combustion systems as well as in systems with reforming of fuel such as IRCC. The reboiler duty in the desorber was found to be 3200 kJ/kg for the standard configuration. Different schemes for energy recuperation in the system were investigated and it was found that the use of a split flow absorber could reduce the heat duty by 22%. An optimized version of the potassium carbonate flowsheet was developed for an IRCC application and the reboiler duty for this case was 1980 kJ/kg.

The third solvent system investigated in this thesis was the chilled ammonia system. A complete flowsheet model was developed for CO<sub>2</sub> capture using chilled ammonia solvent. It was found that in order to control the amount of ammonia that is released to

the atmosphere, a water wash absorber and desorber were needed after the main CO<sub>2</sub> absorber. In order to have a high percentage of capture of CO<sub>2</sub>, a concentrated solution of ammonium carbonate was needed and this led to precipitation in the absorber. The mass transfer rate in the chilled ammonia absorber was estimated to be much lower than in the case of MEA and hence, larger absorbers will be required. Significant refrigeration was also needed in the absorber as well as for flue gas chilling. Since the desorber is operated at a high pressure (30 atm), the compression work was lower than with MEA. The total work for 85% CO<sub>2</sub> capture from a coal fired power plant was estimated to be 0.021 kWh/gmol CO<sub>2</sub> with refrigeration accounting for 44% of the duty. In order to improve the efficiency of the system, the focus needs to be on reducing the refrigeration and chilling loads in the chilled ammonia process.

## 6.2 Future work

A number of research directions can be followed to continue this work further:

- 1. Evaluating activated solvents:** As discussed in this thesis, the addition of an activator to MEA and to K<sub>2</sub>CO<sub>3</sub> will significantly enhance the rate of reaction in these systems and hence have an effect on the energy consumption as well as size of equipment in the system. Flowsheet configurations can be developed for these activated solvents and simulations can be developed to optimize the performance of these systems.
- 2. Design of new solvents:** This thesis has attempted to explore and understand the parameters that influence the performance of different solvent systems. Using this approach, efforts can be made to design new solvent systems that will have lower energy consumption.
- 3. Energy integration with the power plant:** One of the most important means by which to reduce the energy penalty of CO<sub>2</sub> capture is to perform as much energy integration of the power plant with the CO<sub>2</sub> capture system as possible. This will

ensure that all sources of waste heat in the system are utilized. Using software such as GT PRO, a model of the power plant can be built and integrated with the ASPEN models of the capture system and the energy integration between the two systems can be optimized.

- 4. Economic analysis of capture systems:** Since the comprehensive flowsheet models developed as part of this thesis provide estimates of size of equipment as well as energy consumption, they can be used to obtain estimates of costs involved in implementing the capture system on the power plant.

## **Chapter 7**

### **PhD CEP capstone: Case study of different environmental regulations in the US**

One of the biggest holdbacks of implementing carbon capture on power plants has been the lack of environmental regulation on CO<sub>2</sub> emissions. In this project, different environmental regulations that have been successfully implemented in the US, namely the lead phasedown in gasoline, CFC abatement and regulation of SO<sub>2</sub> emissions from utilities have been studied. The study has been done with a particular focus on how environmental regulation affects technology innovation, diffusion and adoption by polluting firms.

#### **7.1 Comparison of command-and-control environmental policies and market-based environmental policies**

A number of environmental policy actions exist to tackle the problem of pollution. The environmental policy actions can be classified as either command-and-control or market-based policies [1]. In general, command-and-control policies are either design standards which dictate that a certain technology should be used or are performance standards which establish a limit on the maximum amount of pollution that each source can emit. Market-based approaches include policies such as the use of taxes on emissions and emissions credit trading [2]. There has been much debate as to which type of policies are best suited for regulating pollutants like CO<sub>2</sub> and for spurring innovation in environmental control technologies. different scenarios by way of case studies. Case

In the past, command-and-control policies have been choice of environmental regulators for enforcing new emission standards. In his paper [1], Stavins presents an excellent discussion on the reasons why this has been the case. It is argued that these policies prevailed because the four main parties who are involved in setting regulations – polluting firms, environmental advocacy groups, organized labor, legislators and policymakers- all favored them.

Existing firms prefer command-and-control policies because of the heavy input that they can provide in writing the standards. It allows them to secure more lenient requirements for existing firms while making the standards stricter for new entrants, thus giving the incumbents a competitive advantage and establishing an entry barrier. This was the case with the Clean Air Act in 1970, where existing coal-fired power plants were given less stringent limits and new firms were mandated to use scrubbing technology. This led to grandfathering of existing coal-fired power plants and led to delays in the launch of new coal-fired power plants in many areas of the country [3]. Stavins argues that since the focus of market-based permits is on the quantity of pollution and not on the source, it reduces the effects of lobbying by powerful interest groups [1]

Stavins [1] argues that environmental groups have also preferred command-and-control approaches because they feel that market-based approaches give firms a “license to pollute” and that they feel that the damage that is caused by pollution cannot be monetized in the form of emission credits or taxes. There have also been suggestions that environmentalists prefer command-and-control policies because they feel that it will be difficult to bring down permit levels and increase taxes once they are established. However, this is not persuasive since it is much harder to change a technology or performance standard once established under the command-and-control policy system. Environmentalists have also voiced the valid concern that the use of tradable permits can cause the concentration of pollution in some areas which will lead to high levels of pollution in these areas.

Both command-and-control environmental policies and market-based environmental policies cause technology innovation and diffusion since they require that some action be taken in order to comply with the mandated standards. However, it has been postulated that market-based approaches are more effective in establishing long-term incentives for technology invention, innovation and diffusion since they establish continuous incentives for emission reductions[2].

In this paper, both command-and-control policies as well as market-based policies are studied in the context of the case studies of the lead phasedown in US gasoline production, reduction in CFC usage in the US and reduction in SO<sub>2</sub> emissions from power plants in the US.

## **7.2 Phasedown of lead in gasoline in the United States**

This case study focused on the phasedown of lead usage in gasoline from 1974-1987. The history of the regulatory program as well as the effects on technology innovation, diffusion and adoption are described.

### **7.2.1 History of lead as a fuel additive and regulations on leaded gasoline**

One of the first successful environmental regulation using market-based-policies was the phasedown of lead in gasoline by U.S. petroleum refineries in the 1970s and 1980s. Since 1923, lead had been added to gasoline as an anti-knocking agent and to improve the octane rating of the gasoline fuel [4]. Leaded gasoline accounted for more than 90% of the automotive fuel sold in the US in the late 1960's. Hence, the use of leaded gasoline was very prevalent in the 1960's. Though concerns about the effect of leaded gasoline on human health were raised as early as 1922, a fierce industry lobbying effort, led by DuPont and General Motors ensured that there was no governmental regulation on lead usage in gasoline [4]. By the late 1960's and early 1970's, the ill effects of lead on human health were becoming more apparent. However, the first regulations on leaded gasoline were not put in place to address the effect on human health, but rather to mandate the use

of unleaded gasoline in new cars that had catalytic converters which controlled emissions of hydrocarbons, nitrogen oxides and carbon monoxide.[4]. This was necessary since lead destroyed the emissions control capacity of catalytic converters. The use of catalytic converters had come about as a requirement of the Clean Air Act of 1970. The EPA required refineries to offer at least one grade of unleaded gasoline no later than July 1974 [5]. It has been estimated that a large part of the phasedown of lead in gasoline in the US has been due to the introduction of the new fleet of cars with catalytic converters [6].

The EPA also mandated that refineries should decrease the average lead content of all the gasoline produced from 1975. However, the implementation of this requirement was delayed until 1979 [5]. The regulations were based on the size of the refinery. The average refinery had a capacity of 67,000 bpd [6]. The requirement was that large refineries – refineries with production capacity of more than 50,000 bpd and those owned by a refiner with a total capacity of 137,500 bpd - must not produce gasoline with a quarterly average of more than 0.8 glpg (grams of lead per gallon) (pooled, leaded and unleaded gasoline) in the first year and 0.5 glpg in the next two years. The restrictions for small refineries – those with a production capacity of less than 50,000 bpd or owned by a refiner with less than 137,500 bpd capacity – and mandated that they have a standard of 0.8 glpg – 2.65 glpg based on size of the refinery [5].

An interesting point here is that the initial restrictions were on pooled lead content. Hence, refineries could produce gasoline with high lead content as long as they produced enough unleaded gasoline to maintain their total lead content within the range. However, in this case, the new fleet of vehicles had catalytic converters and needed to operate on unleaded gasoline. Thus, refineries ended up producing large quantities of unleaded gasoline and gasoline lead levels had declined about 80% [6]. In 1982, further restrictions were put in place that limited the definition of small refineries to refineries with a production capacity of less than 10,000 bpd or those owned by a company with production capacity of less than 70,000 bpd [5]. These refineries were subjected to a pooled standard of 2.16 to 2.65 glpg based on size. Larger refineries faced new restrictions which were calculated only on the basis of the leaded gasoline produced [6].

These restrictions limited the allowable content of lead in leaded gasoline to a quarterly average of 1.1 glpg. Beginning in July 1983, the small refineries were also subjected to the same standard [5]. The allowable lead content was reduced to 0.5 glpg in 1985 and further reduced to 0.1 glpg in 1986, with lead finally being banned as a fuel additive in the US in 1996 [5].

### **7.2.2 Mechanics of the lead trading program in the US**

The mechanics of lead trading in the US had a number of different phases:

- **1974-1982:** In this time period, the EPA established performance standards on refineries with the standards varying according to the size of the refinery. There was no program for trading of lead credits in this time period. However in the early 1980s, when the agency was thinking about further tightening the regulations, it realized that smaller refineries in particular would have difficulty in meeting these standards. In general, smaller refineries did not possess the equipment needed to replace the octane from lead nor did they have the necessary capital to install new technologies such as isomerization. Hence, in order to ease the transition to the tighter standards and to provide the smaller refineries more flexibility, the EPA introduced a lead trading program [6-7].
- **1982-1985:** In 1982, the EPA introduced the inter-refinery lead averaging program which allowed the trading of lead rights between refineries of similar sizes. The refineries which were adding less lead to gasoline than prescribed by regulations accumulated lead credits that they could then trade to refineries that were adding more than the prescribed amount of lead to gasoline [7]. The lead trading program allowed the EPA to progressively tighten the regulations and remove the exemptions for the smaller refineries. While the lead trading program had initially been met with resistance in the 1970s when it was proposed, larger refineries now realized that it was in their competitive interest to remove the exemptions for smaller refineries and began to support the lead trading program [6].

- **1985-1987:** In this time period, the EPA introduced a banking system which allowed the EPA to progressively tighten the lead regulation standards and enable firms to meet these standards by smoothing their abatement costs without being subjected to a sudden spike in abatement cost. In the previous phase of the program, any credits that a refinery had accumulated over a quarter but had not traded by the end of the quarter expired at the end of the quarter [7]. With the introduction of the banking program, firms were allowed to store these rights, either for their own use later or for sale to other firms [7]. Many firms used rights from early 1985 to meet the progressively stringent regulations and hence, smoothed their abatement cost curve. This also allowed them more time to meet the more stringent regulations. While the EPA terminated the lead trading program in 1986, the banked rights were allowed to be used until 1987. Beyond this time, all refineries were subjected to the performance standard of 0.1 g/lpg lead.

The effect of trading and banking lead credits is shown in Figure 7-1 [7]. It can be seen that between 1982-1985, small refineries always exceeded the EPA standard for lead content while large refineries were at or below the standard. Small refineries were hence able to purchase lead credits from large refineries in order to meet the EPA standard. It can also be seen that in the first half of 1985, refineries were below the lead threshold set by the EPA and banked these credits for use in 1986, when the threshold lead limit was reduced and refineries exceeded this limit. Thus, between 1982 to 1987, the EPA introduced a market mechanism for trading of lead rights in order to bring down the lead content in gasoline. This had the effect of allowing firms which had the most cost efficient methods of reducing lead content to bear most of the abatement while the firms which had higher abatement costs bought lead rights from the former. This allowed a cost-effective means of allocating the abatement burden amongst different firms.

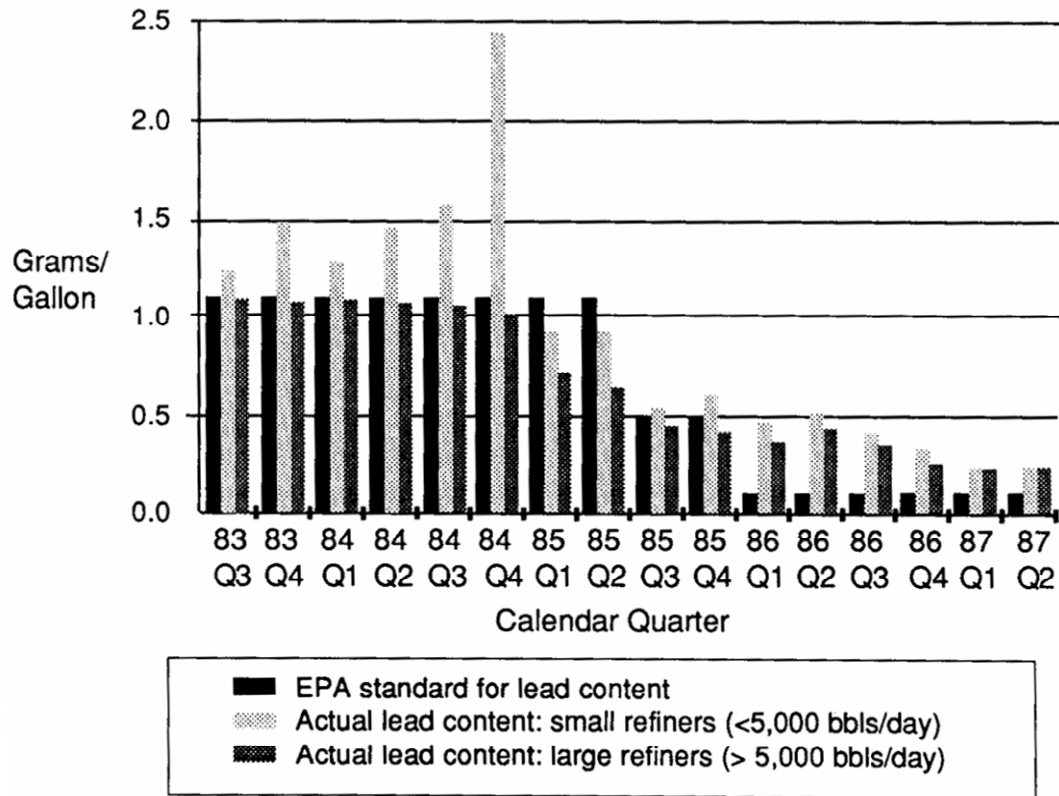


**Figure 7-1: Effect of lead allowances trading on compliance with regulations. Figure adapted from [7]**

Firms also used lead banking rights effectively in order to meet the regulations specified by the EPA. The lead rights banking activity by size is shown in Figure 7-2 [7]. Firms began withdrawing banked lead rights in the third quarter of 1985 in order to meet the tightened regulations set by the EPA. While large refiners had much more volume of activity in banking and withdrawing lead rights, small refiners were able to take advantage of the large volume of banked rights by purchasing rights from the large refiners [7].

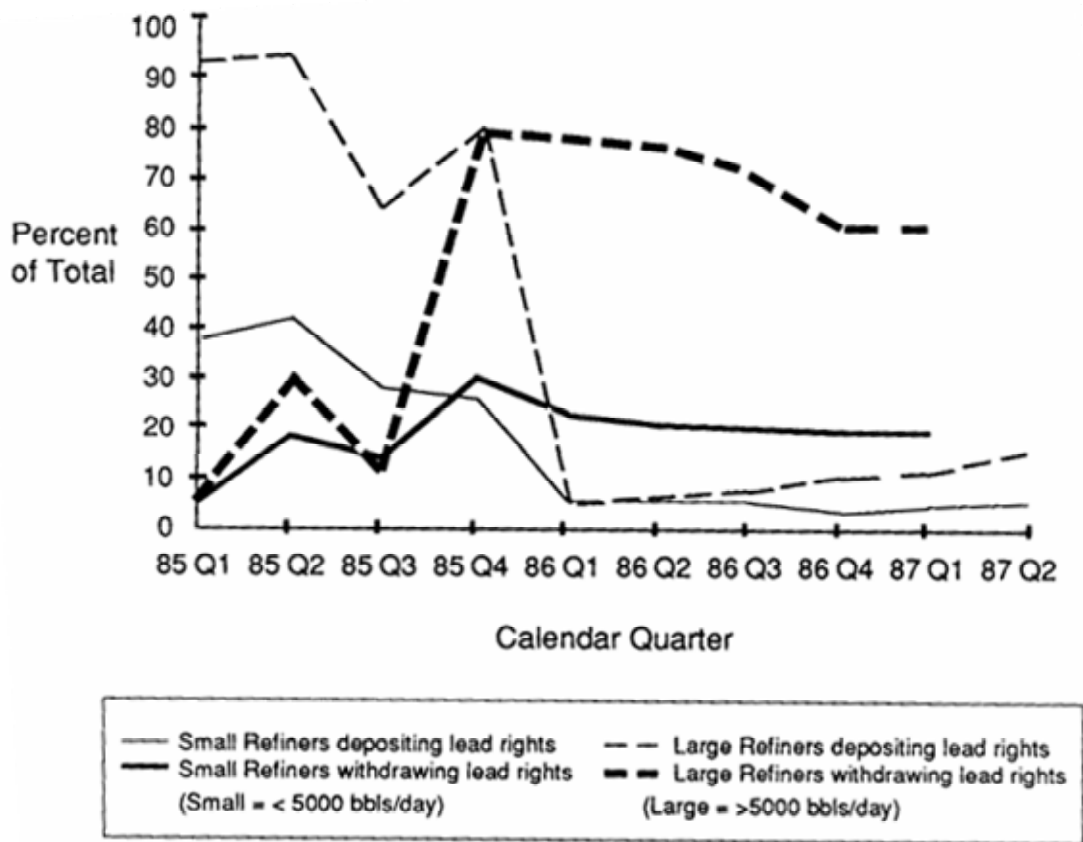


**Figure 7-2: Effect of lead allowances banking on compliance with regulations. Figure adapted from [7]**

In terms of cost savings from the lead trading program, it has been estimated that before banking, the price for lead rights was below one cent per gram and once banking was started, the price fluctuated between two to five cents per gram [7]. The EPA has estimated that banking could have lead to a savings of as much as \$226 million to refiners [7]. Hahn and Hester [7] estimate that the total savings from lead rights trading and banking would have amounted to hundreds of millions of dollars [6].

### **7.2.3 How did refineries adopt to changing lead regulations?**

In order to address the problem of decreasing octane in the gasoline due to reduction in the amount of lead added to gasoline, refineries had two options [5]:

- Use substitutes: Refineries could add substitutes like methyl tertiary-butyl ether (MTBE) to gasoline which act to increase the octane content in the fuel. The problem with these additives was that they were much more costly than lead and hence, the cost of processing gasoline would have gone up with the use of these additives.
- Make process modifications to increase octane rating: Refineries could have made use of their existing equipment and increased the octane rating by running them more intensively. Another option was to use raw material that had a higher octane content. A third option for refineries was to make use of pentane-hexane isomerization, a technology which allows increase in gasoline octane content. The technology could be used in refineries of different sizes [5].

Kerr and Newell [5] performed a study of 378 refineries operating in the period 1971-1995 and studied how the refineries adopted to the changes in lead regulation. They found that the effect of regulation on isomerization adoption was significant and estimated that a 10% increase in the strictness of the regulations led to a 40% increase in probability of adoption of isomerization by refineries [5]. Figure 7-3 shows how the isomerization capacity in refineries increased in this period. In the periods in which performance standards for individual refineries were put in place, the isomerization adoption increases sharply [5].

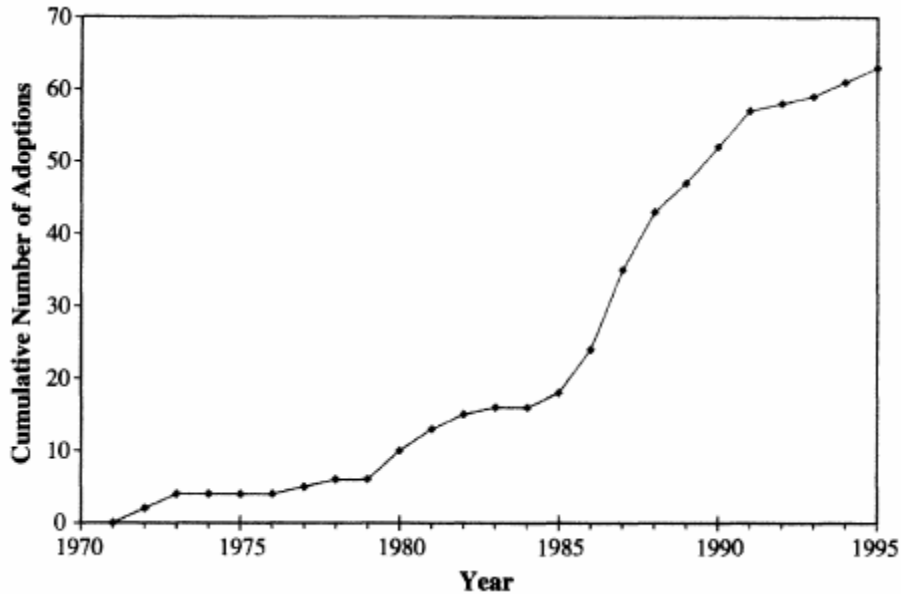


**Figure 7-3: Trend of cumulative number of isomerization adoptions over time. Figure adapted from [5]**

The authors also found a significant difference in the technology adoption behavior of refineries with low and high compliance costs. It was found that refineries with high compliance costs had a much lower tendency to adopt when market-based policies were in place as compared to the phases in which individual performance standards were in place[5]. Refineries with low compliance costs were quick to adopt technology when market-based policies were in place and sold their permits to the refineries with high-compliance cost. This suggests that when market-based instruments are in place, technology adoption will initially be only by those firms with low compliance costs before diffusing to firms with high compliance costs. It was also found that refineries with larger sizes had higher adoption rates. The authors found that a 10% increase from the mean in individual refinery capacity led to a 4% increase in the adoption rate [5]. As is expected, it was also found that more technologically complex refineries had a higher tendency to adopt the isomerization technology.

#### **7.2.4 Conclusion on phasedown of lead usage in gasoline**

The phasedown of lead in gasoline in the United States was achieved through a combination of performance standards and market-based policy measure from 1974 to 1982. The program was successful in achieving its goals and also appears to have done it in an economically feasible way. It serves as a model of an environmental regulation program which is done through a cap and trade policy with a constant reduction on the cap of pollutant allowed to be used. The program was successful in distributing the burden of abatement in a cost-effective manner and in allowing flexibility to refineries to decide the manner in which they should deal with the abatement. It was seen that refineries with lower compliance costs were the first adopters of new, innovative technology and produced gasoline with lower lead content than mandated by the EPA. They were hence able to sell lead rights to refineries with higher compliance costs. Since the allowance for the amount of permissible lead addition to gasoline was progressively tightened and was ultimately changed to a performance mandate, this forced the refineries with higher compliance costs to switch to the new technology at a later stage.

Thus, the lead rights trading program enabled refineries to switch to the new technology after it had been established and the cost had decreased. Forcing them to do it earlier may not have been feasible. In addition, the banking component of the program allowed refineries to smooth the amount of lead added to gasoline and the compliance costs and hence enabled them to meet the tightened regulations.

According to Hahn and Hester [7], the success of the lead rights trading program can in part be attributed to the low administrative requirements for firms engaged in trading. Each quarter, refineries only had to report the amount of lead they had added to gasoline, the volume of rights traded and their trading partners. Since this information was readily available to the refineries, participation in the lead rights trading program did not lead to an undue increase in reporting burdens. In addition, Hahn and Hester [7] postulate that the presence of well-established markets in refinery feedstocks and products enabled the success of the lead rights trading program.

## **7.3 Chlorofluorocarbon (CFC) reduction in the US**

### **7.3.1 What are CFCs and why are they harmful?**

Ozone occurs in the atmosphere at two different levels – the troposphere (below 15 kms from the surface of the earth) and in the stratosphere (between 15-50 kms above the surface of the earth). Ozone that occurs in the troposphere is harmful to human life as high levels of ozone can lead to respiratory diseases and can also damage vegetation. However, ozone in the stratosphere protects the earth from 90% of the UV radiation that comes in and is hence, an essential component of the atmosphere.

Chlorofluorocarbons (CFCs) were developed in the 1930s for use in refrigeration. Their commercial use grew rapidly afterwards and major applications included residential and commercial refrigeration, air-conditioning, plastic insulation, cushioning foams and use as a propellant in aerosol dispensers [8]. In 1974, it was initially identified that CFCs may be responsible for the depletion of stratospheric ozone [9].

The use of CFCs in aerosols results in their immediate release to the atmosphere upon use. In other applications like refrigeration, leakage of CFC can occur and upon disposal, a large portion of the CFC is released to the atmosphere. CFCs are very stable compounds and remain in the troposphere for a very long time, ultimately migrating to the stratosphere [10]. In the middle and upper stratosphere, ultraviolet radiation breaks down the CFCs and causes the release of chlorine atoms. Chlorine and bromine act as catalysts for the destruction process of ozone by ultraviolet radiation. Thus, with the release of chlorine and bromine from the destruction of CFCs, there is a net decrease in the stratospheric ozone content [10].

### **7.3.2 Regulation of CFC use**

Though public concerns about the use of CFCs in aerosols and other applications increased in 1974, there was no Congressional action to regulate the use of CFCs. In 1977, FDA introduced a regulation “prohibiting the use of CFCs as propellants in food,

drug, medical device, or cosmetic products manufactured or packed after December 15, 1978”[10]. The EPA also introduced regulations to “prohibit all manufacture, processing, and distribution in interstate commerce of CFCs for nonessential uses in aerosol propellants”[10]. However, this ban on the use of CFCs in aerosols proved ineffective, because while the use of CFCs in aerosols declined, the use of CFCs in non-aerosol application increased. The production of CFC-11 and CFC-12 in the US declined to 180.7 million kgs in 1982 from 375.8 kgs in 1978 [11]. However, between 1982 to 1988, production again rose to 299.9 million kgs [11] The production of CFCs for aerosol and non-aerosol application in the US between 1972-1989 is shown in Figure 7-4

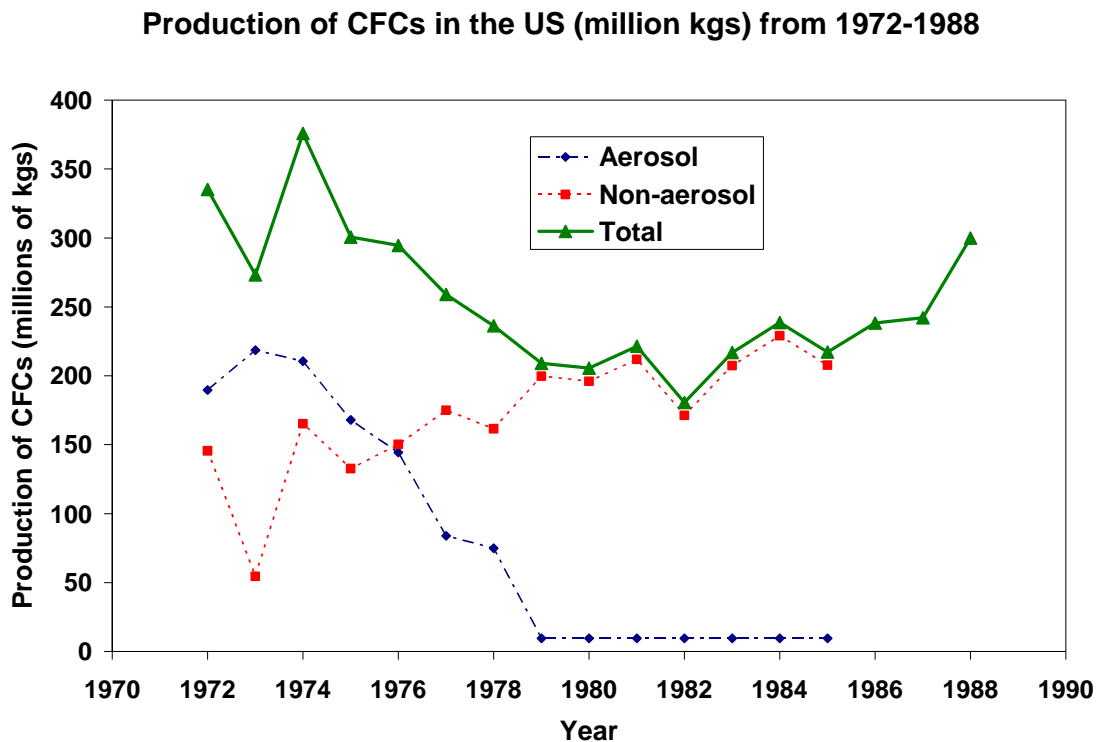


**Figure 7-4: Production of CFCs in the US from 1972 to 1988. Data from [11]**

The government policy in this period failed to increase the price of CFCs and hence development of substitutes was not done because it was not cost-effective. DuPont was the major producer of CFCs and though, it began programs to develop substitutes in

1974, it abandoned these programs because they were not cost-effective [11]. However, since there was a ban on the use of CFCs in aerosols, industry did manage to develop cost-effective substitutes for this application [11].

As the scientific evidence on the destructive effects of CFCs grew more conclusive, there was an increasing realization that a concerted and coordinated international effort would be required. The Vienna Convention in 1985 served to bring the international community together to begin addressing the deleterious effects of the continued use of CFCs. Leading from the Vienna Convention, countries met in Montreal in 1987 to ratify the Montreal Protocol that capped production of a number of CFCs and halons at 1986 levels, reduced them to 82% of 1986 levels by July 1993 and to 50% of 1986 levels by July 1998 [12]. The Montreal Protocol represented the first time that the international community had reached an accord to regulate the use of a product for environmental reasons [10]. The protocol did not place a cap on the production of each substance; but rather, grouped the substances according to their ozone depleting potential into groups and placed a cap on each of these groups. The Montreal Protocol also addressed the concerns of developing countries, by giving an exception to developing countries whose “annual calculated level of consumption of controlled substances is, and remains, less than 0.3 kgs per capita”. These countries were allowed to delay compliance with the Protocol by ten years [10]. The Protocol also gave an exception to developed countries, allowing them to exceed their 1986 levels by up to 10% in order to satisfy the basic domestic needs of developed countries [10].

#### **7.3.2.1 EPA response to Montreal Protocol**

In order to enforce the Montreal Protocol in the US, the EPA had to set a regulatory regime to move forward with. According to Nangle [10], the EPA considered a number of different options – both market-based policy initiatives and command-and-control policies. The following policies were considered:

- **Auction of CFC permits:** The EPA considered an approach whereby it would auction permits to firms that wanted to produce substance containing CFCs. The limit set by the United States' compliance with the Montreal Protocol would determine the amount of permits to be auctioned. The firms would have to use the permits in the specified time period and could not save them for future use. Firms would however have been allowed to trade permits. It was proposed that revenues from the auctions would go to the United States Treasury [10]. The concern with this approach was that it could be legally questionable because of the revenues generated [10]. There was also a concern that if permits were to be auctioned, some big players would buy all the permits allowed for one chemical, thus limiting the allowances for other products and applications [12].
- **Enforcement of production quotas:** Another approach that the EPA considered was to set up production quotas that would govern how much CFC any firm could utilize. The volume of the quotas would be determined, so as to keep the United States in compliance with the Montreal Protocol. As with the permits, firms would have to use the quotas in the specified time period, but would be allowed to trade the quotas [10]. A potential concern with the production quotas was that since this would lead to a scarcity of CFCs in the market, producers of CFCs would see a sudden increase in prices for CFCs and realize a windfall profit.
- **Use of regulatory fees:** The EPA also considered imposing regulatory fees on firms that made use of CFCs. It was proposed that the fee would be determined based on the amount of the chemical that the firm used as well as the ozone depleting potential of the chemical. The thinking behind this was that the fees would deter the use of CFCs and lead to the commercialization of alternatives. It was proposed that the revenues from the fees would go to the United States Treasury [10]. However, it was felt that the use of fees would not necessarily achieve the aim of meeting the regulatory targets, since polluters may just accept fees as a cost of doing business. In

addition, this may have become legally questionable because of the revenue generated to the US Treasury from fees [10].

- **Ban on use of CFCs in some applications:** The EPA also considered a command-and-control approach of employing a ban on use of CFCs in certain applications, and placing controls on the use of CFCs in other applications. It was felt however, that this would restrict the scope of the regulation to some specific industries and products and would not achieve the over-arching goal of reducing and phasing out CFC emissions [10].

Hence, based on these considerations, the EPA decided to allocate permits to CFC producers. The total volume of the allocated permits was determined based on the United States' compliance with the regulations for each class of CFCs and halons as per the Montreal Protocol. The EPA allocated the permits to five domestic CFC producers and ten importers of CFCs and the amount allocated was based on the respective firm's share of the market in 1986 [10]. The regulation stipulated that the firms could not save up the quotas for use in future years and that the permits would expire at the end of the specified period. However, firms would be allowed to trade the permits wherein a firm that expected to produce more CFCs than its allocated quota could buy permits from a firm that produced less CFCs than its allocated quota.

### 7.3.2.2 Introduction of tax on CFCs in the US

A year after the EPA introduced the tradable permit system for the regulation of CFCs, there were two primary concerns about this mechanism in the US:

1. **Windfall profits:** There were concerns that the scarcity caused by the restriction on the volume of production of CFCs would lead to a sharp increase in CFC prices, in turn leading to windfall profits for CFC producers. This would be seen by the public as rewarding the very people who were responsible for the pollution

in the first place. It was felt that a regulatory mechanism to alleviate this would be needed.

- 2. Insufficient reduction in the use of CFCs:** While the cap was meant to constrain the production of CFCs below a certain amount, it would not give producers incentives to reduce their production below the cap. The Montreal Protocol stipulated that the caps be progressively reduced and hence, there was concern about providing enough incentive to consumers and producers to alter their consumption and production behavior accordingly.

It was felt that the best way to address these two concerns was to introduce a tax on the use of ozone depleting substances. This would serve to reduce the windfall profit that producers would receive and also provide incentives for the reduction of the production and consumption of these chemicals below the cap limit set by the regulations. The tax was imposed on the sale or use of the chemicals by manufactures and importers. The tax was applied on a number of specified chemicals and the tax rate was proportional to the ozone depleting potential of the chemical [12]. The ozone depleting potential was calculated by using two considerations – the magnitude of the ozone-depleting effect as well as the persistence of that effect over time [12]. In 1989, Congress passed the Ozone-Depleting Chemicals Tax and it initially covered 8 compounds. In 1990, an additional 12 compounds were added to the list of compounds to be taxed. The tax rate on chemicals was revised subsequently and the rates were increased.

One of the issues with the taxes as designed was that the tax base was formulated to be the amount of CFC that was produced, rather than the CFC that was released. Since it was not the CFC that was produced, but rather the CFC that was released to the atmosphere that caused the damage, this was a problem in how the tax was designed [13]. However, taxing the release on CFCs would be administratively infeasible since it is very hard to track the sources of leaks and the quantity being released from each source.

### **7.3.2.3 Exemptions for exports**

The Ozone Depleting Chemicals Tax had built into it exemptions for exporters in order to maintain the competitiveness of domestic manufacturers who exported compounds with CFCs. This is because the tax was designed on the principle that the tax should be paid in the country in which the product is consumed. This was done for two reasons:

1. There was concern that if a tax was imposed on exports, it would make the prices of exports increase and cause production of CFCs to move abroad to countries that did not employ such a tax. This would not serve the purpose of reducing total worldwide CFC production. This was especially a concern because under the Montreal Protocol, some developing countries were allowed to increase their production of CFCs. Placing a tax on imports to these countries could have forced the countries to develop indigenous methods for production of CFCs, thus increasing the potential worldwide production capacity for CFCs.
2. A tax was also imposed by the EPA on imports of products that contained CFCs. This was to ensure that the use of CFCs in the US did not continue to increase through the import channel. The EPA formulated a list of compounds on which the import tax would be imposed [12].

### **7.3.3 Effectiveness of the regulatory system in decreasing CFC production**

The combination of the cap and trade system with the tax on CFC production was very successful in phasing down the CFC production in the US. Data obtained by Hoerner [12] shows that the production of CFCs has never exceeded 65% of the cap on the production since the introduction of the regulatory system. By 1995, production of ozone depleting chemicals had been lowered to less than half of the level before the regulatory mechanism was put in place.

It appears that both the cap and trade system as well as the tax policy on CFCs were responsible for this rapid phasedown in CFC production. The production of the Montreal Protocol Annex A chemicals in the US after implementation of the regulatory regime is shown in Figure 7-5 [12]. The figure also shows the projected production of CFCs without the regulatory mechanism and the caps that were placed on the production.

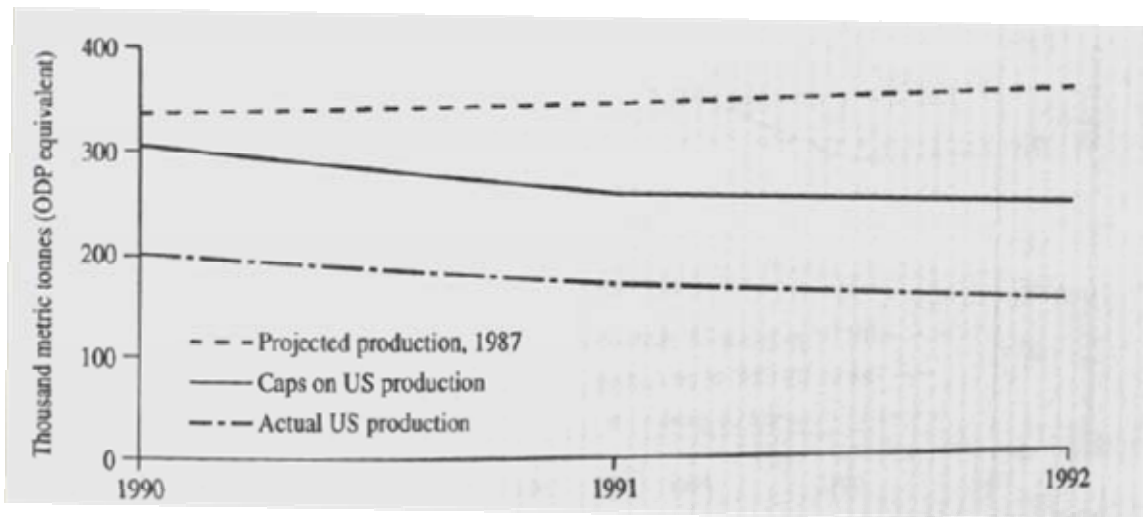


**Figure 7-5: Production of Annex I chemicals in the US after 1990. Figure adapted from [12]**

As can be seen, the actual production of CFCs was much lower than the projected production, and in fact, was lower than the capped production as well. The incentive to produce below the caps was present because of the tax on CFC production. In the absence of a tax, the incentive to lower the total production below the cap would not have been present.

Figure 7-6 shows the total world production of CFCs excluding the US as well as the total US production of CFCs between 1990-1992 [12]. As is seen in the figure, the total US production fell faster than the total world production. This can be attributed to the strict cap and trade system and tax policy employed in the US.

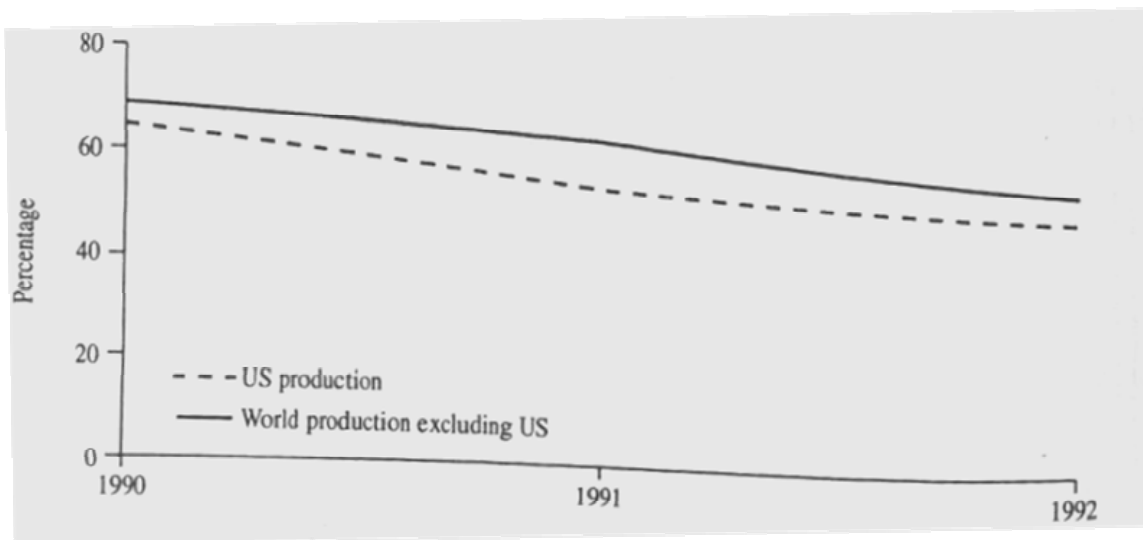


**Figure 7-6: Worldwide production of Annex I chemicals after 1990. Figure adapted from [12]**

With just the imposition of a tax, the industry may have viewed that as a cost of doing business. The caps acted in a way to signal to the industry that the CFC phasedown was definitely going to happen and that the search for alternative products was worth investing in [12]. In addition, because the US was a signatory to the Montreal Protocol and needed to meet certain emission targets, a cap system was required in order to ensure compliance. Charging an appropriate tax rate to ensure compliance would have been difficult.

### **7.3.4 Development of new technology and products**

The actual abatement costs of CFCs has been much lower than what was predicted when then regulatory mechanisms were put in place [8]. This is because of the technology forcing nature of the policy implemented. When the EPA did an assessment in 1982 of the costs of abatement, it was concluded that only a third of CFC usage possessed economically viable alternatives [12]. DuPont which had been working on finding alternatives since 1974 abandoned its efforts in 1982, claiming that there were no feasible alternatives. However, the industry got a stimulus to develop new alternatives once the

Montreal Protocol was signed and it became clear that a reduction in CFC production was necessary. The EPA found in 1988 that a 50% reduction of CFC production by 2000 would entail a cost of US\$ 3 billion [12]. However, in 1990, that number was revised and it was found that a complete elimination of CFCs could be achieved at a lower cost than US\$ 3 billion [12]. This is because the industry was able to come up with substitute products and technologies that eliminated the use of CFCs. This illustrates the need for a regulatory mechanism to be put in place to act as a signal of the seriousness of commitment to reform. The rapid fall in the price of abatement, which was contradictory to everything that industry groups had stated before the regulations were put in place suggests that industry did have viable alternatives available but did not commercialize them because of the lack of regulation.

It should also be noted that in the case of CFC regulation, the reporting requirements were low. This helped keep the administrative costs of compliance for CFC producers low. In addition, the fact that there were only a handful of producers and importers to be regulated made enforcing compliance much easier.

## **7.4 Regulation of SO<sub>2</sub> emissions from power plants in the US**

The issue of SO<sub>2</sub> abatement is an interesting one since the US has tried both a command-and-control approach to control SO<sub>2</sub> emissions as well as moving to a market-based cap and trade policy later. In this section, both policies are discussed and evaluated.

### **7.4.1 Regulation of SO<sub>2</sub> in the 1970s**

The strict regulation of SO<sub>2</sub> emissions in the United States began in 1970 when the EPA introduced the New Source Performance Standards Program (NSPS) [14]. This standard regulated utilities that were built after August 17, 1971 [15] and required these utilities to have emission rates below 1.2 pounds of SO<sub>2</sub> per million BTUs of heat input. The EPA would set national ambient air quality standards for SO<sub>2</sub> under the Clean Air Act and states had to develop a plan in order to achieve the required standards [15]. If a state had more stringent regulations than those promulgated by the EPA under the National

Ambient Air Quality Standards (NAAQS), then the state standards were the one that took precedence. The EPA divided the country into 247 air quality control regions – those regions that were able to achieve the standards set out in NAAQS were called attainment areas and those that were not were called non-attainment areas [16]. It was the state's responsibility to move non-attainment zones into the attainment category. The NSPS required the newly constructed utilities to use an EPA-approved system for controlling emissions of SO<sub>2</sub>. The two EPA approved systems were [14]:

- Installing SO<sub>2</sub> scrubbers to lower the emissions of SO<sub>2</sub> from the electricity generation facility
- Using low-sulfur coal instead of high-sulfur coal as the fuel

It was found that in general, it was cheaper to switch to low-sulfur coal than to install scrubbing technology, since at that time SO<sub>2</sub> scrubbing technology was not well developed. Hence, most of the new utilities that were built after 1971 used low sulfur coal as the fuel [15]. This led to loss of miners' jobs in states that produced high sulfur coal and led to fierce lobbying by this segment to switch back to high sulfur coal as the fuel standard [1].

Right from the point that the NSPS went into effect in 1979, it was felt that the rules were very stringent. The EPA tried to incorporate a number of modifications in order to increase the flexibility afforded by the regulations [16]. The need to incorporate more flexibility, along with complains from interested parties in states with high sulfur coal led to the revamping of the Clean Air Act with the Clean Air Act Amendments of 1977. In the words of the Amendment, it eliminated the “competitive advantage to those States with cheaper low-sulfur coal and....disadvantage for Midwestern and Eastern States where predominantly higher sulfur coal is available”[14]. In order to do this, the language of the Clean Air Act was amended to require the “application of the best technological system of continuous emission reduction which the Administrator determines has been adequately demonstrated” [14].

Since at that time, scrubbing was the only technology that effectively reduced emissions, this was equivalent to mandating the use of scrubbers on utilities. Thus, the EPA shifted from a performance standard that was present before 1977 to a technology standard. The scrubbers had to remove between 70-90% of the sulfur at the exit of the power plant, depending on the type of coal that was used as the fuel. In addition, the EPA promulgated stricter regulations for non-attainment areas [15]. In these areas, new sources of SO<sub>2</sub> needed to install equipment that would allow the achievement of the “lowest achievable emission rate” and existing sources were required to install “reasonably available control technology” [15]. The EPA set up a trading program whereby firms that were reducing emissions below that mandated could apply for a Emission Reduction Credit (ERC) [3]. In addition to making these changes, the EPA also introduced a number of different rules designed to increase the flexibility offered to emission sources in dealing with the regulations. These included:

- **Offsets:** If a firm wanted to build a major new emission source in a non-attainment area, it would be required to offset the increase in emissions from this source with a decrease in the same type of emissions from another part of the non-attainment area [16]. Offsets are basically mandatory for any new entrant in a non-attainment area. Offset trades could be external or internal. Any new firm that wanted to build a source in a non-attainment area would have to buy offsets from an existing source, thus, in effect financing the emission reductions cost of the existing source [3]. While there was some trading activity in offsets, it was found that it was not significant with only 2000 sources using offsets between 1977 and 1986 [16]. In addition, a stable price for offsets in any region was never reached, suggesting that this market was not able to reach equilibrium.
- **Bubbles:** This policy is akin to allowing the firm to place a bubble around their facility and perform any activity that increases the emissions from a particular source within the facility, provided that the total emissions from the entire facility do not increase. For this to be economically feasible, the marginal cost of emission control

at different sources within the facility must be such that an increase in emissions from one source can be economically compensated with a decrease in emissions from another source in the same facility [16]. The use of bubble has been criticized because it is not a policy that causes the total emissions to decrease, which is something that is required in a non-attainment area in order to bring the air quality to acceptable ambient conditions [16].

- **Netting:** With netting, a firm is allowed to increase its emissions from one source as long as it decreases its emissions from another source such that the net increase in emissions is not equivalent to the creation of a new major source [16]. However, the problem with the concept of netting is that though, a new major source may not be created, there can still be a net increase in emissions, thus worsening the ambient air conditions in the area.

In a study, it was found that the most commonly used tool was netting, followed by offsets and bubbles.

These regulations placed existing firms at a significant competitive advantage over new entrants in two ways:

- The use of netting for modifying existing sources provided an avenue for incumbent firms that new entrants did not possess.
- In addition, the requirement on the use of best available control technology applied only to new entrants and not incumbents.
- New firms, in addition to incorporating the best available control technology, also had to buy offsets from existing sources when establishing a source in a non-attainment area.

It is thought that these factors are responsible for the grandfathering of coal plants that was seen in the 1970s and 1980s. The incentive for utilities to build new plants was not

present because of the costs associated with environmental regulation compliance of new generation facilities. A study by Nelson et al. [3] indicates that the regulations of the 1970s increased the average age of fossil-fueled steam generating facilities by 3.29 years.

Between 1971-1988, nationwide SO<sub>2</sub> emissions from anthropogenic sources declined by 28-30% while the use of coal by utilities increased by 80% [17]. However, it was felt that the technology standards enforced by the Clean Air Act Amendments of 1977 were an inefficient and costly method of achieving reduction in SO<sub>2</sub> concentrations and it was seen that many of the non-attainment areas would not be in compliance by the statutory deadline of 1987. It was also felt that the regulations were particularly harsh to new entrants and were not fostering the development of technology that would bring about cost-effective reductions in the level of SO<sub>2</sub> emissions. Hence, in 1990, a decision was made to switch to a market-based cap and trade system of controlling SO<sub>2</sub> emissions.

#### **7.4.2 Regulation of SO<sub>2</sub> emissions from 1990**

The policy shift in 1990 was from one of regulating SO<sub>2</sub> emissions with a command and control approach to one where it was regulated by a market-based policy. In addition, it was decided to pursue an aggregated national plan rather than relying on state-based plans [15]. The goal of the 1990 Clean Air Act Amendments was to reduce SO<sub>2</sub> emissions to half of the 1980 levels with SO<sub>2</sub> emissions being reduced to about 8.5 to 9 million tons by 2000 and placed under a permanent emissions cap of about 8.9 million tons [17]. The new law gave firms significant flexibility in achieving the regulatory standards, with there being no restriction on the technology that could be employed.

The compliance was to be achieved in two phases. The EPA grouped utility boilers under two tiers : Phase I and Phase II units [18]. The first phase was to be implemented from 1995-1999 and phase II was implemented starting in 2000 [17]. The 261 units that were included in Phase I were older, coal-fired boilers and were amongst the highest SO<sub>2</sub> emitters in the nation [19]. These units were required to have an allowance for each unit of SO<sub>2</sub> that they emitted after 1995 [15]. The units were required to emit less than 2.5 lb SO<sub>2</sub> per million BTU of fuel input and were allocated 5 million tons of allowances to

achieve this [17]. In phase II, the remaining generating units that were larger than 25 MW are in size were brought online to the program and the cap on emissions was lowered to 1.2 lb SO<sub>2</sub> per million BTU of fuel input [19]. Thus, the Act granted more time to smaller utilities to adopt the changes and also adopted a phased reduction in the cap in order to allow firms to adapt in an economically viable manner.

It was decided to use a system of allocating allowances for SO<sub>2</sub> emissions to utilities. The number of allowances for each utility would be determined based on the historic fuel usage of the utility as well as the emissions in prior years [19]. If a utility emitted less SO<sub>2</sub> than its allowances permitted, it could sell the excess allowances to another firm whose emissions were greater than the allowances awarded to it. The program also allowed firms to continue the use of bubbles whereby savings in allowances at one source could be transferred to another source of the same utility [17]. Another feature of the regulation was that it allowed utilities to bank emission credits for use in future years [17]. This was meant to help utilities adapt to the gradual reduction in the cap on the emissions and to make the switchover to more efficient technologies easier.

In addition, the EPA decided to set apart about 2.8% of allowances to be auctioned and sold [17]. This was done so as to establish a marketplace for emissions trading – one that was lacking in the previous version of the regulation. It was meant to serve as a mechanism through which a price for a SO<sub>2</sub> allowance credit could be established.

The EPA also wanted to promote the use of scrubbers as a means of achieving the reduction in emissions and so it created a pool of 3.5 million bonus allowances that would be allocated to utilities that installed technologies capable of 90% SO<sub>2</sub> removal [17]. The utilities that chose to proceed with the advanced scrubbers were also given an extra two years to begin compliance with the program and were allocated credits to cover their emissions in the period from 1995 to 1997.

### 7.4.3 Compliance strategies of utilities

Since the Clean Air Act Amendment of 1990 did not mandate a technology standard, but rather a performance standard with a cap and trade system, utilities had a significant degree of flexibility in how they met the regulatory requirement. Utilities employed a number of strategies to achieve the reduction in SO<sub>2</sub> emission and these are described below [19]:

- **Fuel switching and fuel blending:** One of the options that utilities had was to switch to coal with lower sulfur content. For new facilities, an option was to use natural gas instead of coal as a fuel in order to lower compliance costs. In this case, there was a trade-off between the price of natural gas and coal and the SO<sub>2</sub> compliance costs. Utilities could also choose to blend high sulfur coal with lower sulfur coal and lower compliance costs, but this might lead to decreases in the plant's efficiency [19].
- **Use of scrubbing technology:** Utilities could choose to install flue gas desulfurization (FGD) systems that were capable of reducing SO<sub>2</sub> emissions even below the level mandated by the regulation. In such a scenario, utilities could save emission credits and sell them on the trading market.
- **Retiring and repowering of power plants:** Some utilities chose to retire some of their units and to make up for the loss in capacity by increasing generation at their other units. The EPA allowed them to keep the allowances they had received for their old units as long as the loss in generation capacity caused by the retirement of units was made up at other units [19]. In effect, this was positive for the utilities since generation at newer units was more efficient. This acted to prevent the problem of grandfathering that had existed in the 1970s and 1980s. Some utilities chose to keep their old units, but repower them in order to increase efficiency of generation and generation capacity.

- **Demand-side management:** The Clean Air Act Amendment of 1990 created a pool of 300,000 allowances for utilities that adopted demand-side management techniques or used renewable energy sources to aid them in complying with the regulation [19].

#### **7.4.4 Effects of Clean Air Act on SO<sub>2</sub> emissions**

The Clean Air Act Amendment of 1990 has been successful in its primary goal of reducing SO<sub>2</sub> emissions from electricity generating units. Since many units had already implemented some form of SO<sub>2</sub> control before 1990 due to the previous Clean Air Act Amendments, phase I units were consistently able to achieve emissions lower than their allowances in the first phase of the program. Figure 7-7 shows the actual SO<sub>2</sub> emissions from units as compared to EPA's prediction if there had been no enforcement of Title IV of the CAAA of 1990 [20] and Figure 7-8 shows the emissions from phase 1 units between 1995-1999 as well as the allowances that were given to these units in this time frame [21].

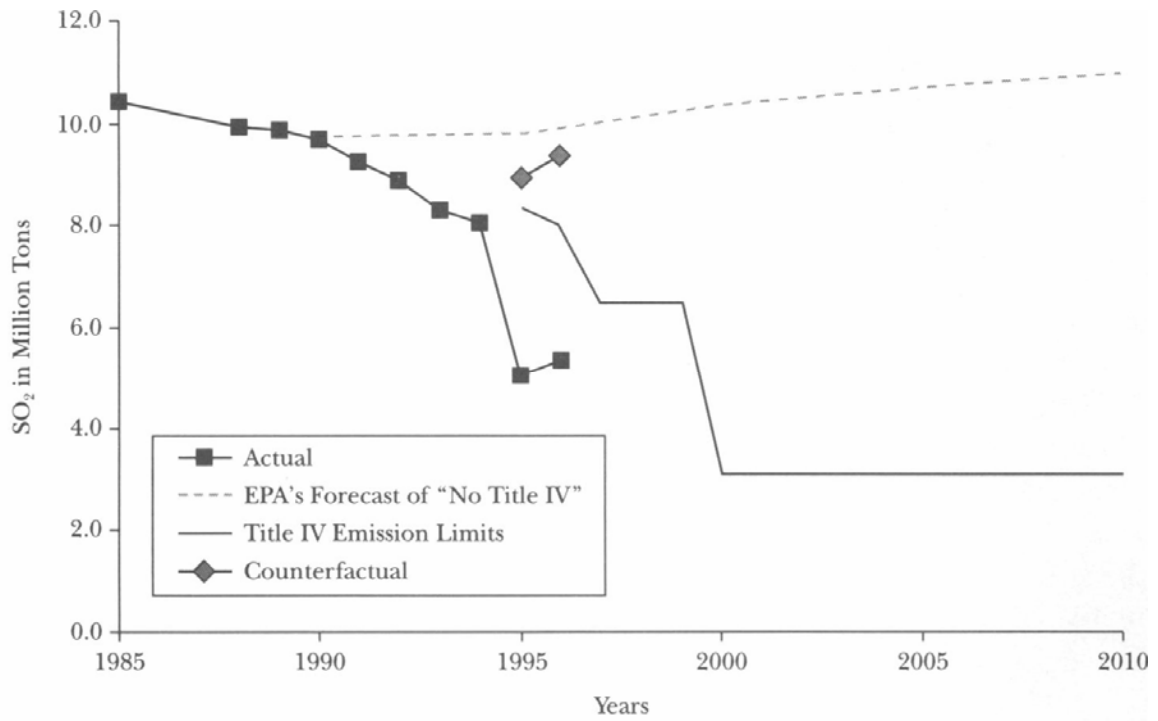


**Figure 7-7: Comparison of actual SO<sub>2</sub> emissions in the US after enactment of Clean Air Act Amendment of 1990 with predicted SO<sub>2</sub> emissions. Figure adapted from [20]**

**Emissions from phase I units compared to allowance caps from 1995 to 1999**

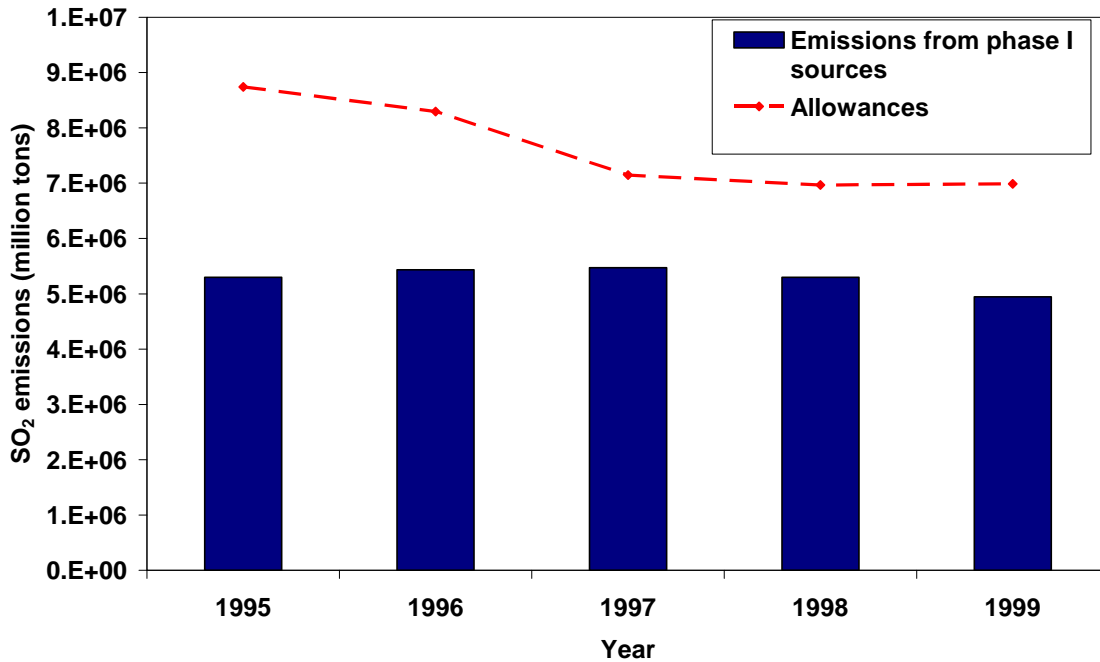


**Figure 7-8: Emissions from phase I units compared to allowance caps from 1995 to 1999. Data from [21]**

Many of the firms chose to lower emissions below the required limit in order to bank allowances for the phase II implementation, in which the standard was stricter. It was also expected that the price of allowances would go up in phase II since there would be more demand for allowances from the smaller utilities.

Much of the reduction in SO<sub>2</sub> was achieved through the use of low sulfur coal. The deregulation of US railroads in the 1980s made the transport of low sulfur coal, which was located primarily in the western states, cheaper and hence, the use of low sulfur coal increased through the 1990s [20]. Figure 7-9 shows the change from 1990 to 1995 in the type of fuel used by generating units.

**Comparison of usage levels of different coal types**

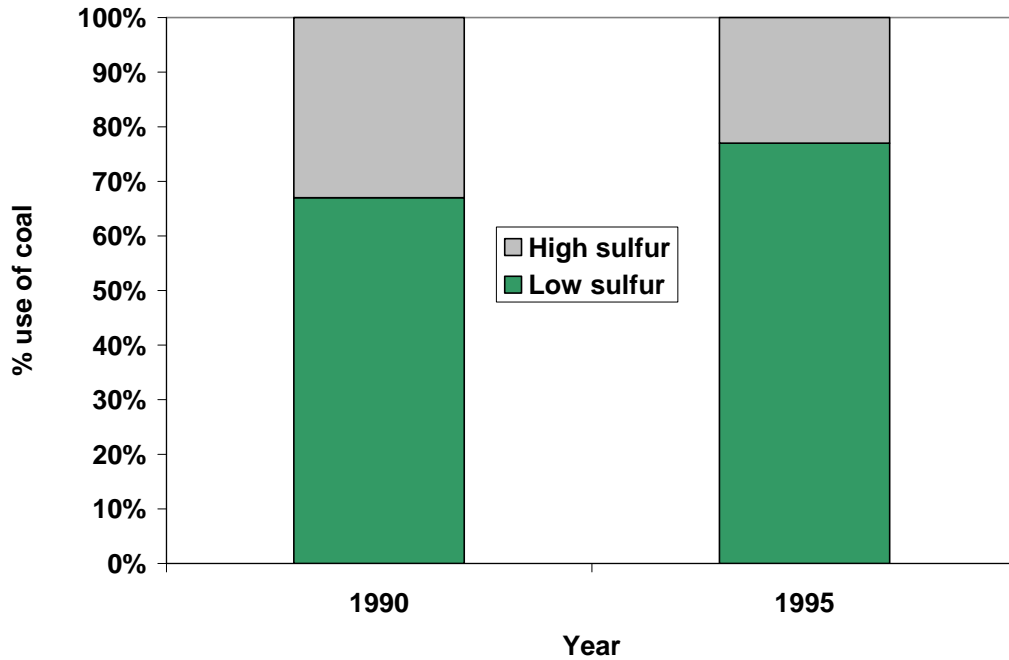


**Figure 7-9: Comparison of usage levels of different coal types in 1990 and 1995. Data from [22]**

It was found that 52% of utilities chose to achieve their compliance with the CAAA regulations by switching to low sulfur coal while 10% chose to do it through installing scrubbers. Figure 7-10 shows the distribution of how units in phase I chose to achieve compliance with the regulation [22] and Figure 7-11 shows the contribution of each of these compliance strategies to the total reduction in SO<sub>2</sub> emissions [22].

**% of units employing each compliance strategy in 1995**

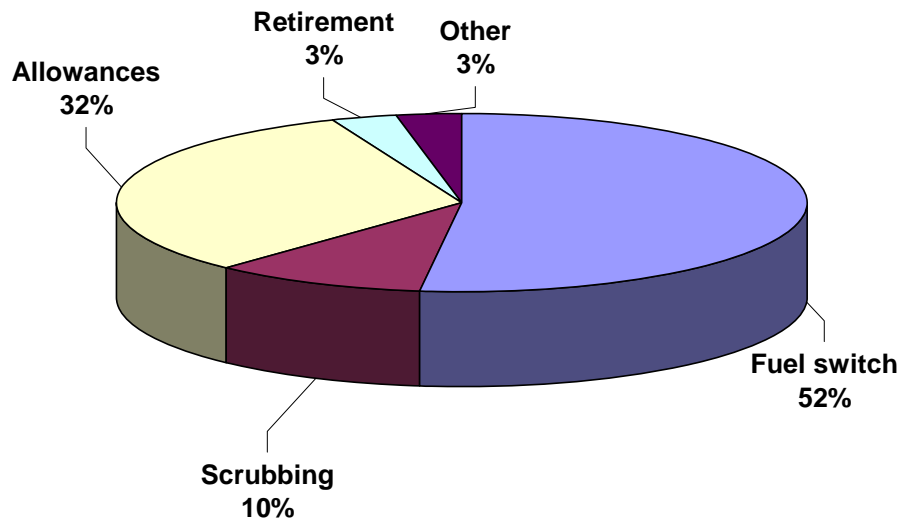


**Figure 7-10: Percentage of electricity generating units employing each compliance strategy in 1995. Data from [22]**

**% Reduction in emissions (1985 base) from each compliance strategy**

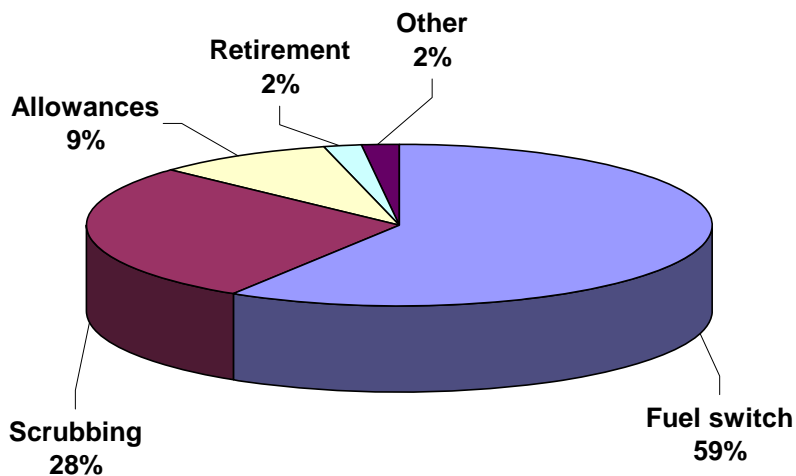


**Figure 7-11: Percentage reduction in emissions from each compliance strategy. Data from [22]**

The fact that only 10% of utilities chose to incorporate scrubbers is surprising since it was expected that this would be the technology of choice. However, the presence of lower cost low-sulfur coal prevented utilities from adopting scrubbing. In addition, since allowance prices were much lower than expected, utilities chose to buy allowances to ensure compliance rather than employ scrubbing.

As phase II was started in 2000, almost every electricity generating unit in the country was required to comply with the lower standard enforced by the Clean Air Act. In order to deal with the stricter standards enforced in phase II of the program, utilities began to withdraw banked allowances for use. Hence, the emissions were higher than the allocated allowances for that year from 2000 till 2005 but lower than the overall emissions allowed

including banked allowances. Figure 7-12 shows the emissions from phase I and II units as well as the allowances for each year and the total allowances including banking [21].

**Total SO<sub>2</sub> emissions and allowed emissions from 1995 to 2006**

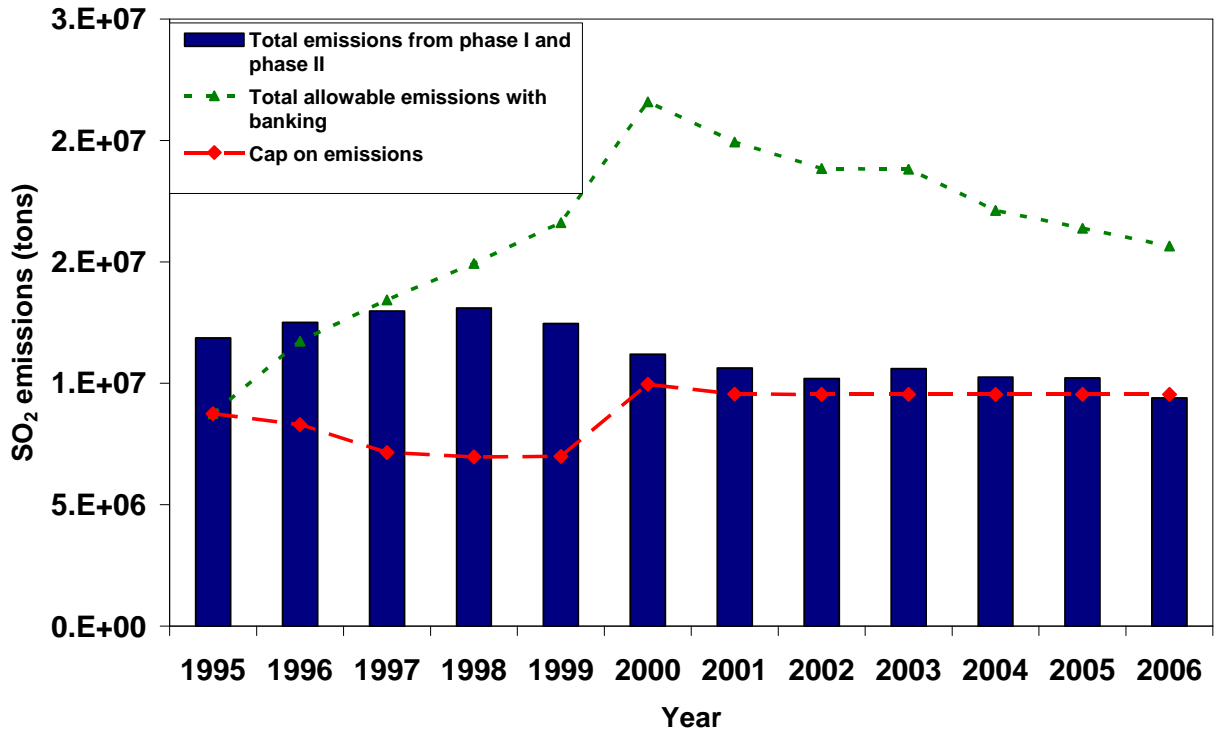


**Figure 7-12: Comparison of total SO<sub>2</sub> emissions from phase I and phase II units with allowed emissions from 1995 to 2006. Data from [21]**

As can be seen from the figure, firms withdrew their banked allowances between 2000-2006 and hence, the total stock of banked allowances decreased in this time period. The decrease in the stock of banked allowances is shown in Figure 7-13 [21].

**Size of emissions bank from 1995-2006**

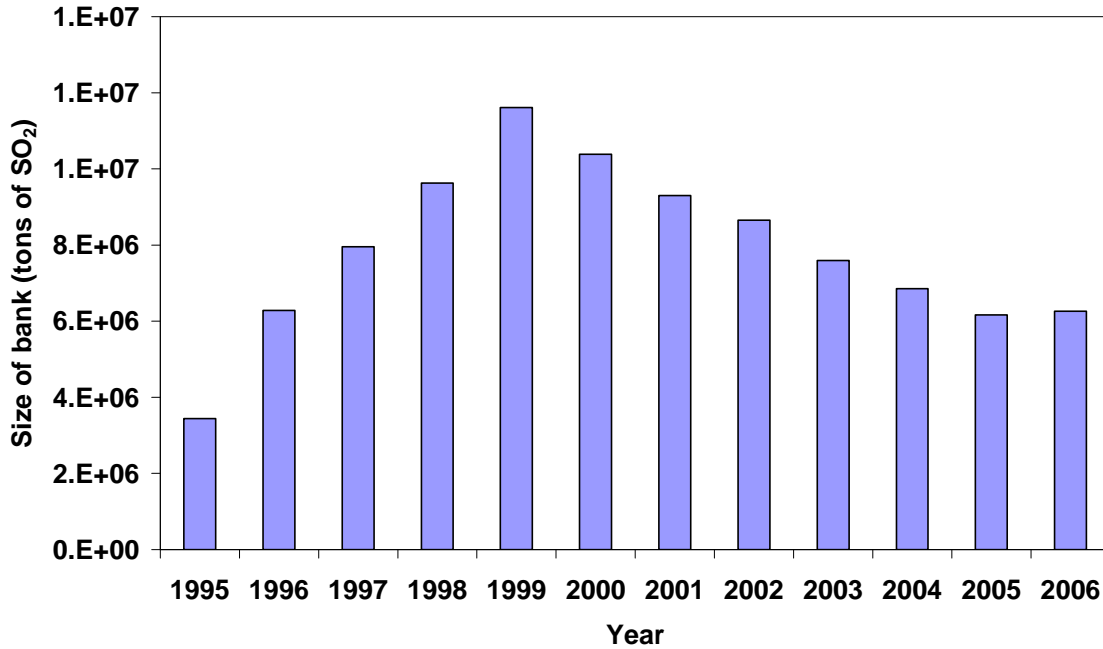


**Figure 7-13: Size of SO<sub>2</sub> emissions bank from 1995-2006. Data from [21]**

It appears that much of the banking in the initial stages of the Phase I program came from utilities that either used fuel switching or incorporated FGDF scrubbing in the power generation. Table 7-1 gives a breakdown of the banking by compliance strategy for 1995 [19].

**Table 7-1: Breakdown of banking of SO<sub>2</sub> allowances by compliance strategy. Data from [19]**

<b>Compliance Strategy</b>	<b>SO<sub>2</sub> emissions (tons)</b>	<b>Allowance allocation (million tons)</b>	<b>Allowances banked (million tons)</b>
<b>Fuel Switching/Blending</b>	2.71	3.32	0.6
<b>Obtaining Additional Allowances</b>	1.33	0.92	-0.41
<b>Installing FGD Equipment</b>	0.28	0.92	0.65
<b>Using Previous Controls</b>	0.14	0.33	0.19
<b>Retiring Facilities</b>	0	0.06	0.06
<b>Boiler Repowering</b>	<0.001	0.004	0.004
<b>Total</b>	4.46	5.55	1.09

In terms of the trading of SO<sub>2</sub> allowances, there has been a significant amount of trade as compared to the years prior to 1990 when no significant market for trade of allowances was established. In 1995, which was the first year of trading for the program, trades for allowances for emission of 2 million tons of SO<sub>2</sub> was completed [23]. In 2003, an average of 10.4 trades were reported per day with an average volume of 4600 tons per trade [23]. Figure 7-14 shows the volume of allowances traded each year ( data from [23]), As can be seen from the figure, the volume of allowances traded increases as the date for phase II compliance grew nearer and stayed high after that.

### Volume of trade in SO<sub>2</sub> allowances

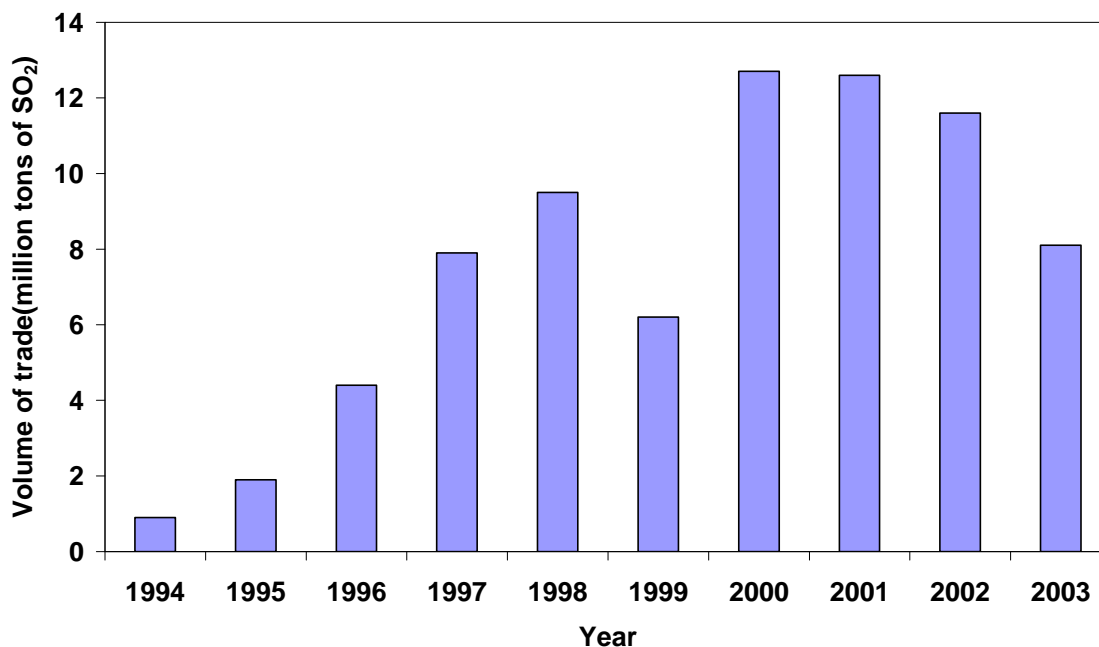


**Figure 7-14: Volume of trade in SO<sub>2</sub> allowances from 1994 to 2003. Data from [23]**

In terms of prices for allowances, the price history has been contrary to what had been predicted. In the early 1990s, it was predicted that the allowance price would be as high as \$1000 to \$1500 per ton over the 2001-2010 period [19]. However, the allowance prices observed were much lower than that. It was observed that in the initial months of the program, the price of allowances was around \$140 per ton and though, this was expected to increase, the price actually fell to \$67 per ton in 1996 [21]. From 1997 to 2003, the average price of allowances was \$150 per ton [21]. A sharp increase in prices was observed in 2005 and this was due to the proposed CAIR regulations, However, when the CAIR regulations were vacated by the DC Court of Appeals, prices again came down. Figure 7-15 shows the price history for SO<sub>2</sub> allowances from 1994 to 2010 [24]



Figure 7-15: Price history for SO<sub>2</sub> allowances from 1994 to 2010. Adapted from [24-25]

A number of explanations can be given for the low prices that have been observed:

- **Over-allocation of permits:** One of the explanations is that there has been an over-allocation of permits that has led to artificially low price of permits [21]. When there is over-allocation of permits, the supply is much greater than the demand and hence, this leads to a reduction in the price that allowances can command. In the case of this regulation, the reason that prices did not collapse is because emissions could be banked indefinitely into the future and hence, there was value in purchasing and holding allowances.
- **Early commitment to other options:** In the early 1990s before trading began, it was expected that the price of allowances would be high and hence, a number of utilities made a commitment to either incorporating scrubbers or to switch to low sulfur coal. Because of the fall in rail transportation rates, it was very cheap to achieve abatement by switching to low-sulfur coal and this was not factored into the expectation of allowance prices. In the case of scrubbing, commitments to install scrubbing were

made in the early 1990s. Through the 1990s, due to improvements in instrumentation, sludge removal techniques and utilization of the scrubbers, the operating cost of the scrubbers decreased substantially to \$65 per ton of SO<sub>2</sub> reduction [20]. Since the initial cost of the scrubbers was sunk, utility operators preferred to use the scrubbers rather than purchasing allowances which were on average more expensive than the operating cost of the scrubbers.

#### **7.4.5 Technology innovation and diffusion under the Clean Air Act**

The effect of SO<sub>2</sub> regulation on technology diffusion and innovation is interesting since there were different regulatory regimes for SO<sub>2</sub> abatement. With the Clean Air Act amendments of 1970 and 1977, a command and control regime was established, wherein the incentive was to lower the cost of the technology that was mandated by the regulation. There was no incentive to increase the scrubbing efficiency beyond that mandated by the Act. Under the Clean Air Act Amendment of 1990, the utilities had two different incentives [15]:

- Minimize cost of meeting the emission standard in order to lower the cost of compliance
- Increase the scrubbing efficiency cost effectively in order to sell emission permits in the trading market.

A number of studies have been carried out to study the effect of governmental regulation on innovative activity, especially as it applies to environmental regulation. A study by Taylor et. al [26] focused on studying patenting behavior during different regulatory regimes of SO<sub>2</sub> abatement. They observed a strong correlation between patenting activity and environmental regulation. Figure 7-16 shows the trend in US patents relevant to SO<sub>2</sub> control technology over the years.

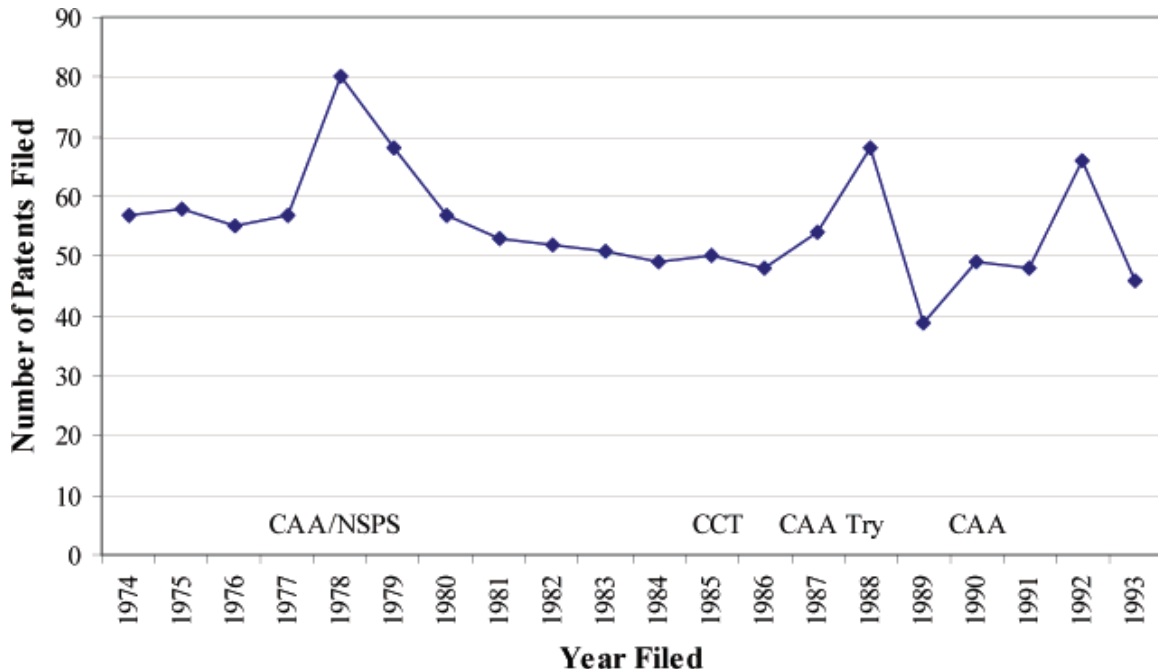


**Figure 7-16: Trend in US patents relevant to SO<sub>2</sub> control technologies from 1974-1993. Adapted from [26]**

As can be seen from the above figure, the level of patenting activity increases with the Clean Air Act Amendment of 1977 as well as with the Amendment of 1990. The peak in 1988 is due to the increased awareness of the acid rain problem and due to anticipation of stricter governmental regulation to control this [26]. In 1988, the Senate unsuccessfully attempted to overhaul the Clean Air Act to have stricter control for acid rain.

In addition, Taylor et al. [26] found that the type of regulation influences strongly the type of innovative activity. As discussed in previous sections, the Clean Air Acts of 1970 and 1990 afforded much more flexibility to utilities in how they met their abatement goals as compared to the Clean Air Act of 1977 which mandated the use of scrubbers. Hence, 1970 and 1990, there was substantial interest in switching to technologies that used low-sulfur coal and in precombustion SO<sub>2</sub> control technologies. Figure 7-17 shows the trend in patenting activity in precombustion SO<sub>2</sub> control technologies over the years [26].

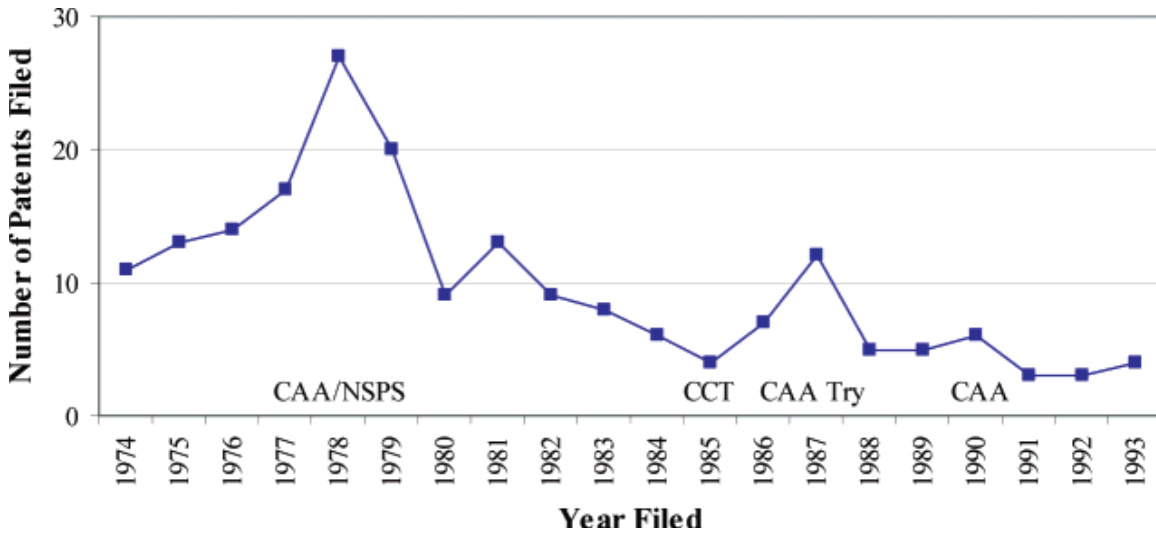


**Figure 7-17: Trend in US patents relevant to precombustion SO<sub>2</sub> control technologies from 1974-1993. Adapted from [26]**

As can be seen from the above figure, the number of patents filed for precombustion SO<sub>2</sub> control technology, the patenting activity in this field increased and peaked in the 1970-1977 period. After 1977, once the New Source Performance Standards regulations were promulgated that mandated the use of scrubbers, the inventive activity in the precombustion SO<sub>2</sub> control technology space tapered off.

However, in 1977, there was renewed interest in scrubbing technology since this was mandated by the regulation. Since the regulation only mandated that a certain emission level had to be met, there was no incentive to reduce emissions beyond this specified level. Hence, in this time period, innovative activity should have focused on being able to reduce cost of installing and operating scrubbers that met the performance standard. Indeed, it was found that there was a steep decline in capital costs of installing scrubbers over the 1980s. While some of the decline in costs was due to factors such as increased competition between technology suppliers, much of the decline in costs has been attributed to technological innovations that occurred as a result of investment in R&D [26]. Figure 7-18 shows the trend in capital costs for a new wet limestone FGD system

for a 500 MW coal-fired power plant in the US as a function of the cumulative capacity of FGD in the US [26].

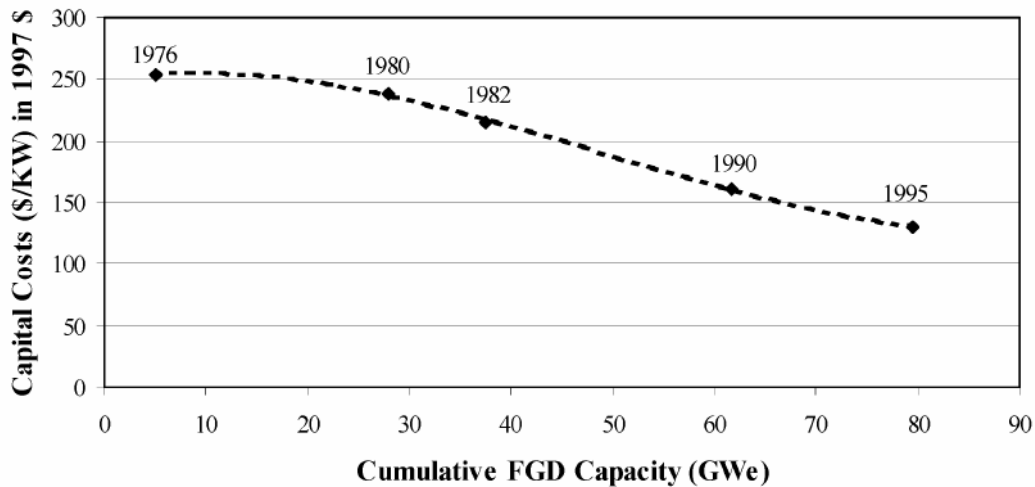


**Figure 7-18: Variation of capital costs of FGD with cumulative FGD capacity. Adapted from [26]**

As is seen in the above figure, the capital costs of installing a scrubber on a 500 MW became 50% of the initial costs over a period of 20 years. In addition, it has been reported that the total adjusted labor cost for operation, maintenance and supervision fell by 83% for each doubling of cumulative power generation at the plant [26].

The period after 1990 is interesting because after the promulgation of the Clean Air Act Amendments of 1990, there was no substantial increase in inventive activity. However, there was an increase in the inventive activity related to increasing the efficiency of SO<sub>2</sub> removal by scrubbing since excess permits could be traded on the market. This led to a case where utilities' decision to install scrubbers was much more sensitive to the marginal abatement cost than it was under the performance standard [27]. It was found that the level of efficiency of scrubbing did increase substantially upon the introduction of a market of tradable SO<sub>2</sub> emission permits. Figure 7-19 [26] shows the increase in scrubbing efficiency with the cumulative FGD installed capacity in the US and Figure

7-20 [15] reflects the increase in scrubbing efficiency with the year that the FGD unit was installed.

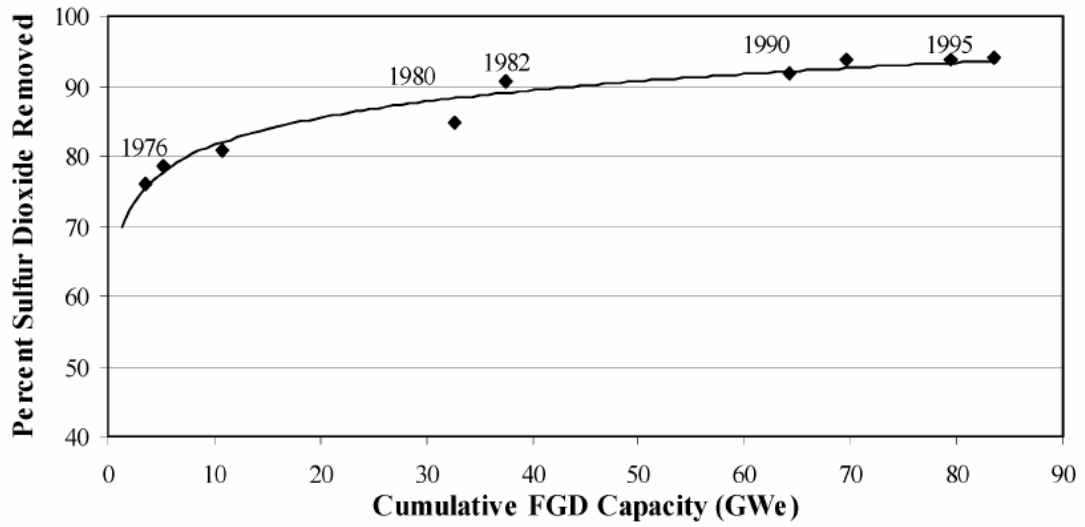


**Figure 7-19: Variation of scrubbing efficiency with cumulative installed FGD capacity in the US. Adapted from [26]**

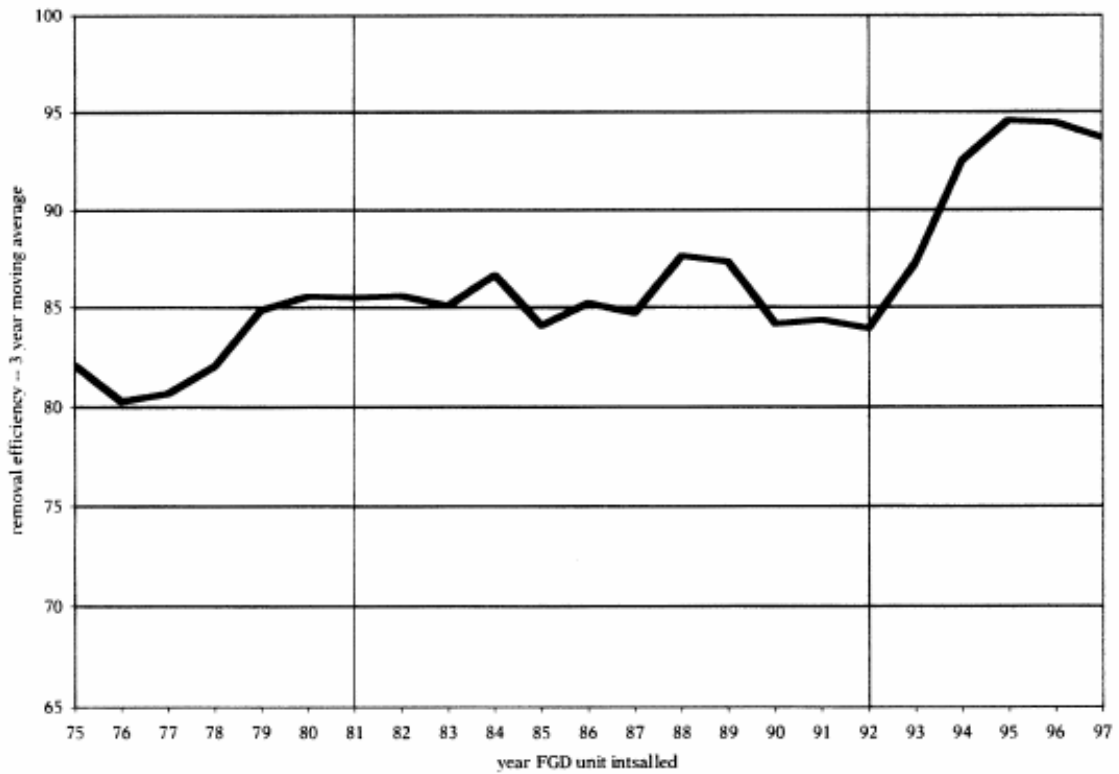


**Figure 7-20: Variation of scrubbing efficiency of FGD with year of installation. Adapted from [15]**

As can be seen from the above figures, there was a substantial increase in the efficiency of scrubbers upon introduction of a tradable permit market in 1990. Table 7-2 shows the percentage of scrubbers with different removal efficiencies under each of the policy regimes [15].

**Table 7-2: Percentage of scrubbers with different removal efficiencies under each regulatory regime. Adapted from [15]**

Removal efficiency	Policy regime		
	1970 (%)	1977 (%)	1990 (phase I) (%)
<70	11	0	0
71-79	1.2	7.3	0
80-89	37.	29.3	0
90	28	43.9	12.5
91-95	8.5	0	8.3
95+	7.3	17.1	79.2

The percentage of scrubbers with different removal efficiencies in each of the policy regimes is shown in Figure 7-21.

**Percentage of scrubbers with different removal efficiencies by regime**

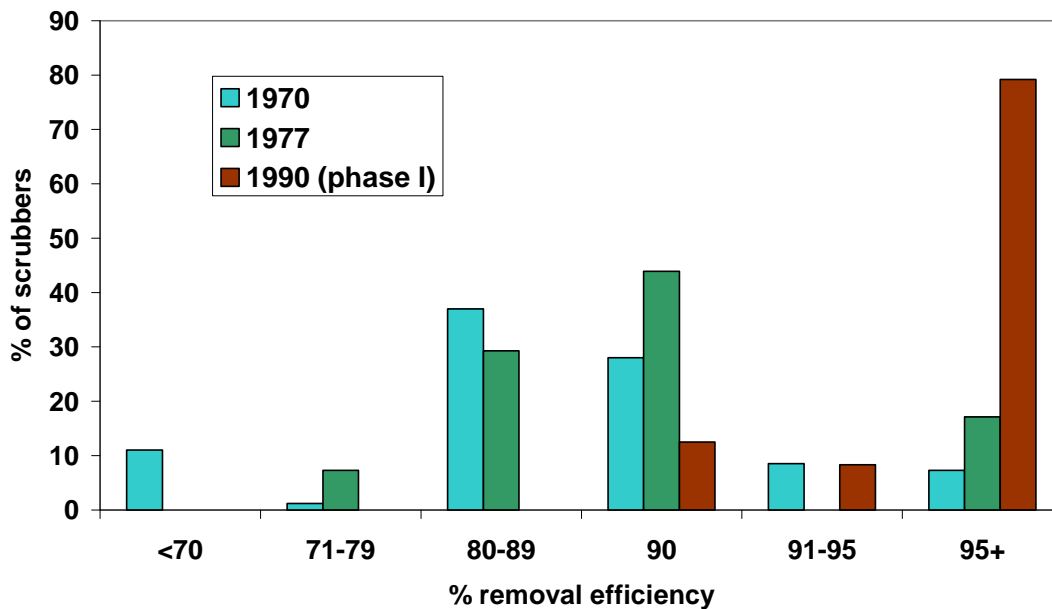


**Figure 7-21: Percentage of scrubbers with different removal efficiencies by regulatory regime. Data from [15]**

As can be seen from the above table and figure, there was a substantial spike in the removal efficiency that scrubbers were able to achieve upon the passage of the Clean Air Act Amendments of 1990. According to the analysis done by Popp [15], scrubbers that were installed under the 1977 policy regime were on average 11.2% less efficient than scrubbers installed in Phase I of the Clean Air Act Amendment of 1990 and scrubbers installed un 1970 were additionally 19.7% less efficient.

This shows the effect that governmental regulation can have on the type of inventive activity that is performed. With the command-and-control policies of the 1977 Clean Air Act Amendment, the incentive for utilities was to lower their cost of meeting the performance standard. Any profits that were captured through the lowering of cost would remain with the utility. However, with the market-based policy of the 1990 Clean Air Act

Amendment, there was an increase in SO<sub>2</sub> removal efficiency which is beneficial to the consumer. Hence, while command-and-control policies do help foster innovation, market oriented policies help foster innovation that may be more beneficial to society at large. In addition, the flexibility afforded by market-based policy instruments allows firms to invest in a variety of different R&D avenues and then choose the one that best fits the portfolio and hence prevents the government from having to make a bet on any particular technology. The market as a whole is allowed to determine the most cost-effective way of dealing with the abatement burden.

One of the differences of the SO<sub>2</sub> abatement program in the US as compared to the lead phasedown and reduction in CFC usage is that the number of sources to be regulated in the case of SO<sub>2</sub> abatement was much larger. While this may have lead to a more efficient market formation for tradable permits, it also made the administration of the program much more difficult. The reporting requirements for utilities were much higher in the SO<sub>2</sub> abatement case. This increased the administrative costs for the utilities as well and made compliance with the program more costly.

Overall, the SO<sub>2</sub> abatement program has been successful in reducing SO<sub>2</sub> emissions from power plants and consequently, improving the air quality in regions in the United States. The market-based policy introduced in 1990 has worked well in supporting technology innovation and diffusion at lower costs than expected. The costs of scrubbing have been much lower than what the industry claimed they would be when the program was being contemplated. Similar to the CFC case, this suggests that a strong commitment to regulation is needed to force industries to bring pollution abatement technologies that are economically viable to commercialization. Further tightening of the emission cap on SO<sub>2</sub> is expected to progressively improve the air quality in regions in the United States.

## **7.5 Conclusion**

In this study, a number of different case studies of environmental control projects have been conducted. We have explored both market-based as well as command-and-control projects. With a market-based approach such as a emission cap and credit trading system,

the brunt of the abatement can be borne by the firms that can perform the abatement most economically with other firms buying emission credits. It was also seen that market-based policies provided incentives for continuously improving the efficiency of technology, whereas with command-and-control policies, the incentive was to minimize the cost of compliance with the performance or technology standard. In addition, a technology standard will inherently slow down the development and diffusion of pollution control technology, since once a standard is established, there will be a lot of resistance to the adoption of a new technology standard. A technology standard also removes the flexibility of allowing firms to meet the required abatement by other methods such as improving efficiency or changing fuel source. Hence, a technology standard is the most inflexible policy instrument of the different instruments available. It may also act in a manner to stifle innovation since it mandates the use of a particular technology, thus removing incentives for continuous improvement in technology.

While a market-based policy can act in a constructive manner to encourage innovation, a proper market needs to be in place for this to happen. As was illustrated in the lead phasedown case study, if the firms involved in the market place are used to trading with one another, it makes the formation of a stable market for emission credits much easier. In addition, the manner in which the allowances are allotted to emitters is important. It may be necessary to charge taxes on emitters in order to prevent windfall profits. This needs to be done to ensure that the pollution emitters do not capture rents from the regulation and that the benefits are passed on to the end consumer.

In addition, for a market-based policy to be effective, it is necessary that the caps on emissions be slowly ratcheted down in order to continuously reduce the level of pollution. To enable firms to do this, policies such as banking and offsets can be employed in order to smooth the emissions curve and hence, prevent the firms from seeing a sudden spike in abatement costs. Such a policy has been successfully adopted in the lead phasedown in gasoline and efforts are ongoing to implement the same in SO<sub>2</sub> abatement.

A market-based-policy should also be designed to ensure that it does not unfairly put undue burden on new entrants into the market. A poorly designed policy can lead to grandfathering of existing capital, thus reducing the efficiency of pollution abatement. While more stringent standards can be placed on new facilities, it is important that emission reductions also be made at existing facilities.

The reporting requirements that may come into existence as a result of market-based policies should be designed such that they do not excessively increase the administrative costs for firms and hence, increase the cost of compliance significantly. This is one of the big concerns that utilities have with respect to potential CO<sub>2</sub> regulation. This assumes particular importance when the number of sources in the market is high, since this makes administration of the program more difficult.

It was also seen in all the case studies that the actual costs of abatement were much lower than what was predicted by industry before regulation was put in place. This shows the necessity of a signal of a strong commitment to regulation from the government in order to force industry to bring environmental control technologies that are potentially economically viable to market.

A properly designed market-based policy for CO<sub>2</sub> control will result in the establishment of competitive markets for the trading of CO<sub>2</sub> emission credits. The policy should be designed with a slowly ratcheting down cap in order to bring down emissions and should also be implemented in stages, with the largest stationary source emitters being targeted first. The policy can also make use of banking and offsets to enable plants to deal with the progressively tightening regulations. Such a policy will result in innovative activity in developing both more cost-effective control technology as well as control technology that can remove more CO<sub>2</sub> than mandated in a cost-effective manner. In this way, the government will not be forced to mandate the use of a particular technology but can allow the market to determine the cost curve of abatement for different technologies and sources and allocate the burden of abatement most cost-effectively.

## 7.6 References

1. Stavins, R.N., *What Can We Learn from the Grand Policy Experiment? Lessons from SO<sub>2</sub> Allowance Trading*. The Journal of Economic Perspectives, 1998. **12**(3): p. 69-88.
2. Jaffe, A.B. and R.N. Stavins, *Dynamic Incentives of Environmental Regulations: The Effects of Alternative Policy Instruments on Technology Diffusion*. Journal of Environmental Economics and Management, 1995. **29**(3): p. S43-S63.
3. Nelson, R.A., T. Tietenberg, and M.R. Donihue, *Differential Environmental Regulation: Effects on Electric Utility Capital Turnover and Emissions*. The Review of Economics and Statistics, 1993. **75**(2): p. 368-373.
4. Nriagu, J.O., *The rise and fall of leaded gasoline*. The Science of The Total Environment, 1990. **92**: p. 13-28.
5. Kerr, S. and R.G. Newell, *Policy-Induced Technology Adoption: Evidence from the U.S. Lead Phasedown*. The Journal of Industrial Economics, 2003. **51**(3): p. 317-343.
6. Newell, R.G. and K. Rodgers, *The Market-based Lead Phasedown*. 2003.
7. Hahn, R.W. and G.L. Hester, *Marketable Permits: Lessons for Theory and Practice*. Ecology Law Quarterly, 1989. **16**: p. 361-406.
8. Hammitt, J.K., *Are The Costs of Proposed Environmental Regulations Overestimated? Evidence from the CFC Phaseout*. Environmental and Resource Economics, 2000. **16**: p. 281-300.
9. Molina, M.J. and R.F. Sherwood, *Stratospheric Ozone Sink for Chlorofluoromethanes: Chlorine Atom Catalyzed Destruction of Ozone*. Nature Biotechnology, 1974. **249**: p. 810-811.
10. Nangle, O.E., *Stratospheric Ozone: United States Regulation of Chlorofluorocarbons*. Boston College Environmental Affairs Law Review, 1989. **16**: p. 531-580.
11. Dudek, D.J., A.M. LeBlanc, and K. Sewall, *Cutting the Cost of Environmental Policy: Lessons from Business Response to CFC Regulation*. Ambio, 1990. **19**(6/7): p. 324-328.
12. Hoerner, J.A., *Tax Tool for Protecting the Atmosphere: The US Ozone-depleting Chemicals Tax*, in *Green Budget Reform*, R. Gale, S. Barg, and A. Gillies, Editors. 1996, Earthscan Publications Ltd.: London.

13. Barthold, T.A., *Issues in the Design of Environmental Excise Taxes*. The Journal of Economic Perspectives, 1994. **8**(1): p. 133-151.
14. Dennis, J.M., *Smoke for Sale: Paradoxes and Problems of the Emissions Trading Program of the Clean Air Act Amendments of 1990*. UCLA Law Review, 1993. **40**.
15. Popp, D., *Pollution Control Innovations and the Clean Air Act of 1990*. Journal of Policy Analysis and Management, 2003. **22**(4): p. 641-660.
16. Hahn, R.W. and G.L. Lester, *Where Did All the Markets Go? An Analysis of EPA's Emissions Trading Program*. Yale Journal on Regulation, 1989. **6**.
17. Torrens, I., M., J.E. Cichanowicz, and J. Platt, B., *The 1990 Clean Air Act Amendments: Overview, Utility Industry Responses, and Strategic Implications*. Annual Review of Energy and the Environment, 1992. **17**: p. 211-233.
18. Dickerman, J. and M. Seweel, *Is it Time to Rethink SO<sub>2</sub> Control Technology Selection?* Power Engineering, 2007. **111**(11): p. 132.
19. Zipper, C. and L. Gilroy, *Sulfur Dioxide Emissions and Market Effects under the Clean Air Act Acid Rain Program*. Air and Waste Management Association, 1998. **48**: p. 829-837.
20. Schmalensee, R., P.L. Joskow, A.D. Ellerman, J.P. Montero, and E.M. Bailey, *An Interim Evaluation of Sulfur Dioxide Emissions Trading*. The Journal of Economic Perspectives, 1998. **12**(3): p. 53-68.
21. McAllister, L., K., *The Overallocation Problem in Cap-And-Trade: Moving Toward Stringency*. Columbia Journal of Environmental Law, 2009. **34**.
22. Energy Information Administration, *The Effects of Title IV of the Clean Air Act Amendments of 1990 on Electric Utilities: An Update*. 1997, EIA: Washington D.C.
23. Chicago Climate Futures Exchange, *The Sulfur Dioxide Emission Allowance Trading Program: Market Architecture, Market Dynamics and Pricing*. 2004: Chicago.
24. Environmental Protection Agency. *Emissions, Compliance and Market Data*. 2009 [cited 2010 May 2nd 2010]; Available from: [http://www.epa.gov/airmarkets/progress/ARP\\_1.html](http://www.epa.gov/airmarkets/progress/ARP_1.html).
25. Environmental Protection Agency. *Emissions, Compliance and Market Data*. 2009 [cited 2010 May 2nd 2010]; Available from: [http://www.epa.gov/airmarkets/progress/ARP\\_1.html](http://www.epa.gov/airmarkets/progress/ARP_1.html).

26. Taylor, M.R., E.S. Rubin, and D.A. Hounshell, *Effect of Government Actions on Technological Innovation for SO<sub>2</sub> Control*. Environmental Science & Technology, 2003. **37**(20): p. 4527-4534.
27. Keohane, N., O. *Environmental Policy and the Choice of Abatement Technique: Evidence from Coal-Fired Power Plants*. 2005 [cited 2010 May 5th]; Available from: <http://www.som.yale.edu/faculty/nok4/files/papers/scrubbers.pdf>.

# Appendix A

## Other post-combustion capture technologies

Previous sections of this thesis have discussed in detail the use of chemical absorption as a post-combustion CO<sub>2</sub> capture technology. In this appendix, other post-combustion CO<sub>2</sub> capture technologies are discussed.

### A.1 Physical absorption

In cases where there is a highly concentrated stream of CO<sub>2</sub> at high pressures, it is advantageous to use a physical solvent that combines less strongly with CO<sub>2</sub> than do chemical solvents. The absorptive capacity of these solvents increases with external gas pressure and decreases with temperature [1]. Hence, CO<sub>2</sub> can be separated from such solvents mainly by reducing the pressure in the desorber, significantly reducing the energy requirements in the desorption process. The main physical solvents that could be employed are cold methanol (Rectisol process), dimethylether of polyethylene glycol (Selexol process), propylene carbonate (Fluor process) and sulpholane. This technology is well established at a large scale in ammonia production plants but needs to be demonstrated in full scale power plants [2].

### A.2 Membrane separation

Gas permeation membranes exploit the difference in physical and chemical interactions between gases and a membrane material, causing one component to pass through the membrane faster than another. Membrane separation has the advantages of steady state operation, absence of moving parts and modular construction and hence has been applied successfully for the separation of CO<sub>2</sub> from light hydrocarbons in the petroleum and natural gas industries. However, in these applications, the partial pressure of CO<sub>2</sub> is much higher than in the flue gases of a power plant. The low partial pressure of CO<sub>2</sub> in the flue gases leads to a low driving force for transport across the membrane. It has been found

that a two-stage system is needed to achieve good separation and that the costs were much higher than those of conventional amine separations [3-4]. The main cost component was that of compressing the gas. A recent study [5] showed that for a flue gas stream containing around 4 vol.% CO<sub>2</sub>, the required membrane area is huge and a membrane process was probably not a viable option. Another study [6] showed that for a 10 vol.% CO<sub>2</sub> flue gas typical of a coal fired power plant, presently available membrane materials do not have the selectivity required to produce the recovery ratios and permeate compositions dictated by government regulations.

Gas absorption membranes are hybrid absorption/membrane systems that involve gas-liquid contacting. The membrane forms a gas permeable barrier between the gaseous and liquid phase. The membrane provides a very high surface to volume ratio for mass exchange between the gas and the liquid. In general, the membrane is not involved in the separation process. The contact surface area is independent of the liquid and gas flowrates [7]. If the membrane is porous, the gaseous component diffuses through the pores and gets absorbed in the solvent. In the case of a non-porous membrane, the gas dissolves in the membrane and then diffuses through it. The selectivity of the process is determined by the selectivity of the solvent. The advantage of this system is that it results in independent control of gas and liquid flows and minimizes entrainment, folding, channeling and foaming [4]. Membrane/solvent systems can be used in both the absorption and desorption steps. A recent development has been the use of amino acid salt solutions as solvents for absorption in membrane processes [8]. These can be used with polyolefin membranes like polypropylene. Units employing membrane separation for CO<sub>2</sub> capture are yet to be demonstrated on a full scale.

### **A.3 Adsorption**

Solid materials with a high surface area such as zeolites and activated carbon can potentially be used to separate CO<sub>2</sub> from flue gases by adsorption. The gas is fed to an adsorbent bed that adsorbs the CO<sub>2</sub> and allows the rest of the gas to pass through. When the bed is fully loaded, the feed is switched to the next bed in the train. The loaded bed is

then regenerated by pressure swing adsorption (PSA) or temperature swing adsorption (TSA). In general, PSA is preferred over TSA because TSA systems are larger in size and involve more cumbersome heating of the adsorbent during regeneration [2]. A disadvantage in adsorption systems is that the gases have to be treated prior to treatment in the adsorbent bed since the stability of adsorbents in the presence of impurities is low [7]. Adsorption systems are used commercially for the removal of CO<sub>2</sub> from natural gas streams but are yet to be demonstrated on a large scale for post-combustion CO<sub>2</sub> capture.

## A.4 References

1. Anderson, S. and R. Newell, *Prospects for carbon capture and storage technologies*. Annual Review of Environment and Resources, 2004. **29**: p. 109-142.
2. Davison, J. and K. Thambimuthu, *Technologies for capture of carbon dioxide*, in *7th International conference on Greenhouse Gas Control Technologies 2004*: Vancouver, Canada.
3. Herzog, H., D. Golomb, and S. Zemba, *Feasibility, modeling and economics of sequestering power plant CO<sub>2</sub> emissions in the deep ocean*. Environmental Progress, 1991. **10**(1): p. 64-74.
4. Meisen, A. and X.S. Shuai, *Research and development issues in CO<sub>2</sub> capture*. Energy Conversion and Management, 1997. **38**: p. S37-S42.
5. Hagg, M.B. and A. Lindbrathen, *CO<sub>2</sub> capture from natural gas fired power plants by using membrane technology*. Industrial & Engineering Chemistry Research, 2005. **44**(20): p. 7668-7675.
6. Bounaceur, R., N. Lape, D. Roizard, C. Vallieres, and E. Favre, *Membrane processes for post-combustion carbon dioxide capture: A parametric study*. Energy, 2006. **31**(14): p. 2220-2234.
7. IPCC, *IPCC Special Report on Carbon Dioxide Capture and Storage*., B. Metz, O. Davidson, H. C. de Coninck, M. Loos, and L. A. Meyer Editor. 2005.
8. Dindore, V. and H.F. Svendsen. *CO<sub>2</sub> capture using amino-acid salt solutions*. 2005. Cincinnati, OH, United States: American Institute of Chemical Engineers, New York, NY 10016-5991, United States.

# Appendix B

## Oxyfuel cycles

In this appendix, a brief overview of different oxyfuel cycles is presented.

### B.1 Oxyfuel power boiler with steam cycle

This mode of oxyfuel combustion is employed in boilers operating with a steam cycle. The heat released from the combustion of the fuel using oxygen as the oxidant is used to indirectly heat water to produce steam which then passes through a steam cycle. A part of the flue gases are recycled and fed to the boiler along with the feed gas in order to moderate the temperature in the boiler and preserve the boiler refractory material. To ensure complete combustion, an excess oxygen content to the percentage of 19% is employed [1]. However, this is not the optimum excess oxygen percentage and this needs to be optimized in order to reduce the energy demand of the ASU. The combustion characteristics were reported to be similar to that in air when the oxygen percentage in the feed gas was 30-35% [2-3]. It is important to prevent air leakage into the boiler in oxyfuel combustion since this causes dilution of the flue gases with nitrogen and can also enhance the formation of  $\text{NO}_x$  [4]. In the case of retrofitting, the air leakage can be as high as 8-16%. New boilers can be built to prevent this. In the absence of air leakage, it was shown that for coal combustion the formation of thermal  $\text{NO}_x$  was much lower as compared to combustion in air [2]. For natural gas, the formation of thermal  $\text{NO}_x$  was close to zero with trace amounts being formed due to the residual nitrogen in the fuel [3].

The boiler heat transfer surfaces need to be suitably modified to account for the change in the composition and the flow through the boiler. In addition, burner modifications may be necessary. Power plants operating on a supercritical steam cycle may be better suited to employing oxyfuel combustion since these plants have an inherently higher efficiency than plants operating on a conventional steam cycle.

## B.2 Oxyfuel fired gas turbine

It is also possible to employ oxyfuel combustion in gas turbines. The feed gas consists of a mixture of oxygen and recycled  $\text{CO}_2$ . The oxygen for combustion is fed in almost stoichiometric proportion. The exhaust gases contain mainly  $\text{CO}_2$  and  $\text{H}_2\text{O}$ . This is expanded in a gas turbine to generate power and is then passed through a heat recovery steam generator (HRSG) to recover the residual heat. The water is then removed by condensation and a fraction of the  $\text{CO}_2$  rich stream is recycled and fed to the gas turbine with the feed gas. The recycle percentage of  $\text{CO}_2$  is to the order of 90% in order to maintain the turbine inlet temperature (TIT) at the required level. The rest of the  $\text{CO}_2$  rich stream is compressed and sent for storage. A schematic of an oxyfuel fired gas turbine cycle is shown in Figure B-1.

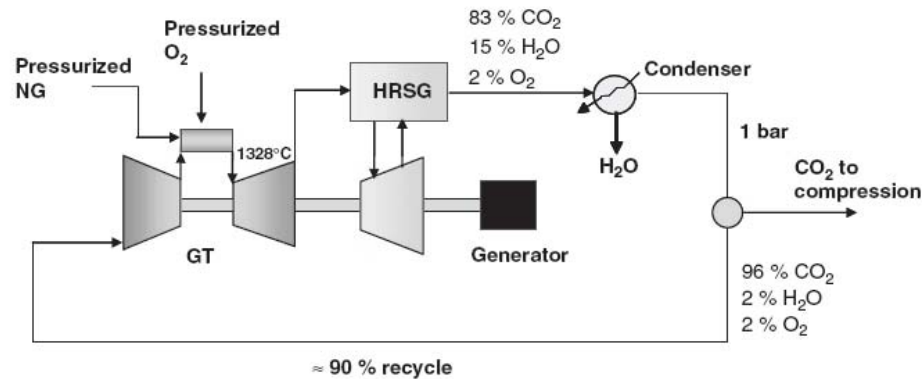


Figure B-1: Schematic of oxyfuel fired gas turbine cycle. Adapted from [5]

One of the major challenges in such a system is the design of a gas turbine operating on  $\text{CO}_2$  as the working fluid. The design of the combustor and the compressor are also affected. The gas density when  $\text{CO}_2$  is used as the working fluid is about 50% higher than when air is used. There is a 7 – 12% lower isentropic exponent that leads to a lower specific compression and expansion work. The gas turbine also operates at a higher pressure ratio of 30-35 as compared to the 18 employed in air combustion. This is done in order to keep the turbine exit temperature at acceptable levels [6]. Due to these changes, a

complete redesign of the combustor, compressor and gas turbine is necessary. This remains one of the biggest developmental challenges to the commercialization of this technology.

### B.3 References

1. Dillon, D.J., Panesar, R.S., Wall, R.A., Allam, R.J., White, V., Gibbons, J., and Haines, M.R., *Oxy-Combustion Processes for CO<sub>2</sub> Capture From Advanced Supercritical PF and NGCC Power Plant*, in *7th International Conference on Greenhouse Gas Control Technologies*. 2004: Vancouver, Canada.
2. Croiset, E., Thambimuthu, K. and Palmer, A., *Coal combustion in O<sub>2</sub>/CO<sub>2</sub> mixtures compared with air*. Canadian Journal of Chemical Engineering, 2000. **78**(2): p. 402-407.
3. Tan, Y., M.A. Douglas, and K.V. Thambimuthu, *CO<sub>2</sub> capture using oxygen enhanced combustion strategies for natural gas power plants*. Fuel, 2002. **81**(8): p. 1007-1016.
4. Herzog, H.J. and E.M. Drake, *Carbon dioxide recovery and disposal from large energy systems*. Annual Review of Energy and the Environment, 1996. **21**: p. 145-166.
5. Kvamsdal, H.M., K. Jordal, and O. Bolland, *A quantitative comparison of gas turbine cycles with CO<sub>2</sub> capture*. Energy. **In Press, Corrected Proof**.
6. Göttlicher, G., *The Energetics of Carbon Dioxide Capture in Power Plants*. 2004, NETL Report.

## Appendix C

### Chemical looping combustion and reforming

The oxygen carriers used in chemical looping combustion are metal-oxide particles on a support material that improves the mechanical strength of the particle. The metal oxide particles need to have the following characteristics:

- High capacity for oxygen transfer
- Fast rates of oxidation and reduction. This gives us flexibility in the operation of the plant
- High attrition resistance
- High cycling capacity
- Good heat transfer characteristics
- Inexpensive

Metals of transition metals like Fe, Co, Cd ,Ni have been receiving particular attention [1-2] In order to increase the reactivity and durability of the oxides, the particles have often been doped with  $\text{Al}_2\text{O}_3$ , yttrium stabilized zirconium (YtZ),  $\text{TiO}_2$  or  $\text{MgO}$ . The particle size of the oxygen carriers is approximately 2mm. The reaction rates vary depending on the metal oxide, the fuel gas, particle size and temperature. Generally, Ni and Co oxides show higher reduction and oxidation rates and greater durability than Fe oxides [3].

The maximum temperature in the reactors is limited to 800 °C when using iron carriers and 1050 °C when using Ni based carriers due to the thermal stability of the material [2, 4]. This is the major thermodynamic difference between CLC and CC. In CC, the turbine inlet temperature is as high as 1200°C. This limits the efficiency of the power cycle in CLC. To overcome this, additional cycle could be burned in the gas turbine. However,

this leads to CO<sub>2</sub> emissions that cannot be captured, thus defeating the purpose of the system.

If a gas turbine is to be used, it may be advantageous to operate the reactor under pressure [5]. In this case, compressed air is supplied to the oxidation reactor. However, it has been observed that an increase in the pressure of the system has a negative impact on the reaction rate [6]. It was proposed that this could be due to a change in the internal structure of the oxygen carriers when pressure is applied. This could have implications for the structural integrity of the particles as well.

It has been shown that there is no significant carbon deposition on the surface of the metal oxide particles during CLC [7]. The reactivity of NiO/SiO<sub>2</sub> particles decreased at 950°C as the number of cycles increased but that this effect was not observed at 850 °C. In CLC, thermal NO<sub>x</sub> formation is reduced or avoided since the flame temperature in the oxidation reactor is less than 2000 K. This has also been confirmed by experiments [5]. If the fuel contains a significant amount of sulfur however, there could be poisoning of the oxide carriers due to sulfur. In such a case, the fuel may need to be desulfurized.

If coal is to be used as the fuel, then, solid-solid heat transfer issues need to be addressed. There may be particulate matter contamination due to the particles present in coal. In addition, separation of ash from oxide particles could be a problem. An additional issue to be addressed is the prevention of leakage of coal from the fuel reactor to the oxidation reactor.

The main thrust of development in chemical looping systems needs to be on the development of more suitable oxygen carrier particles. A demonstration plant needs to be set up in order to gauge the operational feasibility of such a system.

## C.1 Chemical looping steam reforming

A process for chemical looping steam reforming has been conceptualized [8]. This allows the production of hydrogen and a pure stream of carbon dioxide which can be captured. A flowsheet for chemical looping steam reforming is presented in Figure C-1.

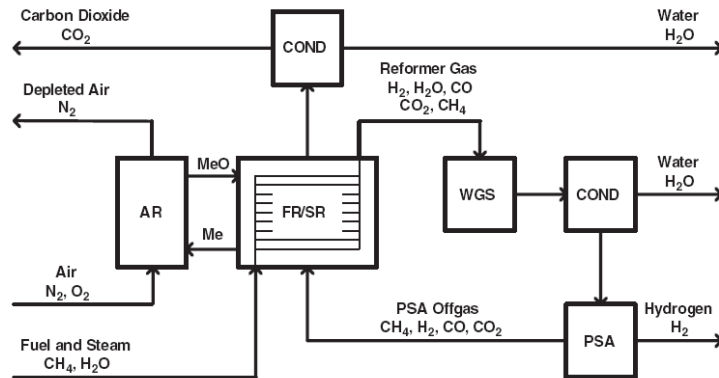


**Figure C-1: Flowsheet of chemical looping steam reforming. Adapted from [8].**

The process is similar to conventional steam reforming but the furnace is replaced with a CLC system. The reformer tubes are located inside the fuel reactor. The fuel and steam are fed to the tubes. The oxidized particles are transferred from the oxidation reactor to the fuel reactor where they transfer oxygen to the PSA offgas. This gas is combusted and provides the heat required for the endothermic steam reforming process. The products of steam reforming are subjected to water gas shift to produce  $\text{CO}_2$  and hydrogen. The water is removed by condensation and then a PSA unit is employed to separate the hydrogen. A pure stream of  $\text{CO}_2$  is obtained which can then be compressed and sent for storage. The PSA offgas consists of methane, hydrogen, carbon monoxide and carbon dioxide and this is sent for firing in the fuel reactor. If necessary, additional fuel in the form of hydrogen obtained from steam reforming can be supplied.

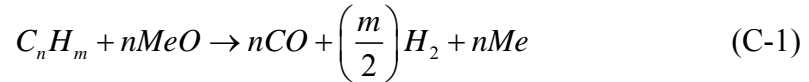
The pressure drop over the fuel reactor may be high if the density of the oxygen carrier and the bed height are large. A low density oxygen carrier is desired; however, this is a

tradeoff with the reactivity and life of the particles. The process if operated at elevated pressures could lead to a better recovery of H<sub>2</sub> in the PSA process. However, higher pressures require higher temperatures in the reformer tubes. A fluidized bed is a harsh environment and there may be erosion of tubes in such an environment. This process is still in the conceptualization stage and is not likely to be operated on a large scale in the near future. In addition, there are exergy losses in the form of loss of fuel heating value due to steam reforming. The produced hydrogen needs to be compressed which also leads to an energy penalty.

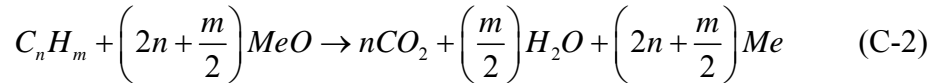
## C.2 Chemical looping autothermal reforming

Autothermal reforming is a combination of steam reforming and partial oxidation of the fuel. The reactions in chemical looping autothermal reforming are shown below:

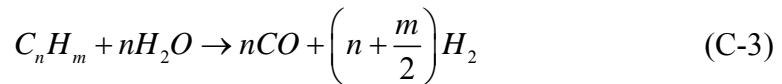
**Partial oxidation:**



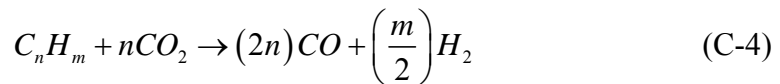
**Complete oxidation:**



**Steam reforming:**



**CO<sub>2</sub> reforming:**



**Oxidation of metal carrier:**



In chemical looping autothermal reforming, most of the fuel should undergo partial oxidation but complete oxidation, steam reforming and  $\text{CO}_2$  reforming also take place. Steam or  $\text{CO}_2$  can be added to enhance the relative importance of (C-3) or (C-4). (C-1), (C-3) and (C-4) are strongly endothermic reactions while (C-5) is strongly exothermic. If the overall sum of the reactions in the fuel reactor is endothermic, heat has to be transferred from the oxidation reactor to the fuel reactor. This is always the case for chemical looping autothermal reforming. A schematic of chemical looping autothermal reforming is shown in Figure C-2.

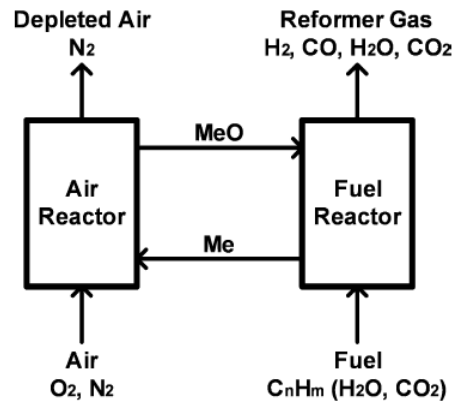


**Figure C-2: Schematic of chemical looping autothermal reforming. Adapted from [9]**

In chemical looping reforming, the exhaust gas from the fuel reactor consists of a mixture of carbon dioxide, carbon monoxide, hydrogen and water. It is similar to what is obtained from a conventional reformer and can be used as a feedstock for the production of chemicals as well as for the production of hydrogen [9]. By subjecting the gas to a shift reaction, we can form a mixture of carbon dioxide and hydrogen. The hydrogen can be separated by PSA and the carbon dioxide can be captured and sent for storage.

A pressurized process has been proposed [10] wherein the chemical looping reforming process is conducted under pressure and is integrated with a power generation process. A flowsheet of the integrated process is presented in Figure C-3.

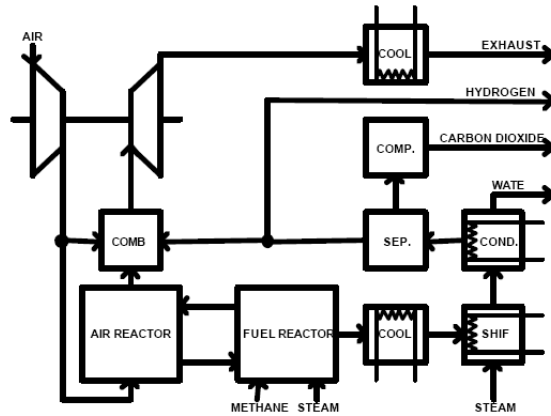


**Figure C-3: Flowsheet of chemical looping autothermal reforming. Adapted from [10]**

However at higher pressures, the thermodynamic equilibrium for the reforming reaction is less favorable and hence higher temperatures will be needed (higher than 850 °C). This may cause a problem in particle reactivity and stability. If the process is done at atmospheric pressure however, the hydrogen produced would have to be compressed and this requires significant energy. Also, the carbon dioxide in this case will have to be separated from the hydrogen by absorption since the required pressure differential for PSA will not be present. This will lead to severe exergy losses in the system making it economically infeasible. Hence, for chemical looping autothermal reforming to be feasible, it is necessary to develop metal oxide carrier particles that can withstand higher pressure and temperatures.

### C.3 References

1. Jin, H.G., T. Okamoto, and M. Ishida, *Development of a novel chemical-looping combustion: Synthesis of a solid looping material of NiO/NiAl<sub>2</sub>O<sub>4</sub>*. Industrial & Engineering Chemistry Research, 1999. **38**(1): p. 126-132.
2. Mattisson, T., A. Lyngfelt, and P. Cho, *The use of iron oxide as an oxygen carrier in chemical-looping combustion of methane with inherent separation of CO<sub>2</sub>*. Fuel, 2001. **80**(13): p. 1953-1962.
3. Lyngfelt, A., B. Leckner, and T. Mattisson, *A fluidized-bed combustion process with inherent CO<sub>2</sub> separation; application of chemical-looping combustion*. Chemical Engineering Science, 2001. **56**(10): p. 3101-3113.
4. Mattisson, T., M. Johansson, and A. Lyngfelt, *The use of NiO as an oxygen carrier in chemical-looping combustion*. Fuel, 2006. **85**(5-6): p. 736-747.
5. Ishida, M. and H.G. Jin, *Fundamental study on a novel gas turbine cycle*. Journal of Energy Resources Technology-Transactions of the Asme, 2001. **123**(1): p. 10-14.
6. Garcia-Labiano, F., Adanez, J., de Diego, L. F., Gayan, P. and Abad, A., *Effect of pressure on the behavior of copper-, iron-, and nickel-based oxygen carriers for chemical-looping combustion*. Energy and Fuels, 2006. **20**(1): p. 26-33.
7. Zafar, Q., T. Mattisson, and B. Gevert, *Redox investigation of some oxides of transition-state metals Ni, Cu, Fe, and supported on SiO<sub>2</sub> and MgAl<sub>2</sub>O<sub>4</sub>*. Energy and Fuels, 2006. **20**(1): p. 34-44.
8. Ryden, M. and A. Lyngfelt, *Using steam reforming to produce hydrogen with carbon dioxide capture by chemical-looping combustion*. International Journal of Hydrogen Energy, 2006. **31**(10): p. 1271-1283.
9. Ryden, M., A. Lyngfelt, and T. Mattisson, *Synthesis gas generation by chemical-looping reforming in a continuously operating laboratory reactor*. Fuel, 2006. **85**(12-13): p. 1631-1641.
10. Ryden, M. and A. Lyngfelt. *Hydrogen and power production with integrated carbon dioxide capture by chemical-looping reforming*. in *Seventh International Conference on Greenhouse Gas Control Technologies*. 2004. Vancouver, Canada.

## Appendix D

### Calculation of minimum work of separation and compression

Consider 1 mole of gas containing 11% CO<sub>2</sub> and 89% N<sub>2</sub>. We will assume separation at 298 K and assume 90% capture of CO<sub>2</sub>. A schematic is shown in Figure D-1.

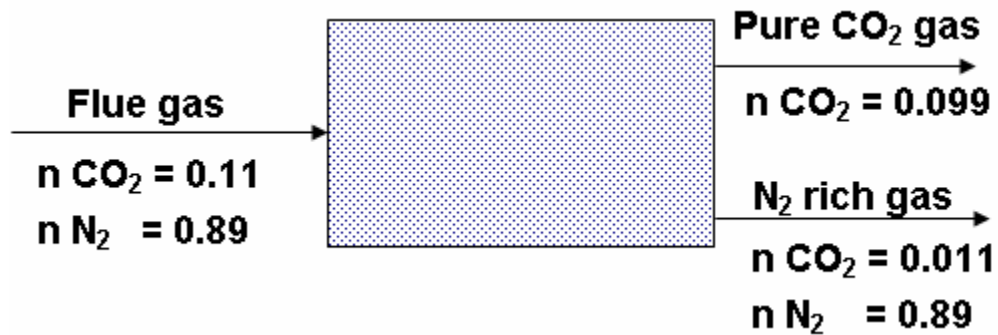


Figure D-1: Schematic of separation system

#### D.1 Minimum work of separation

For a steady flow system, we have the minimum thermodynamic work as:

$$W_{\min} = W_{\text{flue gas}} - W_{\text{CO}_2} - W_{\text{N}_2} \quad (\text{D-1})$$

The reversible separation work per mole of mixture is given by (D-2) [1]:

$$w_{\text{rev}} = -T_o R \sum_i y_i \ln y_i \quad (\text{D-2})$$

$$W_{\min,FG} = -RT \left( \frac{n_{CO_2}}{n_{CO_2} + n_{N_2}} \ln \left( \frac{n_{CO_2}}{n_{CO_2} + n_{N_2}} \right) + \frac{n_{N_2}}{n_{CO_2} + n_{N_2}} \ln \left( \frac{n_{N_2}}{n_{CO_2} + n_{N_2}} \right) \right) \quad (D-3)$$

$$W_{\min,FG} = -8.314 \times 298 \times (0.11 \ln 0.11 + 0.89 \ln 0.89)$$

$$W_{\min,FG} = \mathbf{0.859 \text{ kJ/gmol FG}}$$

**$W_{\min,CO_2} = 0$ , since it is a pure stream**

$$W_{\min,N_2} = -RT \left( \frac{n_{CO_2}}{n_{CO_2} + n_{N_2}} \ln \left( \frac{n_{CO_2}}{n_{CO_2} + n_{N_2}} \right) + \frac{n_{N_2}}{n_{CO_2} + n_{N_2}} \ln \left( \frac{n_{N_2}}{n_{CO_2} + n_{N_2}} \right) \right) \quad (D-4)$$

$$W_{\min,N_2} = -8.314 \times 298 \left( \frac{0.011}{0.011 + 0.89} \ln \left( \frac{0.011}{0.011 + 0.89} \right) + \frac{0.89}{0.011 + 0.89} \ln \left( \frac{0.89}{0.011 + 0.89} \right) \right)$$

$$W_{\min,N_2} = 0.163 \text{ kJ/gmol stream} \times 0.901 \text{ gmol stream/gmol FG}$$

$$W_{\min,N_2} = \mathbf{0.1469 \text{ kJ/gmol FG}}$$

$$W_{\min} = 0.859 - 0.1469$$

$$= 0.7121 \text{ kJ/gmol FG}$$

Since 90% CO<sub>2</sub> is captured i.e. 0.9 x 0.11 = 0.099 gmol CO<sub>2</sub>/gmol flue gas

$$W_{\min, \text{normalized}} = 7.193 \text{ kJ/ gmol CO}_2$$

$$W_{\min, \text{normalized}} = \mathbf{0.001998 \text{ kWh/ gmol CO}_2}$$

The above result holds for 90% capture.

If we were assuming complete capture of CO<sub>2</sub>, then,  $W_{N_2} = 0$  since the stream is pure and

$$W_{\min} = 0.859 \text{ kJ/gmol FG}$$

$$= 7.8 \text{ kJ/gmol CO}_2 \text{ (} N_{CO_2} = 0.11 \text{)}$$

$$W_{\min} = 0.0021 \text{ kWh/gmol CO}_2$$

## D.2 Minimum work of compression

$$\text{Work of compression to 110 bar} = \text{Availability at 110 bar} - \text{Availability at 1 bar} \quad (\text{D-5})$$

From the NIST Chemistry WebBook [2], we can obtain the availability of CO<sub>2</sub> at different pressures. This data is presented in Table D-1.

**Table D-1: Availability data for CO<sub>2</sub> at 1 bar and 110 bar. Data from [2]**

Temperature (K)	Pressure (bar)	H (kJ/mol)	S (J/mol-K)
298	1	22.257	120.54
298	110	11.166	50.979

$$\text{Availability} = H - TS \quad (\text{D-6})$$

$$\text{At 1 bar, availability} = -13.664 \text{ kJ/mol}$$

$$\text{At 110 bar, availability} = -4.0257 \text{ kJ/mol}$$

$$\text{Work of compression} = 9.638 \text{ kJ/mol}$$

$$\text{Ideal work of compression} = 0.002677 \text{ kWh/gmol CO}_2$$

$$\text{Total ideal work of separation and compression for 90\% capture} = 0.004675 \text{ kWh/gmol CO}_2$$

The work calculated for 85% CO<sub>2</sub> capture and compression was 0.01572 kWh/gmol CO<sub>2</sub> in MEA systems and 0.021 kWh/gmol CO<sub>2</sub> for chilled ammonia systems.

### **D.3 References**

1. Smith, J.M., H.C. Van Ness, and M.M. Abbott, *Introduction to Chemical Engineering Thermodynamics*. 6 ed. 2001, New York: McGraw-Hill.
2. NIST Chemistry WebBook. 2008.

# Appendix E

## Definition of terms

Some of the important terms that have been utilized in this thesis are described in Table E-1.

Table E-1: Definition of terms used in thesis

Term	Definition	Unit
<b>Lean stream</b>	Solvent stream that is stripped of CO <sub>2</sub>	-
<b>Rich stream</b>	Solvent stream that has captured CO <sub>2</sub>	-
<b>Reboiler duty</b>	Heat supplied in desorber for each unit of CO <sub>2</sub> that is captured	kJ/kg
<b>L/G</b>	Ratio of total molar liquid flow in absorber to total vapor flow	mol/mol
<b>Loading</b>	Ratio of total moles of CO <sub>2</sub> carrying species to total moles of solvent carrying species	mol/mol
<b>Lean loading</b>	Loading of lean stream	mol/mol
<b>Rich loading</b>	Loading of rich stream	mol/mol
<b>DCC</b>	Direct contact cooling tower	-